



# University of HUDDERSFIELD

## University of Huddersfield Repository

Talbot, Nathan

A Search for Novel Antimicrobials and Novel  $\beta$ -Lactamase Inhibitors

### Original Citation

Talbot, Nathan (2019) A Search for Novel Antimicrobials and Novel  $\beta$ -Lactamase Inhibitors. Doctoral thesis, University of Huddersfield.

This version is available at <http://eprints.hud.ac.uk/id/eprint/34937/>

The University Repository is a digital collection of the research output of the University, available on Open Access. Copyright and Moral Rights for the items on this site are retained by the individual author and/or other copyright owners. Users may access full items free of charge; copies of full text items generally can be reproduced, displayed or performed and given to third parties in any format or medium for personal research or study, educational or not-for-profit purposes without prior permission or charge, provided:

- The authors, title and full bibliographic details is credited in any copy;
- A hyperlink and/or URL is included for the original metadata page; and
- The content is not changed in any way.

For more information, including our policy and submission procedure, please contact the Repository Team at: [E.mailbox@hud.ac.uk](mailto:E.mailbox@hud.ac.uk).

<http://eprints.hud.ac.uk/>

# A Search for Novel Antimicrobials and Novel $\beta$ -Lactamase Inhibitors

Nathan Talbot, BSc (Hons)



*A thesis submitted to the University of Huddersfield in the partial fulfilment of the requirements for the degree of Doctor of Philosophy*

Department of Applied Sciences

October 2018

Word Count Excluding References: 46,454

## Abstract

For almost a century, antibiotics have been used as treatment agents in the combat of infections caused by pathogenic microbes. For a short while, antibiotics were heralded as miracle drugs; their discovery and introduction into the clinic has no doubt saved countless animal and human lives. The use of antibiotics in surgical procedures has ushered in the modern medical era where surgeons are afforded a whole host of cutting edge treatment and ground-breaking surgical techniques thanks to the benefits and treatment options antibiotics offer. The dark times of the pre-antibiotic era where many lives were lost through trivial illnesses have long been forgotten. However, what was once a trickle of reports of antibiotic resistance has since turned into a flood of pandemic proportions; the once lethal actions of antibiotics are threatened by the seemingly unstoppable march of resistance. Pathogenic microbes, once susceptible to the killing mechanisms of antibiotics, are now equipped with several mechanisms capable of shrugging off the previously deadly antibiotics. The main weapon in our antibiotic armamentarium is  $\beta$ -lactam antibiotics, owing to their cheapness, efficacy, and limited side effects. It is perhaps unsurprising then that the main driver of antibiotic resistance is by the production of  $\beta$ -lactamases, enzymes capable of efficiently catalysing the hydrolysis of the  $\beta$ -lactam ring present in  $\beta$ -lactam antibiotics, rendering them useless. Unfortunately, soil which was once a rich source of novel antibiotic producing bacteria has long been described as an over-mined resource and attempts to match the success of natural and semi synthetic antibiotics with truly synthetic antibiotics has largely been a failure.

It is known that the majority of bacteria *in situ* are unculturable in laboratory conditions. The work in this thesis explores novel methods to increase the *in vitro* growth rate of bacteria

in an attempt to revitalise traditional antimicrobial discovery methods, by use of a novel incubation tool known as the isolation chip or “iChip” for short. The iChip is designed in the hope to increase the *in vitro* growth rate of previously unculturable bacteria. The work in this thesis describes the characterisation and antimicrobial activity of a previously little described strain of *Pseudomonas baetica*, a bacterium of little interest, only noted for its pathogenicity towards certain species of fish.

Given the dearth of novel antibiotics,  $\beta$ -lactamase inhibitors represent an alternative mechanism for overcoming antimicrobial resistance as compared to novel antimicrobials. This thesis also explores the potential of novel  $\beta$ -lactamase inhibitors, in the hope of extending the shelf life of existing “resistance vulnerable”  $\beta$ -lactam antibiotics. Several ring-opened carbamate ester analogues of avibactam, a novel  $\beta$ -lactamase inhibitor, were synthesised and their effectiveness as serine- $\beta$ -lactamase inhibitors were assessed. One of the inhibitors was found to be even more effective than avibactam itself. Also, the effect of pH upon inhibition of serine- $\beta$ -lactamases by these inhibitors and the catalytic activity of these enzymes was measured showing that the catalytic machinery is the same for both hydrolysis and inhibition.

Finally, several other existing compounds were tested for their inhibitory effectiveness against  $\beta$ -lactamases. Ellagic acid was found to be a good inhibitor of serine- $\beta$ -lactamases and showed an interesting inhibitory profile dependent upon pH demonstrating that both the mono- and di-anions are effective inhibitors.

## Acknowledgements

My thanks go to my supervisors, Professor Mike Page and Dr. Nicholas Powles, both of whom have given me encouraging and kind words of advice. I would also like to thank Dr. Jürgen Brem of the Professor Schofield Group at Oxford University, for the kind gift of enzymes used throughout this thesis. Finally, I would like to thank Joe Mwansa and the rest of the team at IPOS, for their company, good humour and honest advice throughout the course of my studies.

## Abbreviations

The following is a list of abbreviations the reader may find useful to refer back to throughout this thesis.

AChE	Acetylcholinesterase
ACN	Acetonitrile
AmpC	Class C serine- $\beta$ -lactamase
$\beta$ la	$\beta$ -lactamase
BP	Base Pairs
BuChE	Butyrylcholinesterase
CTX-M-15	Class C serine- $\beta$ -lactamase
DMSO	Dimethylsulfoxide
DNA	Deoxyribonucleic acid
ESBL	Extended spectrum $\beta$ -lactamase
GCMS	Gas chromatography mass spectrometry
HPLC	High performance liquid chromatography
IC <sub>50</sub>	50 % Inhibitory concentration
IMP	Metallo- $\beta$ -lactamase imipenemase
JS-ESI	Jet-Stream electrospray ionisation

LC	Liquid chromatography
LCMS	Liquid chromatography mass spectrometry
MBL	Metallo- $\beta$ -lactamase
MeOH	Methanol
NDM-1	New Delhi metallo- $\beta$ -lactamase 1
PBP	Penicillin binding protein
PCR	Polymerase chain reaction
P99	$\beta$ -Lactamase from <i>E. cloacae</i> strain P99
QqQ	Triple quadrupole mass spectrometry
QToF	Quadrupole time of flight mass spectrometry
RNA	Ribonucleic acid
SBL	Serine- $\beta$ -lactamase
SDS-PAGE	Sodium dodecyl sulfate polyacrylamide gel electrophoresis
TEM-1	Temoniera 1 $\beta$ -lactamase
TSA	Tryptone soy agar
TSB	Tryptone soy broth
UV	Ultraviolet
VIM	Verona integrin-encoded metallo- $\beta$ -lactamase

## Contents

Abstract.....	i
Acknowledgements .....	iii
Abbreviations .....	iv
Chapter One: General Introduction .....	1
1.1: Antimicrobial Chemotherapy .....	1
1.2: Antimicrobials: Examples and Mechanism of Action.....	6
1.3: $\beta$ -Lactam Antibiotics .....	8
1.4: Antibiotic Resistance .....	13
1.5: $\beta$ -Lactamases .....	24
1.5.1: Class A SBLs .....	27
1.5.2: Class B Metallo- $\beta$ -lactamases .....	28
1.5.3: Class C SBLs .....	32
1.5.4: Class D SBLs .....	33
1.5.5: SBLs Mechanism of Action.....	34
1.6: SBL Inhibitors .....	38
1.6.1: Avibactam.....	43
1.7: Search for Novel Antibiotics .....	46
1.8: Summary.....	49
1.9: Project and Research Aims .....	51
1.10: Chapter One References .....	52

Chapter Two: The Search for Novel Antimicrobials from Microbial Origins .....	80
2.1: Introduction.....	80
2.2: Chapter Aims .....	85
2.3: Methods .....	86
2.3.1: Potential Antimicrobials Within a Kombucha Tea Extract .....	86
2.3.2: Isolating Antibiotic Producing Microbes from Soil Samples.....	88
2.3.3: Isolation Chip (iChip) .....	91
2.3.4: Polymerase Chain Reaction (PCR).....	96
2.3.5: Metabolomics .....	102
2.4: Results.....	103
2.4.1: iChip Results.....	103
2.4.1: Inhibition Testing Results .....	104
2.4.2: Polymerase Chain Reaction Results .....	106
2.4.3: Metabolomics .....	111
2.5: Discussion and Conclusion.....	113
2.6: Chapter Two References.....	117
Chapter Three: Novel Avibactam Analogues as Novel Inhibitors of Serine- $\beta$ -Lactamases .....	122
3.1: Introduction.....	122
3.2: Chapter Aims .....	127
3.3: Methods .....	130
3.3.1: Synthesis of Carbamate Inhibitors .....	130

3.3.2: Liquid Chromatography Mass Spectrometry (LCMS) Analysis Methods of the Carbamate Inhibitors .....	133
3.3.3 UV Analysis and Kinetics Determination .....	134
3.3.4: pH Dependence of the Rate of Inactivation Inhibition of SBLs by the Carbamate Inhibitors and pH Dependence of the Rates of Hydrolysis of Substrates by SBLs ...	140
3.3.5: Triple Quadrupole Analysis of Carbamate Inhibitors .....	140
3.3.6: Gas Chromatography Mass Spectrometry Monitoring for Loss of Alcohol....	141
3.4: Results and Discussion .....	142
3.4.1: LCMS Analysis of Carbamates.....	142
3.4.2: QqQ Analysis of Synthesised Compounds for Avibactam Detection .....	144
3.4.3: Liberation of Alcohol.....	147
3.4.4: Detection of Avibactam via LCMS in the Carbamate Derivatives.....	151
3.4.5: Kinetics of Hydrolysis of Substrate by SBLs and Inhibition and pH Dependence .....	154
3.4.6: Kinetics of Inhibition of AmpC, P99, TEM-1 and CTX-M-15 by Methyl ester carbamate and Trifluoroethyl ester Carbamate Derivatives.....	157
3.4.7 Kinetics of Inhibition of CTX-M-15 by Hexafluoroisopropanol and Hexafluoroacetone Derivatives .....	163
3.4.8: Kinetics of Hydrolysis of Substrates by SBLs and pH Dependence .....	173
3.4.9: pH Dependence of Inhibition of SBLs.....	187
3.4.10: Hydrolysis and Inhibition Conclusions.....	205
3.5: Chapter Three References.....	206

Chapter Four: Other Novel $\beta$ -Lactamase Inhibitors .....	213
4.1: Introduction.....	213
4.1.1: Ellagic Acid.....	213
4.1.2: Urolithin A .....	221
4.1.3: Orlistat.....	224
4.1.4: Chapter Four Aims .....	226
4.2: Methods .....	227
4.2.1: UV Methods .....	227
4.2.2: Microbiological Methods .....	229
4.3: Results and Discussion .....	230
4.3.1: Inhibition Results .....	230
4.3.2: Microbial Inhibition by Ellagic Acid .....	247
4.4: Chapter Four Conclusion .....	250
4.5: Chapter Four References .....	251
Chapter Five: Summary and Concluding Remarks .....	262
5.1 Introduction.....	262
5.2: The Search for Novel Antimicrobials from Microbial Origins .....	263
5.3: Novel Avibactam Analogues as Novel Inhibitors of Serine Beta Lactamases.....	264
5.4: Other Novel $\beta$ -Lactamase Inhibitors .....	265
Chapter Six: General Methods .....	267
6.1: Sourcing of Materials .....	267

6.2: Preparation of Tryptone Soy Agar .....	267
6.3: Preparation of Tryptone Soy Broth.....	268
6.4: Polymerase Chain Reaction .....	269
6.4.1: Extraction .....	269
6.4.2: Quantification of Nucleic Acids.....	270
6.4.3: Polymerase Chain Reaction .....	271
6.4.4: Visualisation of PCR Samples by Gel Electrophoresis .....	272
6.4.5: PCR Product Purification.....	272
6.4.6: Sequence Analysis .....	273
6.5: QToF Mass Spectrometry.....	273
6.6: QqQ Mass Spectrometry.....	275
6.7: Gas Chromatography Mass Spectrometry .....	276
6.8: Synthesis of Carbamate Inhibitors.....	277
6.9: Kinetic UV Experiments.....	279
6.10: Scan UV Experiments.....	319
6.11: pH Adjustments .....	320
6.12: Enzyme Preparation and Purifications.....	320
6.13: NMR (Nuclear Magnetic Resonance) Analysis .....	322
6.14 Chapter Six References.....	326

## Chapter One: General Introduction

### 1.1: Antimicrobial Chemotherapy

Infections from microbes have long proved problematic to human health. This can be in the form of innocuous injuries obtained throughout an individual's daily activities, through contagious diseases or infections from a nosocomial origin. Antibiotics are a type of antimicrobial which can be used in the treatment of microbial infections, mainly from bacteria but also from other types of microbes such as protozoa and fungi (Davies, 2006). The first antibiotic synthesised and introduced into a clinical environment in the modern era was arsphenamine (figure 1.1), a drug pioneered by Paul Ehrlich used to treat syphilis infections at the beginning of the 1910's (Williams, 2009). However, whilst arsphenamine was useful in the treatment of syphilis, it was a relatively toxic compound, and was not the 'magic bullet' that Ehrlich had hoped for. However, Ehrlich had shown that chemistry may be used as a weapon in the battle against pathogenic infections.

Spurred on by the horrendous infected wounds witnessed in World War 1, the pharmaceutical company Friedrich Bayer began research into treating bacterial infections with synthetic chemicals inspired by the earlier work of Ehrlich (Bentley, 2009). After a few years, sulfamidochrysoidine, marketed by Bayer as prontosil, was introduced into the clinic in the early 1930s to treat human *Streptococcal* infections. Prontosil acts as an inhibitor in the bacterial folate pathway (Finch, 2010), which in turn prevents the bacteria from synthesising nucleic acids, therefore preventing bacterial growth. Humans do not synthesise folate as it is acquired through diet; therefore, prontosil specifically targets bacteria in bacterial infections. The success of prontosil inspired research into similar compounds,

eventually resulting in modifications to prontosil which spawned the sulfonamide (sulfa) class of antibiotics in the mid-1930s.

While work on the sulfa drugs began and prospered, in 1929 a Scottish physician with an interest in antimicrobials, Alexander Fleming, had serendipitously discovered a fungi capable of inhibiting *Staphylococci*. He noticed on a petri dish in his laboratory on which he was growing *Staphylococci*, there was a contaminant on the dish around which he noticed extensive bacterial lysis (Bentley, 2009). Fleming did not know it yet, but he had discovered what would soon become the basis of our antibiotic armamentarium, penicillin; a  $\beta$ -lactam antibiotic. Crude preparations of the product were made to treat infections at the Sheffield Royal Infirmary. However, no further significant progress was made despite Fleming conceding that there were possible uses for penicillin as an antimicrobial agent. Fleming had struggled to isolate a pure sample of penicillin and had concerns regarding the compound's stability. Thankfully, Fleming maintained the fungal growth in his laboratory for potential future work, but throughout the late 1920's and early 1930's, aside from one paper by Fleming in 1929 (Fleming, 1929), penicillin was mostly relegated to notebooks in the depths of Fleming's laboratory.

Whilst the clinical use of the sulfa drugs continued to grow throughout the mid to late 1930's, it was becoming clear that antimicrobials had an important role to play in the chemotherapy of microbial diseases. Physiologist Howard Florey and biochemist Ernst Chain became interested in Fleming's penicillin. In 1939 with the world on the cusp of World War 2, the two scientists developed a pilot plant for producing penicillin. The antibiotic capability of penicillin was demonstrated, and the two moved their operations to the relative safety of America, where the scale up of operations from their initial pilot plant began. Their operational conditions were optimised, and an efficient fermentation process to produce

penicillin was established, leading to the production and isolation of penicillin G (Bentley, 2009).

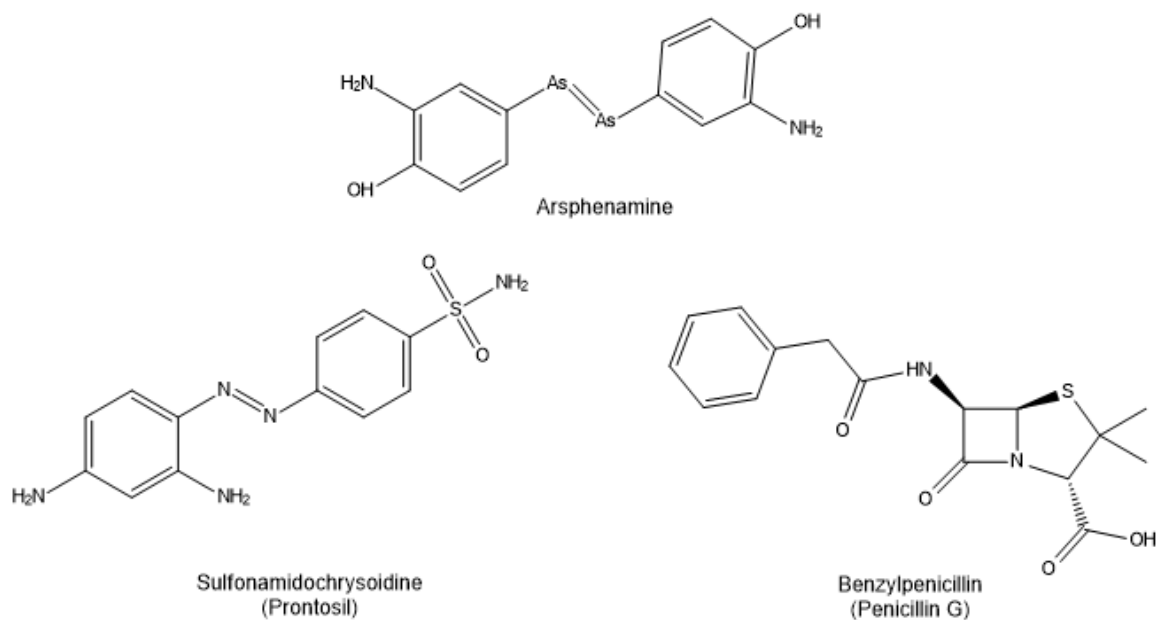


Figure 1.1: Structures of the first marketed antibiotics.

Following the introduction of sulfonamides in the 1930's, there followed a rich discovery period from the 1940's to the 1970's, often termed the 'golden age' of antibiotic discovery (Davies, 2006a). The date of discovery of various antibiotics can be seen in figure 1.2 below.

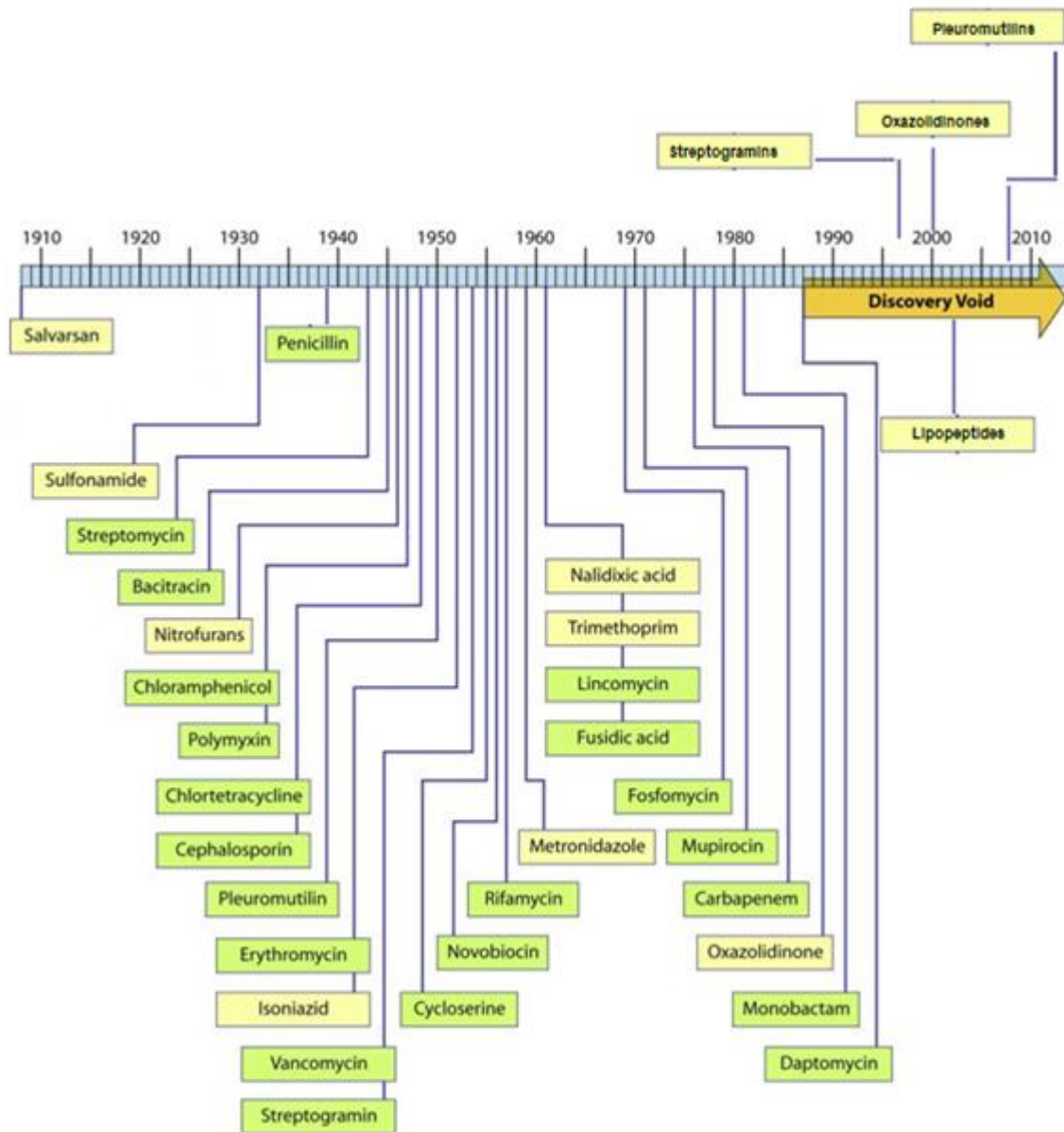


Figure 1.2: Timeline of discovery of different antibiotic classes, showing a rich discovery era in the 1940's-1970's, and a discovery void from 1990 onwards. The introduction of four new classes from 1999 to present reflects a regeneration of interest by pharmaceutical companies in antibiotic development (adapted from Silver, 2011).

The structures of the various classes of antibiotics vary greatly, from small molecules such as the monobactams (Bodey, 1990) to the larger polypeptide antibiotics (Hancock & Chapple, 1999). The molecular mechanisms of action also vary depending on the type of antibiotic, with examples including inhibition of cell wall synthesis and inhibition of protein

synthesis (Kapoor, Saigal & Elongavan, 2017). Due to the relatively wide range of antibiotic classes discovered and introduced into the clinic throughout the prosperous golden era of antibiotic discovery, some healthcare professionals had declared victory over man's war with infectious disease. With the wide array of drugs available and the competitive conditions in this marketplace, pharmaceutical companies looked elsewhere and began scaling back their antibiotic discovery operations, moving resources to combat more lucrative non-infectious diseases such as heart problems and cancer (Cohen, 2000).

Antibiotics are often hailed as a miracle of modern medicine; their discovery and use in the clinic has transformed patient care (Bartlett, Gilbert, & Spellberg, 2013) and has saved millions of patient and animal lives (Ventola, 2015). After the introduction of penicillin, the scientific community, armed with new knowledge of antibiotics and that perhaps they could be readily produced by a wide range of microbes, soil was deemed to be a good medium to screen for microbes exhibiting antimicrobial activity, as soil is an incredibly dense source of microbes, with 1 gram of soil containing one billion bacterial cells on average (Pham & Kim, 2012). However, by the late 1960's this new platform of discovery yielded fewer and fewer results (Lewis, 2013) and soil has since been described as an over-mined resource, as around 99 % of bacteria present in soil are un-culturable in laboratory conditions (Ling et al., 2015), leaving only around 1 % of bacteria present in the soil environment which can be analysed and worked with in a laboratory. Scientists have so far been mostly unable to match the impressive collection of antibiotics that have been isolated from bacteria themselves through synthetic approaches (Berdy, 2012). Alternative approaches to traditional screening platforms are being explored, with the focus on trying to increase the growth rate of microbes *in vitro*. Such approaches have resulted in the discovery of new antibiotics, indicating that there could be potentially be a plethora of interesting discoveries to be made from previously un-culturable bacteria (Ling et al., 2015).

Antibiotics are now considered miracle drugs; common infections which used to result in death are now treatable within a week, and once lethal infections are considered no more than minor inconveniences. It's difficult to imagine a world without antibiotics, but that could be very well what humanity has to face; the efficacy of antibiotics is being severely threatened by antibiotic resistance. Pathogenic microbial strains which were once susceptible to common antibiotics are now resistant to the once lethal killing mechanisms of our antimicrobial armamentarium. Resistant bacteria which were once susceptible to common antibiotics are now estimated to cause the death of over 23,000 people a year in the United States, and over 25,000 people a year in Europe, numbers which are only expected to increase as resistance spreads (World Health Organisation, 2015). Urgent action is needed to overcome the threat of resistance, including the development of novel antibiotics and novel  $\beta$ -lactamase inhibitors to aid in combat of  $\beta$ -lactamases, the main driver of antibiotic resistance.

## **1.2: Antimicrobials: Examples and Mechanism of Action**

Bacteria can be broadly divided into two different categories based upon their structure: Gram-positive and Gram-negative bacteria. Gram-positive bacteria have a thick peptidoglycan cell wall, where-as Gram-negative bacteria have a thinner peptidoglycan cell wall, but are equipped with an additional outer lipopolysaccharide membrane layer. The additional outer membrane layer makes Gram-negative bacteria a more difficult target for antibiotics, presenting challenging scenarios for antibiotic development (Qin, Panunzio & Biondi, 2014). Different antibiotics have different mechanisms of action, for example,  $\beta$ -lactams work by inhibiting cell wall synthesis (Miller, 2002), whilst polymyxins disrupt cell membrane integrity and are therefore useful at combatting Gram-negative bacteria, due to

the structural differences between Gram-positive/negative bacteria (Landman, Georgescu, Martin & Quale, 2008) and rifamycins work by interfering with the enzymes involved in bacterial growth such as RNA polymerases (Floss & Yu, 2005). The origins of most commercially successful antibiotics can be found as secondary metabolites produced by microbes such as bacteria and fungi (Davies, 2006) although many have been chemically altered to increase their microbe killing potential (Todar, 2012a). For example, penicillins can be modified by replacing the acyl group with other substituents through the intermediate formation of aminopenicillanic acid, to give an extended range of activity against Gram-negative bacteria such as *Escherichia coli* and other *Enterobacteriaceae* (Deacon, n.d.).

There was a large effort by the pharmaceutical industry to develop fully synthetic antibiotics. In a perfect world, a resistance-proof, high efficacy synthetic antibiotic would be created which exhibited highly efficient microbial killing capabilities with no side effects. However, given the large amount of effort and resources that went into developing a totally synthetic antibiotic, the mission has been a relative failure with the exception of the sulfa drugs, quinolones, oxazolidinones, and diarylquinolines, being the only examples of synthetic antibiotics to reach the clinic. Natural and semi-synthetic antibiotics outnumber synthetic antibiotics two to one; scientific approaches to developing synthetic antibiotics have simply been unable to replicate the relatively vast library of natural antibiotics. Bacterial resistance has been recorded against all synthetic antibiotics created, meaning science has fallen well short of creating the ‘ultimate’ synthetic antibiotic. Owing to the relative failure of developing synthetic antibiotics, pharmaceutical companies are largely abandoning development of synthetic antimicrobials, instead focusing on semi-synthetic derivatives of natural products (Fair & Tor, 2014). Table 1.1 below shows an overview of the different categories of antimicrobials available and their mechanisms of action. It also shows how resistance inevitably appears a short while after their introduction in the clinic.

Table 1.1: Examples of the different antibiotic classes and their mechanisms of action (Lewis, 2013).

Antibiotic class; example	Year of discovery	Year of introduction	Year resistance observed	Mechanism of action	Activity or target species
Sulfadruugs; prontosil	1932	1936	1942	Inhibition of dihydropteroate synthetase	Gram-positive bacteria
$\beta$ -lactams; penicillin	1928	1938	1945	Inhibition of cell wall biosynthesis	Broad-spectrum activity
Aminoglycosides; streptomycin	1943	1946	1946	Binding of 30S ribosomal subunit	Broad-spectrum activity
Chloramphenicols; chloramphenicol	1946	1948	1950	Binding of 50S ribosomal subunit	Broad-spectrum activity
Macrolides; erythromycin	1948	1951	1955	Binding of 50S ribosomal subunit	Broad-spectrum activity
Tetracyclines; chlortetracycline	1944	1950	1952	Binding of 30S ribosomal subunit	Broad-spectrum activity
Rifamycins; rifampicin	1957	1958	1962	Binding of RNA polymerase $\beta$ -subunit	Gram-positive bacteria
Glycopeptides; vancomycin	1953	1958	1960	Inhibition of cell wall biosynthesis	Gram-positive bacteria
Quinolones; ciprofloxacin	1961	1968	1968	Inhibition of DNA synthesis	Broad-spectrum activity
Streptogramins; streptogramin B	1963	1964	1998	Binding of 50S ribosomal subunit	Gram-positive bacteria
Oxazolidinones; linezolid	1955	2000	2001	Binding of 50S ribosomal subunit	Gram-positive bacteria
Lipopeptides; daptomycin	1986	1987	2003	Depolarization of cell membrane	Gram-positive bacteria
Fidaxomicin (targeting <i>Clostridium difficile</i> )	1948	1977	2011	Inhibition of RNA polymerase	Gram-positive bacteria
Diarylquinolines; bedaquiline	1997	2006	2012	Inhibition of $F_1F_o$ -ATPase	Narrow-spectrum activity ( <i>Mycobacterium tuberculosis</i> )

### 1.3: $\beta$ -Lactam Antibiotics

The  $\beta$ -lactam group of antibiotics consists of four sub classes: penicillins (e.g. benzylpenicillin), cepems (cephalosporins such as cephalothin etc.), penems (carbapenems) and monobactams (for example, aztreonam). Carbapenems exhibit the broadest spectrum of activity against Gram-positive and Gram-negative pathogens and are

often reserved for only the most severe multi drug resistant (MDR) infections when patients are gravely ill, due to drug toxicity concerns (Papp-Wallace, Endimiani, Taracila, & Bonomo, 2011).  $\beta$ -Lactam antibiotics represent some of the most widely used antibiotics in the clinic, owing to their efficacy, low cost and minimal side effects (Wilke, Lovering, & Strynadka, 2005). It is estimated  $\beta$ -lactam antibiotics represent around 60 % of total worldwide usage of antibiotics (Livermore & Woodford, 2006).  $\beta$ -Lactam antibiotics are named as such due to their chemical structure; all  $\beta$ -lactams contain a four membered  $\beta$ -lactam ring, which is the key to the molecule's antimicrobial activity (Poole, 2004). The carbapenems, cephalosporins and penicillins all have a fused bicyclic core; the  $\beta$ -lactam ring may be fused to a thiazolidine ring as is the case for penicillins. The  $\beta$ -lactam ring in cephalosporins is fused to a dihydrothiazine ring. Carbapenems contain a  $\beta$ -lactam ring fused to dihydropyrrole ring. Finally, monobactams only contain one ring system – the  $\beta$ -lactam ring, which is not fused to a secondary ring (figure 1.3).

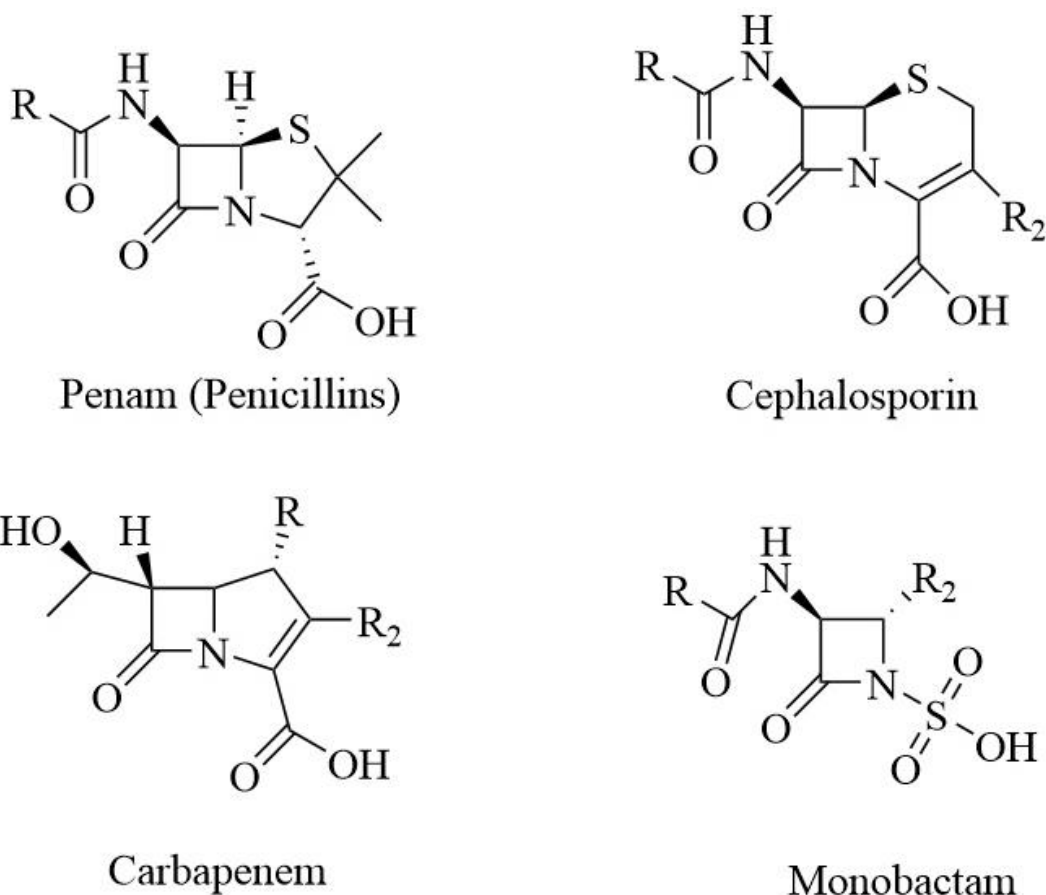
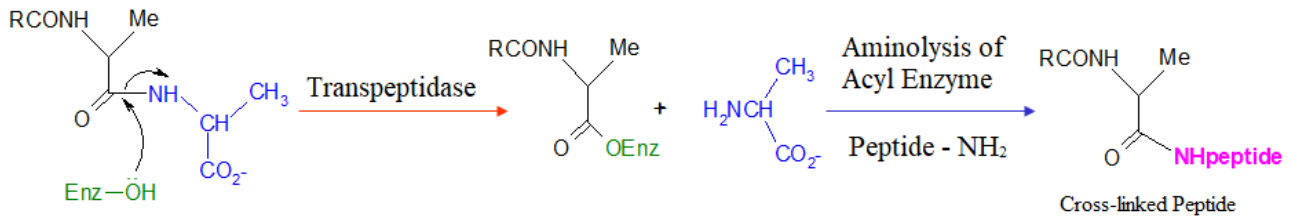


Figure 1.3: Overview of the structure of the different types of  $\beta$ -lactam antibiotics.

$\beta$ -Lactam antibiotics work by inhibiting cell wall synthesis by binding to cell wall transpeptidases – enzymes that are membrane bound outside of the cell's cytoplasmic membrane that facilitate the cross linking of the cell's peptidoglycan cell wall. Therefore, the transpeptidase enzymes which are the target of penicillin are often termed Penicillin Binding Proteins (PBPs) (Wilke et al., 2005). The  $\beta$ -lactam ring mimics the structure of the substrate of the transpeptidase enzyme, the D-Ala-D-Ala peptide terminus (figure 1.5) which is removed from the peptidoglycan precursor by transpeptidase to catalyse the crosslinking of adjacent glycan chains (Tulane University School of Medicine, 2015). Whilst the polysaccharide peptidoglycan units are produced inside the cell, their final crosslinking is catalysed outside of the membrane by transpeptidase enzymes (Poole, 2004).  $\beta$ -Lactam antibiotics therefore prevent the crosslinking of the peptidoglycan cell wall layers, resulting

in inhibition of cell wall synthesis, which results in cell death (Fisher, Meroueh, & Mobashery, 2005). The key to  $\beta$ -lactam antibiotics' success in inhibiting the cell wall transpeptidase enzymes is the fact that the  $\beta$ -lactam ring acts as an acylating agent, resulting in a covalent bond to the active site serine residues, present in the penicillin binding transpeptidase enzymes. As the  $\beta$ -lactam ring occupies the active site of the transpeptidase enzyme, the intended substrate of the enzyme (the D-Ala-D-Ala peptide terminus) cannot be acted upon by the enzyme. This interaction between the  $\beta$ -lactam and the transpeptidase can be considered an un-reversible reaction, as the bacterial cell will eventually lyse well before the acyl-enzyme complex is hydrolysed (Yocum, Waxman, Rasmussen & Strominger, 1979). Therefore, the D-Ala-D-Ala terminus on the PBP is the substrate upon which the penicillin acts to inhibit, and penicillin can therefore be considered an inhibitor of transpeptidase. The reaction schemes of the D-Ala-D-Ala terminus and transpeptidase and penicillin and transpeptidase can be seen in figure 1.4 below.

## D-Ala-D-Ala



## Penicillin

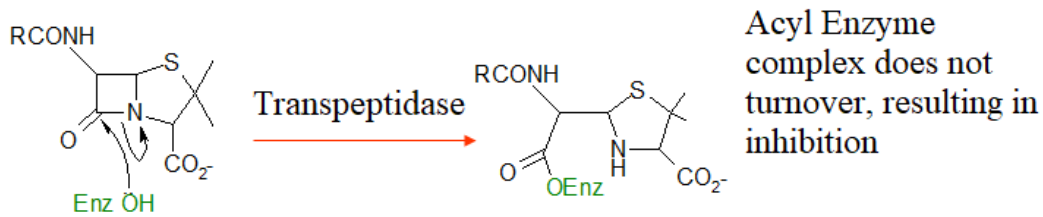


Figure 1.4: Reaction between D-Ala-D-Ala terminus and transpeptidase resulting in cross linkage of cell wall, and the reaction between penicillin and transpeptidase, resulting in inhibition of cell wall synthesis and eventual cell death.

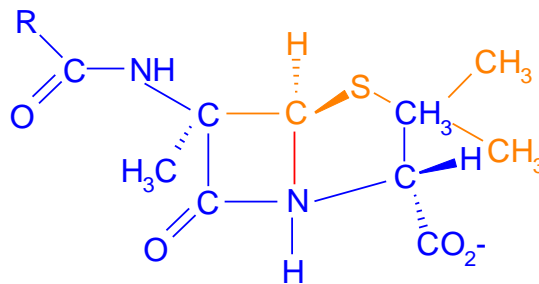


Figure 1.5: Structure of penicillin antibiotic superimposed onto the substrate for PBPs, showing how penicillin acts as a mimic for the substrate.

Humans do not possess any enzymes or proteins which can be considered homologous to the PBPs present in bacterial cell walls. This is important to note, as it results in  $\beta$ -lactam antibiotics having a high specificity towards PBP and preventing side effects in humans.

A major hurdle in the mode of action of other antibiotics is penetrating the cell's membrane or wall (Lewis, 2013).  $\beta$ -Lactam antibiotics therefore avoid this challenge, as their targets (the PBPs) are outside of the cell's cytoplasmic membrane. An overview of the process of transpeptidase inhibition by  $\beta$ -lactam antibiotics is shown below in figure 1.6.

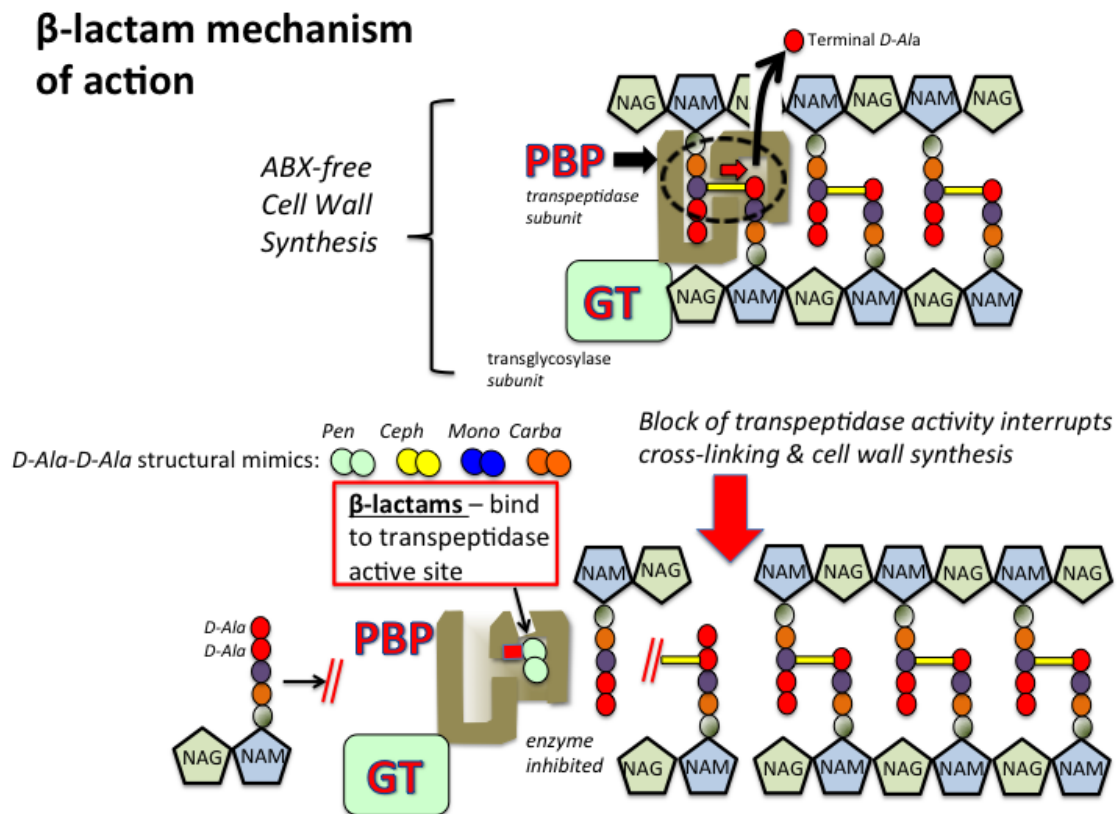


Figure 1.6: Overview of the Mode of Action of  $\beta$ -Lactam Antibiotics.

#### 1.4: Antibiotic Resistance

Although antibiotics have undeniably revolutionised modern medicine, their efficacy is being severely threatened by the onset of antibiotic resistance (Davies & Davies, 2010). Antibiotic resistance is the action of bacteria becoming resistant to the normally lethal

actions of antibiotics and is resulting in bacterial infections which cannot be treated by any available antibiotics, such as multi-drug resistant gonorrhoea, caused by *Neisseria gonorrhoea*, a Gram-negative pathogen typically treated with  $\beta$ -lactam antibiotics such as penicillin (Liu et al., 2015).

Considering that bacteria themselves are the source of around 70 % of commercially available antibiotics (Kitani et al., 2011), it is unsurprising that resistance is present in environments where there is no clinical use of antibiotics. Microbes have been present on Earth for billions of years and over that time, they have had eons to evolve and perfect killing and defensive mechanisms against their microbial neighbours (Bennett, 2008). This is why the majority of antibiotics have been isolated from microbial sources – microbes use antibiotics to kill off surrounding competitors in their never-ending battle for resources. But over this time bacteria have also evolved defensive mechanisms to their neighbours' antibiotics, and although we are witnessing a sharp increase in the number of antibiotic resistant bacteria and multi-drug resistant (MDR) infections (Fair & Tor, 2014), antibiotic resistant genes providing the necessary genetic information to code for  $\beta$ -lactamase production have been isolated from 30,000 year old bacteria located in permafrost sediments in Canada (D'Costa et al., 2011). This finding supports the theory that antibiotic resistance is a natural phenomenon, which greatly pre-dates the invention and mass use of modern antibiotics. Antibiotic resistance therefore seems an unfortunate inevitability, with resistant strains appearing for every single class of antibiotics used against them shortly after the antibiotic is introduced in the clinic (Woodford, 2005). When penicillin was introduced in the early 1940s, almost all *Staphylococcus aureus* strains were susceptible to it. Today, virtually all strains are resistant to natural penicillins (Rice, 2006). Antibiotic resistance continues to spread, whilst the antibiotic development pipeline is drying up (MacGowan & Macnaughton, 2013), presenting a concerning scenario and a desperate need for novel

antimicrobials. In an attempt to overcome antibiotic resistance, work was undertaken to create semi-synthetic derivatives of the original penicillin/cephalosporin antibiotics, resulting in so called third and fourth generation cephalosporins, penicillinase resistant penicillins and carbapenems (Yang, Ramussen & Shlaes, 1999). Exploiting semi-synthetic derivatives of existing antibiotics has been a well explored route by the pharmaceutical industry in the grim dearth of completely novel antibiotic development. At the time of their introduction into the clinic in the 1980s, these drugs were highly resistant to  $\beta$ -lactamases and were poorly hydrolysed (Garau, Wilson, Wood & Carlet, 1997). However, after the introduction of such drugs in the clinic in the 1980s, resistance inevitably arose a short time later.

One of the key concerns of antibiotic resistance is the way in which it is disseminating rapidly and indiscriminately between species of pathogenic and non-pathogenic microbes alike. Antibiotic resistance encoding genes can be spread from one bacterial species to another in several ways. One example is vertical gene transfer; this can come around from selective pressure on the bacteria. Bacteria have incredibly short generation times relative to humans, with some strains of *Escherichia coli* having generation times of around 20 minutes (Fossum, Crooke & Skarstad, 2007), meaning genetic information can be passed on to offspring extremely quickly (Todar, 2012b). When an antibiotic is administered to a patient, some bacteria may survive due to genetic mutations that confer some sort of resistance to the antibiotic (Woodford & Ellington, 2007). The bacterium will then grow and divide, passing down this genetic resistance to all their offspring (Kolář, Urbánek, & Látal, 2001). Also, bacteria can transfer genetic information ‘‘horizontally’’ by several mechanisms on mobile genetic elements. For example, bacteria can transfer plasmids via conjugation, even between different strains. The genes that code for many resistance mechanisms (such as  $\beta$ -lactamase production and efflux pumps) can be coded on plasmids

and transposons, so this provides an efficient way for these resistant genes to be transported between bacterial species (Bennett, 2008). Plasmids are circular rings of DNA found in some bacterial cells that are separate from the chromosomal DNA. Typically, plasmids code for proteins that are not essential for the normal growth of the cell. They are capable of independently replicating, and can be transported amongst different strains, and often species of bacteria (Darnell, Lodish & Baltimore, 1986). Transposons are transportable pieces of DNA, which may be encoded chromosomally or in plasmids (Cooper & Hausman, 2004). Transposons can contain genetic information that codes for  $\beta$ -lactamase production (Bennett, 2008). Transduction is another mechanism of gene transfer; a virus that is able to infect bacteria (bacteriophages) transfers the DNA from one bacterium to another. The genes the bacteriophage transfers can include genes that code for antibiotic resistant traits (Balcazar, 2014). Another method of bacteria spreading antibiotic resistance genes is via transformation. Transformation is where the bacterial cell uptakes, integrates and expresses exogenous DNA (Domingues, Nielsen, & da Silva, 2012). This DNA can include genes that will code for antibiotic resistance traits.

The best way to combat antibiotic resistance is to use antibiotics against which the bacterium has no mechanisms of resistance. However, as eluded to earlier, since the 1980s, pharmaceutical companies have all but lost interest in development of completely novel antimicrobials, with the exception of a few classes. The success of penicillin and altering the core drug scaffold leading to new antibiotics can be a lesson exploited by chemists in the development of novel antimicrobials. This does, however, enter scientists into a race against bacterial evolution, one that we are unlikely to ever win (Chakraborty, 2017).

Although antibiotic resistance is a natural phenomenon, many scientists attribute the accelerated spread of resistance to reckless misuse and overuse of antibiotics (Fair & Tor, 2014). In the United States, it is estimated that 50 % of antibiotic prescriptions are prescribed

incorrectly; either the incorrect antibiotic is prescribed or antibiotics are prescribed for viral infections, both of which can lead to increased resistance (Fair & Tor, 2014) via selective pressure. Antibiotics are used indiscriminately in the meat industry, to prevent infections in livestock when they are kept in crowded conditions, and to promote growth (Fair & Tor, 2014). This irresponsible use of antibiotics promotes the spread of antibiotic resistance, again via selective pressure. One of the latest pieces of evidence showing misuse leading to resistance has been recently documented in China; colistin is a polymyxin antibiotic that is known as one of the ‘‘last line’’ of drugs used, reserved for only the most severe infections of MDR owing to its toxicity in humans (Inamasu, Ishikawa, Oheda, Nakae, Hirose & Yoshida, 2016). But because it is rarely used, resistance to colistin was almost unheard of (Spapen, Jacobs, Van Gorp, Troubleyn, & Honoré, 2011). That was until recently, when a plasmid mediated gene that provides resistance to colistin (MCR-1) was identified in human and animal isolates from *Escherichia coli* in China (Liu et al., 2016). China is one of the world’s highest users of colistin in agriculture, which is attributed to the appearance of colistin resistance in that country (Liu et al., 2016).

Antibiotic resistance is a growing concern amongst scientists and health practitioners for several reasons. Antibiotic resistance is spreading faster than the development of new antibiotics which counter resistance (Ling, et al., 2015). Antibiotic resistant infections are associated with increased patient care costs (Lin. et al., 2015), and increased morbidity amongst patients (Qin, Panunzio & Biondi, 2014). Also, an ever-increasing number of patients susceptible to bacterial infections are being witnessed, due to an ageing population, an increase in the immuno-compromised due to transplant operations and ever increasing advancements in chemotherapy of malignant diseases. Currently, 566 million people are aged 65 and over, with this number predicted to increase to 1.5 billion by 2050 globally (Kline & Bowdish, 2016). The relation between age and a deteriorating immune system has

long been established (Dorrington & Bowdish, 2013), (Kroll, Berger, Lepperdinger, Loebenstein, 2015). Clearly, in an ageing population, infections by bacteria of a pathogenic nature are only likely to increase. As a result, indiscriminate use of antibiotics is increasing, resulting in a dissemination of antibiotic resistant genes (Thomson & Bonomo, 2005). The reliance of antibiotics to treat infections present in the elderly and immunocompromised is therefore only going to increase, meaning there is a desperate need for novel antibiotics.

Since the end of the golden era of discovery in the late 1960s, only 2 new classes of antibiotics have been introduced in the clinic: lipopeptides and oxazolidinones, which can be seen in figure 1.7 below (Butler & Cooper, 2011). The first lipopeptides, daptomycin, was introduced into the clinic in 2003 and is effective against most Gram-positive pathogens and is particularly effective in the treatment of complicated skin and skin structure infections (Lee, Fan, Kuti & Nicolau, 2006). Daptomycin was initially discovered as a secondary metabolite of *Streptomyces roseosporus* (Miao et al., 2005). Daptomycin's mechanism of action is causing cell membrane instability by causing membrane depolarisation and potassium ion reflux, causing the arrest of DNA and RNA synthesis (Steenbergen, Alder, Thorne & Tally, 2005). Linezolid is an example of the oxazolidinone class of synthetic antibiotics, which is effective against Gram-positive pathogens, including methicillin-resistant *Staphylococcus aureus* (MRSA) (Diekema & Jones, 2001). Linezolid exhibits antimicrobial activity by binding to the 50S sub unit of the prokaryotic ribosome, preventing the formation of the initial complex required for protein synthesis (Livermore, 2003). Linezolid was originally developed from a compound that showed activity against plant pathogens. It was investigated further by EI Du Pont in 1987, but was found to be toxic so development of oxazolidinone antibiotics was halted. In 1996, Upjohn Laboratories carried out further work and developed a non-toxic derivative of the original drug and introduced it into the clinic (Bozdogan & Appelbaum, 2004).

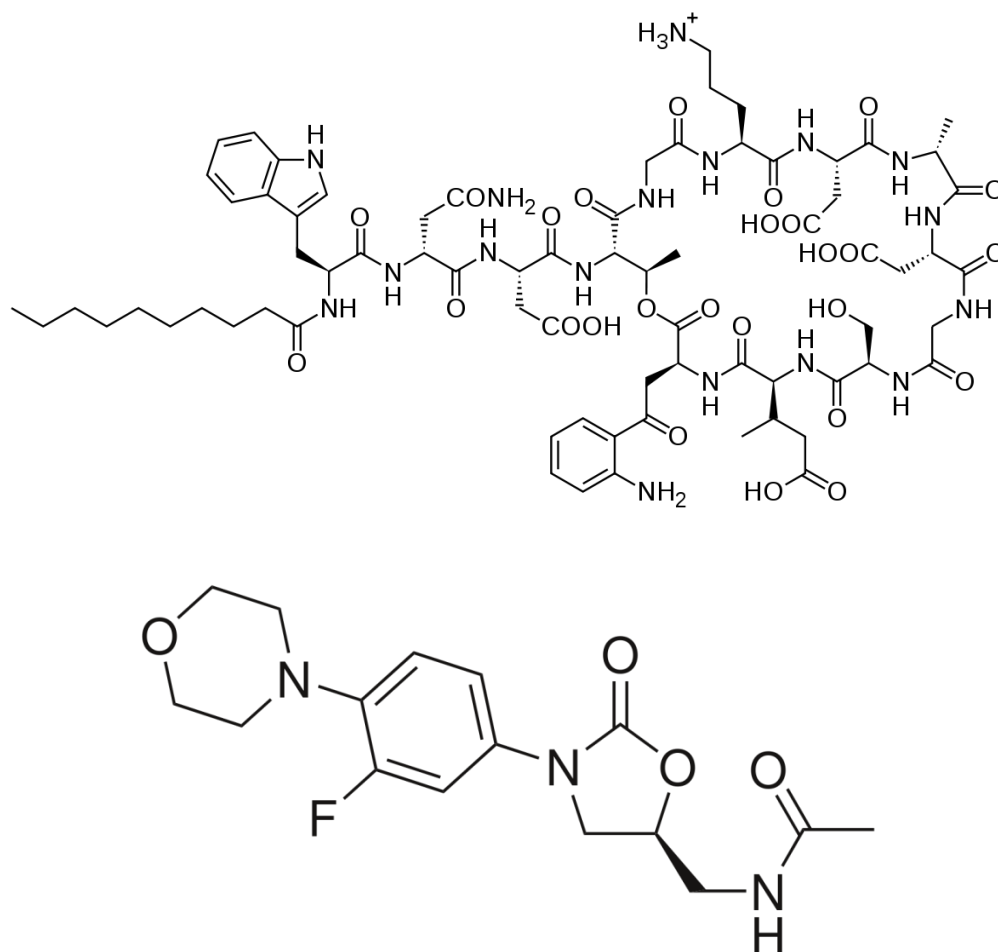


Figure 1.7: Structures of daptomycin (upper), a lipopeptide and linezolid, an oxazolidinone. The structure of daptomycin contains a 13-member amino acid cyclic lipopeptide with a decanoyl side-chain; whilst linezolid is based on an oxazolidinone and acetamide.

Antibiotic resistance is spreading faster than new antibiotic development, leading to a potentially catastrophic scenario unless more work is done in this area to introduce novel antibiotics, preferably with novel modes of action or antibiotics belonging to novel classes. Bacteria of particular concern are Gram-negative bacteria, as these are equipped with an additional outer membrane which makes them much less susceptible to conventional antibiotics. As discussed earlier, bacteria are seemingly always able to evolve resistance mechanisms to any antibiotic introduced against them. New antibiotics are always a welcome addition to our antibiotic armamentarium, but what is really needed are antibiotics

with novel modes of action, against which bacteria will take a longer time to develop resistance to. However, creating new antibiotics is expensive, and many pharmaceutical companies are moving away from new antibiotic development, owing to a multitude of reasons. For example: the high cost it takes to research, develop and manufacture a novel antibiotic, the fact that antibiotics are only used in short courses, so there's never as much demand as for other drugs that are required to be taken daily for life long illnesses, antibiotics are prescribed less owing to better antibiotic stewardship and the fact that antibiotic resistance will arise eventually so the drug will be less effective against its initial target, are just a few reasons pharmaceutical companies are moving away from this area of drug development (Cooper & Shlaes, 2011). This results in a drastic need for novel antibiotics to be introduced into the clinic as soon as possible.

The primary mechanism of antibiotic resistance is the production of  $\beta$ -lactamase enzymes by pathogenic bacteria.  $\beta$ -Lactamases catalyse the hydrolysis of the four membered  $\beta$ -lactam ring present in  $\beta$ -lactam antibiotics. It is the  $\beta$ -lactam ring in  $\beta$ -lactam antibiotics which prevent the crosslinking of cell walls, therefore if this ring is hydrolysed the antibiotic loses its potency and is rendered useless by the  $\beta$ -lactamase (Badarau, Llinás, Laws, Damblon, & Page, 2005). Whilst  $\beta$ -lactamases represent the most important mechanism of antibiotic resistance, this will be explored in much more detail later. Other important mechanisms of antibiotic resistance should be mentioned, and will be described briefly here:

***Efflux systems and alteration of membrane permeability:*** Membrane permeability plays an important role in antibiotic resistance. In Gram-negative bacteria,  $\beta$ -lactam antibiotics must first navigate past the outer membrane before they can carry out inhibition of cell wall synthesis. Efflux pumps located on the outer membrane are a way of the bacteria removing the antibiotic from the periplasm (the space between the outer and inner membrane on Gram-negative bacteria) to the extracellular environment surrounding the cell before the antibiotic

has chance to carry out its intended mechanism. Specifically, they are transport proteins which may act upon a single substrate or a range of different compounds (including antibiotics of different classes, leading to multi drug resistance) (Webber & Piddock, 2003). Whilst efflux pumps are responsible for removing compounds from the cell, porins in the outer membrane allow small hydrophilic compounds (such as  $\beta$ -lactam antibiotics) to enter the cell membrane from the extracellular environment. Therefore, down-regulation of cell membrane porins will permit less antibiotic to pass through the outer membrane of the cell, therefore decreasing the cell's susceptibility to the antibiotic (Delcour, 2009).

***Modification of Penicillin Binding Proteins:*** Mutations at the PBP active site via selective pressure on the bacteria can result in decreased affinity for the antibiotic, whilst maintaining the efficiency of the transpeptidase enzyme. This results in a PBP which the  $\beta$ -lactam antibiotic cannot inhibit, resulting in resistance (Al-Obeid, Gutmann & Williamson, 1990).

***Enzymatic Hydrolysis of the Antibiotic ( $\beta$ -lactamases):*** Enzymes are biological macro molecules that catalyse chemical reactions. They are often highly selective, meaning that specific enzymes will only act upon specific substrates to produce a certain product. Enzymes are typically made up of proteins in a globular structure, they may or may not have cofactors (such as positively charged metal ions [for example  $Zn^{2+}$  in group B metallo- $\beta$ -lactamases]) and can be pH and temperature dependent (Royal Society of Chemistry, 2004). For example, the lactose hydrolysing enzymes produced by species of *Lactobacillus* have a slightly acidic optimum pH of 5.0 and an optimum temperature of 37°C, which is best suited to the environments they operate in, forming part of the gastrointestinal microbiota (Premi, Sandine & Elliker, 1972). By contrast alkaline phosphatases are enzymes that work best in a slightly alkaline environment with an optimum pH of around 8-9.5 (Millán, 2006). Enzymes have an active site which is uniquely shaped so that it will interact with the specific substrate, offering an alternate reaction pathway with lower activation energy, in turn

catalysing the reaction (Royal Society of Chemistry, 2004.). An overview of the four main mechanisms of resistance is shown in figure 1.8 below.

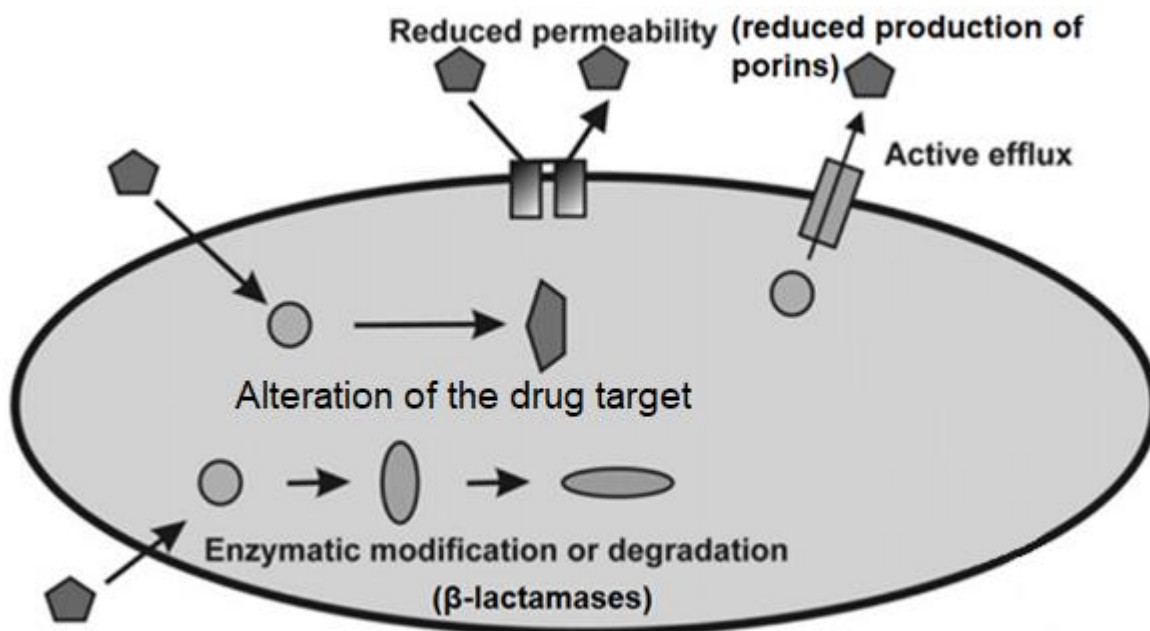


Figure 1.8: Key mechanisms of antibiotic resistance (adapted from Vranakis et al., 2013).

The production of  $\beta$ -lactamase enzymes by pathogens is one of the most significant contributors to modern day antibiotic resistance (Shaikh, Fatima, Shakil, Mohd, Rizvi & Kamal, 2014). The genes which code for  $\beta$ -lactamase production can be coded on plasmid or chromosomal DNA, meaning that the specific gene sequence can easily be transferred between different microbes (Shaikh et al., 2014). Therefore,  $\beta$ -lactamases present an extremely important contributor to resistance mechanisms.

There are four classes of  $\beta$ -lactamase enzymes, the classifications of which are based upon their amino acid sequence. Class B  $\beta$ -lactamase enzymes are unique in that they contain either one or two  $\text{Zn}^{2+}$  ions which are needed to carry out hydrolysis. The positive charge exhibited by the  $\text{Zn}^{2+}$  ions enhances also the attraction between the negatively charged

substrate and the active site, leading to hydrolysis (Drawz & Bonomo, 2010). Table 1.1 below shows an overview of the different classes of  $\beta$ -lactamases and their favoured antibiotic substrates.

Table 1.1: Ambler Classification of  $\beta$ -lactamases showing preferred substrates with examples of enzymes (Adapted from Drawz & Bonomo, 2010).

Ambler Class	Preferred Substrates	Representative Enzyme(s)
A (Serine Penicillinases)	Penicillins	PC1 from <i>S. aureus</i>
	Penicillins, narrow-spectrum cephalosporins	TEM-1, TEM-2, SHV-1
	Penicillins, narrow-spectrum and extended-spectrum cephalosporins	SHV-2 to SHV-6, TEM-3 to TEM-26, CTX-Ms
	Penicillins, carbenicillins	PSE-1
	Extended-spectrum cephalosporins	FEC-1 CepA
	Penicillins, cephalosporins and carbapenems	KPC-2, SME-1, NMC-A
B (Metallo- $\beta$ -lactamases)	Most $\beta$ -lactams (except monobactams), including carbapenems	IMP-1, VIM-1, CcrA and BcII (BL): CphA (B2): L1 (B3)
C (Cephalosporinases)	Cephalosporins	AmpC, CMY-2, ACT-1
D (Oxacillinases)	Penicillins, cloxacillin	OXA-1, OXA-10

Shortly after the introduction of penicillin in the clinic, the first identification of a  $\beta$ -lactamase enzyme capable of hydrolysing penicillin antibiotics was made in 1940 (Abraham & Chain, 1940). Abraham and Chain could not have possibly comprehended the magnitude of their discovery; indeed, at the time  $\beta$ -lactamases were first reported, they were thought of no more than a scientific curiosity. However, since these first early discoveries of resistance,  $\beta$ -lactamases now represent a global health crisis.  $\beta$ -Lactamases have been well classified, with recent studies suggesting the number of unique  $\beta$ -lactamases reported as over 1,300 (Bush, 2013), with these enzymes collectively being able to catalyse the hydrolysis of all classes of  $\beta$ -lactam antibiotics.

### 1.5: $\beta$ -Lactamases

Based upon their amino acid sequence or the mechanism used to catalyse the hydrolysis of the  $\beta$ -lactam ring in  $\beta$ -lactam antibiotics,  $\beta$ -lactamases can be broadly categorised into two different groups: the serine- $\beta$ -lactamases (SBLs), or the metallo- $\beta$ -lactamases (MBLs). The SBLs are the most prevalent type of  $\beta$ -lactamases present in antibiotic resistant bacteria and can be further separated into three subclasses dependent upon their amino acid sequence: class A, C and D. All these proteins contain a similar Ser-Xaa-Xaa-Lys motif, where the serine is the active site residue (Wouters & Bauvois, 2012). The SBLs share a similar reaction mechanism to hydrolyse their  $\beta$ -lactam targets, as seen in figure 1.9 below. Much like PBPs, they employ a nucleophilic serine residue at their active site to catalyse the hydrolysis of  $\beta$ -lactam rings present in  $\beta$ -lactam antibiotics. On the other hand, MBLs require one or two zinc metal ions at their active site to be able to carry out hydrolysis of the  $\beta$ -lactam ring (Brem et al., 2016) (Matagne, Dubus, Galleni & Frère, 1999).

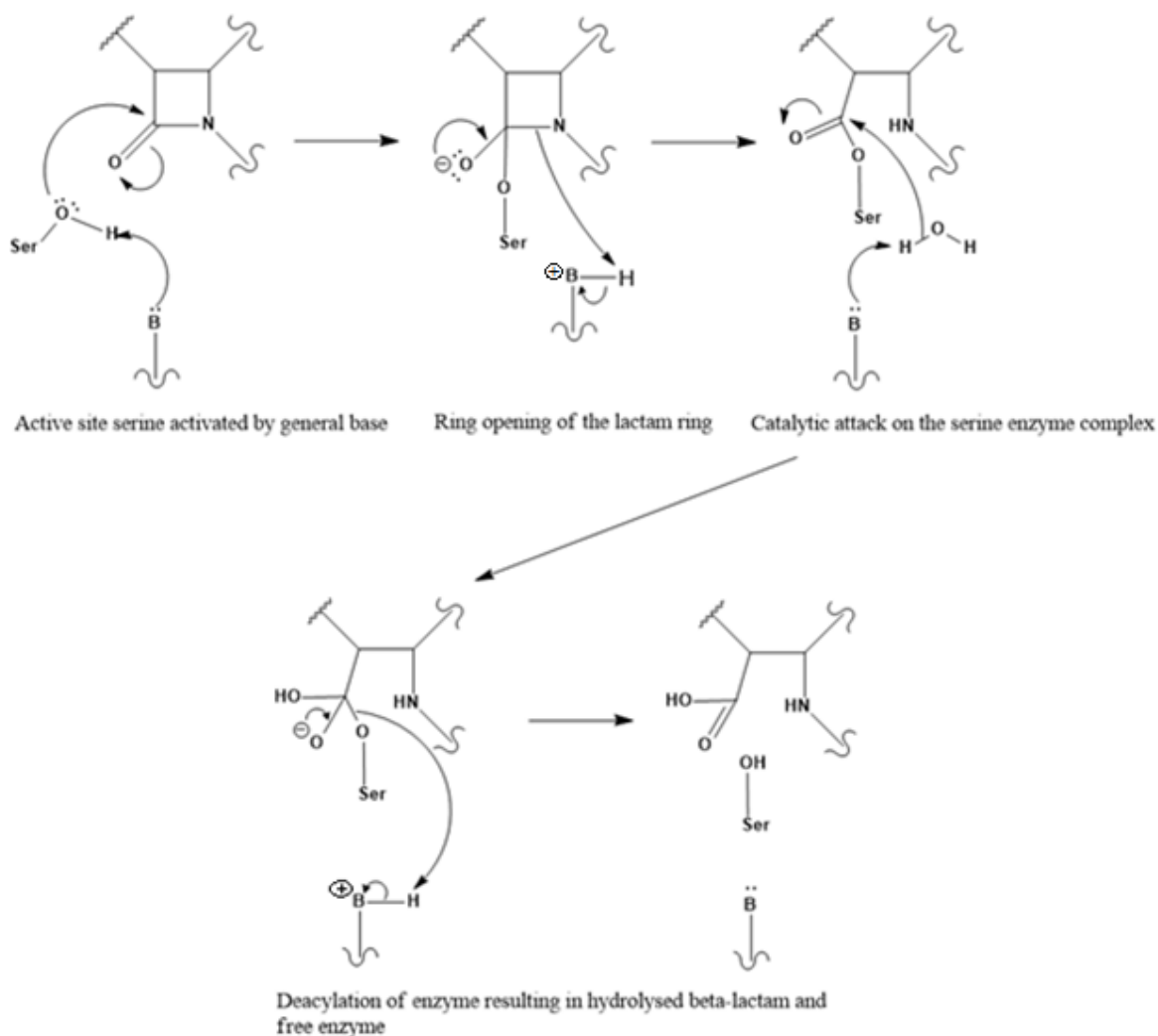


Figure 1.9: General hydrolysis mechanism of SBL.

Although the hydrolysis mechanism is different for each class of SBL on account of the base utilised to deprotonate the active site serine, the general mechanism is similar for the SBLs. The reaction commences by non-covalent formation of a Michaelis complex, followed by nucleophilic attack on the carbonyl carbon of the  $\beta$ -lactam ring by the active site serine residue concerted with proton abstraction by a basic group. Protonation of the  $\beta$ -lactam nitrogen leads to the cleavage of the C-N bond to form a covalent acyl enzyme intermediate. Attack by a catalytic water leads to a high energy deacylation intermediate, with subsequent hydrolysis of the bond between the  $\beta$ -lactam carbonyl and the oxygen of Ser70. This results in the release of the hydrolysed antibiotic and regeneration of free  $\beta$ -lactamase enzyme.

As mentioned, the SBLs can be further categorised into three categories based on their amino acid sequences and substrate preferences; they can be categorised into Ambler classes A, C and D (Ambler, 1980). Problematic Gram-negative pathogens such as strains of *Escherichia coli*, *Pseudomonas aeruginosa* and *Klebsiella pneumoniae* are typical producers of  $\beta$ -lactamases (Zeng & Lin, 2013).

$\beta$ -Lactamases can be inducible or constitutive enzymes. The production of inducible  $\beta$ -lactamases is normally repressed by some mechanism under normal conditions, but can be induced in the presence of a suitable molecular inducer such as a  $\beta$ -lactam antibiotic. This means that when the antibiotic is detected by the bacterial cell, genes coding for the production of  $\beta$ -lactamases are activated and the enzyme is expressed, resulting in hydrolysis of the antibiotic (Bedenic & Zagar, 1995).  $\beta$ -Lactamases may also be constitutive, meaning that the bacterium constantly produces a level of  $\beta$ -lactamase, whether or not a molecular inducer is present. Inducible  $\beta$ -lactamases are most commonly associated with Gram-positive organisms, whilst constitutive  $\beta$ -lactamases are normally found in Gram-negative bacteria (Livermore, 1995).

$\beta$ -Lactamases can be extracellular or intracellular, meaning they can be excreted to the extracellular environment, or remain in the intracellular environment of the periplasmic space in Gram-negative bacteria. It is normally the case for Gram-positive pathogens to excrete the enzyme to the extracellular space, as they do not have an additional outer membrane as Gram-negative bacteria do. Gram-negative are more likely to produce intracellular enzymes within their periplasmic space between their outer membrane and inner cell membrane, where the  $\beta$ -lactam antibiotics are trying to reach to interact with the PBP of the bacteria's cell wall. Although Gram-negative bacteria can also excrete  $\beta$ -lactamases to the extracellular environment more often than not this is due to cell wall

damage resulting in poor cell membrane stability caused by  $\beta$ -lactam antibiotics (Matsumura, Minami, Araki, Hori, Ogake, Watanabe, 2000).

### 1.5.1: Class A SBLs

Group A SBLs consist of the penicillinases, such as Temoneira  $\beta$ -lactamase (e.g. TEM-1), first isolated from a strain of *E. coli* in 1965 (Shaikh et al., 2015) and the plasmid encoded sulfhydryl reagent variable  $\beta$ -lactamase enzymes (SHV) (Philippon, Slama, Deny & Labia, 2016). SHV  $\beta$ -lactamases are most commonly associated with *Klebsiella spp* of bacteria. The gene coding for the precursor of SHV enzymes, SHV-1, is universally found in *Klebsiella pneumoniae* (Shaikh et al., 2015). Class A SBLs are the most widely studied of the SBL classes and are the most commonly encountered class of  $\beta$ -lactamases with more than 550 enzymes being classified (Philippon et al., 2016). Class A SBLs all share a common mechanism of action, which involves a nucleophilic attack at the carbonyl position on the  $\beta$ -lactam ring by the active site serine (Ser70), which is deprotonated by the general base Glu at position 166 (Glu166). This is followed by the formation of an acyl-enzyme intermediate, followed by hydrolysis of this intermediate by a general base activated water molecule, resulting in a cleaved  $\beta$ -lactam ring and the regeneration of free enzyme (Sougakoff, 2012). Class A SBLs are widely recognised to have initially evolved to hydrolyse penicillin (Christensen, Martin, & Waley, 1990). This claim has been given a firm backing by the work of Hardy and Kirsch (1984), that showed the class A SBL  $\beta$ -lactamase I from *Bacillus cereus* operates at the diffusion controlled limit, meaning that the hydrolysis reaction the enzyme catalyses is carried out so efficiently, that the rate limiting step is the diffusion of the substrate into the enzyme's active site (Bulychev & Mobashery, 1999).

Although some class A SBLs are considered extended spectrum  $\beta$ -lactamases (ESBLs), capable of hydrolysing later generation penicillins and cephalosporins such as ceftriaxone (Rawat & Nair, 2010), they typically can be inhibited by some of the clinically available  $\beta$ -lactamase inhibitors (BLIs), such as clavulanic acid (Bush & Jacoby, 2010) and avibactam (Ehmann et al., 2013). Resistance of class A SBLs to the aforementioned inhibitors is difficult to analyse, so specifics of resistance to inhibitors remains unknown. The usual mechanism of resistance for this class of enzymes is to simply mass produce the  $\beta$ -lactamase in high concentrations in the periplasmic space of the bacterial cell, which overwhelms the BLI (Blazquez, Baquero, Canton, Alos & Baquero, 1993), (Martinez, Delgado-Iribarren, Perez-Diaz & Baquero, 1989), (Yang, Ramussen & Shlaes, 1999).

### **1.5.2: Class B Metallo- $\beta$ -lactamases**

The class B  $\beta$ -lactamases are known as the metallo- $\beta$ -lactamases (MBLs). MBLs are a critical concern for physicians as, currently, there are no known clinically significant inhibitors of MBLs (Faridoon & Islam, 2013). Carbapenem  $\beta$ -lactam antibiotics are highly effective antibiotics and are more resistant than other antibiotics to hydrolysis by  $\beta$ -lactamases than other  $\beta$ -lactam antibiotics (Meletis, 2016). Carbapenems are often referred to as the ‘‘last resort’’ antibiotics, owing to their relative toxicity in humans, and as such, use of carbapenems is only recommended after treatment with other  $\beta$ -lactams have had little impact on the infection (Shah & Isaacs, 2003). It is recommended in clinical practice to withhold from the use of carbapenems in the clinic until all other options have been exhausted (Baughman, 2009). Because of the relative scarcity of their use compared to other  $\beta$ -lactam antibiotics, resistance of bacteria towards carbapenems had been practically unheard of until the emergence of MBLs (Codjoe & Donkor, 2018); indeed, carbapenems

themselves have been reported as inhibitors of SBLs by reacting with the serine active site and forming a long-lasting acyl-enzyme intermediate (Palzkill, 2013). MBLs have emerged relatively recently in the last two decades and have become a significant threat in the clinic, owing to the lack of inhibitors and the fact they are capable of hydrolysing carbapenems (Cornaglia, Giamarellou & Rossolini, 2011). The family of MBLs have evolved from seemingly insignificant beginnings to become capable of hydrolysing every class of  $\beta$ -lactam antibiotics except the monobactams (Palzkill, 2013). The first MBL was reported in 1966 by Sabath and Abraham (1966), from a strain of *Bacillus cereus*. Interestingly, although  $\beta$ -lactamases are more typically associated as problematic in Gram-negative pathogens, *Bacillus cereus* is a widespread Gram-positive pathogen, more often typically associated in food poisoning cases (Bottone, 2010). Much like the first reported cases of SBLs, MBLs were considered no more than a scientific curiosity, as they were mainly encountered in non-pathogenic bacteria (Bebrone, 2007) (Walsh et al., 1994). However, curiosity gave way to concern when the unrelenting spread of genes encoding for MBLs transferred from non-pathogenic bacteria to particularly concerning nosocomial strains such as *Pseudomonas aeruginosa* and *Chryseobacterium meningosepticum* (Watanabe, Iyobe, Inoue & Mitsuhashi, 1991), (Rossolini et al., 1998).

Whilst metal ions are required as cofactors for a wide array of enzymes in nature, a unique feature of the MBLs amongst  $\beta$ -lactamases is that they are dependent upon the presence of one or two zinc metal ions at their active site for their catalytic activity (Jiang et al., 2018). The genes that code for MBLs can be found on plasmids, allowing these genes to be transported easily between species of bacteria. As such, a key concern is that non-pathogenic bacteria such as commensal micro flora can act as a source, or a reservoir of genes coding for MBL production, increasing the amount of antibiotic resistance. As the gene can spread from non-pathogenic bacteria to harmful pathogens on mobile genetic elements, resistance

is conferred from one bacterium to another (Machado, Coque, Cantón, Sousa & Peixe, 2013).

MBLs are typically classified into one of four subclasses depending upon their sequences, substrate profiles and structures: B1, B2, B3 and B4, with subclass B4 being a recent addition following the discovery of a novel MBL isolated from *Serratia proteamaculans* (Vella et al., 2013). Although all classes require zinc ions to carry out their catalytic activity (normally  $Zn^{2+}$ ), the classes differ upon the number of Zn ions required. Subgroups B1, B3 and B4 require two Zn ions at their active sites, subgroup B2 needs only one, and are inhibited in the presence of two Zn ions. The notable exception to these general rules is BcII, which is interesting owing to the fact it exhibits catalytic activity in the presence of one or two Zn ions (Jiang et al., 2018).

The most commonly encountered MBLs in the clinic are the carbapenems hydrolysing New Delhi Metallo- $\beta$ -lactamase (NDM-1) and Verona Imipenemase (VIM), both belonging to the B1 subclass of MBL. Almost all clinically significant MBLs are members of the B1 subclass (Logan & Bonomo, 2016).

As mentioned, there are no clinically significant inhibitors of the MBLs available to clinicians (McGeary, Tan & Schenk, 2017). However, work towards a clinical inhibitor has been steadily increasing as the threat posed by the emergence of the MBLs, particularly NDM-1, VIM and IMP variants has become apparent. Two general techniques for MBL inhibition have been identified – Zn dependent and independent inhibition mechanisms (Rotondo & Wright, 2017). Typically, most work into novel MBL inhibitors has been the former, exploiting the Zn ions that are essential for catalysis. Specifically, already approved drugs that are known metal chelators have been screened for inhibitory activity against MBLs. Chelating agents have been shown to be effective inhibitors of certain MBLs by

forming ligands with Zn ions to interfere with their catalytic mechanism, as identified in a study by Klingler and colleagues (2015). This study looked at already approved drugs which are known chelating agents and screened them for inhibition against MBLs. The most effective inhibitor in this study was dimercaprol, a chelating agent used in the treatment of heavy metal poisoning (Rotondo & Wright, 2017). Similarly, another study by Brem and colleagues (2015) found that captopril, a well-established drug that is known to modulate blood pressure by binding to the  $Zn^{2+}$  ion in the human angiotensin converting enzyme causing inhibition (Jenkins, Dreslinski, Tadros, Groel, Fand & Herczeg, 1985) was an effective inhibitor of clinically relevant MBLs in the B1 class (IMP, VIM and BCII); with  $IC_{50}$  values in the sub 10  $\mu M$  range.

The consensus regarding the MBL mechanism of catalysis is that a nucleophilic attack takes place on the carbonyl carbon in the  $\beta$ -lactam ring of  $\beta$ -lactam antibiotics. This is followed by the C-N bond breaking and the protonation of the amide nitrogen before the hydrolysed  $\beta$ -lactam antibiotic is released (Page & Badarau, 2008). An example of the catalytic mechanisms of BCII can be seen in figure 1.10 below.

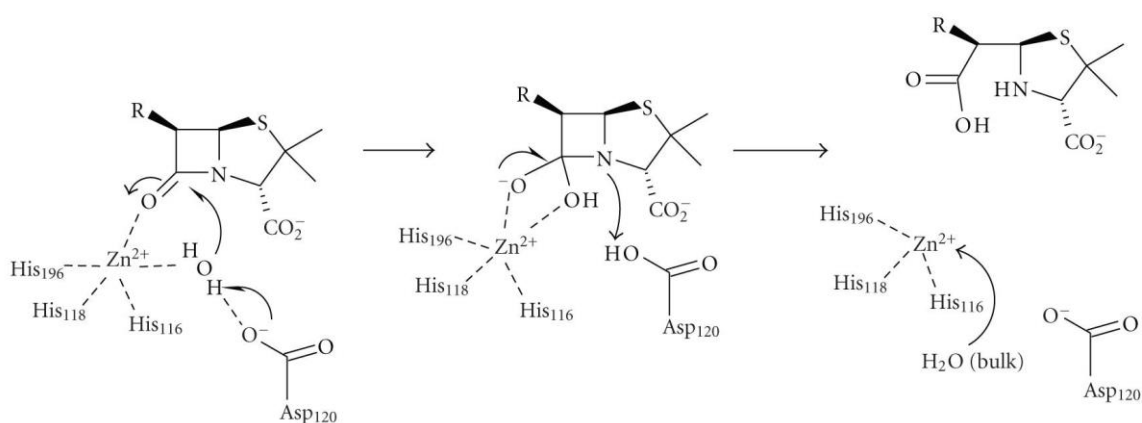


Figure 1.10: Overview of catalytic mechanism of MBLs (Page & Badarau, 2008).

### 1.5.3: Class C SBLs

Class C SBLs are also termed AmpC  $\beta$ -lactamases and are commonly encountered in Gram-negative pathogens such as *Escherichia coli*, *Pseudomonas aeruginosa* and *Serratia marcescens* (Philippon, Arlet & Jacoby, 2002). Class C SBLs represent the second most common class of SBL after class A SBLs (Bush & Mobashery, 1998). Crystallographic structures of class C enzymes have been resolved and help to elucidate the mechanism of hydrolysis employed by this class of enzyme (Powers & Shoichet, 2002). Ser-64 is the active serine and performs the nucleophilic attack onto the  $\beta$ -lactam carbonyl facilitated by Tyr150 acting as the general base to activate the serine residue (Wouters & Bauvois, 2012). Class C SBLs are predominantly chromosomally mediated, although plasmid mediated enzymes do exist, and were first discovered from a *Klebsiella pneumoniae* isolate by Papanicolaou, Medeiros and Jacoby (1990). The preferred substrate of the class C SBLs is cephalosporin  $\beta$ -lactams, but they are also able to catalyse the hydrolysis of penicillins. Similarly to some class A SBLs, it has been shown that class C SBLs can operate at the diffusion limit for their preferred cephalosporin substrates. Specifically, Bulychev and Mobashery have shown that the P99 class C SBL from *Enterobacter cloacae*, reaches the diffusion limit for its preferred cephalosporin substrates. Class C SBLs are typically not inhibited by the two historical  $\beta$ -lactamase inhibitors clavulanic acid and sulbactam, but they are inhibited by the novel non- $\beta$ -lactam  $\beta$ -lactamase diazabicyclooctane inhibitors such as avibactam, relebactam and nacubactam (Lahiri, Johnstone, Ross, McLaughlin, Olivier & Alm, 2014), (Zhanel et al., 2018), (Docquier & Mangani, 2018). AmpCs typically hydrolyse older cephalosporins, such as the first generation cephalothin cephadroxil drugs. Later generations of cephalosporins such as the zwitterionic fourth generation cefpirome, cefepime and carbapenems are not normally hydrolysed by AmpCs. However, the emergence of extended spectrum AmpCs has

been reported, which are able to hydrolyse later generations of cephalosporins and carbapenems, broadening the substrate profile of typical AmpCs (Rodríguez-Martínez et al., 2011).

#### 1.5.4: Class D SBLs

Class D SBLs are also known as oxacillinase enzymes (OXA type) and consist of over 400 genetically diverse enzymes that are largely disseminated from Gram-negative bacteria, with this number steadily increasing (Antunes, Lamoureaux, Toth, Stewart, Frase & Vakulenko, 2014). Like class A and C SBLs, class D SBLs also have a serine active site, but differ from class A and C enough in their structure to require their own class. Class D enzymes have mostly higher rates of hydrolysis for antibiotics such as cloxacillin and oxacillin than for benzylpenicillins (hence the name OXA), but not all class D enzymes have this ability to hydrolyse oxacillins (Poirel, Naas & Nordmann, 2010). Class D enzymes were amongst the first type of  $\beta$ -lactamases discovered, were originally very rare and were only found on plasmid DNA (Evans & Amyes, 2014). OXA enzymes were originally found to be very similar to class A SBLs, having a common substrate profile of being able to hydrolyse penicillins. However, OXA enzymes can be distinguished from class A SBLs by their ability to hydrolyse oxacillin (Evans & Amyes, 2014). The class D SBLs have experienced the largest increase in growth compared to any other class of SBL due to discovery of new enzyme variants (Antunes & Fisher, 2014). Class D SBLs are resistant to inhibition by the classic SBL inhibitors such as clavulanic acid or sulbactam, but are prone to inhibition by halide ions such as  $I^-$  and  $Cl^-$  (Héritier, Poirel, Aubert & Nordmann, 2003), (Stojanoski et al., 2015). The OXA class can be typically classified into narrow and extended spectrum  $\beta$ -lactamases depending upon their substrate profile. OXA-2 and OXA-10 are considered

examples of narrow-spectrum enzymes capable of hydrolysing penicillins and early generation cephalosporins. However, some class D enzymes are capable of hydrolysing carbapenems, which represents serious clinical concern due to the nature of carbapenems as mentioned previously. Such examples of class D carbapenemases include OXA-23, OXA-24 and OXA-51, and are predominantly found in Gram-negative pathogens such as *Acinetobacter baumannii* (Antunes et al., 2014).

For class D  $\beta$ -lactamases an active site lysine (Lys70), serves as the general acid/base to facilitate hydrolysis of  $\beta$ -lactams. Lys70 may be carboxylated as a result of a reaction between  $\epsilon$ -NH<sub>2</sub> of the lysine and carbon dioxide:



The carboxylation of the lysine is pH dependent, and is a compromise between the concentration of CO<sub>2</sub> (favoured by lower pH levels) and deprotonation of CO<sub>2</sub>H (favoured by higher pH levels).

### 1.5.5: SBLs Mechanism of Action

As one might imagine, the catalytic mechanism of the SBL classes of enzymes is very similar to the mechanism of PBPs from which they have evolved; due to similarities in sequence analyses, PBPs and  $\beta$ -lactamases are thought to have emerged from a common ancestor (Kong, Schneper & Mathee, 2010).

The chemistry and sterics of the  $\beta$ -lactam ring makes the antibiotic susceptible to hydrolysis. The carbonyl carbon has a bond angle of 90 °, which is far from the ideal bond angle of 109.5 °, meaning the lactam is susceptible to ring strain. The easiest way for the molecule

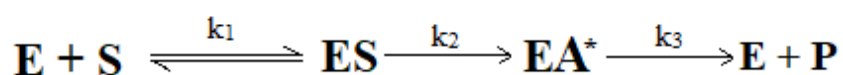
to alleviate this strain is to break the ring by hydrolysing the amide in the  $\beta$ -lactam ring. The cleavage of the amide bond allows the  $\beta$ -lactam ring to open, meaning the bond angle is closer to  $109.5^\circ$ .

Furthermore, resonance has a role to play in facilitating the opening of the  $\beta$ -lactam ring. Linear amides typically have strong resonance, meaning electrons from the nitrogen lone pair are delocalised towards the carbon as they are drawn by the electronegativity of the oxygen atom. This increases the electron density around the carbon, making it less electrophilic and therefore less reactive/susceptible to a nucleophilic attack (considering that the  $\beta$ -lactamase carries out a nucleophilic attack at the carbonyl carbon). Additionally, the nitrogen in the lactam ring cannot be planar due to the sterics of the molecule.

With the chemistry of the lactam ring considered, one might assume it does not take much for a molecule to be able to hydrolyse the ring. However, research has shown that  $\beta$ -lactams are not particularly reactive, showing similar reactivity to normal amides (Page, Laws, Slater & Stone, 1995) (Page, 1999). It is therefore perhaps testament to the evolutionary finesse of SBLs that they are so able to efficiently catalyse the hydrolysis of  $\beta$ -lactam rings. SBLs perform a nucleophilic attack on the carbonyl carbon in order to break open the ring. Typically, a hydroxyl group on a serine residue performs a nucleophilic attack on the carbonyl of the  $\beta$ -lactam ring. The protonation of the  $\beta$ -lactam nitrogen leads to cleavage of the C-N bond and the formation of the covalent acyl enzyme intermediate. This complex is then hydrolysed by water, leading to deacylation of the enzyme from the  $\beta$ -lactam ring, regenerating free enzyme and resulting in a hydrolysed antibiotic. The ability of the SBL enzyme to hydrolyse the acyl-enzyme complex resulting in liberated enzyme and hydrolysed  $\beta$ -lactam antibiotic is what sets them apart from the PBP; the PBPs are unable to efficiently hydrolyse the acyl-enzyme intermediate formed when a  $\beta$ -lactam antibiotic inhibits the PBP, resulting in the  $\beta$ -lactam antibiotic being able to exhibit its antibiotic activity (Hata et al.,

2006). In the case of SBLs, the efficient hydrolysis of this acyl-enzyme intermediate is what allows the SBL to break down the  $\beta$ -lactam ring before it can reach its intended target of the PBP. The fact that Gram-negative pathogens tend to constitutively produce  $\beta$ -lactamases in the periplasmic space of the bacterial cell wall, means that in many cases the  $\beta$ -lactam cannot even reach its intended target of the inner membrane bound PBP before being hydrolysed in the periplasmic space by  $\beta$ -lactamases, representing an extremely challenging scenario for overcoming antimicrobial resistance of this type (Georgopapadakou & Lio, 1980).

The reactions of the SBLs with  $\beta$ -lactam antibiotics, and indeed PBPs and  $\beta$ -lactam antibiotics follow a similar kinetic pathway as detailed below:



Where E is the enzyme, S the substrate, ES is the Michaelis complex, EA\* is the covalent acyl enzyme, and P is the product (Oliva, Dideberg & Field, 2003). As mentioned, the main difference between  $\beta$ -lactamases and PBPs is that the former undergo fast deacylation after ring-opening ( $k_3 \sim 10^3 \text{ s}^{-1}$ ) whereas the latter are inhibited by the antibiotic ( $k_3 \sim 10^{-5} \text{ s}^{-1}$ ) (Oliva, Dideberg & Field, 2003).

Whilst all of the SBLs utilise an active site serine to carry out the nucleophilic attack on the carbonyl carbon, depending upon the class of SBL, different acid/base catalytic residues are used to facilitate hydrolysis of the antibiotic (Hata et al., 2006). Whilst all of the SBLs utilise Ser70 as the active site serine to carry out the nucleophilic attack on the carbonyl carbon, In the case of class A SBLs, a glutamate residue at position 166 (Glu166) is employed as a general base to assist in the deprotonation of the active site serine Ser70, for formation of the acyl enzyme intermediate and also for the hydrolysis of it (Hermann, Ridder, Mulholland

& Holtje, 2003). The mechanism of the first step used by class A SBLs is shown in figure 1.11 below.

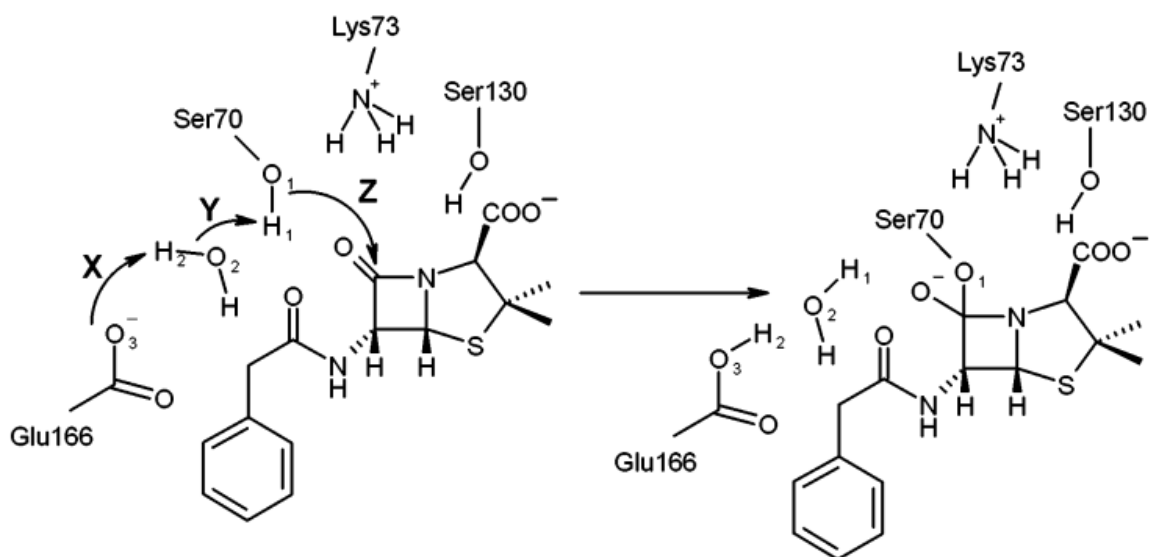
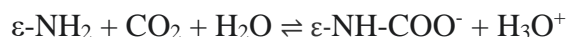


Figure 1.11: Catalytic Mechanism of Class A SBLs showing formation of the tetrahedral intermediate (Hermann et al., 2003).

In the case of class C SBLs, there is no single key amino acid to serve as the general acid/base, but rather an active site hydrogen bonding network that serves as the key to catalysis, unlike class A SBLs where Glu166 is utilised to assist in the deprotonation of the Ser70 residue (Madgwick & Waley, 1987). Asn152, Lys67 and Tyr150 form a hydrogen bonding network between them which is key for the hydrolysis mechanism of class C enzymes (Goldberg, Iannuccilli, Nguyen, Ju & Cornish, 2003). These residues are accompanied with Gln120 and Lys315 and these residues are also considered necessary for catalysis, but are less important than the other residues mentioned previously. The identity of the residue that serves as the general base for the catalysis mechanism is unknown, but can be narrowed down to either Lys67 or Tyr150 (Goldberg et al., 2003).

The class D SBLs rely on a post-translationally modified carboxylated lysine at Lys70 to serve as the general base residue for the enzyme acylation and deacylation steps in their hydrolysis of  $\beta$ -lactams (Golemi, Maveyraud, Vakulenko, Samama & Mobashery, 2001). Lysine reacts with  $\text{CO}_2$  to produce the lysine carbamylate residue that is needed to serve as the general acid/base in the hydrolytic mechanism of class D SBLs (Golemi et al., 2001). The carboxylated lysine is stabilised by an interaction between itself and the indole group of Trp154. Catalytic activity is greatly reduced when Trp154 is replaced with a different amino acid such as Gly, Ala or Phe (Baurin et al., 2009). It is thought that the Lys is carboxylated by reaction of the amino group with  $\text{CO}_2$ , as in the following reaction:



(Maveyraud et al., 2000).

The carbamylated lysine serves as the general base to deprotonate the nucleophilic serine in the first step of the  $\beta$ -lactam hydrolysis and serves as a base once again to abstract a proton of water during the turnover of the acyl-enzyme intermediate (Golemi et al., 2001).

## 1.6: SBL Inhibitors

Due to the rich history of novel antibiotic development in the ‘golden era’ of antibiotic discovery, resistance to antibiotics was seen as more of a minor inconvenience rather than the pandemic health crisis it is today. If resistance arose, it was simply overcome by the development of novel analogues and newer generations of existing cephalosporins and penicillins (Gaude & Hattiholli, 2013).

As mentioned, the predominant method of antibiotic resistance amongst microbes is via the production of  $\beta$ -lactamase enzymes. Owing to the dearth of development of novel antibiotics, pharmaceutical companies have explored the avenue of  $\beta$ -lactamase inhibition, with the aim of restoring the efficacy of  $\beta$ -lactam antibiotics (Drawz & Bonomo, 2010). Inhibitors themselves do not usually possess any antibiotic activity; therefore, they are usually paired with a  $\beta$ -lactam antibiotic, with the aim of preserving the  $\beta$ -lactam core of the antibiotic by inhibiting  $\beta$ -lactamase enzymes produced by the pathogen (King, Sobhanifar & Strynadka, 2016). There are generally 4 widely used examples of  $\beta$ -lactam/ $\beta$ -lactamase inhibitor combinations (BLICs): amoxicillin/clavulanate, ticarcillin/clavulanate, ampicillin/sulbactam, and piperacillin/tazobactam (Toussaint & Gallagher, 2015). BLIC combinations aid in restoring activity to previously susceptible antibiotics. These combinations work well against class A  $\beta$ -lactamases, but are less effective against class C and D enzymes (Toussaint & Gallagher, 2015).

The first SBL introduced into the clinic was clavulanic acid, named after the strain of *Streptomyces clavuligerus* it was isolated from towards the end of the 1970s (Reading & Cole, 1977). Clavulanic acid's structure is similar to that of penicillin, in that it contains a  $\beta$ -lactam ring fused to a 5-membered heterocycle, but contains an oxygen atom compared to penicillin's sulfur (Fulston, Davison, Elson, Nicholson, Tyler & Woroniecki, 2001). Clavulanic acid is approved for use with two  $\beta$ -lactam antibiotics, co-administered with the semi synthetic penicillin antibiotic ticarcillin as timentin (Labia, Morand & Péduzzi, 1986), and with amoxicillin as augmentin (Ball, Mehtar & Watson, 1982) and has restored the efficacious nature of penicillins against infections caused by problematic SBL producing bacteria such as *Acinetobacter baumannii* (Brauers, Frank, Kresken, Rodloff & Seifert, 2005), *Escherichia coli* (Harris et al., 2015) and *Pseudomonas aeruginosa* (Strateva & Yordanov, 2009).

Following the introduction of clavulanic acid in the early 1980s, two synthetic SBL inhibitors were introduced; the penicillinate sulfone sulbactam (Wright & Wise, 1983) and tazobactam (Gutmann, Kitzis, Yamabe & Acar, 1986). Tazobactam is approved for use with the  $\beta$ -lactam antibiotic piperacillin and has been shown to inhibit SBLs caused by infections from *Staphylococci*, *Streptococci*, *Escherichia* and *Klebsiella* families of bacteria (Daniel & Krop, 1996), whilst sulbactam is approved for use with the  $\beta$ -lactam antibiotic ampicillin and is useful in the treatment of intra-abdominal infections associated with SBL producing Gram-negative bacteria such as *Escherichia coli* and *Klebsiella* (Benson & Nahata, 1988). Whilst these  $\beta$ -lactamase inhibitors have little antibacterial activity themselves, the mechanism of their inhibition of SBLs is very similar to the mechanism of inhibition of PBPs by  $\beta$ -lactam antibiotics. The inhibitors react with the active site serine nucleophile forming an acyl-enzyme complex that is subject to low turnover rates, resulting in inhibition of the enzyme (Brown, Aplin & Schofield, 1996), (Thierren & Levesque, 2006).

BLICs have undoubtedly restored efficacy to previously susceptible  $\beta$ -lactam antibiotics leading to improved outcomes in patients suffering infections from SBL producing bacteria, but the previously mentioned inhibitors have no antibiotic capability by themselves, and are only effective against class A SBLs and are typically poor inhibitors of class C and D SBLs. Renewed interest in antibacterials and novel inhibitors of SBL has led to the recent introduction and development of a novel class of  $\beta$ -lactamase inhibitors, the non- $\beta$ -lactam inhibitors such as avibactam (Ehmann et al., 2012), relebactam (Blizzard et al., 2014), nacubactam (Monogue, Giovagnoli, Bissantz, Zampaloni & Nicolau, 2018), zidebactam (Moya et al., 2017) and the cyclic boronic vaborbactam (Lomovskaya et al., 2017). Avibactam is approved for use with the cephalosporin antibiotic ceftazidime, targeting complicated intra-abdominal infections caused by Gram-negative pathogens (Temkin et al., 2017). Relebactam is in clinical trials for use alongside imipenem/cilastin for infections

caused by Gram-negative bacteria (Lob et al., 2017). Nacubactam is in clinical trials in conjunction with meropenem to help combat urinary tract infections caused by SBL producing Gram-negative pathogens (Livermore, 2018). Zidebactam is currently in clinical trials to be used in conjunction with the cephalosporin antibiotic cefepime, targeting infections caused by Gram-negative bacteria (Sader, Castanheira, Huband, Jones & Flamm, 2017). Finally, vaborbactam is approved for use alongside meropenem, marketed as vabormere and is useful to combat infections caused by carbapenemase producing *Klebsiella pneumoniae* (Patel, Pogue, Millis & Kaye, 2018). Figure 1.12 shows an overview of the clinically relevant SBL inhibitors.

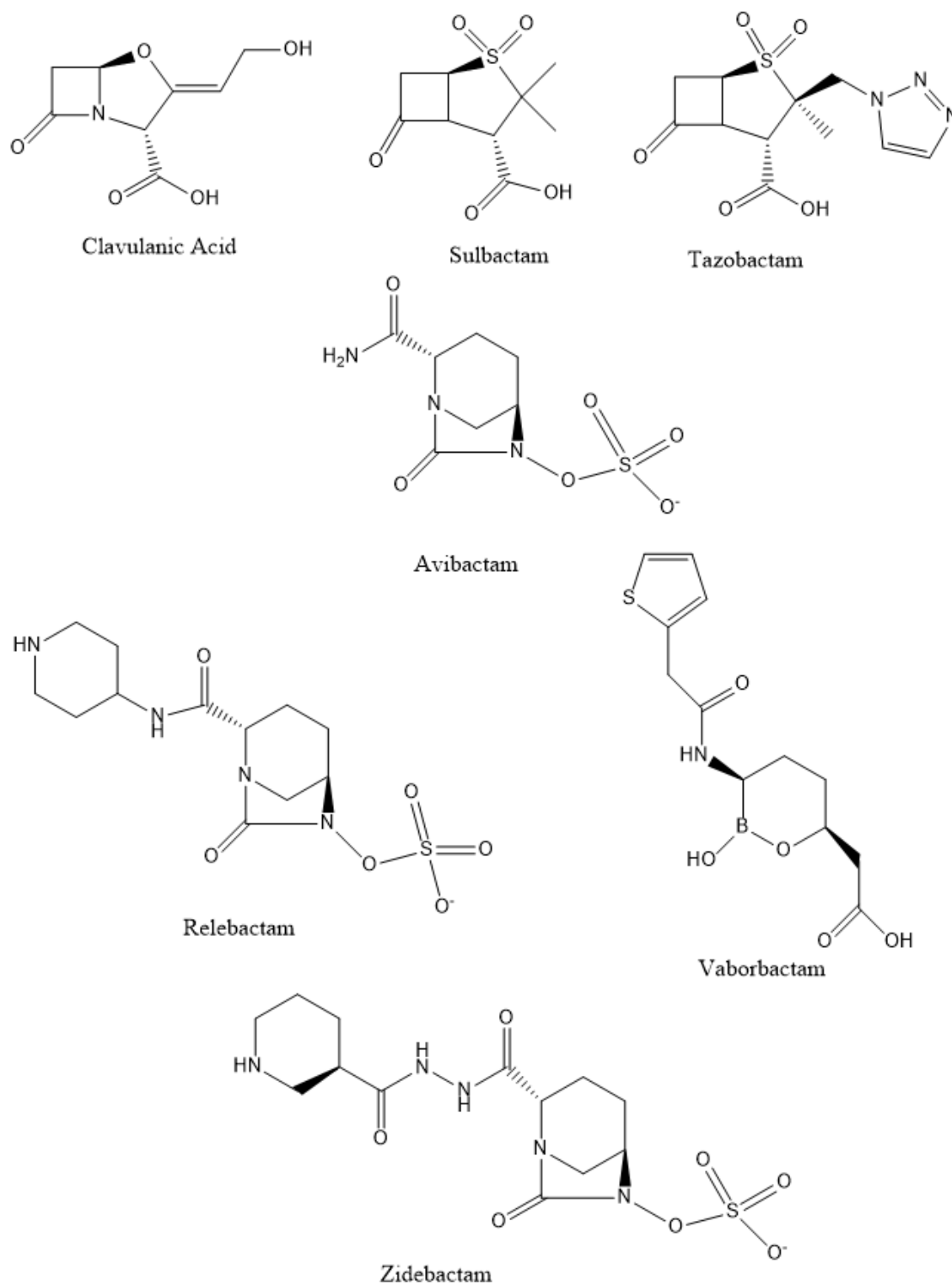


Figure 1.12: Clinically Useful SBL inhibitors. Note how avibactam, relebactam and zidebactam are diazabicyclooctanes whilst vaborbactam is a cyclic boronic compound, representing the novel non- $\beta$ -lactam  $\beta$ -lactamase inhibitors.

Typically,  $\beta$ -lactamase inhibitors can be generally classified in two different ways: the mechanism of their inhibition, or by their structure. Inhibition can be “suicide” inhibition, or reversible inhibition as in the case of avibactam. Suicide inhibition involves inhibitors which permanently inactivate the  $\beta$ -lactamase enzyme via chemical reactions in the enzyme’s active site, resulting in a permanent change in the structure of the active site, resulting in enzyme inhibition (Drawz & Bonomo, 2010). Tazobactam, sulbactam and clavulanic acid are examples of suicide inhibitors. In terms of structure,  $\beta$ -lactamase inhibitors can be classified as being  $\beta$ -lactam, non- $\beta$ -lactam, or diazabicyclooctane. An example of the mechanism of clavulanic acid inhibiting an SBL can be seen in figure 1.13 below.

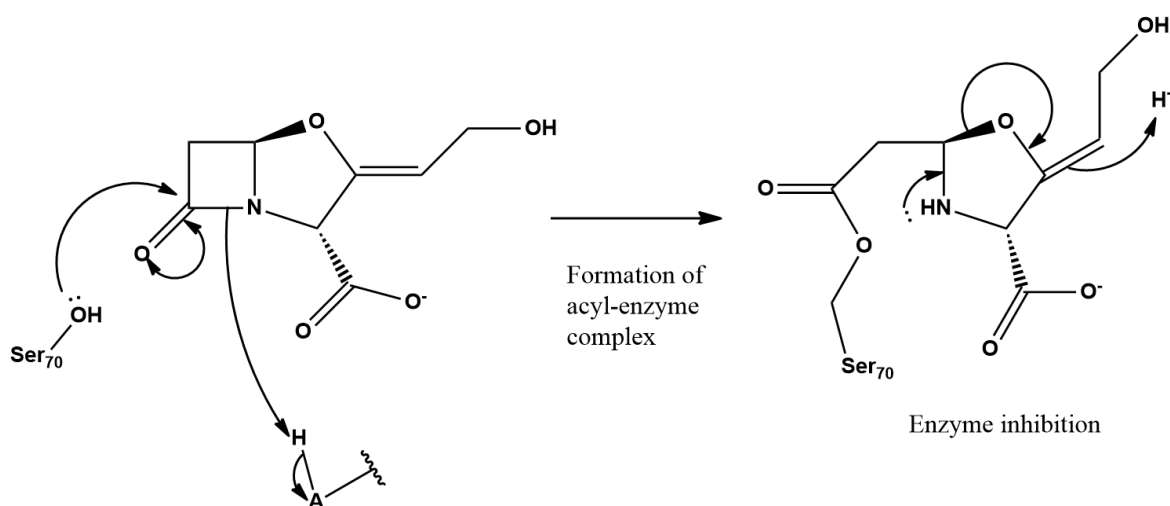


Figure 1.13: Mechanism of inhibition of clavulanic acid and an SBL.

### 1.6.1: Avibactam

Avibactam is a non  $\beta$ -lactam  $\beta$ -lactamase inhibitor developed by Actavis and AstraZeneca (Wang, Abboud, Markoulides, Brem, & Schofield, 2016). It is a good inhibitor of class A  $\beta$ -lactamase enzymes, with less inhibition exhibited against class C and D  $\beta$ -lactamases.

Avibactam is the first non- $\beta$ -lactam  $\beta$ -lactamase inhibitor developed for clinical use (Wang et al., 2016). In terms of its chemical nature, avibactam is a diazabicyclooctane, which is capable of reversibly inhibiting target  $\beta$ -lactamases via covalent bonding. Although not a  $\beta$ -lactam, the structure of avibactam strongly resembles that of a  $\beta$ -lactam.

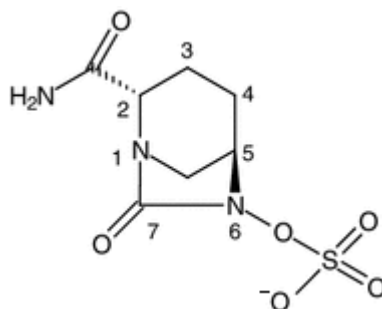


Figure 1.14: Chemical structure of avibactam (Zhanel et al., 2013).

The carbonyl at position 7 in figure 1.14 above mimics those found in  $\beta$ -lactam antibiotics such as penicillins and cephalosporins and the anionic sulfamate on the nitrogen at position 6 mimics the carboxylate anion found in other  $\beta$ -lactams (Zhanel et al., 2013). This allows avibactam, to have 2 anchor points to inhibit  $\beta$ -lactamase enzymes. Hydrogen bonding occurs to the O on the carbonyl at position 7 between avibactam and the amino acids round the active site of the enzyme, where-as the negatively charged sulfamate group is attracted to the positive charge of lysine amino acids. An example of the reversible inhibition of a SBL by avibactam can be seen in figure 1.15 below.

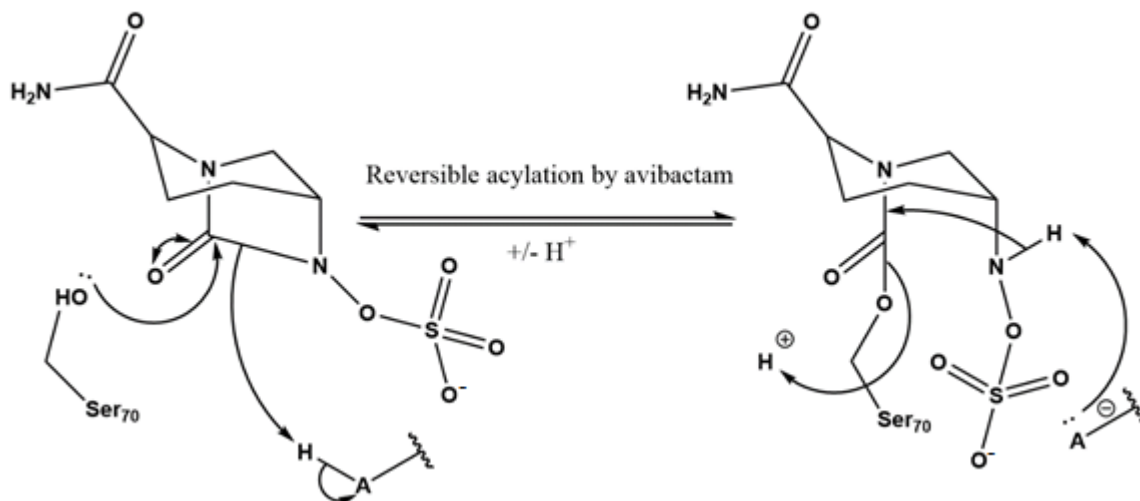


Figure 1.15: Reversible inhibition of SBL by avibactam

The introduction of avibactam in the clinic has led to the development of similar non- $\beta$ -lactam  $\beta$ -lactamase inhibitors, including relebactam (Merck) and nacubactam (Fedora Pharmaceuticals/Roche). Both are structurally similar analogues to avibactam, with different groups being added to the amide at position 2 in figure 1.15 above. The structures of relebactam and nacubactam are shown below in figure 1.16.

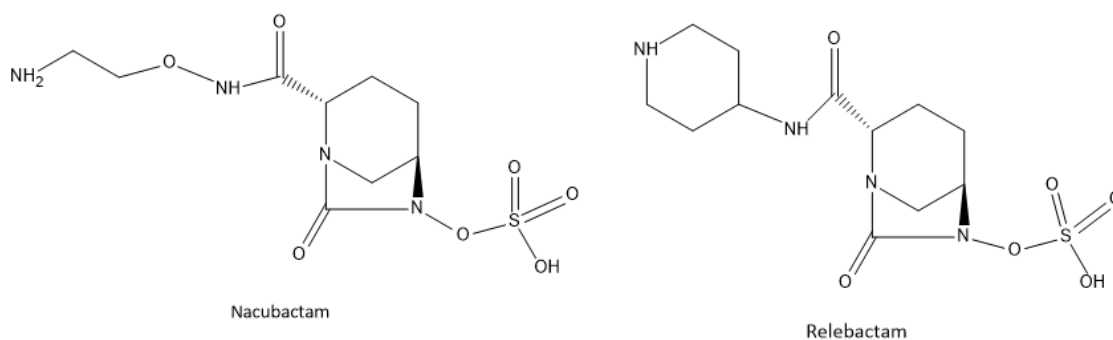


Figure 1.16: Chemical structures of nacubactam and relebactam

Nacubactam is currently nearing the end of phase 1 clinical trials (Roche, 2016), with the intention of it being partnered with  $\beta$ -lactam antibiotics (much like avibactam) to assist in restoring efficacy to  $\beta$ -lactam antibiotics. Relebactam has entered phase 3 clinical trials, with

the intention of it being partnered with imipenem to treat patients with complicated urinary tract infections (Merck, 2016). Initial studies against gram-negative pathogens show promise, with activity against troublesome pathogens including multidrug resistant *Pseudomonas aeruginosa* (Lapuebla et al., 2015).

### 1.7: Search for Novel Antibiotics

The majority of antibiotics first introduced in the clinic over 40 years ago had microbial origins. These drugs were found and developed by screening samples for antimicrobial activity against common pathogens, in what is known as the Waksman Platform of discovery (Lewis, 2013). Soil provided a rich source of antimicrobial compounds, with more than 70 % of commercially important antibiotics being derived from the secondary metabolites of the *Streptomyces* genus of bacteria (Kitani et al., 2011), which are ubiquitous in soil (Seipke, Kaltenpoth, & Hutchings, 2012). However, as described earlier, this once rich source of novel compounds yielded diminishing results, and this approach has now been largely abandoned. The problem of antibiotic resistance is compounded by the fact there is a desperate lack of novel antibiotics in clinical development. Almost all antibiotics in clinical use were first developed in the golden era of antibiotic discovery, during the 1940s to 1960s (Lewis, 2013), with resistance more often than not appearing shortly after their introduction in the clinic (Ventola, 2015). There is a steady, but slow continued stream of antibiotic compounds in development, and many are derivatives of old compounds that were initially thought to be unsuccessful but have gained renewed interest largely due to the desperate need for novel antibiotics (Lewis, 2013). Some “new” antibiotics in development are simply old derivatives combined with novel  $\beta$ -lactamase inhibitors, such as ceftolozane, a combination of a cephalosporin and tazobactam (Draenert, Seybold, Grütznert, & Bogner,

2015) and Ceftazidime-avibactam, a combination of a cephalosporin and avibactam, a novel  $\beta$ -lactamase inhibitor with inhibitory action against class D  $\beta$ -lactamases (Theuretzbacher, 2015). As discussed, synthetic approaches to antibiotics have largely been unsuccessful, despite the massive effort pharmaceutical companies invested into discovering novel synthetic compounds (Lewis, 2013). One of the main problems with synthetic antibiotics is ensuring their uptake into the cell, a process that is made more difficult in Gram-negative bacteria. This approach has now largely been abandoned due to the minimal return in investment. The most successful discovery platform to date for novel antibiotics has clearly been the screening of natural products. One pitfall of this discovery platform is that around 99 % of bacteria present in the environment do not grow *in vitro*. This means there's potentially a huge source of interesting, novel antimicrobial compounds waiting to be discovered in this un-explored resource (Ling, Schneider, Peoples, Spoering, Engels, Conlon, Mueller, Schaberle, et al., 2015). One of the greatest conundrums that is pondered by modern microbiologists is the sheer lack of colonies that are able to be cultivated *in vitro* compared with the amount of organisms observed directly from environmental samples. Whether observing through a light microscope, or metagenomic analysis direct from samples, it is clear that the amount and diversity of microbes that are present in the sample but do not grow *in vitro* is staggering.

As mentioned, around 99 % of bacteria present in the environment are not grown under standard laboratory conditions, including the classic incubation technique of growing microbes on agar plates. Agar plates consist of a medium, containing salts and nutritional substituents that give microbes everything that they are needed to grow. These can be strain specific, such as MacConkey agar for Gram-negative organisms (Mossel, Mengerink & Scholts, 1962) or malt extract agar for selective fungi growth (Skaar & Stenwig, 1996). It is ironic in a way, that scientists seemingly give microbes everything they need to grow, from

nutrients, pH adjustments, temperature and atmospheric conditions tailored to specific microbes, but still microbes are simply unable to be grown in laboratory conditions. We are seemingly unable to replicate the infinitely intricate and sensitive environments in which these microbes prosper.

One recent study used a novel method of growing previously uncultivable bacteria by use of an ‘‘iChip’’ (Ling et al., 2015), a multi wellled plastic device which allows the growth of bacteria *in situ*. After incubation in the environment, the iChip and its contents are transported to the laboratory and disassembled for further analyses. The use of the iChip raised the *in vitro* growth rate of microbes in soil from 1 % up to 50 %. This novel method of growing previously un-grown microbes could lead to the discovery of a wealth of novel metabolites, and potentially novel antibiotics. Ling’s team has discovered one such antibiotic, teixobactin, which is currently in clinical trials. Teixobactin belongs to a new class of antibiotics, presenting a novel method of inhibiting microbial growth, by binding to lipid pre-cursor molecules needed in cell wall formation (Ling et al., 2015). It is likely that there is potentially a plethora of novel and useful antibiotic producing organisms present in the environment which scientists are unable to cultivate in the laboratory. Novel approaches to growing previously un-cultivable bacteria appear to be a pathway to revitalising the Waksman platform approach to discovering novel antimicrobials. The iChip essentially aims not to replicate the environment in which the microbes grow, but utilise the actual environment itself to allow microbes to grow in their unadulterated natural environment (Kaeberlein, Lewis & Epstein, 2002). From this work, the group were able to grow previously uncultivated bacteria *in vitro*.

In a similar vein of research, the work of Rappé, Connon, Vergin & Giovannoni (2002), involved collecting samples of sea water and taking them back to the laboratory, from which the bacteria were isolated, rather than attempting to replicate the environment in the media

used in a petri dish. From this work, they were able to cultivate and characterise the previously uncultivated SAR11 carbon-oxidising bacteria. SAR11 bacteria represent some of the most ubiquitous bacteria present in sea-water, but had long avoided *in vitro* cultivation.

Aside from novel incubation techniques taking place *in-situ*, metagenomics has been identified as a potential solution to probing the unknowns of unculturable bacteria. Metagenomics is described as the culture-independent analysis of microbial genomes (Scholes & Handelsman, 2005). Metagenomics unravels the secrets of unculturable microbes by extracting the DNA straight from the environmental sample, rather than relying on incubation first. Whilst the metagenomic approach can provide clues to the yet to be cultivated microbes lurking in the environment, even the largest metagenomic studies are only capable of identifying fractions of genes; discovering novel antimicrobials from sequence data is essentially impossible. It is much more feasible to identify novel methods to cultivate previously unculturable microbes. As discussed, novel cultivation methods have resulted in identification of novel bacteria and so far, have represented the most feasible way of cultivating previously un-culturable bacteria *in vitro*.

## 1.8: Summary

Antibiotics are rightly held in high esteem, and their discovery and introduction to the clinic is regarded as one of human kind's finest accomplishments in modern medical sciences (Aminov, 2010). However, the action of pathogenic bacteria becoming resistant to the once lethal actions of antibiotics by the mechanisms previously discussed and the spread of said mechanisms of antibacterial resistance is a pandemic health crisis and is recognised by the

World Health Organisation (WHO) as being one of the greatest clinical threats to human health (World Health Organisation, 2018). By a considerable margin, the key driver of antibiotic resistance is the evolution and spread of  $\beta$ -lactamase enzymes, which confer resistance to bacteria by producing enzymes which are capable of hydrolysing the  $\beta$ -lactam ring present in  $\beta$ -lactam antibiotics. Despite their age and the rise of resistant bacteria,  $\beta$ -lactam antibiotics are still the most prescribed class of antibiotics, representing around 70 % of all prescribed antibiotics worldwide annually (Versporten, Bielicki, Drapier, Sharland & Goossens, 2016). Whilst science cannot possibly hope to have an ever-lasting victory over bacteria in battle of antibiotic resistance, it has clearly been shown that development of novel  $\beta$ -lactamase inhibitors can provide renewed action to once susceptible antibiotics, including action against carbapenemase producing *Enterobacteriaceae*. Therefore, the development of novel  $\beta$ -lactamase inhibitors, particularly compounds capable of inhibiting class C and D SBLs are of great clinical interest and significance.

Antibiotics are expensive to develop, time consuming to research and introduce into the clinic, and do not offer a huge return of investment for pharmaceutical companies. They are inexpensive to patients, clinicians are being encouraged to reduce the number of prescriptions for antibiotics, and resistance will inevitably rise to the drug leading to their inefficacy and eventual decline. Therefore, large pharmaceutical companies have been pulling out of the field of antibiotic development altogether (Lewis, 2013). This presents a bleak scenario in the battle against antibiotic resistance; development of new compounds is essential in order to turn the tide in our favour. Clearly, novel antibiotics are needed desperately.

Antibiotics from natural sources vastly outnumber completely synthetic antibiotics in the clinic. Natural sources have provided us with the vast majority of the antibiotics used in the clinic, and science has simply been unable to replicate the success of these products via

synthetic drugs. Therefore, antibiotics from natural sources represent our best discovery platform for antibiotics. Microbes have had eons to evolve and develop lethal killing mechanisms aimed towards their microbial neighbours in the never ending competition for resources. However, more than 98 % of microbes present in the environment cannot be cultured in the laboratory. Metabolites from bacteria or their derivatives account for a staggering 50 % of all commercially available pharmaceuticals (Demain & Sanchez, 2009). Novel incubation methods are needed to attempt to increase the *in vitro* growth rate. Even managing to increase the percentage of culturable organisms from 2 % to 10 % would represent a huge achievement, and a massive potential for the discovery of novel metabolites, potentially including bacteria. These unculturable bacteria could potentially represent a vast treasure trove of interesting discoveries, potentially giving humanity an untapped supply of novel antibiotics, able to combat antimicrobial resistance.

### 1.9: Project and Research Aims

The project will begin by attempting to isolate an antibiotic from a soil environment. Once an antibiotic producing microbe has been isolated, a method will be developed to identify the bacteria's metabolites. Samples will be analysed via liquid chromatography mass spectrometry (LC-MS), specifically, by use of a quadrupole time of flight (Q-TOF) instrument. A Q-TOF is favourable over other instruments owing to being more suited to screen for a wide variety of substances when attempting to locate an unknown sample, and also because it can report results to its accurate mass. Use of an iChip will also be investigated in an attempt to discover and isolate a novel antibiotic. Furthermore, analogues of avibactam, a novel non- $\beta$ -lactam  $\beta$ -lactamase inhibitor will be synthesised and tested for their inhibitory effects against SBL enzymes from classes A, C and D. The pH dependence

of these enzymes will also be investigated, as this will provide useful information regarding their kinetic properties. Finally, potential novel  $\beta$ -lactamase inhibitors will be investigated and screened for inhibitory effects.

### 1.10: Chapter One References

Abraham, E.P. & Chain, E. (1940). An enzyme from Bacteria able to Destroy Penicillin. *Nature*, 146 (1), 837-837. doi: 10.1038/146837a0.

Al-Obeid, S., Gutmann, L., & Williamson, R. (1990). Modification of penicillin-binding proteins of penicillin-resistant mutants of different species of enterococci. *Journal of Antimicrobial Chemotherapy*, 26 (1), 613-618. Retrieved from [https://watermark.silverchair.com/26-5-613.pdf?token=AQECAHi208BE49Ooan9kkhW\\_Ercy7Dm3ZL\\_9Cf3qfKAc485ysgAAAcgwgGHEBkgkqhkiG9w0BBwaggG1MIIBsQIBADCCAaoGCSqGSIb3DQEHATAeBgIghkgBZQMEAS4wEQQMkoZt0Yz7RWvqHm1JAgeQgIIBeyKJesjrwLDQSCXGRg7b\\_S5GDHVazXZsdFrhEUAO0ICR5bb4AcwwalieygpKKKZgbEVnBUXOa5AsAUngREmq-aVYb94jumU8hbP0KcC3wOYeYgrbYjQdjYa2r9W6Q-ix7GQ\\_mU4lhc8iZ7cCV\\_\\_nHK2HKGEHvSy7Y-Norb7DTwbXw\\_SNC3ZznTj2W1bNfDRiYqM9snLjr7aExcz7gw4gQVYr\\_PE0lqu9uCpYsnuMb8e0dsQEhb4E7uQLrSjnZqwy7xYsoNjngE8AI\\_mJe-9nIdKu4q2pDyGF6fuqNvICiElvZUGTaednpNug6ZP6LGBBf0XwltVf3Qn-4IJFV11789kJfuVPpkLaUEcIEhmWP6djJXmFvBLXjDpJqhiw5Ty\\_5zAsGbU3GIQNwyBP5OIN0w7b\\_sUhwYfgUPkVdkaa6RhJxaPS4l8AsKrR6lTiRXXx2iuF4HKlnBzpjXzhtrd5x0gKugeI68LCnFn-DwVpxdRd9tyYWAzOdFAf2c\\_w](https://watermark.silverchair.com/26-5-613.pdf?token=AQECAHi208BE49Ooan9kkhW_Ercy7Dm3ZL_9Cf3qfKAc485ysgAAAcgwgGHEBkgkqhkiG9w0BBwaggG1MIIBsQIBADCCAaoGCSqGSIb3DQEHATAeBgIghkgBZQMEAS4wEQQMkoZt0Yz7RWvqHm1JAgeQgIIBeyKJesjrwLDQSCXGRg7b_S5GDHVazXZsdFrhEUAO0ICR5bb4AcwwalieygpKKKZgbEVnBUXOa5AsAUngREmq-aVYb94jumU8hbP0KcC3wOYeYgrbYjQdjYa2r9W6Q-ix7GQ_mU4lhc8iZ7cCV__nHK2HKGEHvSy7Y-Norb7DTwbXw_SNC3ZznTj2W1bNfDRiYqM9snLjr7aExcz7gw4gQVYr_PE0lqu9uCpYsnuMb8e0dsQEhb4E7uQLrSjnZqwy7xYsoNjngE8AI_mJe-9nIdKu4q2pDyGF6fuqNvICiElvZUGTaednpNug6ZP6LGBBf0XwltVf3Qn-4IJFV11789kJfuVPpkLaUEcIEhmWP6djJXmFvBLXjDpJqhiw5Ty_5zAsGbU3GIQNwyBP5OIN0w7b_sUhwYfgUPkVdkaa6RhJxaPS4l8AsKrR6lTiRXXx2iuF4HKlnBzpjXzhtrd5x0gKugeI68LCnFn-DwVpxdRd9tyYWAzOdFAf2c_w)

613.pdf?token=AQECAHi208BE49Ooan9kkhW\_Ercy7Dm3ZL\_9Cf3qfKAc485ysgAAAcgwgGHEBkgkqhkiG9w0BBwaggG1MIIBsQIBADCCAaoGCSqGSIb3DQEHATAeBgIghkgBZQMEAS4wEQQMkoZt0Yz7RWvqHm1JAgeQgIIBeyKJesjrwLDQSCXGRg7b\_S5GDHVazXZsdFrhEUAO0ICR5bb4AcwwalieygpKKKZgbEVnBUXOa5AsAUngREmq-aVYb94jumU8hbP0KcC3wOYeYgrbYjQdjYa2r9W6Q-ix7GQ\_mU4lhc8iZ7cCV\_\_nHK2HKGEHvSy7Y-Norb7DTwbXw\_SNC3ZznTj2W1bNfDRiYqM9snLjr7aExcz7gw4gQVYr\_PE0lqu9uCpYsnuMb8e0dsQEhb4E7uQLrSjnZqwy7xYsoNjngE8AI\_mJe-9nIdKu4q2pDyGF6fuqNvICiElvZUGTaednpNug6ZP6LGBBf0XwltVf3Qn-4IJFV11789kJfuVPpkLaUEcIEhmWP6djJXmFvBLXjDpJqhiw5Ty\_5zAsGbU3GIQNwyBP5OIN0w7b\_sUhwYfgUPkVdkaa6RhJxaPS4l8AsKrR6lTiRXXx2iuF4HKlnBzpjXzhtrd5x0gKugeI68LCnFn-DwVpxdRd9tyYWAzOdFAf2c\_w.

Ambler, R.P. (1980). The structure of  $\beta$ -lactamases. *Philosophical Transactions of the Royal Society of Biological Sciences*, 286 (1036), 321-331. doi: DOI: 10.1098/rstb.1980.0049.

Aminov, R.I. (2010). A Brief History of the Antibiotic Era: Lessons Learned and Challenges for the Future. *Frontiers in Microbiology*, 1 (134), 1-7. doi: 10.3389/fmicb.2010.00134.

Antunes, N.T. & Fisher, J.F. (2014). Acquired Class D  $\beta$ -Lactamases. *Antibiotics*, 3 (3), 398-434. doi: 10.3390/antibiotics3030398.

Antunes, N.T., Lamoureaux, T.L., Toth, M., Stewart, N.K., Frase, H., & Vakulenko, S.B. (2014). Class D  $\beta$ -Lactamases: Are They All Carbapenemases? *Antimicrobial Agents and Chemotherapy*, 58 (4), 2119-2125. doi: 10.1128/AAC.02522-13.

Badarau, A., Llinás, A., Laws, A. P., Damblon, C., & Page, M. I. (2005). Inhibitors of Metallo- $\beta$ -lactamase Generated from  $\beta$ -Lactam Antibiotics. *Biochemistry*, 44(24), 8578-8589. doi:10.1021/bi050302j.

Balcazar, J. L. (2014). Bacteriophages as Vehicles for Antibiotic Resistance Genes in the Environment. *PLoS Pathogens*, 10(7), e1004219. doi:10.1371/journal.ppat.1004219.

Ball, A.P., Mehtar, S., & Watson, A. (1982). Clinical efficacy and tolerance of Augmentin in soft tissue infection. *Journal of Antimicrobial Chemotherapy*, 1 (1), 67-74. doi: 10.1093/jac/17.suppl\_C.17.

Bartlett, J. G., Gilbert, D. N., & Spellberg, B. (2013). Seven Ways to Preserve the Miracle of Antibiotics. *Clinical Infectious Diseases*, 56(10), 1445-1450. doi:10.1093/cid/cit070.

Baughman, R.P. (2009). The use of Carbapenems in the Treatment of Serious Infections. *Journal of Intensive Medical Care*, 24 (4), 230-241. Retrieved from <http://journals.sagepub.com/doi/pdf/10.1177/0885066609335660>.

Baurin, S., Vercheval, L., Bouillenne, F., Falzone, C., Brans, A., Jacquamet, L. ... Kerff, F. (2009). Critical Role of Tryptophan 154 for the Activity and Stability of Class D  $\beta$ -Lactamases. *Biochemistry*, 48 (47), 11252-11263. doi: 10.1021/bi901548c.

Bebrone, C. (2007). Metallo- $\beta$ -lactamases (classification, activity, genetic organization, structure, zinc coordination) and their superfamily. *Biochemical Pharmacology*, 74 (12), 1686-1701. doi: 10.1016/j.bcp.2007.05.021.

Bedenic, B. & Zagar, Z. (1995). Clinical and laboratory significance of inducible beta-lactamases. *Lijec Vjesn*, 117 (9), 249-253. Retrieved from <https://www.ncbi.nlm.nih.gov/pubmed/8643019>.

Bennett, P. M. (2008). Plasmid encoded antibiotic resistance: acquisition and transfer of antibiotic resistance genes in bacteria. *British Journal of Pharmacology*, 153(Suppl 1), S347-S357. doi:10.1038/sj.bjp.0707607.

Benson, J.M. & Nahata, M.C. (1988). Sulbactam/ampicillin, a new beta-lactamase inhibitor/beta-lactam antibiotic combination. *Drug Intelligence & Clinical Pharmacy*, 7 (8), 534-541. Retrieved from <https://www.ncbi.nlm.nih.gov/pubmed/3046887>.

Bentley, R. (2009). Different roads to discovery; Prontosil (hence sulfa drugs) and penicillin (hence  $\beta$ -lactams). *Journal of Industrial Microbiology & Biotechnology*, 36 (6), 775-786. Retrieved from <https://link.springer.com/article/10.1007%2Fs10295-009-0553-8>.

Berdy, J. (2012). Thoughts and facts about antibiotics: Where we are now and where we are heading. *The Journal of Antibiotics*, 65 (1), 385-395. doi: 10.1038/ja.2012.27.

Blazquez, J., Baquero, J., Canton, R., Alos, I., & Baquero, F. (1993). Characterization of a new TEM-type  $\beta$ -lactamase resistant to clavulanate, sulbactam and tazobactam in a clinical

isolate of *Escherichia coli*. *Antimicrobial Agents and Chemotherapy*, 37 (1), 2059-2063. doi: 10.1128/CMR.00019-15.

Blizzard, T.A., Chen, H., Kim, S., Wu, J., Bodner, R., Gude, C. ... Hammond, M.L. (2014). Discovery of MK-7655, a  $\beta$ -lactamase inhibitor for combination with Primaxin. *Bioorganic & Medicinal Chemistry Letters*, 24 (3), 750-785. doi: 10.1016/j.bmcl.2013.12.101.

Bodey, G.P. (1990). Penicillins, Monobactams and Carbapenems. Texas Heart Institute, 17 (4), 315-329. Retrieved from <https://www.ncbi.nlm.nih.gov/pmc/articles/PMC324942/>.

Bottone, E.J. (2010). *Bacillus cereus*, a Volatile Human Pathogen. *Clinical Microbiology Reviews*, 23 (2), 382-398. doi: 10.1128/CMR.00073-09.

Bozdogan, B. & Appelbaum, P.C. (2004). Oxazolidinones: activity, mode of action, and mechanism of resistance. *International Journal of Antimicrobial Agents*, 23 (1), 113-119. doi: 10.1016/j.ijantimicag.2003.11.003.

Brauers, J., Frank, U., Kresken, M., Rodloff, A.C., & Seifert, H. (2005). Activities of various  $\beta$ -lactams and  $\beta$ -lactam/ $\beta$ -lactamase inhibitor combinations against *Acinetobacter baumannii* and *Acinetobacter* DNA group 3 strains. *Clinical Microbiology and Infection*, 11 (1), 24-30. doi: 10.1111/j.1469-0691.2004.01015.x.

Brem, J., van Berkel, S.S., Zolman, D., Lee, S.Y., Gileadi, O., McHugh, P.J. ... Schofield, C.J. (2015). Structural basis of metallo- $\beta$ -lactamase inhibition by captopril stereoisomers. *Antimicrobial Agents and Chemotherapy*, 60 (1), 142-150. doi: 10.1128/AAC.01335-15.

Brem, J., Cain, R., Cahill, S., McDonough, M.A., Clifton, I.J., Jiménez-Castellanos, J.C. ... Schofield, C.J. (2016). Structural basis of metallo- $\beta$ -lactamase, serine- $\beta$ -lactamase and penicillin-binding protein inhibition by cyclic boronates. *Nature Communications*, 7 (12406), doi: 10.1038/ncomms12406 .

Brown, R.P.A., Aplin, R.T., & Schofield, C.J. (1996). Inhibition of TEM-2  $\beta$ -Lactamase from *Escherichia coli* by Clavulanic Acid: Observation of Intermediates by Electrospray Ionization Mass Spectrometry. *Biochemistry*, 35 (38), 12421-12432. doi: 10.1021/bi961044g.

Bulychev, A. & Mobashery, S. (1999). Class C  $\beta$ -Lactamases Operate at the Diffusion Limit for Turnover of Their Preferred Cephalosporin Substrates. *Antimicrobial Agents and Chemotherapy*, 43 (7), 1743-1746. Retrieved from <https://www.ncbi.nlm.nih.gov/pmc/articles/PMC89354/#B16>.

Bush, K. (2013). The ABCD's of  $\beta$ -lactamase nomenclature. *Journal of Infection and Chemotherapy*, 19 (4), 549-559. doi: 10.1007/s10156-013-0640-7.

Bush, K., & Jacoby, G. A. (2010). Updated Functional Classification of  $\beta$ -Lactamases. *Antimicrobial Agents and Chemotherapy*, 54(3), 969-976. doi:10.1128/AAC.01009-09.

Bush, K. & Mobashery, S. (1998). How  $\beta$ -lactamases have driven pharmaceutical discovery: from mechanistic knowledge to classical circumvention. In B . P. Rosen & S. Mobashery (Eds.) *Resolving the Antibiotic Paradox: Progress in Understanding Drug Resistance and Development of New Antibiotics* (pp. 71-98). New York, NY: Plenum Press.

Butler, M.S. & Cooper, M.A. (2011). Antibiotics in the clinical pipeline in 2011. *The Journal of Antibiotics*, 64 (1), 413-425. doi: 10.1038/ja.2011.44.

Chakraborty, A.K. (2017). Mechanisms of AMR: Bacteria Won the Battle Against Antibiotics. *Insights in Biomedicine*, 2 (18), 1-6. doi: 10.21767/2572-5610.100034.

Christensen, H., Martin, M.T., & Waley, S.G. (1990). Beta-lactamases as fully efficient enzymes. Determination of all the rate constants in the acyl-enzyme mechanism. *Journal of*

Biochemistry, 266 (3), 853-861. Retrieved from <https://www.ncbi.nlm.nih.gov/pmc/articles/PMC1131217/>.

Codjoe, F.S. & Donkor, E.S. (2018). Carbapenem Resistance: A Review. *Medical Sciences*, 6 (1), 1-28. doi: 10.3390/medsci6010001.

Cohen, M.L. (2000). Changing patterns of infectious disease. *Nature*, 406 (1), 762-767. doi: 10.1038/35021206.

Cooper, G.M. & Hausman, R.E. (2004). *The Cell A Molecular Approach* (Third ed.). Washington DC, United States of America: ASM Press.

Cooper, M.A. and Shlaes, D., 2011. Fix the antibiotics pipeline. *Nature*, 472(7341), pp. 32.

Cornaglia, G., Giamarellou, H., & Rossolini, G.M. (2011). Metallo- $\beta$ -lactamases: a last frontier for  $\beta$ -lactams? *The Lancet Infectious Diseases*, 11 (5), 381-393. doi: 10.1016/S1473-3099(11)70056-1.

Daniel, K.P. & Krop, L.C. (1996). Piperacillin-Tazobactam: A new B-Lactam-B-Lactamase Inhibitor Combination. *Pharmacotherapy*, 16 (2), 149-162. Retrieved from <https://onlinelibrary.wiley.com/doi/epdf/10.1002/j.1875-9114.1996.tb02933.x>.

Darnell, J., Lodish, H., & Baltimore, D. (1986). *Molecular Cell biology*. New York, United States of America: Scientific American Books.

Davies, J. (2006). Are antibiotics naturally antibiotics? *Journal of Industrial Microbiology and Biotechnology*, 33 (7), 496-499. doi: 10.1007/s10295-006-0112-5.

Davies, J. (2006a). Where have all the antibiotics gone? *Canadian Journal of Infectious Diseases and Medical Microbiology*, 17 (5), 287-290. Retrieved from <https://www.ncbi.nlm.nih.gov/pmc/articles/PMC2095086/>.

Davies, J., & Davies, D. (2010). Origins and Evolution of Antibiotic Resistance. *Microbiology and Molecular Biology Reviews*, 74(3), 417-433. doi:10.1128/membr.00016-10.

D'Costa, V. M., King, C. E., Kalan, L., Morar, M., Sung, W. W. L., Schwarz, C., . . . Wright, G. D. (2011). Antibiotic resistance is ancient. *Nature*, 477(7365), 457-461. doi:<http://www.nature.com/nature/journal/v477/n7365/abs/nature10388.html#supplementary-information>.

Deacon, J. (N.D.). The Microbial World. Retrieved from <http://archive.bio.ed.ac.uk/jdeacon/microbes/penicill.htm>.

Delcour, A.H. (2009). Outer Membrane Permeability and Antibiotic Resistance. *Biochimica et Biophysica Acta (BBA) - Proteins and Proteomics*, 1794 (5), 808-816. doi: 10.1016/j.bbapap.2008.11.005.

Demain, A.L. & Sanchez, S. (2009). Microbial drug discovery: 80 years of progress. *The Journal of Antibiotics*, 62 (1), 5-16. Retrieved from 10.1038/ja.2008.16.

Diekema, D.J. & Jones, R.N. (2001). Oxazolidinone antibiotics. *The Lancet*, 358 (9297), 1975-1982. doi: 10.1016/S0140-6736(01)06964-1.

Docquier, J.D. & Mangani, S. (2018). An update on  $\beta$ -lactamase inhibitor discovery and development. *Drug Resistance Updates*, 36 (1), 13-29. doi: 10.1016/j.drug.2017.11.002.

Domingues, S., Nielsen, K. M., & da Silva, G. J. (2012). Various pathways leading to the acquisition of antibiotic resistance by natural transformation. *Mobile Genetic Elements*, 2(6), 257-260. doi:10.4161/mge.23089

Dorrington, M.G. & Bowdish, D.M.E. (2013). Immunosenescence and Novel Vaccination Strategies for the Elderly. *Frontiers in Immunology*, 4 (171), 1-10. doi: 10.3389/fimmu.2013.00171.

Draenert, R., Seybold, U., Grütznert, E., & Bogner, J. R. (2015). Novel antibiotics: are we still in the pre-post-antibiotic era? *Infection*, 43(2), 145-151. doi:10.1007/s15010-015-0749-y.

Drawz, S. M., & Bonomo, R. A. (2010). Three Decades of  $\beta$ -Lactamase Inhibitors. *Clinical Microbiology Reviews*, 23(1), 160–201. doi: 10.1128/CMR.00037-09.

Ehmann, D.E., Jahic, H., Ross, P.L., Gu, R.F., Hu, J., Kern, G. ... Fisher, S.L. (2012). Avibactam is a covalent, reversible, non- $\beta$ -lactam  $\beta$ -lactamase inhibitor. *Proceedings of the National Academy of Sciences of the United States of America*, 109 (26), 11663-11668. doi: 10.1073/pnas.1205073109.

Ehmann, D.E., Jahic, H., Ross, P.L., Gu, R.F., Durand-Reveille, T.F., Lahiri, S. ... Fisher, S.L. (2013). Kinetics of avibactam inhibition against Class A, C, and D  $\beta$ -lactamases. *Journal of Biological Chemistry*, 288 (1), 27960-27971. doi: 10.1074/jbc.M113.485979.

Evans, B.A. & Amyes, S.G.B. (2014). OXA  $\beta$ -Lactamases. *Clinical Microbiology Reviews*, 27 (2), 241-263. doi: 10.1128/CMR.00117-13.

Fair, R. J., & Tor, Y. (2014). Antibiotics and Bacterial Resistance in the 21st Century. *Perspectives in Medicinal Chemistry*, 6, 25-64. doi:10.4137/PMC.S14459.

Faridoun, U.I. & Islam, N. (2013). An Update on the Status of Potent Inhibitors of Metallo- $\beta$ -Lactamases. *Scientia Pharmaceutica*, 81 (2), 309-327. doi: 10.3797/scipharm.1302-08.

Finch, R.G., Greenwood, D., Norrby, S.R., & Whitley, R.J. (Eds.) (2010). *Antibiotic and Chemotherapy* (9th ed.). Edinburgh: Elsevier.

Fisher, J. F., Meroueh, S. O., & Mobashery, S. (2005). Bacterial Resistance to  $\beta$ -Lactam Antibiotics: Compelling Opportunism, Compelling Opportunity. *Chemical reviews*, 105(2), 395-424. doi:10.1021/cr030102i.

Fleming, A. (1929). On the Antibacterial Action of Cultures of a *Penicillium*, with Special Reference to their Use in the Isolation of *B. influenzae*. *The British Journal of Experimental Pathology*, 10 (3), 226-236. Retrieved from <https://www.ncbi.nlm.nih.gov/pmc/articles/PMC2048009/pdf/brjexppathol00255-0037.pdf>.

Floss, H. G., & Yu, T.-W. (2005). Rifamycin-mode of action, resistance, and biosynthesis. *Chemical reviews*, 105(2), 621-632. doi:10.1021/cr030112j.

Fossum, S., Crooke, E., & Skarstad, K. (2007). Organization of sister origins and replisomes during multifork DNA replication in *Escherichia coli*. *The EMBO Journal*, 26 (21), 4514-4522. doi: 10.1038/sj.emboj.7601871.

Fulston, M., Davison, M., Elson, S.W., Nicholson, N.H., Tyler, J.W., & Woroniecki, S.R. (2001). Clavulanic acid biosynthesis; the final steps. *Journal of the Chemical Society, Perkin Transactions 1*, 0 (1), 1122-1130. doi: 10.1039/B007009M.

Garau, J., Wilson, W., Wood, M., & Carlet, J. (1997). Fourth-generation cephalosporins: a review of in vitro activity, pharmacokinetics, pharmacodynamics and clinical utility. *Clinical Microbiology and Infection*, 3 (1), 87-101. Retrieved from [https://ac.els-cdn.com/S1198743X14642543/1-s2.0-S1198743X14642543-main.pdf?\\_tid=eb37d228-](https://ac.els-cdn.com/S1198743X14642543/1-s2.0-S1198743X14642543-main.pdf?_tid=eb37d228-)

4f17-4083-8262-

35122a96736a&acdnat=1534153269\_b4768f533dc98669fdecfdb6ebcc84ff.

Gaude, G.S. & Hattiholli, J. (2013). Rising bacterial resistance to beta-lactam antibiotics: Can there be solutions? *Journal of Dr. NTR University of Health Sciences*, 2 (1), 4-9. doi: 10.4103/2277-8632.108504.

Georgopapadakou, N.H. & Liu, F.Y. (1980). Penicillin-Binding Proteins in Bacteria. *Antimicrobial Agents and Chemotherapy*, 18 (1), 148-157. Retrieved from <https://www.ncbi.nlm.nih.gov/pmc/articles/PMC283955/pdf/aac00387-0156.pdf>.

Goldberg, S.D., Iannuccilli, W., Nguyen, T., Yu, J., & Cornish, V. (2003). Identification of residues critical for catalysis in a class C  $\beta$ -lactamase by combinatorial scanning mutagenesis. *Protein Science*, 12 (8), 1633-1645. doi: 10.1110/ps.0302903.

Golemi, D., Maveyraud, L., Vakulenko, S., Samama, J.P., & Mobashery, S. (2001). Critical involvement of a carbamylated lysine in catalytic function of class D  $\beta$ -lactamases. *Proceedings of the National Academy of Sciences of the United States of America*, 98 (25), 14280-14285. doi: 10.1073/pnas.241442898.

Gutmann, L., Kitzis, M.D., Yamabe, S., & Acar, J.F. (1986). Comparative Evaluation of a New  $\beta$ -Lactamase Inhibitor, YTR 830, Combined with Different  $\beta$ -Lactam Antibiotics against Bacteria Harboring Known  $\beta$ -Lactamases. *Antimicrobial Agents and Chemotherapy*, 29 (5), 955-957. Retrieved from <http://aac.asm.org/content/aac/29/5/955.full.pdf>.

Hancock, R.E.W. & Chapple, D.S. (1999). Peptide Antibiotics. *Antimicrobial Agents and Chemotherapy*, 43 (6), 1317-1323. Retrieved from <https://www.ncbi.nlm.nih.gov/pmc/articles/PMC89271/>.

Hardy, L.W. & Kirsch, J.F. (1984). Diffusion-limited component of reactions catalyzed by *Bacillus cereus* beta-lactamase I. *Europe Pub Med Central*, 23 (6), 1275-1282. doi: 10.1021/bi00301a040.

Harris, P.N.A., Yin, M., Chew, J., Ali, J., Paytner, S., Paterson, D.L., & Tambyah, P.A. (2015). Comparable outcomes for  $\beta$ -lactam/ $\beta$ -lactamase inhibitor combinations and carbapenems in definitive treatment of bloodstream infections caused by cefotaxime-resistant *Escherichia coli* or *Klebsiella pneumoniae*. *Antimicrobial Resistance & Infection Control*, 1 (1), 1-14. doi: 10.1186/s13756-015-0055-6.

Hata, M., Fujii, Y., Tanaka, Y., Ishikawa, H., Ishii, M., Neya, S. ... Hoshino, T. (2006). Substrate Deacylation Mechanisms of Serine- $\beta$ -lactamases. *Biological and Pharmaceutical Bulletin*, 29 (11), 2151-2159. doi: 10.1248/bpb.29.2151.

Héritier, C., Poirel, L., Aubert, D., & Nordmann, P. (2003). Genetic and Functional Analysis of the Chromosome-Encoded Carbapenem-Hydrolyzing Oxacillinase OXA-40 of *Acinetobacter baumannii*. *Antimicrobial Agents and Chemotherapy*, 47 (1), 268-273. doi: 10.1128/AAC.47.1.268-273.2003.

Hermann, J.C., Ridder, L., Mulholland, A.J., & Holtje, H.D. (2003). Identification of Glu166 as the General Base in the Acylation Reaction of Class A  $\beta$ -Lactamases through QM/MM Modeling. *Journal of the American Chemical Society*, 125 (32), 9590-9591. doi: 10.1021/ja034434g.

Inamasu, J., Ishikawa, K., Oheda, M., Nakae, S., Hirose, Y., & Yoshida, S. (2016). Intrathecal administration of colistin for meningitis due to New Delhi metallo- $\beta$ -lactamase 1(NDM-1)-producing *Klebsiella pneumoniae*. *Journal of Infection and Chemotherapy*, 22 (3), 184-186. doi: 10.1016/j.jiac.2015.10.007.

Jenkins, A.C., Dreslinski, G.R., Tadros, S.S., Groel, J.T., Fand, R., & Herczeg, S.A. (1985). Captopril in Hypertension: Seven Years Later. *Journal of Cardiovascular Pharmacology*, 7 (1), 96-101. Retrieved from file:///C:/Users/u1151564/Desktop/Captopril\_in\_Hypertension\_\_Seven\_Years\_Later.19.pdf.

Jiang, X.W., Cheng, H., Huo, Y.Y., Xu, L., Wu, Y.H., Liu, W.H. ... Zhang, B.W. (2018). Biochemical and genetic characterization of a novel metallo- $\beta$ -lactamase from marine bacterium *Erythrobacter litoralis* HTCC 2594. *Scientific Reports*, 8 (803), 1-9. doi: 10.1038/s41598-018-19279-0.

Kaeberlein, T., Lewis, K., & Epstein, S.S. (2002). Isolating "Uncultivable" Microorganisms in Pure Culture in a Simulated Natural Environment. *Science*, 296 (5570), 1127-1129. doi: 10.1126/science.1070633.

Kapoor, G., Saigal, S., & Elongavan, A. (2017). Action and resistance mechanisms of antibiotics: A guide for clinicians. *Journal of Anaesthesiology Clinical Pharmacology*, 33 (3), 300-305. doi: 10.4103/joacp.JOACP\_349\_15.

King, D.T., Sobhanifar, S., & Strynadka, N.C.J. (2016). One ring to rule them all: Current trends in combating bacterial resistance to the  $\beta$ -lactams. *The Protein Society*, 25 (1), 787-803. Retrieved from <https://onlinelibrary.wiley.com/doi/epdf/10.1002/pro.2889>.

Kitani, S., Miyamoto, K. T., Takamatsu, S., Herawati, E., Iguchi, H., Nishitomi, K., . . . Nihira, T. (2011). Avenolide, a *Streptomyces* hormone controlling antibiotic production in *Streptomyces avermitilis*. *Proceedings of the National Academy of Sciences*, 108(39), 16410-16415. doi:10.1073/pnas.1113908108.

Kline, K.A. & Bowdish, D.M.E. (2016). Infection in an aging population. *Current Opinion in Microbiology*, 29 (1), 63-67. doi: 10.1016/j.mib.2015.11.003 1369-5274.

Klingler, F.M., Wichelhaus, T.A., Frank, D., Cuesta-Bernal, J., El-Delik, J., Muller, H. ... Proschak, E. (2015). Approved Drugs Containing Thiols as Inhibitors of Metallo- $\beta$ -lactamases: Strategy To Combat Multidrug-Resistant Bacteria. *Journal of Medicinal Chemistry*, 58 (8), 3626-3630. doi: 10.1021/jm501844d.

Kolář, M., Urbánek, K., & Látal, T. (2001). Antibiotic selective pressure and development of bacterial resistance. *International Journal of Antimicrobial Agents*, 17(5), 357-363. doi: 10.1016/S0924-8579(01)00317-X.

Kong, K.F., Schneper, L., & Mathee, K. (2010). Beta-lactam Antibiotics: From Antibiosis to Resistance and Bacteriology. *Journal of Pathology Microbiology and Immunology*, 118 (1), 1-36. doi: 10.1111/j.1600-0463.2009.02563.x.

Kroll, C.G., Berger, P., Lepperdinger, G., & Loebeinstein, B.G. (2015). How sex and age affect immune responses, susceptibility to infections and response to vaccination. *Aging Cell*, 14 (3), 309-321. doi: 10.1111/accel.12326.

Labia, R., Morand, A., & Péduzzi, J. (1986). Timentin and  $\beta$ -lactamases. *Journal of Antimicrobial Chemotherapy*, 17 (1), 17-26. doi: 10.1093/jac/17.suppl\_C.17.

Lahiri, S.D., Johnstone, M.R., Ross, P.L., McLaughlin, R.E., Olivier, N.B., & Alm, R.A. (2014). Avibactam and Class C  $\beta$ -Lactamases: Mechanism of Inhibition, Conservation of the Binding Pocket, and Implications for Resistance. *Antimicrobial Agents and Chemotherapy*, 58 (10), 5704-5713. doi: 10.1128/AAC.03057-14.

Landman, D., Georgescu, C., Martin, D.A., & Quale, J. (2008). Polymyxins Revisited. *Clinical Microbiology Reviews*, 21 (3), 449-465. doi: 10.1128/CMR.00006-08.

Lapuebla, A., Abdallah, M., Olafisoye, O., Cortes, C., Urban, C., Landman, D., & Quale, J. (2015). Activity of Imipenem with Relebactam against Gram-Negative Pathogens from New York City. *Antimicrobial Agents and Chemotherapy*, 59 (8), 5029-5031. doi: 10.1128/AAC.00830-15.

Lee, S.Y., Fan, H.W., Kuti, J.L., & Nicolau, D.P. (2006). Update on daptomycin: the first approved lipopeptide antibiotic. *Expert Opinion on Pharmacotherapy*, 7 (10), 1381-1397. doi: 10.1517/14656566.7.10.1381.

Lewis, K., 2013. Platforms for antibiotic discovery. *Nature Reviews. Drug Discovery*, 12(5), pp. 371-87.

Lin, J., Nishino, K., Roberts, M. C., Tolmasky, M., Aminov, R., & Zhang, L. (2015). Mechanisms of antibiotic resistance. *Frontiers in Microbiology*, 6. doi:10.3389/fmicb.2015.00034.

Ling, L. L., Schneider, T., Peoples, A. J., Spoering, A. L., Engels, I., Conlon, B. P., . . . Lewis, K. (2015). A new antibiotic kills pathogens without detectable resistance. *Nature*, 517(7535), 455-459. doi:10.1038/nature14098.

Liu, Y.-Y., Wang, Y., Walsh, T. R., Yi, L.-X., Zhang, R., Spencer, J., . . . Shen, J. (2016). Emergence of plasmid-mediated colistin resistance mechanism MCR-1 in animals and human beings in China: a microbiological and molecular biological study. *The Lancet. Infectious diseases*, 16(2), 161-168. doi:10.1016/S1473-3099(15)00424-7.

Livermore, D.M. (1995).  $\beta$ -Lactamases in Laboratory and Clinical Resistance. *Clinical Microbiology Reviews*, 8 (4), 557-584. Retrieved from <https://www.ncbi.nlm.nih.gov/pmc/articles/PMC172876/pdf/080557.pdf>.

Livermore, D.M. (2003). Linezolid in vitro: mechanism and antibacterial spectrum. *Journal of Antimicrobial Chemotherapy*, 51 (2), 9-16. doi: 10.1093/jac/dkg249.

Livermore, D.M. & Woodford, N. (2006). The  $\beta$ -lactamase threat in Enterobacteriaceae, Pseudomonas and Acinetobacter. *Trends in Microbiology*, 14 (9), 413-420. doi: 10.1016/j.tim.2006.07.008.

Livermore, D.M. (2018). The 2018 Garrod Lecture: Preparing for the Black Swans of Resistance. *Journal of Antimicrobial Chemotherapy*, , . doi: 10.1093/jac/dky265.

Lob, S.H., Hackel, M.A., Kazmierczak, K.M., Young, K., Motyl, M.R., Karlowsky, J.A., & Sahm, D.H. (2017). In Vitro Activity of Imipenem\_relebactam against Gram-Negative ESKAPE Pathogens Isolated by Clinical Laboratories in the United States in 2015 (Results from the SMART Global Surveillance Program). *Antimicrobial Agents and Chemotherapy*, 61 (6), . doi: 10.1128/AAC.02209-16.

Logan, L.K. & Bonomo, R.A. (2016). Metallo- $\beta$ -Lactamase (MBL)-Producing Enterobacteriaceae in United States Children. *Open Forum Infectious Diseases*, 3 (2), 1-4. doi: 10.1093/ofid/ofw090.

Lomovskaya, O., Rubio-Aparicio, D., Nelson, K., Tsivkosvski, R., Griffith, D.C., Dudley, M.N., & Sun, D. (2017). Vaborbactam: Spectrum of Beta=Lactamase Inhibition and Impact of Resistance Mechanisms of Activity in Enterobacteriaceae. *Antimicrobial Agents and Chemotherapy*, 61 (1), 443-517. doi: 10.1128/AAC.01443-17.

MacGowan, A., & Macnaughton, E. (2013). Antibiotic resistance. *Medicine*, 41(11), 642-648. doi: <http://dx.doi.org/10.1016/j.mpmed.2013.08.002>.

Machado, E., Coque, T.M., Cantón, R., Sousa, J.C., & Peixe, L. (2013). Commensal Enterobacteriaceae as reservoirs of extended-spectrum beta-lactamases, integrons and sul genes in Portugal. *Frontiers in Microbiology*, 4 (80), 1-7. doi: 10.3389/fmicb.2013.00080.

Madgwick, P.J. & Waley, S.G. (1987). B-Lactamase I from *Bacillus cereus*. *Biochemical Journal*, 248 (3), 657-662. Retrieved from <https://www.ncbi.nlm.nih.gov/pmc/articles/PMC1148599/>.

Martinez, J.L., Vicente, M.F., Delgado-Iribarren, A., Perez-Diaz, J.C., & Baquero, F. (1989). Small plasmids are involved in amoxicillin-clavulanate resistance in *Escherichia coli*. *Antimicrobial Agents and Chemotherapy*, 33 (4), 595-595. Retrieved from <https://www.ncbi.nlm.nih.gov/pmc/articles/PMC172490/>.

Matagne, A., Dubus, A., Galleni, M., & Frère, J.M. (1999). The b-lactamase cycle: a tale of selective pressure and bacterial ingenuity. *Natural Product Reports*, 16 (1), 1-19. Retrieved from <http://pubs.rsc.org/en/content/articlepdf/1999/np/a705983c>.

Matsumura, N., Minami, S., Araki, H., Hori, R., Ogake, N., & Watanabe, Y. (2000). Determination of intracellular and extracellular B-lactamase activities of *Pseudomonas aeruginosa* after exposure to B-lactams in vitro and in vivo. *Journal of Infection and Chemotherapy*, 6 (4), 200-205. doi: 10.1007/s101560070003.

Maveyraud, L., Golemi, D., Kotra, L.P., Trainer, S., Vakulenko, S., Mobashery, S., & Samama, J.P. (2000). Insights into Class D  $\beta$ -Lactamases Are Revealed by the Crystal Structure of the OXA10 Enzyme from *Pseudomonas aeruginosa*. *Structure*, 8 (12), 1289-1298. doi: 10.1016/S0969-2126(00)00534-7.

McGeary, R.P., Tan, D.T.C., & Schenk, G. (2017). Progress toward inhibitors of metallo- $\beta$ -lactamases. *Future Medicinal Chemistry*, 9 (7), 855-863. doi: 10.4155/fmc-2017-0007.

Meletis, G. (2016). Carbapenem resistance: overview of the problem and future perspectives. *Therapeutic Advances in Infectious Disease*, 3 (1), 15-21. doi: 10.1177/2049936115621709.

Merck. (2016). Results of Phase 2 Study of Merck's Investigational Beta-Lactamase Inhibitor Relebactam in Combination with Imipenem/Cilastatin Presented at ASM Microbe. Retrieved from <http://investors.merck.com/news/press-release-details/2016/Results-of-Phase-2-Study-of-Mercks-Investigational-Beta-Lactamase-Inhibitor-Relebactam-in-Combination-with-ImipenemCilastatin-Presented-at-ASM-Microbe/default.aspx>.

Miao, V., Coeffet-Legal, M.F., Brian, P., Brost, R., Penn, J., Whiting, A. ... Baltz, R.H. (2005). Daptomycin biosynthesis in *Streptomyces roseosporus*: cloning and analysis of the gene cluster and revision of peptide stereochemistry. *Microbiology*, 151 (5), 1507-1523. doi: 10.1099/mic.0.27757-0.

Millán, J.L. (2006). Alkaline Phosphatases. *Purinergic Signalling*, 2 (2), 335-341. doi: 10.1007/s11302-005-5435-6.

Miller, E.L. (2002). The penicillins: A review and update. *Journal of Midwifery & Women's Health*, 47 (6), 426-434. doi: 10.1016/S1526-9523(02)00330-6.

Monogue, M.L., Giavagnoli, S., Bissantz, C., Zampaloni, C., & Nicolau, D.P. (2018). In Vivo Efficacy of Meropenem, with a novel non- $\beta$ -lactam  $\beta$ -lactamase Inhibitor, Nacubactam, against Gram-negative Organisms Exhibiting Various Resistance Mechanisms in a Murine Complicated Urinary Tract Infection Model. *Antimicrobial Agents and Chemotherapy*, 17 (1), doi: 10.1128/AAC.02596-17.

Mossel, D.A.A., Mengerink, W.H.J., & Scholts, H.H. (1962). Use of a Modified MacConkey Agar Medium for the Selective Growth and Enumeration of Enterobacteriaceae.

Journal of Bacteriology, 84 (2), 381-381. Retrieved from <https://www.ncbi.nlm.nih.gov/pmc/articles/PMC277879/>.

Moya, B., Barcelo, I.M., Bhagwat, S., Patel, M., Bou, G., Papp-Wallace, K.M. ... Oliver, A. (2017). WCK 5107 (Zidebactam) and WCK 5153 Are Novel Inhibitors of PBP2 Showing Potent “-Lactam Enhancer” Activity against *Pseudomonas aeruginosa*, Including Multidrug-Resistant Metallo-- Lactamase-Producing High-Risk Clones. *Antimicrobial Agents and Chemotherapy*, 61 (6), doi: 10.1128/AAC .02529-16.

Oliva, M., Dideberg, O., & Field, M.J. (2003). Understanding the acylation mechanisms of active-site serine penicillin-recognizing proteins: A molecular dynamics simulation study. *Proteins*, 53 (1), 88-100. doi: 10.1002/prot.10450.

Page, M.I., Laws, A.P., Slater, M.J., & Stone, J.R. (1995). Reactivity of B-lactams and phosphoramidates and reactions with B-Lactamase. *Pure and Applied Chemistry*, 67 (5), 711-717. Retrieved from <http://eprints.hud.ac.uk/id/eprint/6099/1/6705x0711.pdf>.

Page, M.I. (1999). The reactivity of beta-lactams, the mechanism of catalysis and the inhibition of beta-lactamases. *Current Pharmaceutical Design*, 5 (11), 895-913. Retrieved from <https://www.ncbi.nlm.nih.gov/pubmed/10539995>.

Page, M.I. & Badarau, A. (2008). The Mechanisms of Catalysis by Metallo  $\beta$  -Lactamases. *Bioinorganic Chemistry and Applications*, 2008 (1), 14-pages. doi: 10.1155/2008/576297.

Palzkill, T. (2013). Metallo- $\beta$ -lactamase structure and function. *Annals of the New York Academy of Sciences*, 1277 (1), 91-104. doi: 10.1111/j.1749-6632.2012.06796.x.

Papanicolaou, G.A., Medeiros, A.E., & Jacoby, G.A. (1990). Novel Plasmid-Mediated 1-Lactamase (MIR-1) Conferring Resistance to Oxyimino- and ot-Methoxy 1-Lactams in

Clinical Isolates of *Klebsiella pneumoniae*. *Antimicrobial Agents and Chemotherapy*, 34 (11), 2200-2209. doi: 10.1128/AAC.34.11.2200.

Papp-Wallace, K. M., Endimiani, A., Taracila, M. A., & Bonomo, R. A. (2011). Carbapenems: Past, Present, and Future. *Antimicrobial Agents and Chemotherapy*, 55(11), 4943-4960. doi:10.1128/AAC.00296-11.

Patel, T.S., Pogue, J.M., Mills, J.P., & Kaye, K.S. (2018). Meropenem-vaborbactam: a new weapon in the war against infections due to resistant Gram-negative bacteria. *Future Microbiology*, 13 (9),doi: 10.2217/fmb-2018-0054.

Pham, V.H.T. & Kim, J. (2012). Cultivation of unculturable soil bacteria. *Trends in Biotechnology*, 30 (9), 475-484. doi: 10.1016/j.tibtech.2012.05.007.

Philippon, A., Arlet, G., & Jacoby, G.A. (2002). Plasmid-Determined AmpC-Type  $\beta$ -Lactamases. *Antimicrobial Agents and Chemotherapy*, 46 (1), 1-11. doi: 10.1128/AAC.46.1.1-11.2002.

Philippon, A., Slama, P., Deny, P., & Labia, R. (2016). A Structure-Based Classification of Class A  $\beta$ -Lactamases, a Broadly Diverse Family of Enzymes. *Clinical Microbiology Reviews*, 29 (1), 29-57. doi: 10.1128/CMR.00019-15.

Poirel, L., Naas, T., & Nordmann, P. (2010). Diversity, Epidemiology, and Genetics of Class D  $\beta$ -Lactamases. *Antimicrobial Agents and Chemotherapy*, 54 (1), 24-38. doi: 10.1128/AAC.01512-08.

Poole, K. (2004). Resistance to  $\beta$ -lactam antibiotics. *Cellular and Molecular Life Sciences CMLS*, 61(17), 2200-2223. doi:10.1007/s00018-004-4060-9.

Powers, R.A. & Shoichet, B.K. (2002). Structure-Based Approach for Binding Site Identification on AmpC  $\beta$ -Lactamase. *Journal of Medicinal Chemistry*, 45 (1), 3222-3234. Retrieved from <https://pubs.acs.org/doi/pdf/10.1021/jm020002p>.

Premi, L., Sandine, W.E., & Elliker, P.R. (1972). Lactose-Hydrolyzing Enzymes of *Lactobacillus* Species. *Applied Microbiology*, 24 (1), 51-57. Retrieved from <https://www.ncbi.nlm.nih.gov/pmc/articles/PMC380546/pdf/applmicro00048-0069.pdf>.

Qin, W., Panunzio, M., & Biondi, S. (2014).  $\beta$ -Lactam Antibiotics Renaissance. *Antibiotics*, 3 (2), 193-215. doi: 10.3390/antibiotics3020193.

Rappé, M.S., Connon, S.A., Vergin, K.L., & Giovannoni, S.J. (2002). Cultivation of the ubiquitous SAR11 marine bacterioplankton clade. *Nature*, 413 (1), 630-633. doi: 10.1038/nature00917.

Rawat, D. & Nair, D. (2010). Extended-spectrum  $\beta$ -lactamases in Gram Negative Bacteria. *Journal of Global Infectious Disease*, 2 (3), 263-274. doi: 10.4103/0974-777X.68531.

Reading, C. & Cole, M. (1977). Clavulanic Acid: a Beta-Lactamase-Inhibiting Beta-Lactam from *Streptomyces clavuligerus*. *Antimicrobial Agents and Chemotherapy*, 11 (5), 852-857. Retrieved from <https://www.ncbi.nlm.nih.gov/pmc/articles/PMC352086/pdf/aac00299-0090.pdf>.

Rice, L. B. (2006). Antimicrobial resistance in gram-positive bacteria. *AJIC: American Journal of Infection Control*, 34(5), S11-S19. doi:10.1016/j.ajic.2006.05.220.

Roche. (2016). Annual Report 2016. Retrieved from <http://www.roche.com/dam/jcr:ee2f197f-5487-4629-9e28-66b77c9cbbab/en/ar16e.pdf>.

Rodríguez-Martínez, J.M., Fernández-Echauri, P., Fernández-Cuenca, F., de Alba, P.D., Briaies, A., & Pascual, A. (2011). Genetic characterization of an extended-spectrum AmpC cephalosporinase with hydrolysing activity against fourth-generation cephalosporins in a clinical isolate of *Enterobacter aerogenes* selected in vivo. *Journal of Antimicrobial Chemotherapy*, 67 (1), 64-68. doi: 10.1093/jac/dkr423.

Rossolini, G.M., Franceschini, N., Riccio, M.L., Mercuri, P.S., Perilli, M., Galleni, M. ... Amicosante, G. (1998). Characterization and sequence of the *Chryseobacterium* (*Flavobacterium*) *meningosepticum* carbapenemase: a new molecular class B  $\beta$ -lactamase showing a broad substrate profile. *Biochemical Journal*, 15 (332), 145-152. Retrieved from <https://www.ncbi.nlm.nih.gov/pubmed/9576862>.

Rotondo, C.M. & Wright, G.D. (2017). Inhibitors of metallo- $\beta$ -lactamases. *Current Opinion in Microbiology*, 39 (1), 96-105. doi: 10.1016/j.mib.2017.10.026.

Royal Society of Chemistry. (2004). Enzymes. Retrieved from <http://www.rsc.org/Education/Teachers/Resources/cfb/enzymes.htm>.

Sabath, L.D. & Abraham, E.P. (1966). Zinc as a cofactor for Cephalosporinase from *Bacillus cereus*. *Biochemical Journal*, 98 (1), 11-12. Retrieved from <https://www.ncbi.nlm.nih.gov/pmc/articles/PMC1264844/pdf/biochemj00759-0380.pdf>.

Sader, H.S., Castanheira, M., Huband, M., Jones, R.N., & Flamm, R.K. (2017). WCK 5222 (Cefepime-Zidebactam) Antimicrobial Activity against Clinical Isolates of Gram-Negative Bacteria Collected Worldwide in 2015. *Antimicrobial Agents and Chemotherapy*, 61 (5), . doi: 10.1128/AAC.00072-17.

Scholes, P.D. & Handelsman, J. (2005). Metagenomics for studying unculturable microorganisms: cutting the Gordian knot. *Genome Biology*, 6 (8), 1-4. doi: 10.1186/gb-2005-6-8-229.

Seipke, R. F., Kaltenpoth, M., & Hutchings, M. I. (2012). Streptomyces as symbionts: an emerging and widespread theme? *FEMS Microbiology Reviews*, 36(4), 862-876. doi:10.1111/j.1574-6976.2011.00313.x.

Shah, P.M. & Isaacs, R.B. (2003). Ertapenem, the first of a new group of carbapenems. *Journal of Antimicrobial Chemotherapy*, 52 (4), 538-542. doi: 10.1093/jac/dkg404.

Shaikh, S., Fatima, J., Shakil, S., Rizvi, S.M.D., & Kamal, M.A. (2015). Antibiotic resistance and extended spectrum beta-lactamases: Types, epidemiology and treatment. *Saudi Journal of Biological Sciences*, 22 (1), 90-101. doi: 10.1016/j.sjbs.2014.08.002.

Silver, L.L. (2011). Challenges of antibiotic discovery. *Clinical Microbiology Reviews*, 24 (1), 71-109. doi: 10.1128/CMR.00030-10.

Skaar, I. & Stenwig, H. (1996). Malt-yeast extract-sucrose agar, a suitable medium for enumeration and isolation of fungi from silage. *Applied and Environmental Microbiology*, 62 (10), 3614-3619. Retrieved from <https://www.ncbi.nlm.nih.gov/pmc/articles/PMC168168/>.

Sougakoff, W. (2012). Structure of Class A Beta-Lactamases. In J . M. Frere (Ed.) *Beta-Lactamases* (pp. 21-39). New York: Nova Science Publishers.

Spapen, H., Jacobs, R., Van Gorp, V., Troubleyn, J., & Honoré, P. M. (2011). Renal and neurological side effects of colistin in critically ill patients. *Annals of Intensive Care*, 1(1), 1-7. doi:10.1186/2110-5820-1-14.

Steenbergen, J.N., Alder, J., Thorne, G.M., & Tally, F.P. (2005). Daptomycin: a lipopeptide antibiotic for the treatment of serious Gram-positive infections. *Journal of Antimicrobial Chemotherapy*, 3 (1), 283-288. doi: 10.1093/jac/dkh546.

Stojanoski, V., Chow, D.C., Fryszczyn, B., Hu, L., Nordmann, P., Poirel, L. ... Palzkill, T. (2015). Structural Basis for Different Substrate Profiles of Two Closely Related Class D  $\beta$ -lactamases and Their Inhibition by Halogens. *Biochemistry*, 54 (21), 3370-3380. doi: 10.1021/acs.biochem.5b00298.

Strateva, T. & Yordanov, D. (2009). *Pseudomonas aeruginosa* - a phenomenon of bacterial resistance. *Journal of Medical Microbiology*, 58 (1), 1133-1148. doi: 10.1099/jmm.0.009142-0.

Temkin, E., Cisneros, J.T., Beovic, B., Benito, N., Giannella, M., Gilarranz, R. ... Carmeli, Y. (2017). Ceftazidime-avibactam as salvage therapy for infections caused by Carbapenem-resistant organisms: a case series from the compassionate-use program. *Antimicrobial Agents and Chemotherapy*, 61 (2), 1-29. doi: 10.1128/AAC.01964-16.

Theuretzbacher, U. (2015). Recent FDA Antibiotic Approvals: Good News and Bad News. Retrieved from [http://cddep.org/blog/posts/recent\\_fda\\_antibiotic\\_approvals\\_good\\_news\\_and\\_bad\\_news#sthash.EAhqTX9K.dpbs](http://cddep.org/blog/posts/recent_fda_antibiotic_approvals_good_news_and_bad_news#sthash.EAhqTX9K.dpbs).

Thierren, C. & Levesque, R.C. (2006). Molecular basis of antibiotic resistance and  $\beta$ -lactamase inhibition by mechanism-based inactivators: perspectives and future directions. *FEMS Microbiology Reviews*, 24 (3), 251-262. doi: 10.1111/j.1574-6976.2000.tb00541.x.

Thomson, J. M., & Bonomo, R. A. (2005). The threat of antibiotic resistance in Gram-negative pathogenic bacteria:  $\beta$ -lactams in peril! *Current Opinion in Microbiology*, 8(5), 518-524. doi: <http://dx.doi.org/10.1016/j.mib.2005.08.014>.

Todar, K. (2012a). Control of Microbial Growth. Retrieved from [http://textbookofbacteriology.net/control\\_4.html](http://textbookofbacteriology.net/control_4.html).

Todar, K. (2012b). The Growth of Bacterial Populations (Page 3). Retrieved from [http://textbookofbacteriology.net/growth\\_3.html](http://textbookofbacteriology.net/growth_3.html).

Toussaint, K.A. & Gallagher, J.C. (2015).  $\beta$ -Lactam/ $\beta$ -Lactamase Inhibitor Combinations: From Then to Now. *Annals of Pharmacotherapy*, 49 (1), 86-98. doi: 10.1177/1060028014556652.

Tulane University School of Medicine. (2015). Beta-Lactam Chemistry. Retrieved from [http://tmedweb.tulane.edu/pharmwiki/doku.php/beta\\_lactam\\_working\\_rough\\_draft\\_-\\_not\\_ready\\_for\\_prime\\_time](http://tmedweb.tulane.edu/pharmwiki/doku.php/beta_lactam_working_rough_draft_-_not_ready_for_prime_time).

Velho-Pereira, S., & Kamat, N. M. (2011). Antimicrobial Screening of Actinobacteria using a Modified Cross-Streak Method. *Indian Journal of Pharmaceutical Sciences*, 73(2), 223-228. Retrieved from <http://www.ncbi.nlm.nih.gov/pmc/articles/PMC3267309/>.

Vella, P., Miraula, M., Phelan, E., Leung, E.W.W., Ely, F., Ollis, D.L. ... Mitic, N. (2013). Identification and characterization of an unusual metallo- $\beta$ -lactamase from *Serratia proteamaculans*. *Journal of Biological Inorganic Chemistry*, 18 (7), 855-863. doi: 10.1007/s00775-013-1035-z.

Ventola, C. L. (2015). The Antibiotic Resistance Crisis: Part 1: Causes and Threats. *Pharmacy and Therapeutics*, 40(4), 277-283. Retrieved from <http://www.ncbi.nlm.nih.gov/pmc/articles/PMC4378521/>.

Versporten, A., Bielicki, J., Drapier, N., Sharland, M., & Gossens, H. (2016). The Worldwide Antibiotic Resistance and Prescribing in European Children (ARPEC) point prevalence survey: developing hospital-quality indicators of antibiotic prescribing for children. *Journal of Antimicrobial Chemotherapy*, 71 (4), 1106-1117. doi: 10.1093/jac/dkv418.

Vranakis, I., Goniotakis, I., Psaroulaki, A., Sandalakis, V., Tselentis, Y., Gevert, K., & Tsiotis, G. (2014). Proteome studies of bacterial antibiotic resistance mechanisms. *Journal of Proteomics*, 97 (1), 88-99. doi: 10.1016/j.jprot.2013.10.027.

Walsh, T.R., Hall, L., Assinder, S.J., Nichols, W.W., Cartwright, S.J., Macgowan, A.P., & Bennett, P.M. (1994). Sequence analysis of the L1 metallo- $\beta$ -lactamase from *Xanthomonas maltophilia*. *Biochimica et Biophysica Acta (BBA) - Gene Structure and Expression*, 1218 (2), 199-201. doi: 10.1016/0167-4781(94)90011-6.

Wang, D.Y., Abboud, M.I., Markoulides, M.S., Brem, J., & Schofield, C.J. (2016). The road to avibactam: the first clinically useful non-B-lactam working somewhat like a B-lactam. *Future Medicinal Chemistry*, 8 (10), 1063-1084. doi: 10.4155/fmc-2016-0078.

Watanabe, M., Iyobe, S., Inoue, M., & Mitsuhashi, S. (1991). Transferable Imipenem Resistance in *Pseudomonas aeruginosa*. *Antimicrobial Agents and Chemotherapy*, 35 (1), 147-151. Retrieved from <https://www.ncbi.nlm.nih.gov/pmc/articles/PMC244956/pdf/aac00046-0189.pdf>.

Webber, M.A. & Piddock, L.J.V. (2003). The importance of efflux pumps in bacterial antibiotic resistance. *Journal of Antimicrobial Chemotherapy*, 51 (1), 9-11. doi: 10.1093/jac/dkg050.

Wilke, M. S., Lovering, A. L., & Strynadka, N. C. J. (2005).  $\beta$ -Lactam antibiotic resistance: a current structural perspective. *Current Opinion in Microbiology*, 8(5), 525-533. doi: <http://dx.doi.org/10.1016/j.mib.2005.08.016>.

Williams, K.J. (2009). The introduction of chemotherapy using arsphenamine - the first magic bullet. *Journal of the Royal Society of Medicine*, 1 (102), 343-348. doi: 10.1258/jrsm.2009.09k036.

Woodford, N. (2005). Biological counterstrike: antibiotic resistance mechanisms of Gram-positive cocci. *Clinical Microbiology & Infection*, 11(s3), 2-21. doi:10.1111/j.1469-0691.2005.01140.x.

Woodford, N. & Ellington, M.J. (2007). The emergence of antibiotic resistance by mutation. *Clinical Microbiology and Infection*, 13 (5), 5-18. doi: 10.1111/j.1469-0691.2006.01492.x.

World Health Organisation. (2015). Antibiotic Resistance. Retrieved from <http://www.who.int/mediacentre/factsheets/antibiotic-resistance/en/>.

World Health Organisation. (2018). Antibiotic Resistance. Retrieved from <http://www.who.int/news-room/fact-sheets/detail/antibiotic-resistance>.

Wouters, J. & Bauvois, C. (2012). Structure of Class C Beta-Lactamases and Perspectives in Drug Design. In J . M. Frere (Ed.) *Beta-Lactamases* (pp. 79-101). New York: Nova Science Publishers.

Wright, N. & Wise, R. (1983). The elimination of sulbactam alone and combined with ampicillin in patients with renal dysfunction. *Journal of Antimicrobial Chemotherapy*, 1 (11), 583-587. Retrieved from [https://watermark.silverchair.com/11-6-583.pdf?token=AQECAHi208BE49Ooan9kkhW\\_Ercy7Dm3ZL\\_9Cf3qfKAc485ysgAAAcgwgGHEBqkqhkIG9w0BBwagggG1MIIBsQIBADCCAaoGCSqGSIb3DQEHATAeBglghkgBZQMEAS4wEQQM12nrOFoMpBsTChnuAgEQgIIBe-c4KSNPyUT4g1s6vX\\_TwniDMajg6DTrj6NjVzWsbHF990MszpIKGDmfvhieQYL8W1dkExETNFFO4C77YjxshEjsQPtrnGA09a2K9w5opTSAOC2UC6mJV3mn-nMIImI-C3EigU\\_l3uRHovNRshsxpIW8DQe6GbYKK-N9F\\_w-SdFRyF3Mj7r4GNvmizjD98Kr6qNEcMkUpZrCgiQ0iJOoWKRc57peBCF15GjOukDNZwObmWceGzLGP9NWPv7qqOZSpcP67WRLzlelqI1Sxp2J9\\_ZEEhRvMg4EAePXxaYfWGHCcPtQfWha1NqNwfxeyUH3S8l\\_9rxCwYCd0KH1SIVdaBf0XI0Orbj-D5-dms-exLKcjHihQcWDcujoF-0eP1Nbg7SE5jzRydmxXpvzxCSjdSDZIW-cbiuhaHBurLvtUfiwrPZEnOBICP5a7Gn3clx446OyWEUCzcc\\_xQcKvpTYIe74xNZL60ZViFZQUle9GF1BJDD7FiHnNkImqI0](https://watermark.silverchair.com/11-6-583.pdf?token=AQECAHi208BE49Ooan9kkhW_Ercy7Dm3ZL_9Cf3qfKAc485ysgAAAcgwgGHEBqkqhkIG9w0BBwagggG1MIIBsQIBADCCAaoGCSqGSIb3DQEHATAeBglghkgBZQMEAS4wEQQM12nrOFoMpBsTChnuAgEQgIIBe-c4KSNPyUT4g1s6vX_TwniDMajg6DTrj6NjVzWsbHF990MszpIKGDmfvhieQYL8W1dkExETNFFO4C77YjxshEjsQPtrnGA09a2K9w5opTSAOC2UC6mJV3mn-nMIImI-C3EigU_l3uRHovNRshsxpIW8DQe6GbYKK-N9F_w-SdFRyF3Mj7r4GNvmizjD98Kr6qNEcMkUpZrCgiQ0iJOoWKRc57peBCF15GjOukDNZwObmWceGzLGP9NWPv7qqOZSpcP67WRLzlelqI1Sxp2J9_ZEEhRvMg4EAePXxaYfWGHCcPtQfWha1NqNwfxeyUH3S8l_9rxCwYCd0KH1SIVdaBf0XI0Orbj-D5-dms-exLKcjHihQcWDcujoF-0eP1Nbg7SE5jzRydmxXpvzxCSjdSDZIW-cbiuhaHBurLvtUfiwrPZEnOBICP5a7Gn3clx446OyWEUCzcc_xQcKvpTYIe74xNZL60ZViFZQUle9GF1BJDD7FiHnNkImqI0).

Yang, Y., Ramussen, B.A., & Shlaes, D.M. (1999). Class A  $\beta$ -lactamases—enzyme-inhibitor interactions and resistance. *Pharmacology & Therapeutics*, 83 (1), 141-151. Retrieved from [https://ac.els-cdn.com/S0163725899000273/1-s2.0-S0163725899000273-main.pdf?\\_tid=33b014a2-5a35-430e-b700-c927de518aa4&acdnat=1534151832\\_423e48aff65e360f6e0965c6f5e27b3](https://ac.els-cdn.com/S0163725899000273/1-s2.0-S0163725899000273-main.pdf?_tid=33b014a2-5a35-430e-b700-c927de518aa4&acdnat=1534151832_423e48aff65e360f6e0965c6f5e27b3).

Yocum, R.R., Waxman, D.J., Rasmussen, J.R., & Strominger, J.L. (1979). Mechanism of penicillin action: penicillin and substrate bind covalently to the same active site serine in two bacterial D-alanine carboxypeptidases. *Proceedings of the National Academy of Sciences of the United States of America*, 76 (6), 2730-2734. Retrieved from <https://www.ncbi.nlm.nih.gov/pmc/articles/PMC383682/>.

Zeng, X. & Lin, J. (2013). Beta-lactamase induction and cell wall metabolism in Gram-negative bacteria. *Frontiers in Microbiology*, 4 (128), 1-9. doi: 10.3389/fmicb.2013.00128.

Zhanel, G.G., Lawson, C.D., Adam, H., Schweizer, F., Zelenitsky, S., Lagacé-Wiens, P.R.S. ... Karlowsky, J.A. (2013). Ceftazidime-Avibactam: a Novel Cephalosporin/ $\beta$ -lactamase Inhibitor Combination. *Drugs*, 73 (2), 159-177. doi: 10.1007/s40265-013-0013-7.

Zhanel, G.G., Lawrence, C.K., Adam, H., Schweizer, F., Zelenitsky, S., Zhanel, M. ... Karlowsky, J.A. (2018). Imipenem–Relebactam and Meropenem–Vaborbactam: Two Novel Carbapenem- $\beta$ -Lactamase Inhibitor Combinations. *Drugs*, 78 (1), 65-98. doi: 10.1007/s40265-018-0910-x.

## Chapter Two: The Search for Novel Antimicrobials from Microbial Origins

*The author acknowledges the kind gift of *Pseudomonas baetica* from Professor Jesus L. Romalde from Santiago University, Portugal.*

### 2.1: Introduction

As discussed in the general introduction, the vast majority of current antibiotics used in the clinic originated as being identified as secondary metabolites of bacteria. Specifically, more than 70 % of commercial antibiotics were isolated from strains of *Streptomyces* (Raja & Prabakarana, 2011). Examples of antibiotics isolated from *Streptomyces* include the aminoglycoside antibiotic neomycin and the macrolytic peptide antibiotic bottromycin (Bibb, 2013). It was the pioneering work of Ukrainian scientist Selman Waksman (Waksman & Woodruff, 1940) that first identified soil as being a potentially rich source of novel antimicrobial products with the discovery of *Actinomycetes antibioticus* which produced actinomycin, which had bacteriostatic and bactericidal properties (Kresge, Simoni & Hill, 2004). Whilst actinomycin had potent effects against Gram-positive organisms, it had little effect on Gram-negative pathogens, and was also found to be extremely toxic in animal test cases and was therefore of little clinical value.

Despite this initial relative failure, Waksman had clearly shown soil to be a potential source of novel antimicrobials in the emerging era of antibiotics. He developed a platform for the screening of novel antimicrobial products from bacteria isolated from soil. Briefly, this comprised of suspending a sample of soil in sterile liquid, carrying out serial dilutions and

then streaking a sample of this soil solution onto an agar plate. Even with serial dilutions, the concentration of microbes in soil is estimated to be in the region of 1 billion cells per gram of soil. Therefore, the plates will still contain thousands of microbes in close proximity with each other. This close proximity will increase competition for resources from the agar plate during incubation. Therefore, this will initiate microbes capable of producing antibiotics to do so, resulting in inhibitory effects on their immediate microbial neighbours. The plates were then incubated and antimicrobial producing organisms were identified by observing for inhibition zones around the microbe in question. Figure 2.1 below is taken from Waksman's paper (1940) showing the examples of inhibition zones around antimicrobial producing microbes.

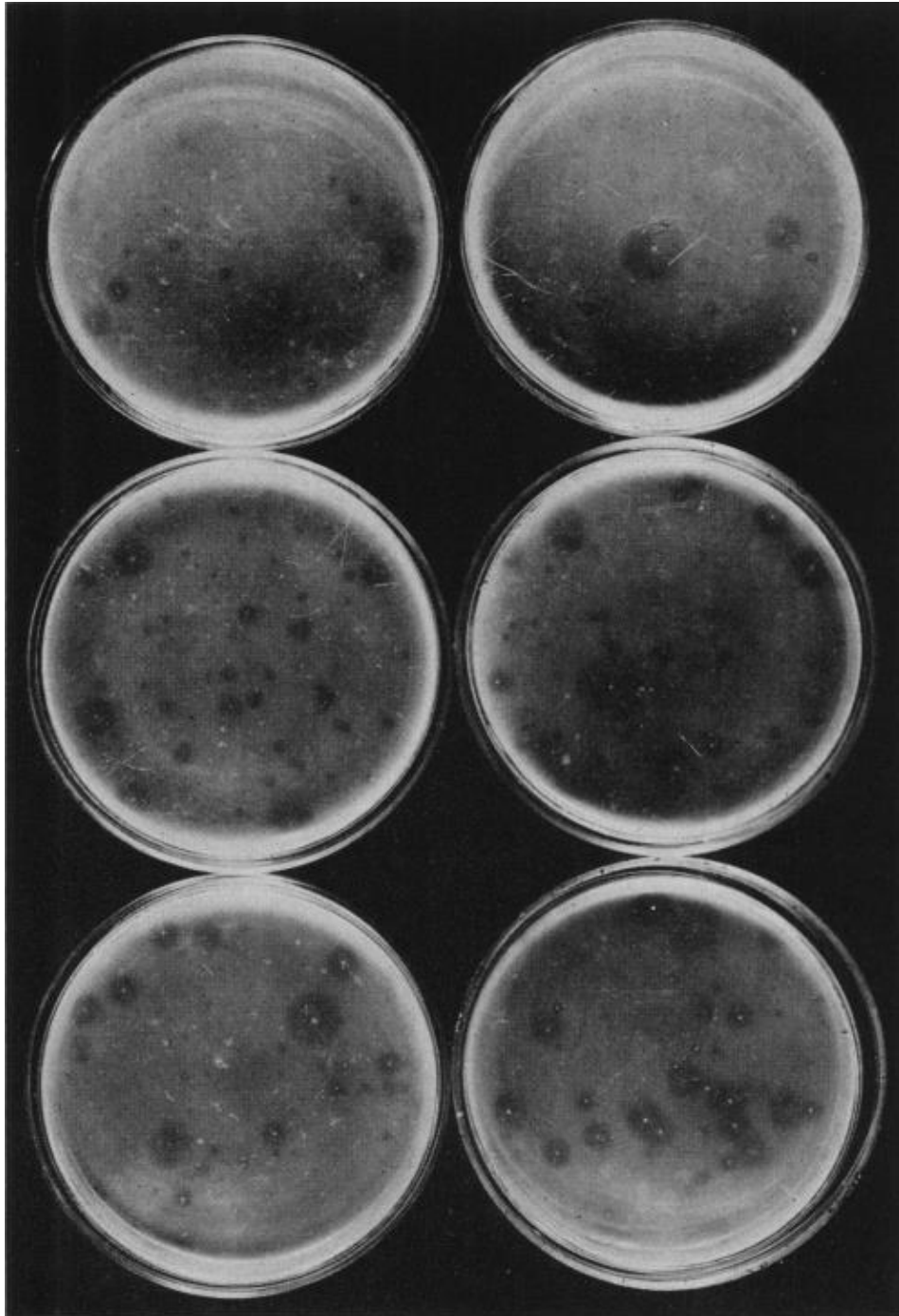


Figure 2.1: Examples of microbes producing antimicrobial products resulting in inhibition of growth of their neighbouring organisms (Waksman & Woodruff, 1940).

Once inhibition zone inducing microbes had been identified, they were then isolated so further analyses could be commenced. Waksman, along with the help of others in his laboratory (namely Woodruff and a post graduate student, Schatz) pioneered a cross-

streaking technique for fast, qualitative analysis of a microbe's antimicrobial potential. Briefly, the now isolated antimicrobial producing organism in question would be streaked vertically down the centre of an agar plate. Pathogenic organisms would be streaked in perpendicular to the antimicrobial producing isolate. If the organism produced inhibition zones where they came into close contact with each other, then the antimicrobial producing organism showed potential with producing a useful, potent antibiotic (Woodruff, 2014). A visual example of this technique is shown in figure 2.2 below.

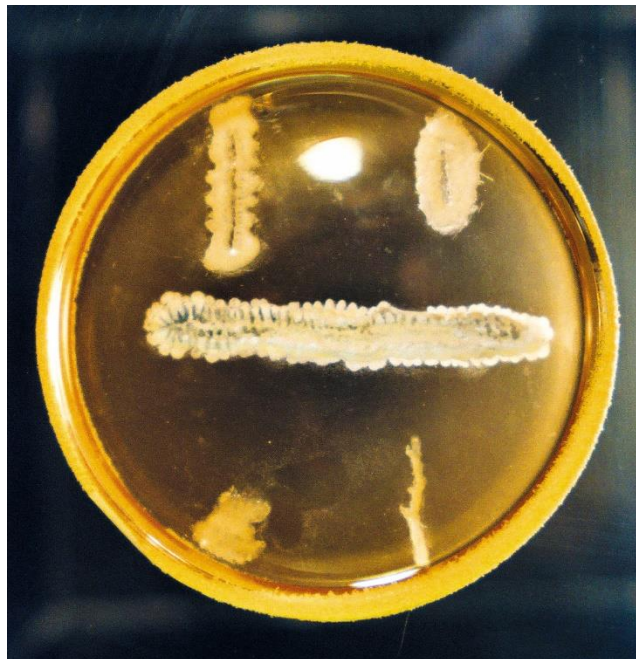


Figure 2.2: Example of the cross-streak method pioneered by Waksman and colleagues (American Chemical Society, 2005).

Waksman continued with this discovery platform and soon after his initial discovery of *Actinomyces antibioticus*, he and his team discovered streptomycin in 1944, isolated from *Actinomyces griseus* (Schatz, Bugle & Waksman, 1944). Streptomycin, an aminoglycoside protein synthesis inhibitor (Demirci et al., 2013) was a breakthrough for Waksman and his team, as it was not only effective against Gram-positive and negative bacteria, but most importantly was not toxic, like the other antibiotics he had isolated previously. His work laid

the foundation for future work isolating antibiotic producing bacteria from soil, which for many years throughout the golden era of antibiotic discovery provided a rich source of novel antibiotics (Lyddiard, Jones & Greatrex, 2016). However, as discussed in the general introduction, this platform of discovery yielded fewer and fewer novel prospects up to the point that most “new” antibiotics introduced into the clinic were simply novel analogues of existing antibiotics, with no novel mode of action.

The fact that more than 98 % of bacteria are unculturable in laboratory conditions has spurred research into novel methods of culturing bacteria, with the aim of increasing the *in vitro* growth rate (Wade, 2002). Scientists know that the vast majority of bacteria are unculturable through various ways. Chiefly, one simply has to look down a microscope to see that in an environmental sample, the number of microbes that can be seen visually far outweigh the number that has grown from the same sample on a petri dish. Furthermore, PCR analysis of environmental samples shows there is simply a huge array of bacteria present in the sample that have not grown on the dish (Stewart, 2012). It is not fully understood why microbes fail to grow *in vitro*, but the chief suspicion amongst scientists is that we are simply unable to exactly replicate the incredibly unique conditions of the environment from which samples are taken. It goes much more beyond simple pH and temperature adjustments. Nevertheless, it is not for lack of effort or cleverness that science has been unable to answer this quandary, but there are many intricate factors which must be replicated which in most cases are simply not feasible to attempt. Therefore, the attitude towards growing unculturable bacteria has moved from simply trying different compositions of media in the microbiology laboratory to completely novel growth techniques that try to simulate the *in situ* growth environment as much as possible. One such novel technique is that of the isolation chip or “iChip”.

As discussed in the general introduction, the iChip aims to increase the *in vitro* growth rate of microbes by first growing the microbes *in situ* in the iChip device, and then transferring the iChip to the laboratory to continue the culturing of the microbes. This is thought to increase the *in vitro* growth rate from 2 % to above 15 %, which is in the region of a tenfold increase of *in situ* growth rate (Nichols et al., 2010). Clearly, this is an extremely promising avenue of research; as human kind has simply been unable to recreate the successfulness of antibiotics in a synthetic sense, novel techniques for growing previously un-culturable bacteria that could potentially yield many novel classes of antimicrobials is an area of research that has been growing intensely in recent years (Vartoukian, Palmer & Wade, 2010).

## 2.2: Chapter Aims

The aims of this chapter were to investigate novel microbes which may show inhibitory effects on pathogenic bacteria. First, an extract of kombucha tea was analysed to detect for the presence of an inhibitory effect on pathogenic microbes. Then, the Waksman platform of discovery was first utilised to attempt to find antibiotic producing microbes from a soil environment. This work was expanded by use of an iChip to attempt to grow previously unculturable bacteria, and then investigate whether any novel antimicrobial producing microbes could be isolated. LCMS analysis then took place to attempt to identify any metabolites responsible for any detected inhibition.

## 2.3: Methods

### 2.3.1: Potential Antimicrobials Within a Kombucha Tea Extract

The search for novel antibiotics began by investigating a kombucha tea, also known as a symbiotic culture of bacteria and yeast (SCOBY). Kombucha tea is a generic term for any fermented tea product that is drunk for supposed health benefits. A kombucha tea sample was obtained from the Department of Human and Health Sciences at the University of Huddersfield. The kombucha tea contained a cellulose layer created by the microbes present in the culture. This cellulose layer was collected with a sterile hook and samples were taken using an autoclaved 10 mm cork borer. Plates of pathogenic bacteria were prepared by suspending a loop full of culture in 9 ml of maximum recovery diluent (MRD) solution and vortexing for 60 seconds. Concentrations were corrected to  $10^6$  cells per ml using a spectrophotometer operating at specific wavelengths for the bacterium in question. The optical density (OD) is the turbidity created in the sample by the scattering of light by the microbial cells. If more cells are present, there will be more turbidity (light scattering), and therefore a higher concentration of microbes. The optical density is therefore proportional to the concentration of cells and can be used to standardise the amount of cells/ml (Widdel, 2010). Tryptone Soy agar (TSA) plates were prepared by dissolving 37.5 g of TSA powder (Lab M) in 1,000 ml of deionised water and poured into sterile petri dishes and allowed to dry in a laminar flow hood. 100  $\mu$ l of the test suspension containing the pathogen was spread onto the TSA plates using a sterile plate spreader and was allowed to dry for 3-5 minutes in a laminar flow hood until no obvious sign of wetness was visible. The 10 mm cellulose plug was aseptically transferred to the pre-inoculated plates of *Escherichia coli* (NCIMB: 8879), *Enterococcus hirae* (NCIMB: 8191), *Pseudomonas aeruginosa* (NCIMB: 10421) and *Staphylococcus aureus* (NCIMB: 9518) and were incubated for 48 hours at 37 °C. After the

incubation period, the plates were removed and examined for areas of inhibition. The results were varying and indeterminate, but the SCOBY sample showed best action against *E. hirae*, with inhibition zones of up to 3 mm, which can be seen in figure 2.3 below.

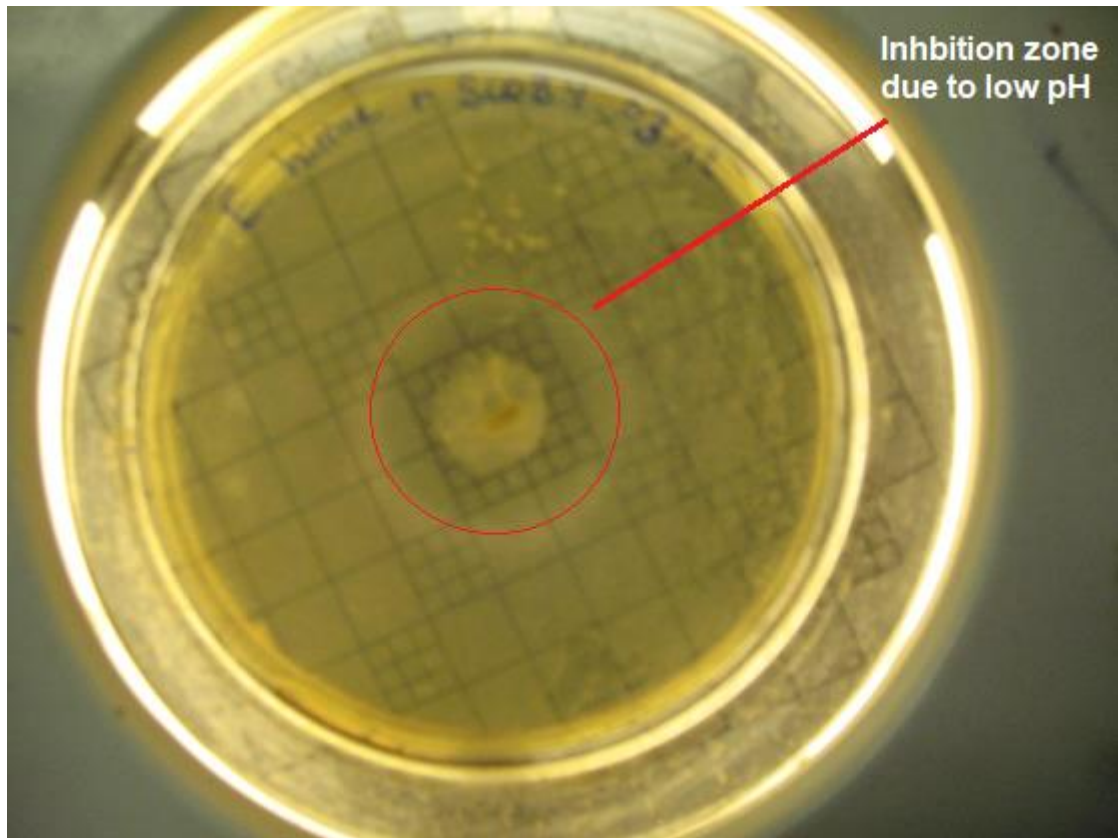


Figure 2.3: Antimicrobial effect of SCOBY on *E. hirae*.

The pH of the SCOBY culture was measured and recorded as  $3.5 \pm 0.5$ . This low pH was due to the acids produced by the microbes during fermentation, which lowered the pH of the culture. To determine if it was the low pH that was inhibiting growth or if it was indeed microbial action, the experiment was repeated but once the sample of the cellulose layer had been collected, it was rinsed and soaked in a pH 7 phosphate buffer. Once the pH of the SCOBY culture had reached  $7 \pm 0.5$ , it was added to the pre-inoculated TSA plates as before and incubated. When the pH had been adjusted, there were no zones of inhibition. This confirmed that it was the low pH of the fluid in the cellulose layer that had probably

inhibited growth, not any specific anti-microbial action exhibited by the microbes present in the culture. As such, this line of investigation was not pursued.

### **2.3.2: Isolating Antibiotic Producing Microbes from Soil Samples**

It was deemed important to attempt to isolate an antibiotic from an environmental sample rather than just purchase one from a laboratory supplier, as this would allow training on how to isolate an antibiotic from a culture, and eventually how to analyse the antibiotic using analytical techniques such as gas chromatography mass spectrometry (GCMS), liquid chromatography mass spectrometry (LCMS). To do this, a soil sample was taken from a garden environment and collected in a sterile bag and transferred to the laboratory under aseptic conditions and stored at 4 °C. The sample was taken from a grassy shaded area in a semi-urban area in the district of Wakefield, West Yorkshire, 10cm below the surface of top soil. To begin the search for an antibiotic producing microbe, the crowded plate technique was followed (Waksman, 1945). Briefly, 1 g of the soil sample was measured out and added to 9 ml of MRD to give an initial starting sample. Two 1 in 10 serial dilutions (1 cm<sup>3</sup> sample added to 9 ml MRD) were carried out to give a sample concentration of 10<sup>-2</sup> in relation to the initial starting sample. It was important that the microbes would not get too diluted, as crowded plates would allow the microbes to compete with each other and inhibition zones would be obvious. 100 µl of the dilutions were spread onto sterile TSA plates using a plate spreader and allowed to dry. The plates were incubated at room temperature (as they were collected during winter, so the traditional incubator temperature of 37 °C may be too high for some of the bacteria) until sufficient growth had occurred that the plates were completely covered in a lawn of bacteria; this was typically around 1-2 weeks. After this time period, the plates were examined for any areas of inhibition. Where inhibition had occurred, the

microbe assumed responsible was sub-sampled off the sample plate and streaked onto a fresh TSA plate. The streak plate process was repeated until the strain was isolated and pure, which was confirmed by a visual inspection of the plate and examining colonies via light microscopy. Phenotypic characteristics were examined using the naked eye (features such as colony shape, colour, speed of growth) to give a simple indication of the purity of the bacterial strains on the plate. The streak plate method was followed further until single colonies could be isolated. These colonies were incubated and were further assessed for their purity using other analytical techniques, such as Gram staining, and light microscopy analysis. Gram staining gave a good indication that all the cells present were of the same cell wall type, and although light microscopy does not give detailed insights into the very small cell components of bacterial cells, it gives a good indication of basic cell morphology such as shape. This gave further confidence that the isolated strains were pure and suitable for further downstream analyses.

Once pure isolates of the potential antibiotic producers had been collected, they were screened against 4 pathogenic organisms: *Escherichia coli* (NCIMB: 8879), *Enterococcus hirae* (NCIMB: 8191), *Pseudomonas aeruginosa* (10421) and *Staphylococcus aureus* (9518), the same microbes used in the SCOPY experiments. The cross streak method (Velho-Pereira & Kamat, 2011) was used to examine any antimicrobial activity that might be exhibited by the collected isolates. A single colony of the isolate was spread vertically down the centre of the plate. The plate was then incubated at room temperature for 5-7 days, or until a band with a 1 cm width had grown. This allowed time for metabolites to diffuse through the agar, including any antibiotic if present. A single colony of each of the 4 pathogenic test organisms was streaked perpendicularly across the plate towards the test isolate. The pathogenic organisms were streaked close to, but not touching the test isolate, and allowed to grow for a further 5-7 days at room temperature. After the incubation period,

the plates were examined for any inhibition zones. An example of a typical cross streak test can be seen in figure 2.4 below.

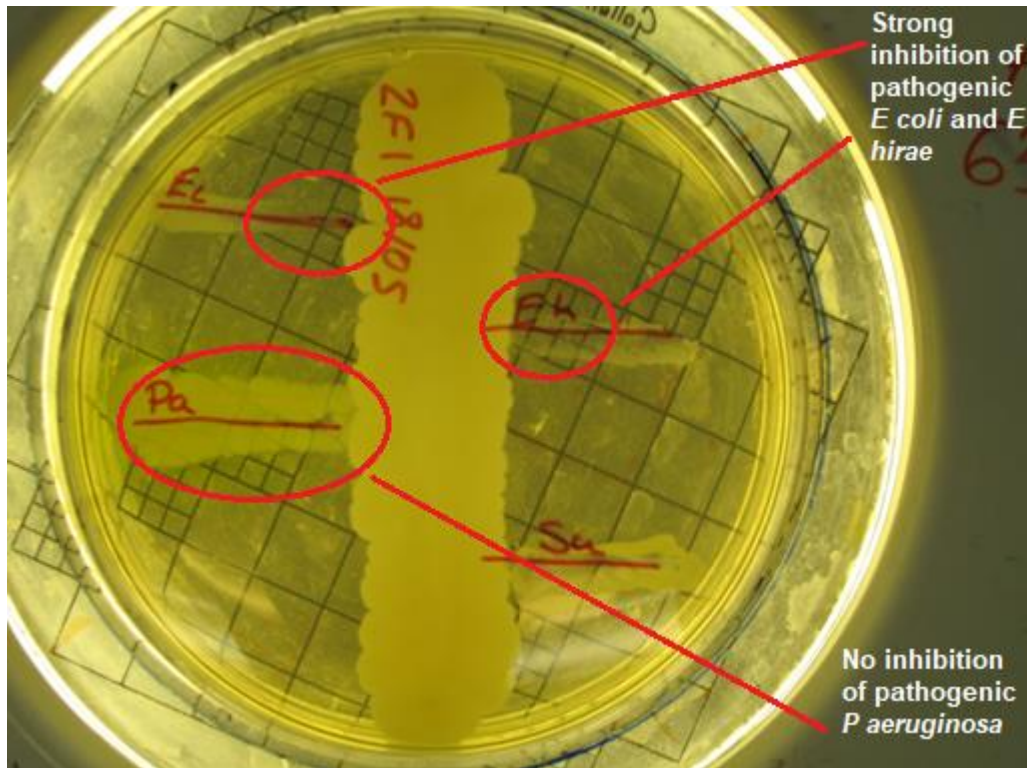


Figure 2.4: An example of cross streak testing against antibiotic resistant bacteria, showing intermediate inhibition of *E. coli* and weak inhibition of *E. hirae*.

Most antibiotics in use today have microbial origins. The *Streptomyces* genus produce more than 70 % of commercially available antibiotics (Kitani et al., 2011). Therefore, actinomycete isolation agar was prepared in an attempt to isolate bacteria from the *Streptomyces* genus. *Streptomyces* bacteria typically have a rough, white, leathery appearance and produce geosmin, a volatile metabolite which produces a typically earthy odour (Bizuye, Moges, & Andualem, 2013). Bacteria matching these phenotypic characteristics (i.e. having a rough, white, leathery appearance) were carefully selected off the agar using a sterile inoculating loop and purified using the isolation method described previously and tested for antimicrobial activity, as with the crowded plate bacteria above. However, no *Streptomyces* bacteria were found that exhibited any antimicrobial activity.

### 2.3.3: Isolation Chip (iChip)

As described previously, the iChip is a novel method for growing previously un-cultivable bacteria in a laboratory environment. The iChip is a multi-channel device made up of two exterior plates and a central interior plate. The central plate is submerged in molten agar containing an environmental sample and allowed to dry. The iChip is then assembled and incubated in-situ in an attempt to raise the in-vitro growth rate of microbes from 1 % to nearer 15 % (Nichols et al., 2010). The iChip assembly can be seen in figure 2.5 below.

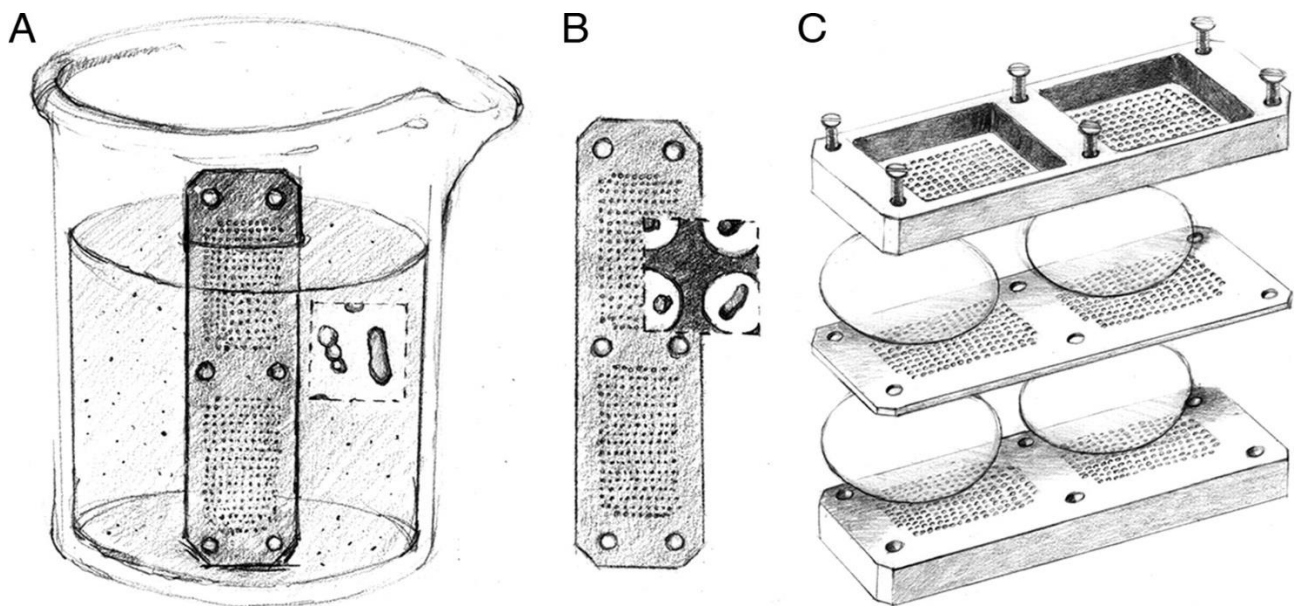


Figure 2.5: iChip assembly showing (A) the central plate being submerged in molten agar containing environmental sample, (B) how the iChip's wells "capture" bacteria in solidified agar plugs and (C) the assembly of the iChip containing suitable membranes allowing nutrients to diffuse into the agar from the external environment, but restricts the movement of bacteria (Ling et al., 2015).

An iChip style device was manufactured via 3-D printing by The Department of Forensic Engineering at the University of Huddersfield and was assessed for suitability in future experiments (see figure 2.6 below). Appropriate nuts and bolts to screw the iChip together were obtained along with 0.03  $\mu\text{m}$  membranes. The membranes had to be small enough to restrict movement of bacterial cells, but still allow nutrients to move through from the external environment. The components of the iChip were sterilised by autoclaving and were aseptically transferred to sterile petri dishes until needed. It was important to test the effectiveness of the iChip's seal; this was done by preparing the iChip containing only sterile agar and then incubating the iChip overnight in a broth containing *Escherichia coli* NCTC 10418. The iChip was disassembled and the agar plugs in the central plate were examined for microbial growth by light microscope. The plugs examined remained sterile, so this proved that the membranes prevent movement of microbes from the external environment into the iChip and that the tightened nuts and bolts provided an adequate seal from the external environment.

The iChip was prepared for microbial incubation by the method of Nichols et al., (2010). Briefly, 100  $\mu\text{g}$  of soil was suspended in 100 ml MRD and vortexed until homogenous. 100 ml of molten agar was prepared and stored in a sterile 100 ml falcon tube. 1 ml of the soil solution was pipetted into the molten agar. The central plate of the iChip was added and mixed slowly. The molten agar was allowed to cool and form plugs in the iChip's central plate. The aim was to "trap" bacteria in the wells of the central plate, so they can be incubated *in situ*. The 0.03  $\mu\text{m}$  membranes were applied to each set of holes around the central plate (4 in total). Finally, the two outer plates are attached to the central plate and screwed tightly together with appropriate nuts and bolts to form a pressurised seal around the central plate. The iChip was incubated *in situ* in 10  $\text{cm}^3$  of soil in a garden style environment, providing the microbial cells with the nutrients from their natural environment.

The iChip was incubated for 7-10 days 10 cm below the surface in a grassy, shaded area next to St Paul's Hall at the University of Huddersfield during the month of April 2016. The area was 10 m away from a main road and approximately 10 m away from the Applied Sciences building at the university, with a footpath through the area. In the area there are several mature tall trees, with a variety of wildlife including squirrels, jackdaws and other typical birds native to England. The iChip was buried 30 cm away from one of the trees, with the location marked and signed appropriately. After the incubation period *in situ*, the iChip was retrieved and transported back to the laboratory in sealed, sterile bag. The iChip was then washed vigorously in DNA grade water before being disassembled.

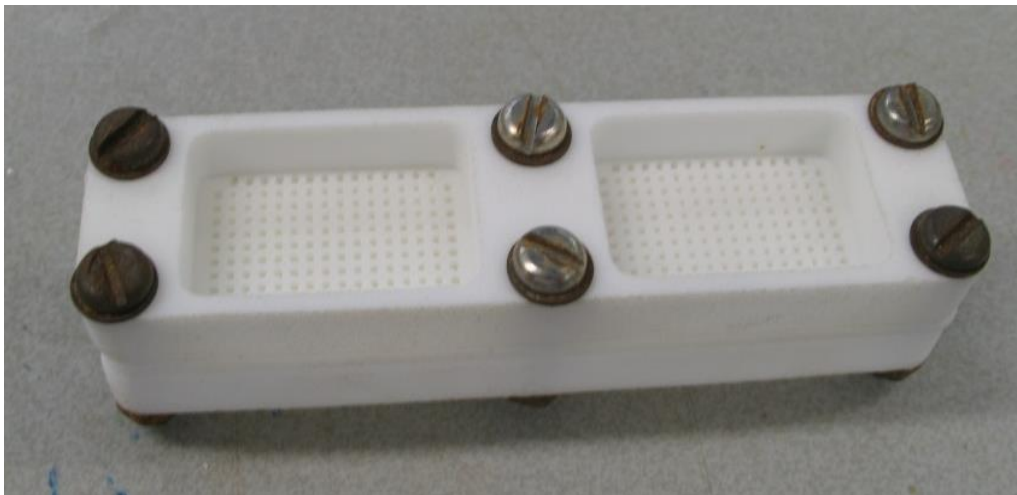


Figure 2.6: Assembled 3-D printed iChip.

The iChip was disassembled and agar plugs were removed by sterile unwound paper clips. The agar plugs were then examined under light microscope to look for microbial growth. Agar plugs that exhibited growth were aseptically transferred to agar plates and streaked across the plate using a sterile plate spreader. The plates were incubated and allowed to grow for 5-7 days until there was a lawn of bacteria covering the plate.

As in the crowded soil plate experiments, the crowded plates were examined for inhibition zones. The microbes presumed responsible for producing the inhibition zones were identified by placing the agar plate on a colony counting unit. Using the light from the colony counting unit, one could clearly see a single colony of microbes at the centre of each inhibition zone (see figure 2.11 below). It was therefore simple to identify the microbes which were exhibiting an antimicrobial effect on their neighbours. These colonies at the centre of each inhibition zone were carefully selected off the plate using a sterile inoculating loop and purified by using the streak plate method to obtain pure colonies, as described previously (Sanders, 2012). These isolates were examined for the antimicrobial activity against seven pathogenic organisms, specifically,  $\beta$ -lactamase producing bacteria. The pathogens were purchased from Public Health England (PHE) and included: the carbapenemase KPC-3 producing *Klebsiella pneumoniae* NCTC strain 13438, the VIM-1 producing *Klebsiella pneumoniae* NCTC strain 13440, the OXA-48 producing *Klebsiella pneumoniae* NCTC 13442, the NDM-1 producing *Klebsiella pneumoniae* NCTC 13443, methicillin resistant *Staphylococcus aureus* NCTC 12493, the IMP producing *Escherichia coli* NCTC 13476 and finally a  $\beta$ -lactamase negative *Escherichia coli* NCTC 10418. Over 200 cross streak plates were prepared for potential antimicrobial producing organisms isolated from iChip testing. Once replicate testing had taken place, the initial number was reduced from over 200 organisms to 7 organisms that were observed to consistently inhibit the same pathogens upon repeats.

Results of the cross streaking were recorded as showing weak inhibition (1-2 mm inhibition zones), intermediate inhibition (2-4 mm inhibition zones) or strong inhibition (>4 mm inhibition zones). An example of a cross streak test using the  $\beta$ -lactamase producing bacteria can be seen in figure 2.7 below.

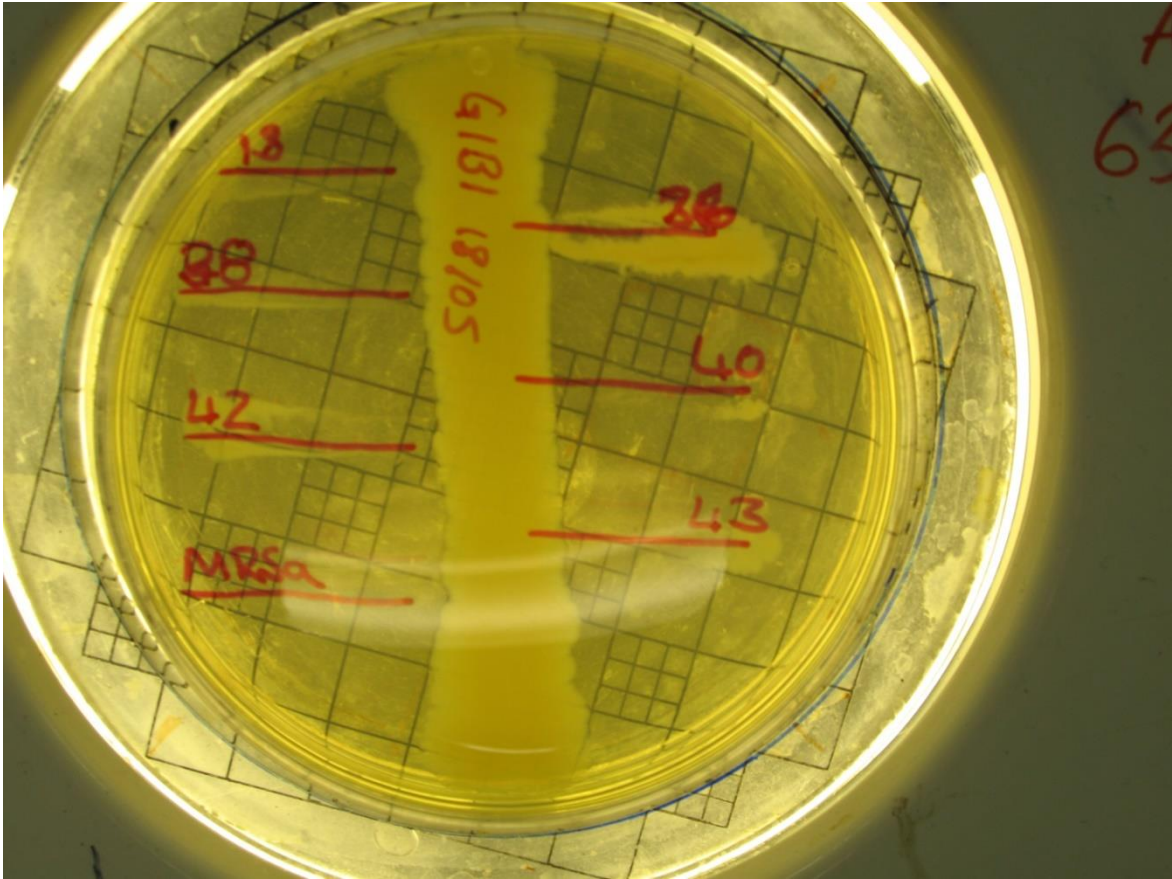


Figure 2.7: An example of cross streak testing against antibiotic resistant bacteria, showing strong inhibition against *Escherichia coli* NCTCC 10418, *Klebsiella pneumoniae* NCTCC 13340 and *Klebsiella pneumoniae* NCTCC 13343.

### 2.3.4: Polymerase Chain Reaction (PCR)

The key concept of the iChip is that it facilitates the growth of previously unculturable bacteria. To test this hypothesis, polymerase chain reaction (PCR) took place to examine the specific strains of microbes that the iChip had cultivated.

The 7 organisms were identified by polymerase chain reaction (PCR) experiments. PCR can be used to identify microbial organisms based upon their DNA sequence. DNA sequences are unique to individual strains and can be used to confidently identify the species and specific strain of an organism. PCR for microbial identification is a process which involves amplifying a target area of the 16S rDNA gene to a certain concentration so that the gene can be sequenced and the organism identified. Specific primers are used so that only the required region of the 16S rDNA gene is amplified. Although all organisms have a unique DNA sequence, there are conserved regions across all bacterial species, and this is also true in the 16S rDNA gene, as shown in figure 2.8 below. The variable region allows identification of the bacteria.

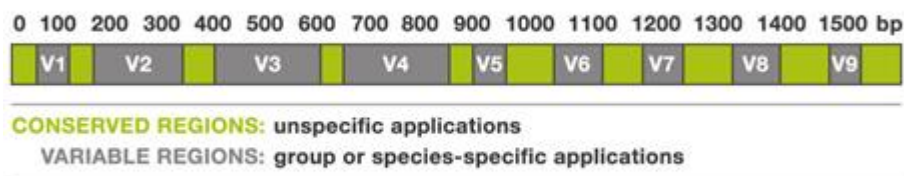


Figure 2.8: Variable and conserved regions found in the 16S rDNA gene (Alimetrics, n.d.).

A Mo Bio Ultra-Clean Microbial Isolation Kit was ran in accordance to the manufacturer's instructions (Mo Bio, n.d.), but will be briefly described here. The sample is first prepared by adding appropriate amounts of initial bacterial sample, primer and polymerase/base

mixture into solution. The cells are ruptured in this process, releasing the DNA into the extracellular environment. The samples are centrifuged and filtered a number of times so that only the DNA is left in the sample. At this stage, the samples are run through an electrophoresis gel, which is created by dissolving 1 g of agarose powder in 100 ml of ultra-pure water. The aim of the electrophoresis is to ensure that there is actually DNA present in the sample, without contamination, and that the preparation procedure to isolate the correct DNA from the bacteria has been a success. An example of an electrophoresis from the PCR process can be seen in figure 2.9 below. The lane on the far left hand side of the agarose gel was the reference ladder used for determining the size of the DNA fragment present in the PCR mixture. This contained reference DNA fragments, of which the molecular weight (and base pair [BP] length) is known and standardised, against which samples obtained from PCR were compared. The length of the 16s rDNA gene in the PCR experiment was approximately 1500 BP; the obtained samples were compared to the reference marker in the ladder (which contained a 1500 BP marker), to give an indication to whether the PCR had been successful.

DNA has a net negative charge owing to the phosphate backbone of the DNA chain (Yamasaki, Teramoto & Yoshikawa, 2001). The agarose gel works by separating components based on size. Smaller DNA fragments can traverse the viscous gel medium more quickly, so move closer to the positive anode, whilst the opposite is true for longer DNA fragments. This allows DNA fragments to be reliably separated based upon their length and compared to a reference ladder.

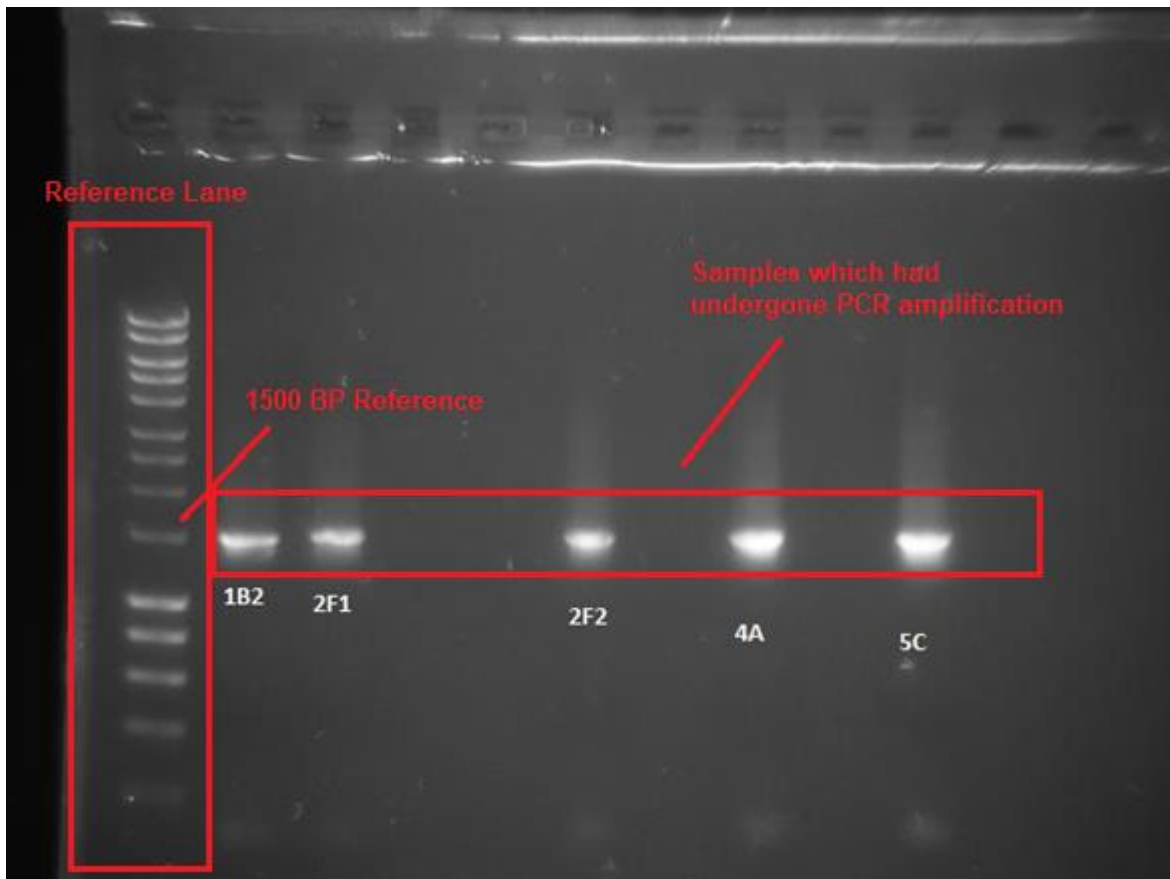


Figure 2.9: Example of electrophoresis run on samples, clearly showing the PCR products being the desired length in the region of 1500 BP (owing to the tight banding to the 1500 BP reference marker in the ladder), indicating successful PCR amplification for the region of interest.

The first step in the PCR process is to separate the double helix strands of DNA in the denaturation process, which takes place at 95 °C. At this temperature, the DNA denatures and essentially unravels to form an upper (sense) and lower (anti sense) strands. This allows the primers present in the primer mix (myTaq) to begin pairing up to the exposed strands of DNA. The second process is the annealing process of the primers. Appropriate primers must be selected that will match the gene of interest to be amplified. In taxonomic identification, the fact there is a conserved region in the 16S rDNA across all bacterial species is exploited: an 8F1510R primer is used that will begin the amplification process in the conserved regions

of the 16S rDNA gene. The primer works from both the 8 forward position and the 1510 reverse position on separate DNA strands (hence the name of the primer, 8F1510R). The annealing stage operates at 60 °C, which is cool enough to allow the reaction of the primers present in the primer mix to react and form pairs with the exposed bases on the strands of DNA. The final stage is the elongation stage; the temperature is raised to a value specific to the polymerase enzyme being used (72 °C in the current experiment) which binds the nucleotide bases to the rest of the DNA strand, completing the replication process. Normally, 72 °C would cause enzymes to denature, but the polymerase typically used in PCR experiments is extracted from a strain of *Thermus aquaticus*, which are present in the hot springs of Yellowstone National Park, USA, which are capable of living at high temperatures (University of Utah, 2016). These 3 stages are repeated a total of 33 times to amplify the required 16s rDNA gene. The PCR schematic is shown in figure 2.10 below.

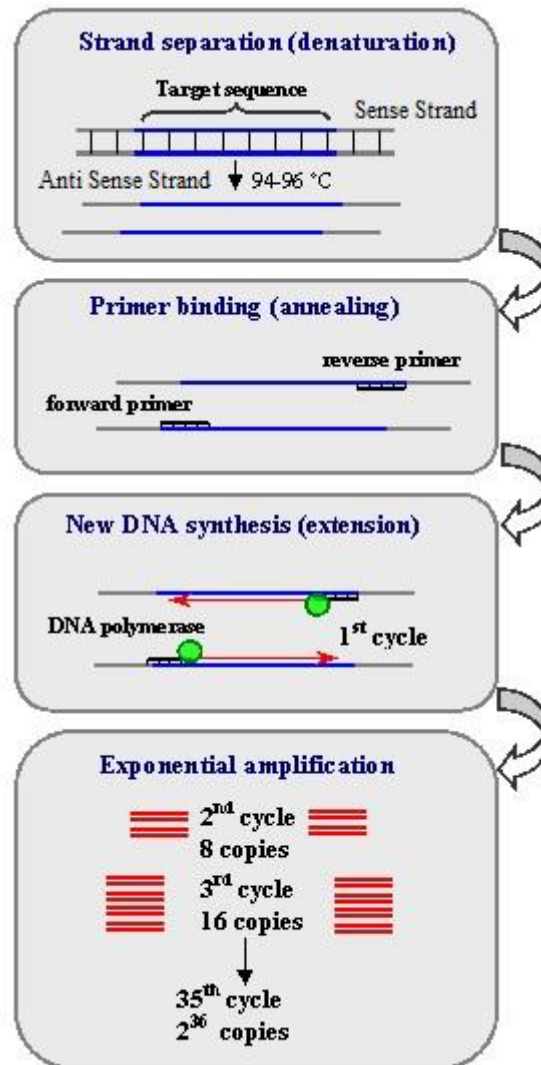


Figure 2.10: Overview of PCR Process (National Centre Biotechnology Information, 2014).

Importantly, the primer mix used contains dideoxy nucleotides – also known as chain terminating nucleotides. These specific nucleotides are the same as regular nucleotides also contained in the primer mix, apart from the fact they lack a hydroxyl (OH) group on the 3' carbon. The lacking OH group prevents other nucleotides bonding to the chain terminating nucleotide. This therefore terminates the sequencing of this chain, preventing the elongation of this specific chain of DNA. The dideoxy nucleotides present in the primer mix are approximately present at a 100 fold lower concentration than the regular nucleotides. The fact that there are billions of copies of the replicated DNA strand allows the statistical

inevitability that there will be a chain terminating dideoxy nucleotide present at every possible position in the replicated DNA strands. The dideoxy nucleotides are also labelled with a specific colour dye, which allows the specific nucleotides to be identified in downstream processing. After this process, the DNA samples were purified and corrected to appropriate concentration levels in DNA/RNA treated water. The replicated DNA strands were sent for external sequencing at Eurofins Laboratories in Wolverhampton, where the Sanger sequencing method was employed. The Sanger sequencing method takes advantage of the fact that there will be a dideoxy nucleotide base at every possible sequence in the DNA strand. The DNA samples are then ran through a capillary gel electrophoresis. The DNA strands exit the capillary gel electrophoresis tube in size order, as according to their molecular weight, with the DNA strands terminating after just one sequence exiting the gel first, and so on. The DNA strands are illuminated with a laser which allows the fluorescence emitted by the specific dye colour to be detected by a fluorescence detector. This therefore allows for the detection of the specific base at that position in the sequence. This process is repeated until all of the chains have been processed by the electrophoresis gel, allowing the complete DNA chain to be sequenced. The sequences were then compared to an academic database containing the DNA sequence of every characterised microbe. This allows analysis of the extracted DNA sequences and the percentage similarity gives an indication of the novelty of the microbe. Different academic sources may have different cut offs for defining a sample as a completely novel strain, but generally a similarity percentage of less than 97 % can be grounds for claiming a completely novel, previously uncharacterised microbial strain (Fenollar, Roux, Stein, Drancourt, Raoult, 2006), (Srinivasan et al., 2015), (Reller, Weinstein, Petti, 2007). A similarity score of between 97 % and 99 % allows microbiologists to classify the genus, whilst a similarity score of more than 99 % allows classification to the species level (for example, a similarity score of more than 99 % would indicate a species

match, whereas a similarity score of between 97-99 % indicates a genus match). A match of less than 97 % allows a claim for a novel strain to be made and is the generally accepted cut off points in academic literature within the field of microbiology.

### 2.3.5: Metabolomics

Once the bacterial isolates showing antimicrobial activity had been identified by PCR experiments, the next stage of the experiment was to attempt to identify the metabolites being produced and investigate what may be causing antimicrobial activity. The samples were grown in Tryptone soy broth (TSB), which essentially contain the same ingredients as TSA, but contain fewer solidifying agents, so would remain in liquid state even at room temperatures. Samples were incubated for 7 days in an orbital incubator operating at 30 °C / 100 RPM. After the incubation period, samples were centrifuged using a large rotor at 4°C / 8,500 RPM for 20 minutes.

The supernatant was collected and filter sterilised so the samples could be transported to non-class 2 laboratories and analysed. The supernatant was added to equal volumes of various solvents, including ethyl acetate, dichloromethane and chloroform shaken vigorously and incubated once again in an orbital incubator overnight to allow the solvent to extract any potential antibiotic from the TSB supernatant. Along with solvent extraction taking place, the neat aqueous solution was freeze dried in an attempt to concentrate any potential antibiotic. After incubation, the solvent phase was collected using an extracting funnel and allowed to dry in a fume cabinet. The aqueous phase was also collected and stored separately. Once the solvent samples were dry, a yellow/brown gummy layer was collected. The first attempt to re-dissolve the samples used ultra-pure water, but after several

attempts the gummy brown layer remained un-dissolved. It was decided to try and use a different solvent; dimethyl sulfoxide (DMSO) was selected and seemed to work well to dissolve the gummy brown substance. A method to identify the metabolites was developed using an Agilent 6500 series LC-MS Q-TOF. A 1 µl injection was analysed over a 15 minute draw time using an Agilent Zorbax SB-C18 column. A jet stream electrospray ionisation source was used to ionise the sample, running in positive polarity mode. Samples were analysed in triplicate. De-ionised water was used as a system blank and a sterile sample of TSB was used as a sample blank. The rotary evaporated solvent extracts and the freeze dried aqueous solution were dissolved in DMSO and ran on LCMS-QToF in an attempt to identify any potential antibiotics.

## **2.4: Results**

### **2.4.1: iChip Results**

The crowded plates created from the agar plugs of the iChip were examined for the presence of antimicrobial producing microbes, as identified by an inhibition zone. Visual inspection of the iChip crowded plates showed many zones of inhibition, as shown in figure 2.11 below.

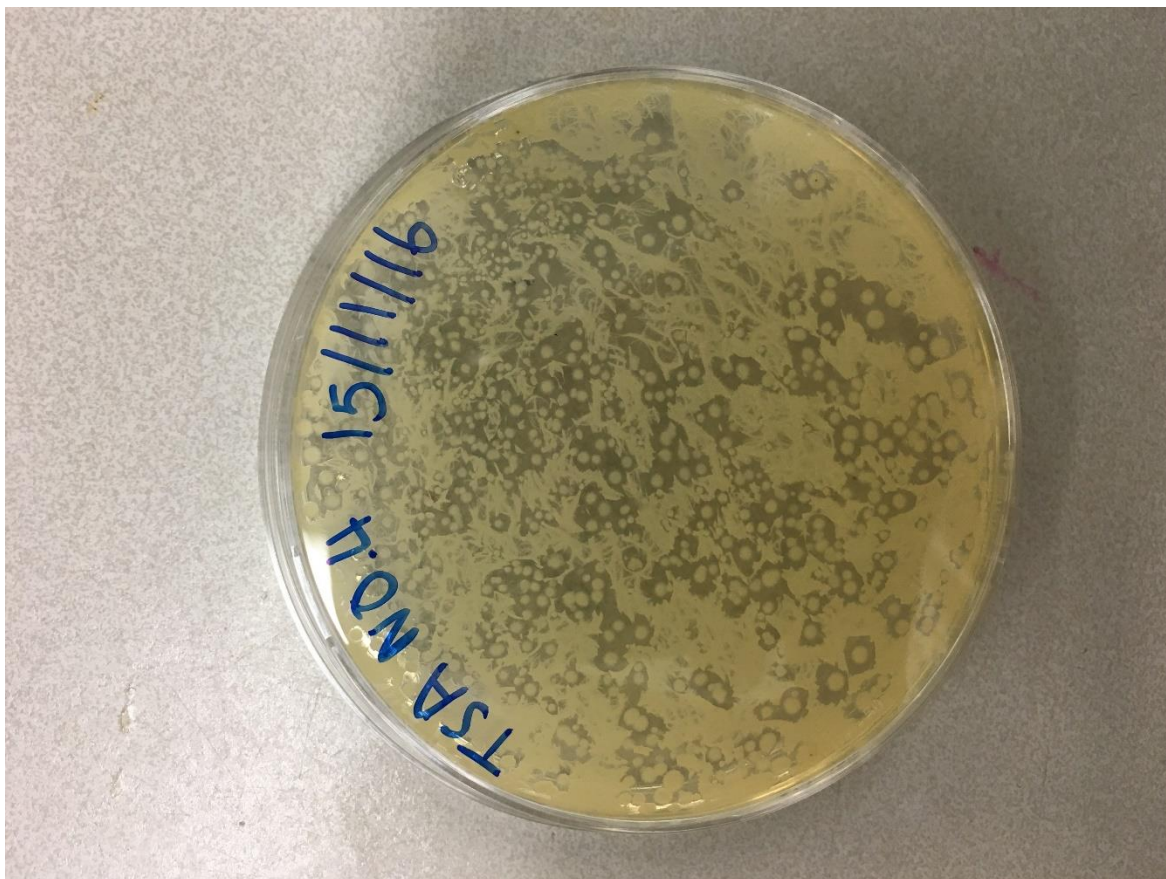


Figure 2.11: Typical example of an iChip crowded plate.

Over 200 antimicrobial producing microbes were isolated and purified as described previously and after repeated tests, these were narrowed down to 7 organisms. The PCR sequences of these organisms are discussed further in this chapter.

#### 2.4.1: Inhibition Testing Results

Inhibition zones for the  $\beta$ -lactamase producing bacteria were graded as showing weak inhibition (1-2 mm inhibition zones) recorded as '1', intermediate inhibition (2-4 mm inhibition zones) recorded as '2', or strong inhibition (>4 mm inhibition zones) recorded as '3' (raw data tables can be found in the appendix). The 7 test organisms used were *Klebsiella*

*pneumoniae* 13438, *Klebsiella pneumoniae* 13440, *Klebsiella pneumoniae* 13443, *Klebsiella pneumoniae* 13442, *Escherichia coli* 13476, a strain of Methicillin Resistant *Staphylococcus aureus* and *Escherichia coli* 10418 as a  $\beta$ -lactamase negative control.

The total inhibition scores were averaged, and the numerical values were used to create a heat map using RStudio and can be seen in figure 2.12 below.

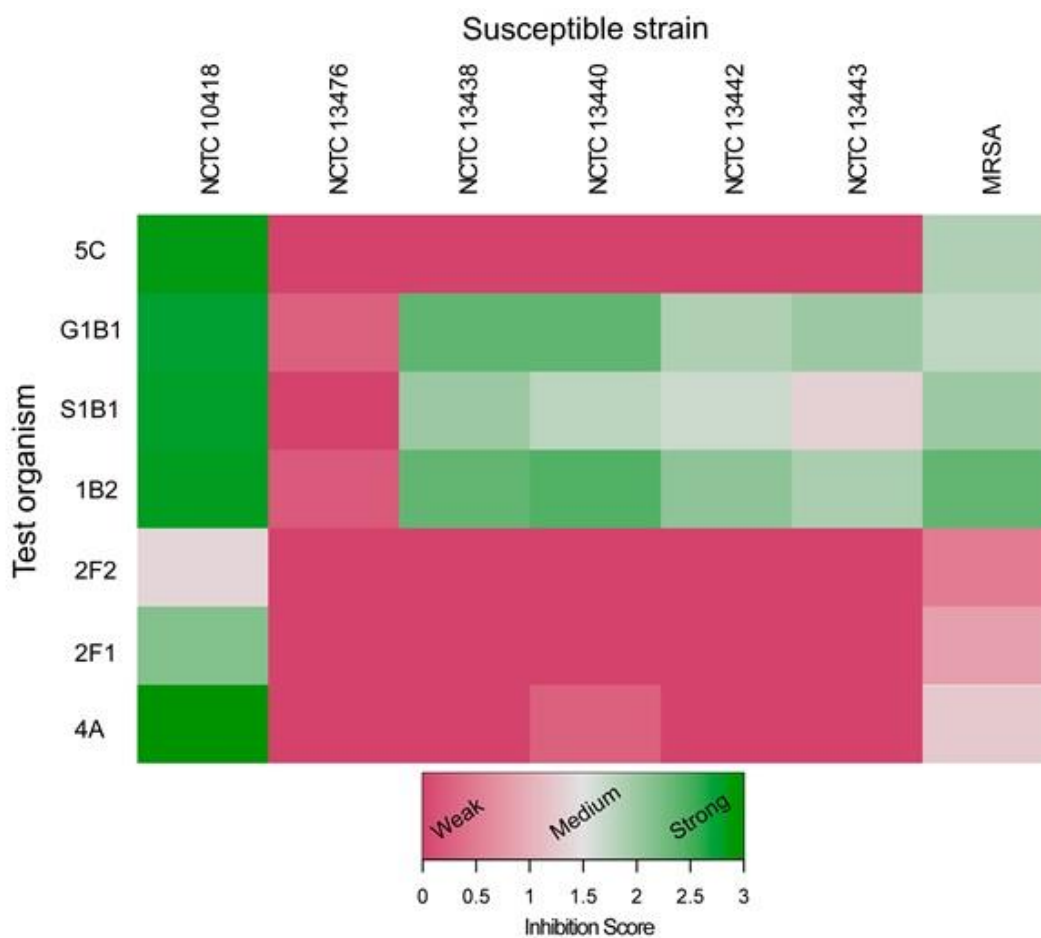


Figure 2.12: Heat map of inhibition scores.

On figure 2.12 above, green colours indicate cross streak tests where strong inhibition was noted against the pathogenic strain, and red colours indicate where weak to no inhibition was recorded. As can be seen, the strongest inhibition was shown against *E. coli* NCTC 10418 by almost all the antimicrobial producing test organisms. This is perhaps

unsurprising, as this was a  $\beta$ -lactamase negative control pathogen, perhaps indicating it lacks the defensive capability to protect itself from whatever the antimicrobial producing test organisms may be creating to exhibit their lethal effect on this organism. Practically no microbial inhibition was seen against *E. coli* NCTC 13476, which is an MBL, IMP producing microbe. Test organisms 5C, 2F1, 2F2 and 4A are largely ineffective against the other  $\beta$ -lactamase producing bacteria, but G1B1, S1B1 and 1B2 show medium to strong inhibition of these pathogenic microbes. G1B1 and 1B2 seemed to be strong inhibitors of these pathogenic,  $\beta$ -lactamase (including MBL) producing bacteria.

#### **2.4.2: Polymerase Chain Reaction Results**

After the purified PCR samples had been sequenced, the sequencing information was processed using National Centre for Biotechnology Information's Basic Local Alignment Search Tool (BLAST) database (National Centre for Biotechnology, 2016). The figures below show the top matches for the isolated potential antibiotic producers when compared to the BLAST database. The sequences were then analysed using Molecular Evolutionary Genetics Analysis (MEGA) software (Molecular Evolutionary Genetics Analysis, 2016). The BLAST tool is a library containing the genetic information of many different microbial species and strains, against which the sequenced 16S rDNA gene can be compared and the closest matches can be given.

Figure 2.13 below shows the closest DNA BLAST matches for G1B1.

Alignments <a href="#">Download</a> <a href="#">GenBank</a> <a href="#">Graphics</a> <a href="#">Distance tree of results</a>						
Description	Max score	Total score	Query cover	E value	Ident	Accession
<input checked="" type="checkbox"/> <a href="#">Pseudomonas baetica strain a390 16S ribosomal RNA gene, partial sequence</a>	1580	1580	99%	0.0	100%	<a href="#">NR_116899.1</a>
<input checked="" type="checkbox"/> <a href="#">Pseudomonas umsongensis strain Ps 3-10 16S ribosomal RNA gene, partial sequence</a>	1568	1568	99%	0.0	99%	<a href="#">NR_025227.1</a>
<input checked="" type="checkbox"/> <a href="#">Pseudomonas jessenii strain CIP 105274 16S ribosomal RNA gene, partial sequence</a>	1554	1554	99%	0.0	99%	<a href="#">NR_024918.1</a>
<input checked="" type="checkbox"/> <a href="#">Pseudomonas helmanticensis strain OHA11 16S ribosomal RNA gene, partial sequence</a>	1552	1552	99%	0.0	99%	<a href="#">NR_126220.1</a>
<input checked="" type="checkbox"/> <a href="#">Pseudomonas reinekei strain MT1 16S ribosomal RNA gene, partial sequence</a>	1546	1546	99%	0.0	99%	<a href="#">NR_042541.1</a>
<input checked="" type="checkbox"/> <a href="#">Pseudomonas moorei strain RW10 16S ribosomal RNA gene, partial sequence</a>	1541	1541	99%	0.0	99%	<a href="#">NR_042542.1</a>
<input checked="" type="checkbox"/> <a href="#">Pseudomonas vancouverensis strain DhA-51 16S ribosomal RNA gene, partial sequence</a>	1541	1541	99%	0.0	99%	<a href="#">NR_041953.1</a>
<input checked="" type="checkbox"/> <a href="#">Pseudomonas migulae strain NBRC 103157 16S ribosomal RNA gene, partial sequence</a>	1539	1539	99%	0.0	99%	<a href="#">NR_114223.1</a>
<input checked="" type="checkbox"/> <a href="#">Pseudomonas migulae strain CIP 105470 16S ribosomal RNA gene, partial sequence</a>	1539	1539	99%	0.0	99%	<a href="#">NR_024927.1</a>
<input checked="" type="checkbox"/> <a href="#">Pseudomonas koreensis strain Ps 9-14 16S ribosomal RNA gene, partial sequence</a>	1535	1535	99%	0.0	99%	<a href="#">NR_025228.1</a>
<input checked="" type="checkbox"/> <a href="#">Pseudomonas mohnii strain lpA-2 16S ribosomal RNA gene, partial sequence</a>	1533	1533	99%	0.0	99%	<a href="#">NR_042543.1</a>
<input checked="" type="checkbox"/> <a href="#">Pseudomonas fluorescens Pf0-1 strain Pf0-1 16S ribosomal RNA, complete sequence</a>	1524	1524	99%	0.0	99%	<a href="#">NR_102835.1</a>
<input checked="" type="checkbox"/> <a href="#">Pseudomonas moraviensis strain 1B4 16S ribosomal RNA gene, partial sequence</a>	1524	1524	99%	0.0	99%	<a href="#">NR_043314.1</a>
<input checked="" type="checkbox"/> <a href="#">Pseudomonas putida KT2440 strain KT2440 16S ribosomal RNA, complete sequence</a>	1519	1519	99%	0.0	99%	<a href="#">NR_074596.1</a>
<input checked="" type="checkbox"/> <a href="#">Pseudomonas brenneri strain CFML 97-391 16S ribosomal RNA gene, partial sequence</a>	1517	1517	99%	0.0	99%	<a href="#">NR_025103.1</a>
<input type="checkbox"/> <a href="#">Pseudomonas monteilii 16S ribosomal RNA, complete sequence</a>	1513	1513	99%	0.0	99%	<a href="#">NR_121767.1</a>
<input type="checkbox"/> <a href="#">Pseudomonas entomophila strain L48 16S ribosomal RNA gene, complete sequence</a>	1513	1513	99%	0.0	99%	<a href="#">NR_102854.1</a>
<input type="checkbox"/> <a href="#">Pseudomonas putida F1 strain F1 16S ribosomal RNA, complete sequence</a>	1513	1513	99%	0.0	99%	<a href="#">NR_074739.1</a>
<input type="checkbox"/> <a href="#">Pseudomonas taiwanensis strain BCRC 17751 16S ribosomal RNA gene, partial sequence</a>	1513	1513	99%	0.0	99%	<a href="#">NR_116172.1</a>
<input checked="" type="checkbox"/> <a href="#">Pseudomonas panacis strain CG20106 16S ribosomal RNA gene, partial sequence</a>	1511	1511	99%	0.0	99%	<a href="#">NR_043195.1</a>
<input type="checkbox"/> <a href="#">Pseudomonas monteilii strain NBRC 103158 16S ribosomal RNA gene, partial sequence</a>	1507	1507	99%	0.0	98%	<a href="#">NR_114224.1</a>
<input checked="" type="checkbox"/> <a href="#">Pseudomonas mosselii strain CFML 90-83 16S ribosomal RNA gene, partial sequence</a>	1507	1507	99%	0.0	98%	<a href="#">NR_024924.1</a>

Figure 2.13: Closest DNA BLAST matches for G1B1.

Figure 2.14 below shows the closest DNA BLAST matches for S1B1.

Alignments <a href="#">Download</a> <a href="#">GenBank</a> <a href="#">Graphics</a> <a href="#">Distance tree of results</a>						
Description	Max score	Total score	Query cover	E value	Ident	Accession
<input checked="" type="checkbox"/> <a href="#">Pseudomonas baetica strain a390 16S ribosomal RNA gene, partial sequence</a>	1659	1659	100%	0.0	99%	<a href="#">NR_116899.1</a>
<input checked="" type="checkbox"/> <a href="#">Pseudomonas umsongensis strain Ps 3-10 16S ribosomal RNA gene, partial sequence</a>	1648	1648	100%	0.0	99%	<a href="#">NR_025227.1</a>
<input checked="" type="checkbox"/> <a href="#">Pseudomonas helmanticensis strain OHA11 16S ribosomal RNA gene, partial sequence</a>	1631	1631	100%	0.0	99%	<a href="#">NR_126220.1</a>
<input checked="" type="checkbox"/> <a href="#">Pseudomonas jessenii strain CIP 105274 16S ribosomal RNA gene, partial sequence</a>	1629	1629	100%	0.0	99%	<a href="#">NR_024918.1</a>
<input checked="" type="checkbox"/> <a href="#">Pseudomonas reinekei strain MT1 16S ribosomal RNA gene, partial sequence</a>	1622	1622	100%	0.0	99%	<a href="#">NR_042541.1</a>
<input checked="" type="checkbox"/> <a href="#">Pseudomonas moorei strain RW10 16S ribosomal RNA gene, partial sequence</a>	1620	1620	100%	0.0	99%	<a href="#">NR_042542.1</a>
<input checked="" type="checkbox"/> <a href="#">Pseudomonas vancouverensis strain DhA-51 16S ribosomal RNA gene, partial sequence</a>	1620	1620	100%	0.0	99%	<a href="#">NR_041953.1</a>
<input checked="" type="checkbox"/> <a href="#">Pseudomonas migulae strain NBRC 103157 16S ribosomal RNA gene, partial sequence</a>	1618	1618	99%	0.0	99%	<a href="#">NR_114223.1</a>
<input checked="" type="checkbox"/> <a href="#">Pseudomonas migulae strain CIP 105470 16S ribosomal RNA gene, partial sequence</a>	1618	1618	99%	0.0	99%	<a href="#">NR_024927.1</a>
<input checked="" type="checkbox"/> <a href="#">Pseudomonas koreensis strain Ps 9-14 16S ribosomal RNA gene, partial sequence</a>	1615	1615	100%	0.0	99%	<a href="#">NR_025228.1</a>
<input checked="" type="checkbox"/> <a href="#">Pseudomonas mohnii strain lpA-2 16S ribosomal RNA gene, partial sequence</a>	1613	1613	100%	0.0	99%	<a href="#">NR_042543.1</a>
<input checked="" type="checkbox"/> <a href="#">Pseudomonas moraviensis strain 1B4 16S ribosomal RNA gene, partial sequence</a>	1605	1605	100%	0.0	99%	<a href="#">NR_043314.1</a>
<input checked="" type="checkbox"/> <a href="#">Pseudomonas fluorescens Pf0-1 strain Pf0-1 16S ribosomal RNA, complete sequence</a>	1604	1604	100%	0.0	99%	<a href="#">NR_102835.1</a>
<input checked="" type="checkbox"/> <a href="#">Pseudomonas putida KT2440 strain KT2440 16S ribosomal RNA, complete sequence</a>	1598	1598	100%	0.0	99%	<a href="#">NR_074596.1</a>
<input checked="" type="checkbox"/> <a href="#">Pseudomonas brenneri strain CFML 97-391 16S ribosomal RNA gene, partial sequence</a>	1596	1596	99%	0.0	99%	<a href="#">NR_025103.1</a>
<input checked="" type="checkbox"/> <a href="#">Pseudomonas monteilii 16S ribosomal RNA, complete sequence</a>	1592	1592	100%	0.0	99%	<a href="#">NR_121767.1</a>
<input type="checkbox"/> <a href="#">Pseudomonas entomophila strain L48 16S ribosomal RNA gene, complete sequence</a>	1592	1592	100%	0.0	99%	<a href="#">NR_102854.1</a>
<input type="checkbox"/> <a href="#">Pseudomonas putida F1 strain F1 16S ribosomal RNA, complete sequence</a>	1592	1592	100%	0.0	99%	<a href="#">NR_074739.1</a>
<input checked="" type="checkbox"/> <a href="#">Pseudomonas taiwanensis strain BCRC 17751 16S ribosomal RNA gene, partial sequence</a>	1592	1592	100%	0.0	99%	<a href="#">NR_116172.1</a>
<input checked="" type="checkbox"/> <a href="#">Pseudomonas panacis strain CG20106 16S ribosomal RNA gene, partial sequence</a>	1591	1591	99%	0.0	99%	<a href="#">NR_043195.1</a>

Figure 2.14: Closest DNA BLAST matches for S1B1.

Figure 2.15 below shows the closest DNA BLAST matches for 1B2.

Alignments <a href="#">Download</a> <a href="#">GenBank</a> <a href="#">Graphics</a> <a href="#">Distance tree of results</a>						
Description	Max score	Total score	Query cover	E value	Ident	Accession
<a href="#">Pseudomonas baetica strain a390 16S ribosomal RNA gene, partial sequence</a>	1500	1500	100%	0.0	99%	<a href="#">NR_116899.1</a>
<a href="#">Pseudomonas umsongensis strain Ps 3-10 16S ribosomal RNA gene, partial sequence</a>	1483	1483	100%	0.0	99%	<a href="#">NR_025227.1</a>
<a href="#">Pseudomonas iessenii strain CIP 105274 16S ribosomal RNA gene, partial sequence</a>	1476	1476	100%	0.0	99%	<a href="#">NR_024918.1</a>
<a href="#">Pseudomonas helmanticensis strain OHA11 16S ribosomal RNA gene, partial sequence</a>	1472	1472	100%	0.0	99%	<a href="#">NR_126220.1</a>
<a href="#">Pseudomonas reinkei strain MT1 16S ribosomal RNA gene, partial sequence</a>	1469	1469	100%	0.0	99%	<a href="#">NR_042541.1</a>
<a href="#">Pseudomonas moorei strain RW10 16S ribosomal RNA gene, partial sequence</a>	1456	1456	100%	0.0	98%	<a href="#">NR_042542.1</a>
<a href="#">Pseudomonas koreensis strain Ps 9-14 16S ribosomal RNA gene, partial sequence</a>	1456	1456	100%	0.0	99%	<a href="#">NR_025228.1</a>
<a href="#">Pseudomonas vancooverensis strain DhA-51 16S ribosomal RNA gene, partial sequence</a>	1456	1456	100%	0.0	99%	<a href="#">NR_041953.1</a>
<a href="#">Pseudomonas miqulae strain NBRC 103157 16S ribosomal RNA gene, partial sequence</a>	1454	1454	98%	0.0	99%	<a href="#">NR_114223.1</a>
<a href="#">Pseudomonas miqulae strain CIP 105470 16S ribosomal RNA gene, partial sequence</a>	1454	1454	98%	0.0	99%	<a href="#">NR_024927.1</a>
<a href="#">Pseudomonas mohnii strain IpA-2 16S ribosomal RNA gene, partial sequence</a>	1448	1448	100%	0.0	98%	<a href="#">NR_042543.1</a>
<a href="#">Pseudomonas moraviensis strain 1B4 16S ribosomal RNA gene, partial sequence</a>	1447	1447	100%	0.0	98%	<a href="#">NR_043314.1</a>
<a href="#">Pseudomonas fluorescens Pf0-1 strain Pf0-1 16S ribosomal RNA, complete sequence</a>	1445	1445	100%	0.0	98%	<a href="#">NR_102835.1</a>
<a href="#">Pseudomonas putida KT2440 strain KT2440 16S ribosomal RNA, complete sequence</a>	1434	1434	100%	0.0	98%	<a href="#">NR_074596.1</a>
<a href="#">Pseudomonas brenneri strain CFML 97-391 16S ribosomal RNA gene, partial sequence</a>	1432	1432	98%	0.0	99%	<a href="#">NR_025103.1</a>
<a href="#">Pseudomonas monteilii 16S ribosomal RNA, complete sequence</a>	1428	1428	100%	0.0	98%	<a href="#">NR_121767.1</a>
<a href="#">Pseudomonas entomophila strain L48 16S ribosomal RNA gene, complete sequence</a>	1428	1428	100%	0.0	98%	<a href="#">NR_102854.1</a>
<a href="#">Pseudomonas putida F1 strain F1 16S ribosomal RNA, complete sequence</a>	1428	1428	100%	0.0	98%	<a href="#">NR_074739.1</a>
<a href="#">Pseudomonas taiwanensis strain BCRC 17751 16S ribosomal RNA gene, partial sequence</a>	1428	1428	100%	0.0	98%	<a href="#">NR_116172.1</a>

Figure 2.15: Closest DNA BLAST matches for 1B2.

Figure 2.16 below shows the closest DNA BLAST matches for 2F1.

Alignments <a href="#">Download</a> <a href="#">GenBank</a> <a href="#">Graphics</a> <a href="#">Distance tree of results</a>						
Description	Max score	Total score	Query cover	E value	Ident	Accession
<a href="#">Bacillus mycoides strain NBRC 101228 16S ribosomal RNA gene, partial sequence</a>	1639	1639	99%	0.0	99%	<a href="#">NR_113990.1</a>
<a href="#">Bacillus mycoides strain ATCC 6462 16S ribosomal RNA gene, partial sequence</a>	1639	1639	99%	0.0	99%	<a href="#">NR_115993.1</a>
<a href="#">Bacillus weihenstephanensis strain DSM 11821 16S ribosomal RNA gene, partial sequence</a>	1639	1639	99%	0.0	99%	<a href="#">NR_024697.1</a>
<a href="#">Bacillus mycoides strain 273 16S ribosomal RNA gene, partial sequence</a>	1639	1639	99%	0.0	99%	<a href="#">NR_036880.1</a>
<a href="#">Bacillus weihenstephanensis KBAB4 strain KBAB4 16S ribosomal RNA, complete sequence</a>	1628	1628	99%	0.0	99%	<a href="#">NR_074926.1</a>
<a href="#">Bacillus anthracis str. Ames strain Ames 16S ribosomal RNA, complete sequence</a>	1611	1611	99%	0.0	99%	<a href="#">NR_074453.1</a>
<a href="#">Bacillus cereus ATCC 14579 16S ribosomal RNA (rrnA) gene, complete sequence</a>	1611	1611	99%	0.0	99%	<a href="#">NR_074540.1</a>
<a href="#">Bacillus cereus strain JCM 2152 16S ribosomal RNA gene, partial sequence</a>	1611	1611	99%	0.0	99%	<a href="#">NR_113266.1</a>
<a href="#">Bacillus cereus strain CCM 2010 16S ribosomal RNA gene, complete sequence</a>	1611	1611	99%	0.0	99%	<a href="#">NR_115714.1</a>
<a href="#">Bacillus cereus strain NBRC 15305 16S ribosomal RNA gene, partial sequence</a>	1611	1611	99%	0.0	99%	<a href="#">NR_112630.1</a>
<a href="#">Bacillus cereus strain ATCC 14579 16S ribosomal RNA gene, partial sequence</a>	1611	1611	99%	0.0	99%	<a href="#">NR_114582.1</a>
<a href="#">Bacillus cereus strain IAM 12605 16S ribosomal RNA gene, partial sequence</a>	1611	1611	99%	0.0	99%	<a href="#">NR_115526.1</a>
<a href="#">Bacillus thuringiensis Bt407 16S ribosomal RNA, complete sequence</a>	1605	1605	99%	0.0	99%	<a href="#">NR_102506.1</a>
<a href="#">Bacillus thuringiensis strain NBRC 101235 16S ribosomal RNA gene, partial sequence</a>	1602	1602	99%	0.0	99%	<a href="#">NR_112780.1</a>

Figure 2.16: Closest DNA BLAST matches for 2F1.

Figure 2.17 below shows the closest DNA BLAST matches for 2F2.

Alignments						
Description	Max score	Total score	Query cover	E value	Ident	Accession
<a href="#">Bacillus mycoides strain NBRC 101228 16S ribosomal RNA gene, partial sequence</a>	1600	1600	100%	0.0	99%	<a href="#">NR_113990.1</a>
<a href="#">Bacillus mycoides strain ATCC 6462 16S ribosomal RNA gene, partial sequence</a>	1600	1600	100%	0.0	99%	<a href="#">NR_115993.1</a>
<a href="#">Bacillus weihenstephanensis strain DSM 11821 16S ribosomal RNA gene, partial sequence</a>	1600	1600	100%	0.0	99%	<a href="#">NR_024697.1</a>
<a href="#">Bacillus mycoides strain 273 16S ribosomal RNA gene, partial sequence</a>	1600	1600	100%	0.0	99%	<a href="#">NR_036880.1</a>
<a href="#">Bacillus weihenstephanensis KBAB4 strain KBAB4 16S ribosomal RNA, complete sequence</a>	1594	1594	100%	0.0	99%	<a href="#">NR_074926.1</a>
<a href="#">Bacillus thuringiensis Bt407 16S ribosomal RNA, complete sequence</a>	1572	1572	100%	0.0	99%	<a href="#">NR_102506.1</a>
<a href="#">Bacillus anthracis str. Ames strain Ames 16S ribosomal RNA, complete sequence</a>	1572	1572	100%	0.0	99%	<a href="#">NR_074453.1</a>
<a href="#">Bacillus cereus ATCC 14579 16S ribosomal RNA (rrnA) gene, complete sequence</a>	1572	1572	100%	0.0	99%	<a href="#">NR_074540.1</a>
<a href="#">Bacillus cereus strain JCM 2152 16S ribosomal RNA gene, partial sequence</a>	1572	1572	100%	0.0	99%	<a href="#">NR_113266.1</a>
<a href="#">Bacillus cereus strain CCM 2010 16S ribosomal RNA gene, complete sequence</a>	1572	1572	100%	0.0	99%	<a href="#">NR_115714.1</a>
<a href="#">Bacillus cereus strain NBRC 15305 16S ribosomal RNA gene, partial sequence</a>	1572	1572	100%	0.0	99%	<a href="#">NR_112630.1</a>
<a href="#">Bacillus cereus strain ATCC 14579 16S ribosomal RNA gene, partial sequence</a>	1572	1572	100%	0.0	99%	<a href="#">NR_114582.1</a>
<a href="#">Bacillus anthracis strain ATCC 14578 16S ribosomal RNA gene, partial sequence</a>	1572	1572	100%	0.0	99%	<a href="#">NR_041248.1</a>
<a href="#">Bacillus cereus strain IAM 12605 16S ribosomal RNA gene, partial sequence</a>	1572	1572	100%	0.0	99%	<a href="#">NR_115526.1</a>
<a href="#">Bacillus thuringiensis strain NBRC 101235 16S ribosomal RNA gene, partial sequence</a>	1568	1568	100%	0.0	99%	<a href="#">NR_112780.1</a>
<a href="#">Bacillus tovonensis strain BCT-7112 16S ribosomal RNA gene, complete sequence</a>	1567	1567	100%	0.0	99%	<a href="#">NR_121761.1</a>

Figure 2.17: Closest DNA BLAST matches for 2F2.

Figure 2.18 below shows the closest DNA BLAST matches for 4A.

Alignments						
Description	Max score	Total score	Query cover	E value	Ident	Accession
<a href="#">Bacillus mycoides strain NBRC 101228 16S ribosomal RNA gene, partial sequence</a>	1594	1594	100%	0.0	99%	<a href="#">NR_113990.1</a>
<a href="#">Bacillus mycoides strain ATCC 6462 16S ribosomal RNA gene, partial sequence</a>	1594	1594	100%	0.0	99%	<a href="#">NR_115993.1</a>
<a href="#">Bacillus weihenstephanensis strain DSM 11821 16S ribosomal RNA gene, partial sequence</a>	1594	1594	100%	0.0	99%	<a href="#">NR_024697.1</a>
<a href="#">Bacillus mycoides strain 273 16S ribosomal RNA gene, partial sequence</a>	1594	1594	100%	0.0	99%	<a href="#">NR_036880.1</a>
<a href="#">Bacillus weihenstephanensis KBAB4 strain KBAB4 16S ribosomal RNA, complete sequence</a>	1589	1589	100%	0.0	99%	<a href="#">NR_074926.1</a>
<a href="#">Bacillus thuringiensis Bt407 16S ribosomal RNA, complete sequence</a>	1567	1567	100%	0.0	99%	<a href="#">NR_102506.1</a>
<a href="#">Bacillus anthracis str. Ames strain Ames 16S ribosomal RNA, complete sequence</a>	1567	1567	100%	0.0	99%	<a href="#">NR_074453.1</a>
<a href="#">Bacillus cereus ATCC 14579 16S ribosomal RNA (rrnA) gene, complete sequence</a>	1567	1567	100%	0.0	99%	<a href="#">NR_074540.1</a>
<a href="#">Bacillus cereus strain JCM 2152 16S ribosomal RNA gene, partial sequence</a>	1567	1567	100%	0.0	99%	<a href="#">NR_113266.1</a>
<a href="#">Bacillus cereus strain CCM 2010 16S ribosomal RNA gene, complete sequence</a>	1567	1567	100%	0.0	99%	<a href="#">NR_115714.1</a>
<a href="#">Bacillus cereus strain NBRC 15305 16S ribosomal RNA gene, partial sequence</a>	1567	1567	100%	0.0	99%	<a href="#">NR_112630.1</a>
<a href="#">Bacillus cereus strain ATCC 14579 16S ribosomal RNA gene, partial sequence</a>	1567	1567	100%	0.0	99%	<a href="#">NR_114582.1</a>
<a href="#">Bacillus anthracis strain ATCC 14578 16S ribosomal RNA gene, partial sequence</a>	1567	1567	100%	0.0	99%	<a href="#">NR_041248.1</a>
<a href="#">Bacillus cereus strain IAM 12605 16S ribosomal RNA gene, partial sequence</a>	1567	1567	100%	0.0	99%	<a href="#">NR_115526.1</a>

Figure 2.18: Closest DNA BLAST matches for 4A.

Figure 2.19 below shows the closest DNA BLAST matches for 5C.

Alignments <a href="#">Download</a> <a href="#">GenBank</a> <a href="#">Graphics</a> <a href="#">Distance tree of results</a>						
Description	Max score	Total score	Query cover	E value	Ident	Accession
<input type="checkbox"/> <a href="#">Bacillus aerius strain 24K 16S ribosomal RNA gene, partial sequence</a>	1589	1589	99%	0.0	99%	<a href="#">NR_118439.1</a>
<input type="checkbox"/> <a href="#">Bacillus stratosphericus strain 41KF2a 16S ribosomal RNA gene, partial sequence</a>	1589	1589	99%	0.0	99%	<a href="#">NR_042336.1</a>
<input type="checkbox"/> <a href="#">Bacillus stratosphericus strain 41KF2a 16S ribosomal RNA gene, partial sequence</a>	1589	1589	99%	0.0	99%	<a href="#">NR_118441.1</a>
<input type="checkbox"/> <a href="#">Bacillus altitudinis strain 41KF2b 16S ribosomal RNA gene, partial sequence</a>	1589	1589	99%	0.0	99%	<a href="#">NR_042337.1</a>
<input type="checkbox"/> <a href="#">Bacillus pumilus SAFR-032 strain SAFR-032 16S ribosomal RNA, complete sequence</a>	1567	1567	99%	0.0	99%	<a href="#">NR_074977.1</a>
<input type="checkbox"/> <a href="#">Bacillus safensis strain NBRC 100820 16S ribosomal RNA gene, partial sequence</a>	1567	1567	99%	0.0	99%	<a href="#">NR_113945.1</a>
<input type="checkbox"/> <a href="#">Bacillus pumilus strain NBRC 12092 16S ribosomal RNA gene, partial sequence</a>	1567	1567	99%	0.0	99%	<a href="#">NR_112637.1</a>
<input type="checkbox"/> <a href="#">Bacillus safensis strain FO-36b 16S ribosomal RNA gene, partial sequence</a>	1567	1567	99%	0.0	99%	<a href="#">NR_041794.1</a>
<input type="checkbox"/> <a href="#">Bacillus pumilus strain ATCC 7061 16S ribosomal RNA gene, partial sequence</a>	1567	1567	99%	0.0	99%	<a href="#">NR_043242.1</a>
<input type="checkbox"/> <a href="#">Bacillus pumilus strain CIP 52.67 16S ribosomal RNA gene, partial sequence</a>	1567	1567	99%	0.0	99%	<a href="#">NR_115334.1</a>
<input type="checkbox"/> <a href="#">Bacillus pumilus strain SBMP2 16S ribosomal RNA gene, partial sequence</a>	1517	1517	99%	0.0	98%	<a href="#">NR_118381.1</a>
<input type="checkbox"/> <a href="#">Bacillus idriensis strain SMC 4352-2 16S ribosomal RNA gene, partial sequence</a>	1483	1483	98%	0.0	98%	<a href="#">NR_043268.1</a>
<input type="checkbox"/> <a href="#">Bacillus pumilus strain NRRL NRS-272 16S ribosomal RNA gene, partial sequence</a>	1463	1463	92%	0.0	99%	<a href="#">NR_116191.1</a>
<input type="checkbox"/> <a href="#">Bacillus subtilis strain 168 16S ribosomal RNA gene, complete sequence</a>	1445	1445	99%	0.0	97%	<a href="#">NR_102783.1</a>

Figure 2.19: Closest DNA BLAST matches for 5C.

The DNA of the isolated potential antibiotic producers was compared using MEGA to see if any of the organisms were genetically identical. Samples G1B1, S1B1 and 1B2 were compared, as they were all found to be *Pseudomonas baetica* and their morphology appeared similar. After analysis on MEGA it appeared that samples G1B1 and S1B1 were genetically identical over the extracted 16S rDNA gene, but 1B2 was different. Also, samples 2F1, 2F2 and 4A all appeared to have similar morphology, so were also compared on MEGA. Samples 2F1 and 2F2 appear to be genetically identical, whilst 4A was different. Therefore, for the purpose of future experiments, it will be assumed that samples G1B1 and S1B1 are the same, and samples 2F1 and 2F2 are also identical.

### 2.4.3: Metabolomics

All 7 samples were prepared for LC-MS analysis as described in the methods section. The rotary evaporated solvent extracts were analysed along with the freeze dried aqueous sample. The LC-MS analysis identified 1,915 unique compounds across all the samples. The sample information was extracted from Agilent Technologies' MassHunter Workstation Qualitative Analysis Software into Agilent Technologies' chemometric analysis software Mass Profiler Professional. Figure 2.20 below is an example of the data obtained from the LCMS QToF experiments and shows the initial volcano plot showing all the compounds identified by the Q-TOF, grouped together by sample in the aqueous freeze dried sample.

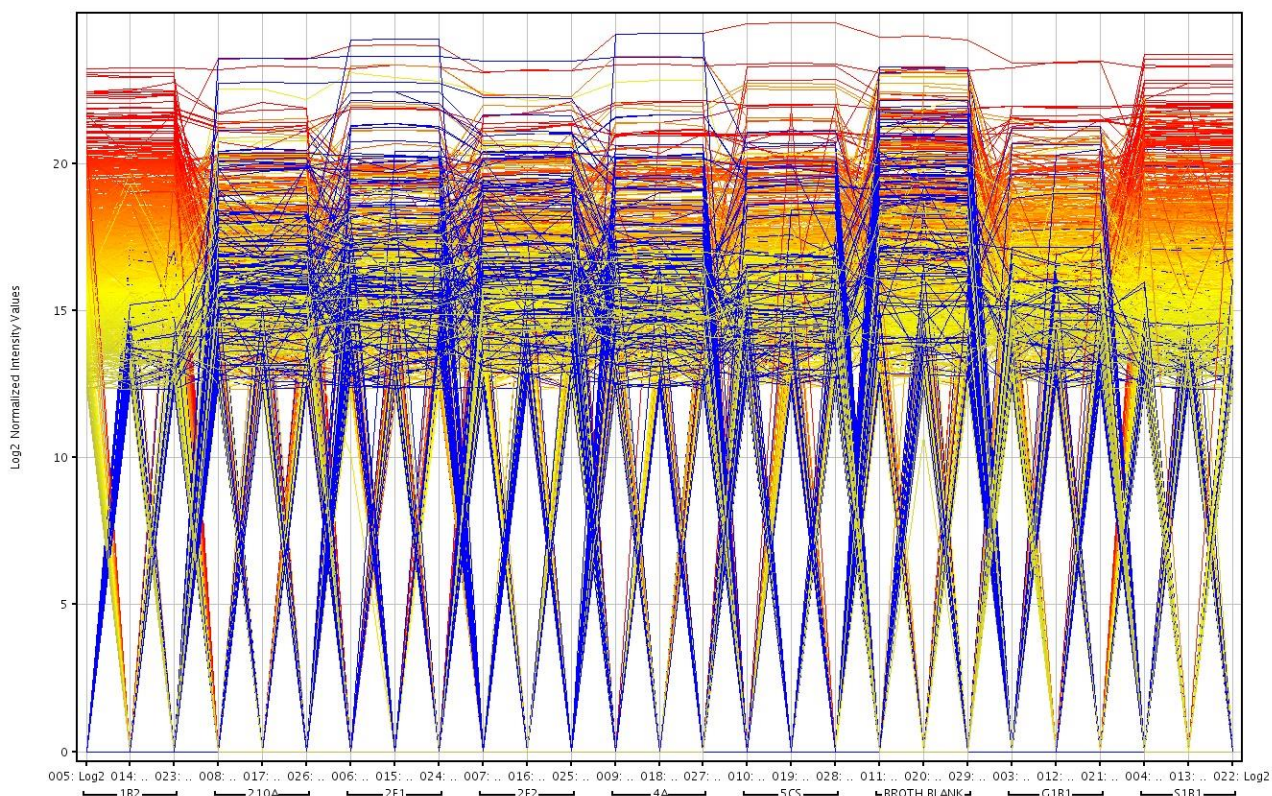


Figure 2.20: Initial volcano plot showing compounds identified grouped by sample.

Samples could then be compared against the blank to see how many unique compounds were in the sample. Figure 2.21 below shows sample 1B2 compared against the TSB blank.

Figure 2.20 above shows the relative abundance of unique compounds identified in the LCMS assay, colour coded with blue colours showing compounds that are lower intensity, towards yellow, orange and red colours that represent compounds that are highly abundant in the sample. Blue colours represent lower abundance compounds. Lines that go vertically from the X axis indicate compounds that are unique to that specific sample, whereas lines that go horizontally indicate compounds that are present in all of the samples. Lines that go vertical from the X axis from one sample and then go across only over a few are present in those specific compounds.

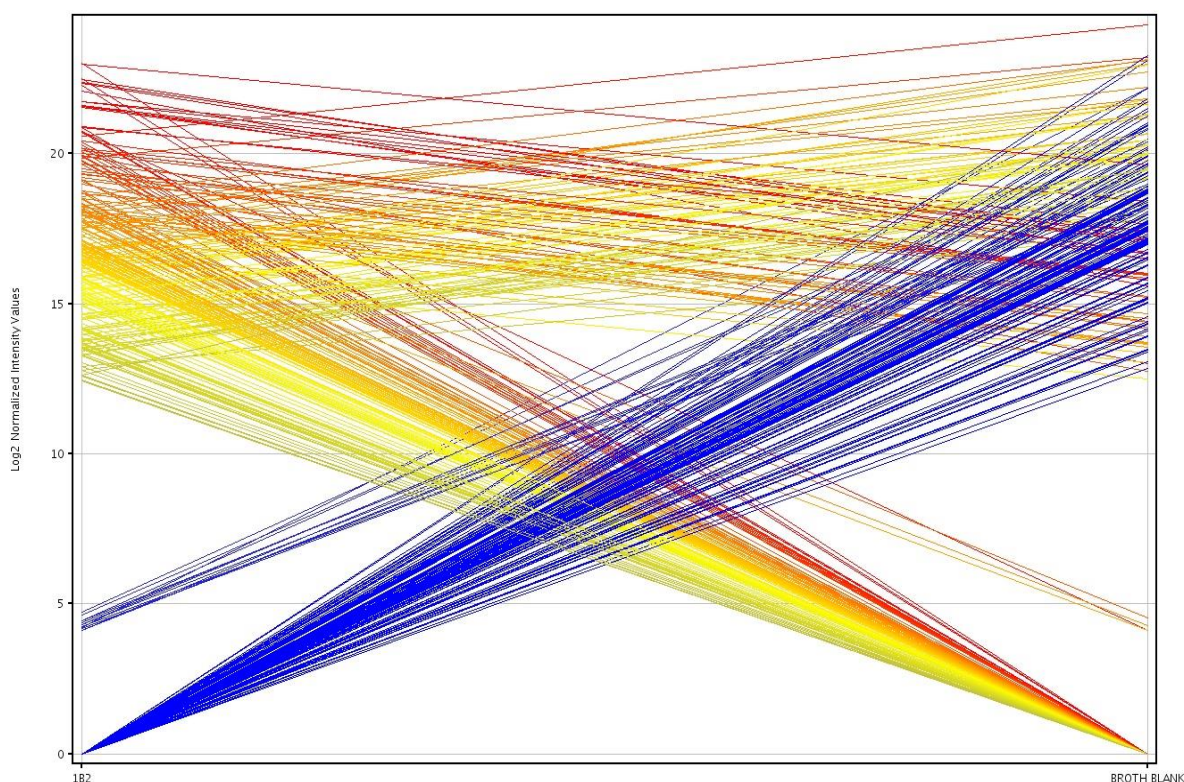


Figure 2.21: Sample 1B2 compared against the TSB blank.

Figure 2.21 above shows all the compounds present the TSB blank and sample 1B2. The blue lines represent compounds that are at overall relative low abundance, whilst the yellow-red lines represent an increase in overall relative compound abundance. The lines coming from the origin on the primary Y axis are compounds that are only present in the 1B2 sample,

whereas lines coming from the origin on the secondary Y axis represent compounds that are only present in the broth blank. The primary and secondary Y axis represents the abundance of the compound in that specific sample. For example, a line originating from 5 on the primary Y axis that goes to a higher position on the secondary Y axis represent compounds that are present in both 1B2 and the broth blank, but are more abundant in the broth blank. Figure 2.21 shows a large number of compounds that are only present in both 1B2 and the broth blank. However, the fact that there are no blue lines on the secondary Y axis shows that there are no compounds present in the broth blank in a low abundance which are not present in the test sample (1B2), but the opposite is true for the test sample. This means that there are many more compounds present in the test sample at a lower abundance than are not present at all in the broth blank. It is highly probable, that if any antibiotic is being produced, it is one of these compounds that is coloured blue and comes from the origin on the primary Y axis. However, this compound is present amongst a slew of other metabolites. Further work is needed to try and reduce this number down to a more reasonable amount, where a realistic chance is possible for the antibiotic to be characterised from the LCMS data.

## 2.5: Discussion and Conclusion

The results from the cross streak testing from antibiotic producing bacteria isolated from the iChip crowded plates indicate that 7 potential antibiotic producing bacteria have been identified. Three strains in particular (G1B1, S1B1 and 1B2) seemed to show good inhibition against  $\beta$ -lactamase producing pathogens. Of particular interest is inhibition of *K pneumoniae* 13443, a Gram negative metallo- $\beta$ -lactamase producer (NDM-1). A surface pH

probe was used to measure the pH of the agar in the inhibition zones and showed a pH of 8.2. Although this is not optimum for growth of *K. pneumoniae*, it should not be inhibitory. Also, the fact that other strains of *K. pneumoniae* grew on these plates indicates that, hopefully, there is a compound that the test microbe is producing that is inhibiting growth, and it is not just that (for example) an acidic substance is being produced that inhibits growth. This theory can be supported by the fact that *E. coli* 10418 experienced the most inhibition out of any test pathogen. *E. coli* 10418 is a negative control for  $\beta$ -lactamase production, so the observation that it is inhibited the most suggests that it is because it cannot protect itself against whatever potential antibiotic compounds the test organism is producing, but some of the other  $\beta$ -lactamase positive pathogens can.

The closest match to test organisms G1B1, S1B1 and 1B2 was *Pseudomonas baetica*, as it was the closest match on the BLAST search and also when examining the phylogenetic tree. *Pseudomonas baetica* was described as a novel fish pathogen as recently as 2012 (López et al., 2012). It is not known for producing antibiotics, so perhaps this could be a novel discovery and further metabolomics of the test microbes that showed good results against the  $\beta$ -lactamase producing pathogens is certainly worth exploring. It is known that *Pseudomonas* spp. can produce antibiotics, including: 1-phenazinecarboxylic acid, 2, 4-diacetylphloroglucinol, pyrrolnitrin, phenazine and pyoluteorin (Raaijmakers, Weller & Thomashow, 1997). However, the formulas and molecular weights of these samples were not found when checking the metabolomics results in Agilent's MassHunter software, further indicating that perhaps a novel metabolite may be inhibiting the test pathogens. Samples 2F1 and 2F2 appear to be the same organism, according to the PCR results. Samples 2F1, 2F2, 4A and 5C all had negligible inhibitory effects against the test  $\beta$ -lactamase producers, although they had good results against the non  $\beta$ -lactamase producing bacteria in the first round of antibiotic susceptibility testing. Future work will most likely focus on

working with bacteria that showed good inhibition against the  $\beta$ -lactamase producing bacteria, such as 1B1G, 1B1S and 1B2.

The results from the LC-MS identified 1,915 compounds. The results from 1B2 showed over 400 differences from the blank TSB sample when analysed at  $p < 0.01$  and 16 fold difference. This represents a good result in one way, because it shows that the LC-MS method developed is capable of identifying a large amount of compounds from the samples, but over 400 compounds is far too many to try and identify and quantify.

There is possibly a huge potential for discovery of novel microbial strains and novel antimicrobials using the iChip. As stated earlier, the vast majority of microbes present in the environment are unculturable in laboratory conditions. Secondary metabolites of the remaining culturable organisms have been described as a long over-mined source of antimicrobials, with the chance of discovering a novel antimicrobial metabolite estimated to be  $10^{-7}$  (Nichols et al., 2010).

In an attempt to reduce the number of compounds found in the sample, isolates G1B1, S1B1 and 1B2 were incubated in Tryptone Soy Broth at 30 °C in a rotating incubator for 7 days. The samples were centrifuged and the supernatant was collected and filter sterilised. The supernatant was subject to freeze drying which resulted in the production of a brown powder for each sample. The freeze dried product was collected and subjected to antimicrobial testing using the streak plate method described previously. This was attempted in the hope that the antimicrobial the isolates produce was a secondary metabolite, as most antibiotics are from microbial sources; and the freeze drying would concentrate the compounds responsible for the inhibition seen. However, the freeze dried isolate showed no signs of inhibition, as was seen in the cross streak testing. This indicates that perhaps the compound is not stable enough to survive the freeze drying process, or that perhaps the compound is

not produced whilst the bacteria grows in a broth. Further work is needed to attempt to isolate the antibiotic.

The work done in this chapter found a previously little described strain of *Pseudomonas baetica*, not previously known for producing antimicrobials (López et al., 2007), (López, Navas, Thanantong, Herran, Sparagano, 2012). Previous interest in this microbe had mostly only been concerned with its pathogenicity towards fish, specifically wedge sole. This isolate exhibited repeated inhibition in subsequent cross streak tests against  $\beta$ -lactamase producing bacteria. LCMS analysis of the isolate revealed over 400 unique compounds not identified in blank samples. Further work is needed to reduce this amount to a manageable figure, where identification of specific compounds responsible for causing the inhibition may be possible. Further work could include more statistical analysis involving Agilent Technologies' Mass Profiler Professional; more blank samples could be prepared against which the test sample could be compared to “subtract” blank metabolites (i.e. metabolites which are not involved in any sample inhibition). Blank samples could be taken such as TSA dissolved in a suitable solvent, and then areas around the pathogen growing on TSA, and then areas around the *Pseudomonas baetica* growing on TSA. These metabolites could be logged as “blank” metabolites. Then, the test could be repeated but agar taken directly from the zone of inhibition on TSA plates where *Pseudomonas baetica* and test pathogens are incubated together. These “blank” metabolites could then be “subtracted” from the total metabolites in the test sample. This would then account for metabolites produced without the presence of an inducer (the pathogen, in the case of the antibiotic producing *Pseudomonas baetica*). Although the blank TSB was accounted for in the current experiment, passive metabolites were not. Single bacterial strains are capable of producing thousands of unique metabolites (Sajed et al., 2016), therefore being able to “subtract” several insignificant passive metabolites would be a helpful step in the experimental

procedure towards reducing the number of unique compounds found in the test sample. Also, as shown here, the potential for novel microbes incubated using the iChip is huge and represents a promising way of eventually identifying novel antimicrobials.

## 2.6: Chapter Two References

Alimetrics. (n.d.). DNA Sequence Analysis. Retrieved from <http://www.alimetrics.net/en/index.php/dna-sequence-analysis>.

American Chemical Society. (2005). Selman Waksman and Antibiotics. Retrieved from <https://www.acs.org/content/acs/en/education/whatischemistry/landmarks/selmanwaksman.html#discovery-of-streptomycin-controversy>.

Bibb, M.J. (2013). Understanding and manipulating antibiotic production in actinomycetes. *Biochemical Society Transactions*, 41 (6), 1355-1364. doi: 10.1042/BST20130214.

Bizuye, A., Moges, F., & Andualem, B. (2013). Isolation and screening of antibiotic producing actinomycetes from soils in Gondar town, North West Ethiopia. *Asian Pacific Journal of Tropical Disease*, 3(5), 375-381. doi:10.1016/S2222-1808(13)60087-0

Demirci, H., Murphy IV, F., Murphy, E., Gregory, S.T., Dahlberg, A.E., & Jogl, G. (2013). A structural basis for streptomycin-induced misreading of the genetic code. *Nature Communications*, 4 (1355), . doi: 10.1038/ncomms2346.

Fenollar, F., Roux, V., Stein, A., Drancourt, M., & Raoult, D. (2006). Analysis of 525 Samples To Determine the Usefulness of PCR Amplification and Sequencing of the 16S

rRNA Gene for Diagnosis of Bone and Joint Infections. *Journal of Clinical Microbiology*, 44 (3), 1018-1028. doi: 10.1128/JCM.44.3.1018-1028.2006.

Kitani, S., Miyamoto, K. T., Takamatsu, S., Herawati, E., Iguchi, H., Nishitomi, K., . . . Nihira, T. (2011). Avenolide, a *Streptomyces* hormone controlling antibiotic production in *Streptomyces avermitilis*. *Proceedings of the National Academy of Sciences*, 108(39), 16410-16415. doi:10.1073/pnas.1113908108.

Kresge, N., Simoni, R.D., & Hill, R.L. (2004). Selman Waksman: The Father of Antibiotics. *The Journal of Biological Chemistry*, 279 (48), 101-102. Retrieved from <http://www.jbc.org/content/279/48/e7.full.pdf>.

Ling, L. L., Schneider, T., Peoples, A. J., Spoering, A. L., Engels, I., Conlon, B. P., . . . Lewis, K. (2015). A new antibiotic kills pathogens without detectable resistance. *Nature*, 517(7535), 455-459. doi:10.1038/nature14098.

López, J. R., Diéguez, A. L., Doce, A., De la Roca, E., De la Herran, R., Navas, J. I., . . . Romalde, J. L. (2012). *Pseudomonas baetica* sp. nov., a fish pathogen isolated from wedge sole, *Dicologlossa cuneata* (Moreau). *International Journal of Systematic and Evolutionary Microbiology*, 62(4), 874-882. doi:doi:10.1099/ijs.0.030601-0.

López, J.R., Navas, J.I., Thanantong, N., Herran, R.D.L., & Sparagano, O.A.E. (2012). Simultaneous identification of five marine fish pathogens belonging to the genera *Tenacibaculum*, *Vibrio*, *Photobacterium* and *Pseudomonas* by reverse line blot hybridization. *Aquaculture*, 324 (1), 33-88. doi: 10.1016/j.aquaculture.2011.10.043.

Lyddiard, D., Jones, G.L., & Greatrex, B.W. (2016). Keeping it simple: lessons from the golden era of antibiotic discovery. *FEMS Microbiology Letters*, 363 (8), doi: 10.1093/femsle/fnw084.

Molecular Evolutionary Genetics Analysis. (2016). Home. Retrieved from <http://www.megasoftware.net/>.

Mo Bio. (n.d.). UltraClean® Microbial DNA Isolation Kit. Retrieved from <https://mobio.com/media/wysiwyg/pdfs/protocols/12224.pdf>.

National Centre for Biotechnology Information. (2014). Polymerase Chain Reaction (PCR). Retrieved from <http://www.ncbi.nlm.nih.gov/probe/docs/techpcr/>.

National Centre for Biotechnology Information. (2016). Standard Nucleotide BLAST. Retrieved from <https://blast.ncbi.nlm.nih.gov/Blast.cgi>.

Nichols, D., Cahoon, N., Trakhtenberg, E. M., Pham, L., Mehta, A., Belanger, A., . . . Epstein, S. S. (2010). Use of IChip for High-Throughput In Situ Cultivation of “Uncultivable” Microbial Species. *Applied and Environmental Microbiology*, 76(8), 2445-2450. doi:10.1128/aem.01754-09.

Raaijmakers, J.M., Weller, D.M., & Thomashow, L.S. (1997). Frequency of Antibiotic-Producing *Pseudomonas* spp. in Natural Environments. *Applied and Environmental Microbiology*, 63 (3), 881-887. Retrieved from <http://aem.asm.org/content/63/3/881.full.pdf>.

Raja, A. & Prabakarana, P. (2011). Actinomycetes and Drugs - an Overview. *American Journal of Drug Discovery and Development*, 1 (2), 75-84. doi: 10.3923/ajdd.2011.75.84.

Reller, L.B., Weinstein, M.P., & Petti, C.A. (2007). Detection and Identification of Microorganisms by Gene Amplification and Sequencing. *Clinical Infectious Diseases*, 44 (8), 1108-1114. doi: 10.1086/512818.

Sajed, T., Marcu, A., Ramirez, M., Pon, A., Guo, A.C., Knox, C. ... Wishart, D.S. (2016). ECMDB 2.0: A richer resource for understanding the biochemistry of *E. coli*. *Nucleic Acids Research*, 44 (44), 495-501. doi: 10.1093/nar/gkv1060.

Sanders, E.R. (2012). Aseptic Laboratory Techniques: Plating Methods. *Journal of Visualized Experiments*, 63(3064), 1-18. doi: 10.3791/3064.

Schatz, A., Bugle, E., & Waksman, S.A. (1944). Streptomycin, a Substance Exhibiting Antibiotic Activity Against Gram-Positive and Gram-Negative Bacteria. *Experimental Biology and Medicine*, 55 (1), 66-69. doi: 10.3181/00379727-55-14461.

Srinivasan, R., Karaoz, U., Volegova, M., Mackichan, J., Kato-Maeda, M., Miller, S. ... Lynch, S.V. (2015). Use of 16S rRNA Gene for Identification of a Broad Range of Clinically Relevant Bacterial Pathogens. *Public Library of Science*, 10 (2), 1-22. doi:10.1371/journal.pone.0117617.

Stewart, E.J. (2012). Growing Unculturable Bacteria. *Journal of Bacteriology*, 194 (16), 4151-4160. Retrieved from <https://jb.asm.org/content/jb/194/16/4151.full.pdf>.

University of Utah. (2016). *PCR*. Retrieved from <http://learn.genetics.utah.edu/content/labs/pcr/>.

Vartoukian, S.R., Palmer, R.M., & Wade, W.G. (2010). Strategies for culture of 'unculturable' bacteria. *FEMS Microbiology Letters*, 309 (1), 1-7. doi: 10.1111/j.1574-6968.2010.02000.x.

Velho-Pereira, S., & Kamat, N. M. (2011). Antimicrobial Screening of Actinobacteria using a Modified Cross-Streak Method. *Indian Journal of Pharmaceutical Sciences*, 73(2), 223-228. Retrieved from <http://www.ncbi.nlm.nih.gov/pmc/articles/PMC3267309/>.

Wade, W. (2002). Unculturable bacteria - the uncharacterized organisms that cause oral infections. *Journal of the Royal Society of Medicine*, 95 (2), 81-83. Retrieved from <https://www.ncbi.nlm.nih.gov/pmc/articles/PMC1279316/>.

Waksman, S.A. (1945). *Microbial Antagonisms and Antibiotic Substances*. New York: The Common Wealth Fund.

Waksman, S.A. & Woodruff, H.B. (1940). The Soil as a Source of Microorganisms Antagonistic to Disease-Producing Bacteria. *Journal of Bacteriology*, 40 (4), 581-600. Retrieved from <https://www.ncbi.nlm.nih.gov/pmc/articles/PMC374661/>.

Widdel, F. (2010). Theory and Measurement of Bacterial Growth . Retrieved from <https://www.mpi-bremen.de/Binaries/Binary307/Wachstumsversuch.pdf>.

Woodruff, H.B. (2014). Selman A Waksman, Winner of the 1952 Nobel Prize for Physiology or Medicine. *Applied and Environmental Microbiology*, 80 (1), 2-8. doi: 10.1128/AEM.01143-13.

Yamasaki, Y., Teramoto, Y., & Yoshikawa, K. (2001). Disappearance of the Negative Charge in Giant DNA with a Folding Transition. *Biophysical Journal*, 80 (6), 2823-2832. doi: 10.1016/S0006-3495(01)76249-2.

## Chapter Three: Novel Avibactam Analogues as Novel Inhibitors of Serine- $\beta$ -Lactamases

*The author wishes to acknowledge the kind gift of avibactam from Astra Zeneca. The author also wishes to acknowledge the kind gift of SBL enzymes from Christopher Schofield's Group at the University of Oxford.*

### 3.1: Introduction

As discussed in the general introduction, there are existing inhibitors of the SBLs. However, there are only four approved for clinical use; clavulanic acid, sulbactam, tazobactam, and more recently avibactam (figure 3.1 below). With the exception of avibactam, the existing inhibitors typically only inhibit class A and C SBLs. The combination of  $\beta$ -lactam antibiotics with SBL inhibitors has been utilised to give previously susceptible  $\beta$ -lactam antibiotics renewed activity against SBL producing bacteria.

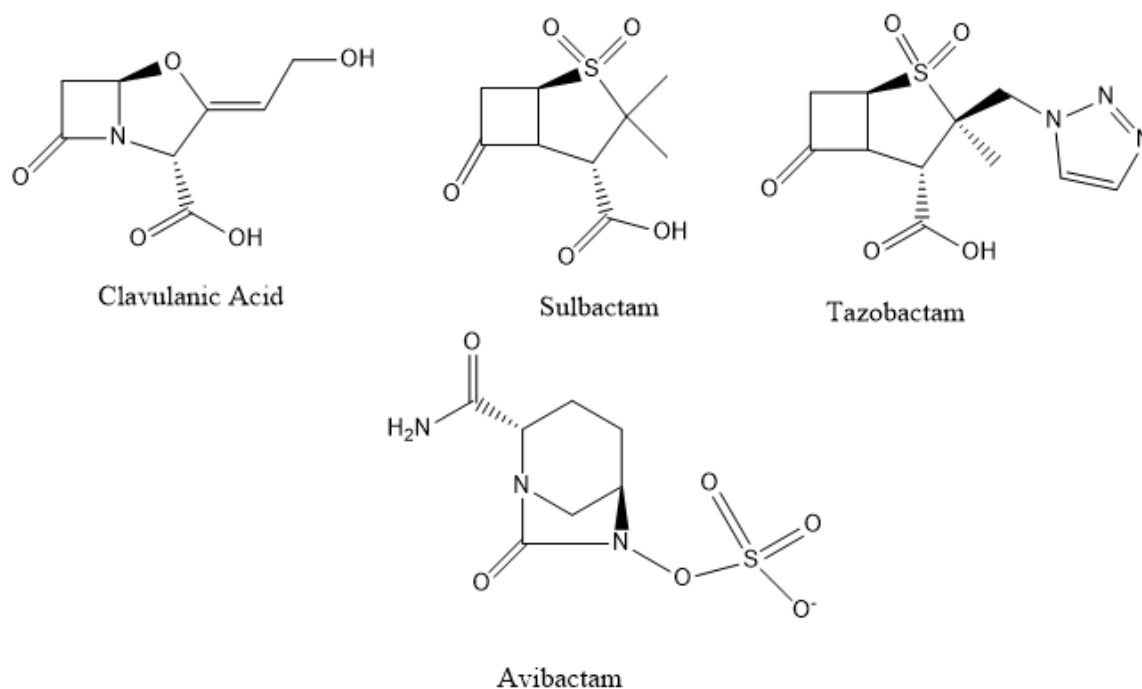


Figure 3.1: SBL inhibitors approved for clinical use; the  $\beta$ -lactam containing clavulanic acid, sulbactam and tazobactam and the non- $\beta$ -lactam diazabicyclooctane avibactam.

Bacteria have developed resistance for every antibiotic introduced into the clinic so far, so the development of novel SBL inhibitors is of the greatest importance in order to increase the susceptibility of ESBL producing bacteria to existing  $\beta$ -lactam antibiotics.

In an effort to combat the ever increasing threat posed by  $\beta$ -lactamases, inhibitors have been developed with the intention of being used in conjunction with  $\beta$ -lactam antibiotics to restore antibiotic activity to previously susceptible antibiotics. Examples of  $\beta$ -lactam  $\beta$ -lactamase inhibitor combinations (BLBLIC) include: ceftazidime-avibactam, ceftolozane-tazobactam, amoxicillin-clavulanate and ampicillin-sulbactam (Toussaint & Gallagher, 2015). Data show that BLBLIC produce lower minimum inhibitory concentrations (MIC) than treatment without  $\beta$ -lactamase inhibitors (Reading & Cole, 1977), (Jones, Barry, Thornsberry & Wilson, 1985), and can be as powerful as carbapenems – our most potent antibiotics of ‘‘last resort’’, held in reserve for only the most severe bacterial infections. BLBLIC therefore

represent an alternate treatment pathway for serious infections caused by extended spectrum  $\beta$ -lactamase producing bacteria – drugs of “last resort”, (such as carbapenems and polymyxins), can be reserved for the most severe infections, therefore limiting bacterial exposure to such drugs, thereby reducing the chance for resistance to arise to said drugs; whereas BLBLIC can be used to extend and prolong the life of our existing  $\beta$ -lactam antibiotic arsenal. Development of novel  $\beta$ -lactam antibiotics has been scarce in recent times, and existing discovery platforms have yielded insignificant results. Developing novel SBL inhibitors for use in conjunction with  $\beta$ -lactam antibiotics is an attractive development option for medicinal chemists, in order to restore the functionality of existing  $\beta$ -lactam antibiotics.

Whilst clavulanic acid and the related inhibitors sulbactam and tazobactam have been in clinical use for some time, they are good inhibitors of class A SBLs but are generally poorer inhibitors of class C and D enzymes. The newer inhibitor, avibactam, has a wider range of activity than the existing SBL inhibitors, being able to inhibit enzymes from class A, C and some D. Vaborbactam is also a novel, non- $\beta$ -lactam SBL inhibitor, but only has activity against class A and C SBLs. Therefore the need for the development of a novel  $\beta$ -lactamase inhibitor with action against all 3 classes of SBLs is of great clinical significance.

Given the frequency of administration of BLBLIC, as well as the fast generation times of bacteria, it is perhaps unsurprising that there are reports describing resistance of bacteria to BLBLIC medication. Avibactam has been approved for clinical use alongside the cephalosporin antibiotic ceftazidime in a BLBLIC marketed as Avycaz and has been shown to be effective against infections mediated by SBL producing bacteria (Mosley, Smith, Parke, Brown, Wilson & Gibbs, 2016). Whilst BLBLIC resistance was initially described in the combination of amoxicillin and clavulanic acid, there are concerning reports that resistance has already been noted against avibactam/ceftazidime (Shields, Nguyen, Press,

Chen, Kreiswirth & Clancy, 2017). The mechanism of resistance to BLBLIC is primarily through the hyper-production of  $\beta$ -lactamase enzymes that simply overwhelm the inhibitor and antibiotic, resulting in a net hydrolysis compared to inhibition (Martinez, Vicente, Delgado-Iribarren, Perez-Diaz & Baquero, 1989), (Wu, Shannon & Phillips, 1994), (Wu, Shannon & Phillips, 1995), by modification of outer membrane proteins, decreasing the permeability of the cell membrane (Reguera, Baquero, Perez-Diaz & Martinez, 1991), as well as variations of the  $\beta$ -lactamase which is less susceptible to covalent inhibition by the commercially available inhibitors (Bonomo & Rice, 1999), (Nicolas-Chanoine, 1997).

Diazabicyclooctane inhibitors such as avibactam, relebactam and vaborbactam are promising developments in the campaign against antibiotic resistance, as previous inhibitors were all based on the  $\beta$ -lactam scaffold. These are novel inhibitors in the sense that they do not contain a  $\beta$ -lactam group, and represent a significant step forward in the development of SBL inhibitors. Up until avibactam, all SBLs had operated using a  $\beta$ -lactam scaffold, and limited development options. Since the introduction of avibactam, there has been the development of further non- $\beta$ -lactam inhibitors entering into clinical trials. These include the diazabicyclooctanes relebactam, nacubactam, zidebactam and the boronic acid vaborbactam, the latter has recently passed clinical trials in 2017 for use in conjunction with meropenem for use against carbapenemase producing *Klebsiella pneumoniae* (Hecker et al., 2015). Although vaborbactam has only been recently introduced into the clinic, the concept of using boron derived electrophilic agents to inhibit SBLs is not new. Work in the early 1970s showed that an SBL from *Bacillus cereus* was reversibly inhibited by borate ions (Kiener & Waley, 1978). The structures of these inhibitors are seen in figure 3.2 below.

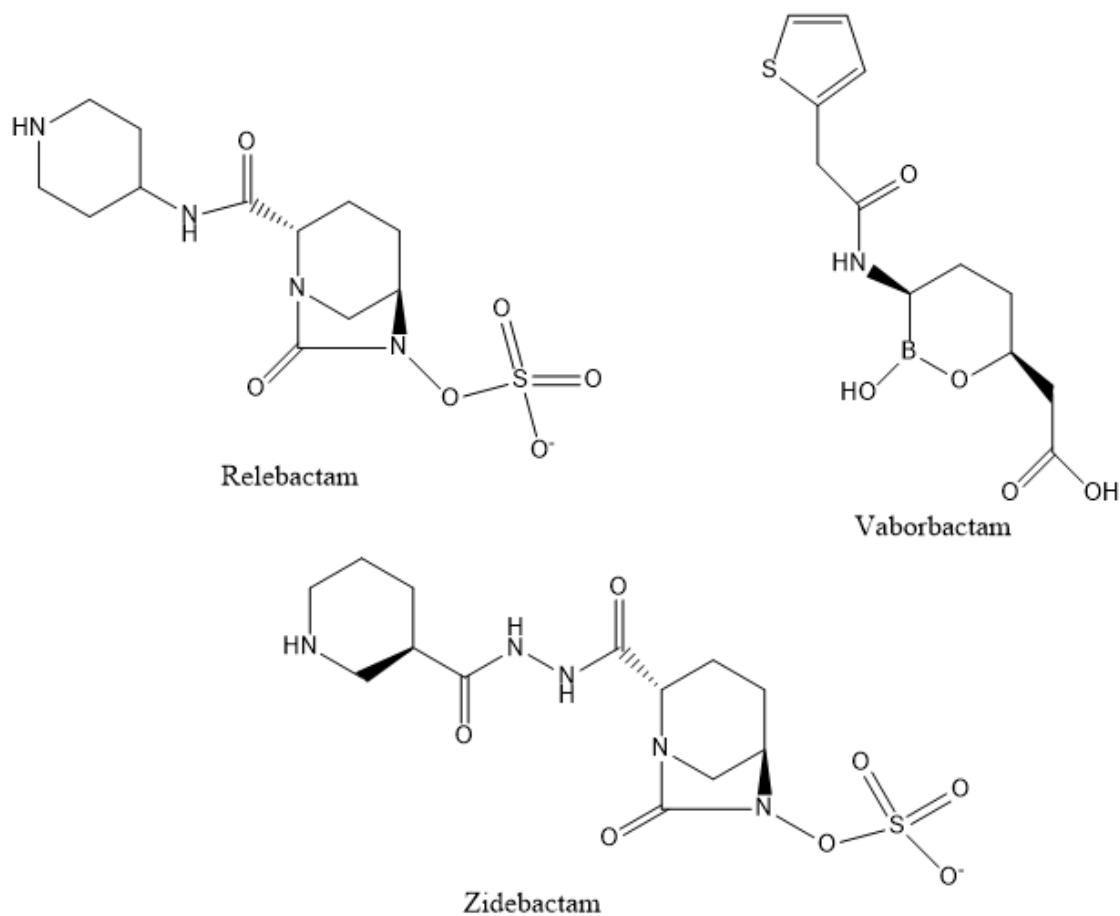


Figure 3.2: The non- $\beta$ -lactam SBL inhibitors in clinical development and the recently approved vaborbactam.

Development of non- $\beta$ -lactam SBL inhibitors is a significant step forward in the battle against antibiotic resistance, owing to the novelty of their structures and explores a fresh avenue of research previously restricted to  $\beta$ -lactam containing compounds.

History has taught us that antibiotic resistance will eventually overcome any treatment we can produce, so the development or the expansion of knowledge regarding novel inhibitors is a desperate priority. Clearly,  $\beta$ -lactamase inhibitors are a desirable addition for medicinal chemists in order to extend the life and dwindling effectiveness of our current  $\beta$ -lactam antibiotics. However, over the course of the last 70 years, the evolutionary pressure forced onto microbes has afforded them with many mechanisms of resistance. Bacteria are able to

combat  $\beta$ -lactamase inhibitors by hyper-production of the enzyme (Wu, Shannon & Phillips, 1994), or by producing strains of  $\beta$ -lactamases that are resistant to inhibitors (Chaïbi, Sirot, Paul & Labia, 1999). With the ever looming threat of resistance, novel antimicrobials including novel  $\beta$ -lactamase inhibitors are needed.

### 3.2: Chapter Aims

This study aimed to produce novel inhibitors derived from avibactam based on the mechanism of action. Here, four such novel inhibitors are reported and their inhibitory activity is discussed.

It is known that inactivation of the  $\beta$ -lactamases by avibactam occurs by acylation of the active site serine residue (Wang et al., 2016). This acyl enzyme complex is not readily further hydrolysed and is relatively stable, leading to termination of catalytic activity of the  $\beta$ -lactamase enzyme, resulting in inhibition. The aim of this project was to investigate the possibility of generating the acyl enzyme from derivatives of avibactam, for example, the ring opened carbamate ester. The ester function may act as a substrate for the enzyme, displacing the alcohol and so generating the same acyl enzyme complex. An overview of the intended reaction scheme is shown below in figure 3.3.

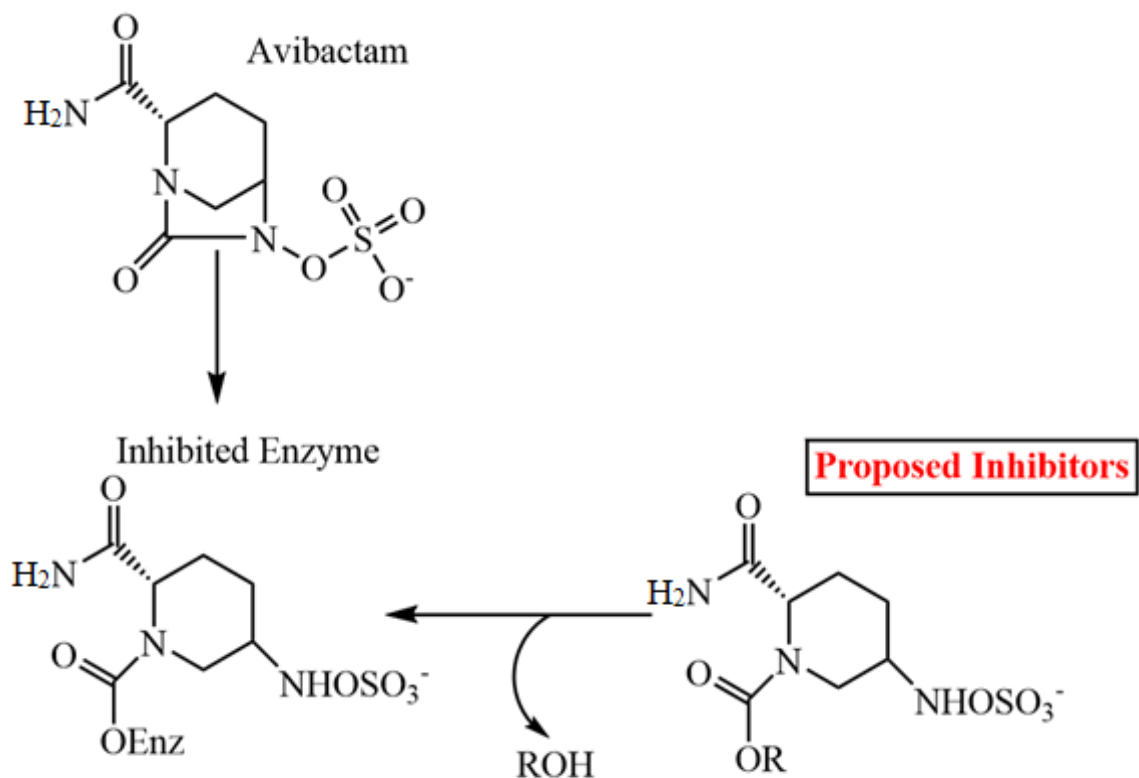


Figure 3.3: Avibactam and proposed inhibitor mechanisms.

Carbamates are half ester/half amide derivatives of carbonic acid and are more reactive than amides but less reactive than esters. Carbamates derived from carbamic acid have long been used as a pesticide owing to the fact they inhibit the two forms of acetylcholinesterase (AChE) found in mammals – AChE and butyrylcholinesterase (BuChE) (Bajda, Latka, Hebda, Jonczyk & Malawska, 2018), (Chiou, Huang, Hwang & Lin (2009)). Cholinesterases are responsible for the termination of impulse response in controlling muscles by efficiently catalysing the hydrolysis of the neurotransmitter acetylcholine at synapses into choline and acetic acid (Colovic, Kristic, Pasti, Bondzic & Vasic, 2013). Acetylcholine is released from the pre-synaptic neuron into the synapse to transmit the nerve impulse across the synaptic cleft by binding to receptors on the post synaptic neuron, which causes sodium channels on the post synaptic neuron, generating an action potential and causing muscle contraction. After the acetylcholine is released from the receiving neuron, it is hydrolysed by AChE into

its substituents (acetic acid and choline). Acetic acid diffuses through the synaptic cleft, whereas the choline is taken back up into the presynaptic neuron by a sodium ion dependent choline transporter, where it is used to resynthesize acetylcholine (Titus, Revest & Shortland, 2010). Acetylcholine and the nerve transmission pathway is obviously a very important mechanism within mammals, and therefore represent an important therapeutic target for a variety of medications (Mehta, Adem & Sabbagh, 2012). Indeed, recent work has highlighted the link between decreased levels of acetylcholine and progression of Alzheimer's disease, leading to dementia (Ayllon, Small, Avila & Valero, 2011), (McGleenon, Dynan & Passmore, 1999), (Tabet, 2006). Obviously, as acetylcholinesterase is responsible for catalysing the hydrolysis of acetylcholine which therefore leads to a decrease in physiological concentrations of the neurotransmitter, inhibitors of acetylcholinesterase has been of interest to the pharmaceutical community. Carbamates are well known inhibitors of acetylcholinesterase; an example of which is rivastigmine, which contains a carbamate group capable of binding covalently with the serine active site of the acetylcholinesterase and has a very slow turnover in which it is only very slowly removed by hydrolysis of the enzyme carbamate complex (Yanovsky et al., 2012). Rivastigmine is used in the treatment and prevention of Alzheimer's disease, the mechanism of action is to inhibit acetylcholinesterase, helping to prevent the hydrolysis of the neurotransmitter acetylcholine.

Although carbamates show therapeutic potential in the treatment and prevention of Alzheimer's, historically they have a rather more sinister use. Carbamate inhibitors have been heavily used in agriculture as insecticides, fungicides, herbicides, biocides and pesticides for common pests (Struger, Grabuski, Cagampan, Sverko & Marvin, 2016). Carbamates are often preferred compared to traditional organophosphates owing to the latter's toxicity (Queensland Department of Health, 2002). Levels of acetylcholine in

mammals is closely regulated via the previously mentioned actions of AChE. If this enzyme is inhibited in mammals, it can cause rapid onset of symptoms including paralysis leading to death arising from the interruption of normal nerve transmissions (Risher, Mink & Stara, 1987).

X-ray crystallography studies have shown AChE to have a serine group in its active site (Dvir, Silman, Harel, Rosenberry & Sussman, 2010), (Johnson et al., 2003). Knowing that carbamates can act as effective inhibitors of AChE (McHardy, Wang, McCowen & Valdez, 2017), a serine enzyme, it was hoped that the synthesised carbamates based on avibactam may show inhibitory activity for SBL enzymes.

### **3.3: Methods**

*All chemicals used were of reagent grade and acquired from Sigma Aldrich unless otherwise stated.*

#### **3.3.1: Synthesis of Carbamate Inhibitors**

Four derivatives were synthesised based on the schemes below in figures 3.4 and 3.5 to give a variety of carbamates with leaving groups.

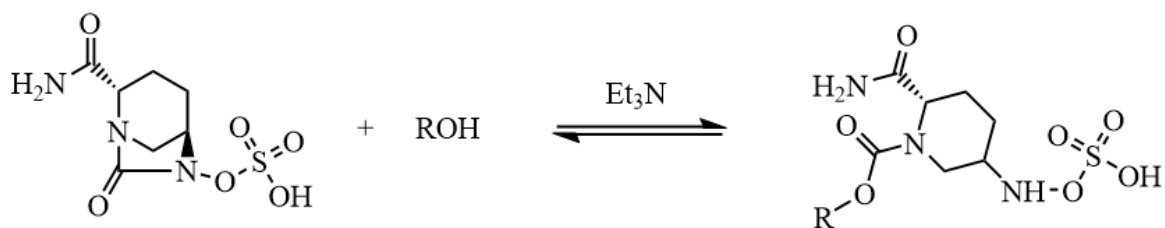


Figure 3.4: Overview of the synthesis of the carbamates of avibactam.

The alcohol (ROH) used in each instance was: methanol (MeOH), trifluoroethanol ( $\text{CF}_3\text{CH}_2\text{OH}$ ), hexafluoroisopropanol ( $\text{CF}_3)_2\text{CHOH}$  (HFIP) and hexafluoroacetone hydrate ( $\text{CF}_3)_2\text{C}(\text{OH})_2$  (HFA) was used as per the scheme below.

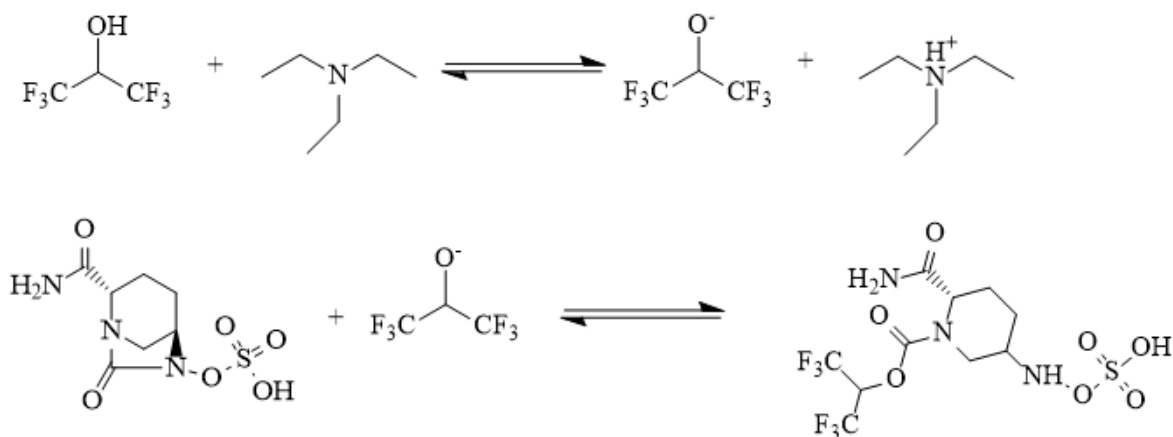
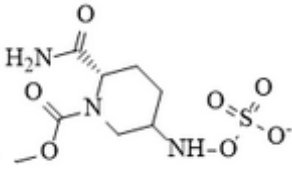
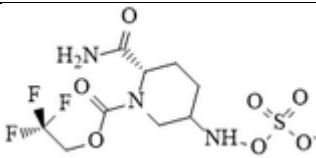
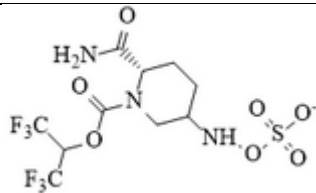
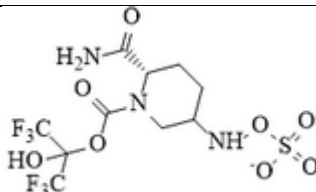
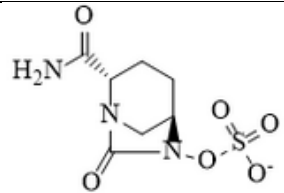


Figure 3.5: Overview of the synthesis of the HFA analogue.

For the synthesis of all the derivatives, triethylamine (TEA) was utilised as a base to enhance the nucleophilicity of the alcohol, for attack at the carbonyl carbon on the  $\beta$ -lactam ring of avibactam to cause ring opening. It is unlikely that these weakly basic conditions would lead to any epimerisation of the chiral centres. Table 3.1 below shows the expected structure, formula, and molecular weight (MW) of each compound.

Table 3.1: Information and structures of carbamate inhibitors. Further analytical data is given in the methods section.

Compound Name	$pK_a$ of ROH	Structure in negative ionisation mode	Mass to Charge (M/Z)	Formula
Methyl Carbamate (MA)	16		296.0561	$C_{11}H_{20}N_3O_6S^-$
Trifluoroethyl Carbamate (TA)	12.4		364.0439	$C_9H_{13}F_3N_3O_6S^-$
Hexafluoroisopropanol (HFIP)	9.3		432.0318	$C_{10}H_{12}F_6N_3O_6S^-$
Hexafluoroacetone Hydrate (HFA)	6.58		447.03	$C_{10}H_{12}F_6N_3O_8S^-$
Avibactam	N/A		264.0296	$C_7H_{10}N_3O_6S^-$

One equivalent of TEA base was added to one equivalent of the avibactam starting material in the alcohol as the solvent. The reaction mixture was stirred under reflux in a  $N_2$  atmosphere. Samples were periodically taken to monitor the disappearance of avibactam and

the appearance of the product which was analysed by LCMS and will be described more fully in the LCMS method section. Typically, the reaction would be complete after 36 hours. Once avibactam could no longer be seen by the LCMS detection method, the sample was rotary evaporated under reduced pressure to form a dry powder. The powder was kept under  $N_2$  and stored at  $-20\text{ }^\circ\text{C}$ .

### **3.3.2: Liquid Chromatography Mass Spectrometry (LCMS) Analysis Methods of the Carbamate Inhibitors**

An Agilent 1260 LC system coupled to an Agilent 6545 Quadrupole Time of Flight Mass Spectrometer (QToF-MS) system was utilised for LCMS analysis of the carbamate inhibitors, with the method of Beaudoin & Gangl (2016) utilised to provide acceptable LCMS parameters. The carbamates were dissolved in pH 7 4-(2-hydroxyethyl)-1-piperazineethanesulfonic acid (HEPES) buffer and sonicated prior to LCMS analysis and made to a concentration of 100 ppm. The mobile phases used were LCMS water 0.1 % formic acid on pump line A and LCMS acetonitrile (ACN) 0.1 % formic acid on pump line B. An ACE 5 C18-AR (3  $\mu\text{m}$ , 150 x 4.6 mm) column maintained at  $30\text{ }^\circ\text{C}$  was used to provide retention of the inhibitors. The binary pump flow rate was 0.8 ml with an injection volume of 5  $\mu\text{l}$ . The elution method was as follows: 3 % B for 1 minute, then a linear increase from 3 to 50 % B in 1.4 minutes, followed by another linear increase from 50 to 99 % B in 1.6 minutes, hold at 99 % B for 0.5 minutes, then a return to 3 % B for 3.5 minutes, followed by an equilibration time of 10 minutes before the next sample was injected.

The mass spectrometer employed a jet stream electrospray ionisation (JS-ESI) and the conditions were as follows: gas temperature,  $320\text{ }^\circ\text{C}$ ; gas flow, 8 L/min; nebuliser. 35 psig;

sheath gas temp, 350 °C; ion polarity, negative; nozzle voltage, 1000 V; fragmentor voltage, 175 V.

### 3.3.3 UV Analysis and Kinetics Determination

It was necessary to develop a method to determine both the rates of hydrolysis of the carbamates and the rates of inhibition of the SBLs by the carbamates, and the rates of antibiotic hydrolysis by the SBLs.

The hydrolysis of the carbamates in pH 14 sodium hydroxide (NaOH) was measured by recording a decrease in absorbance at 305 nm for the HFIP carbamate, 221 nm for the TFA carbamate and 235 nm for the MA carbamate. A baseline blank consisting of NaOH (1 M) corrected to pH 14 using a calibrated pH probe was first taken. 0.1 mM solutions of each carbamate were prepared and then added to the NaOH and the UV spectra were recorded over a period of 12 hours to deduce the hydrolysis of the carbamates as monitored by a loss in absorbance at the already mentioned wavelengths.

The rate of hydrolysis of SBLs against various  $\beta$ -lactam antibiotic substrates was first measured as a control (initial antibiotic substrates used included benzylpenicillin and cephalosporin based antibiotics such as cephalothin and cefpirome). These were considered blanks, against which the activity of inhibition would be compared to give insights into the kinetics of inhibition of the SBLs by the carbamates. The various SBLs used were prepared in appropriate buffer and used in nM range concentration solutions. This solution was placed into an Agilent Technologies Cary 4000 Series UV Vis Spectrophotometer thermostatted to 30 °C controlled by Cary Win UV Scan/Kinetics software. The instrument was zeroed in the presence of enzyme and buffer, but with the absence of antibiotic substrate. Appropriate

wavelengths were used to monitor for the decrease in absorbance of each antibiotic used, with 240 nm being used for benzylpenicillin and 260 nm being used for the cephalosporin based substrates. A 40 mM stock solution of substrate antibiotic was used with a final concentration in the cuvette being 0.2 mM. As soon as the substrate was added to the cuvette, the solution was shaken and immediately placed in the UV instrument so the loss of absorbance of the antibiotic as it was hydrolysed by the SBL could be measured. Penicillin was found to have a very high  $K_m$  compared to the cephalosporin based antibiotic used, cephalothin. Therefore, after initial experiments cephalothin was used as the substrate of choice to measure hydrolysis/inhibition, as it had a lower  $K_m$  and was easier to use to deduce kinetic information. An example of the data produced by these experiments is shown in figure 3.6 below.

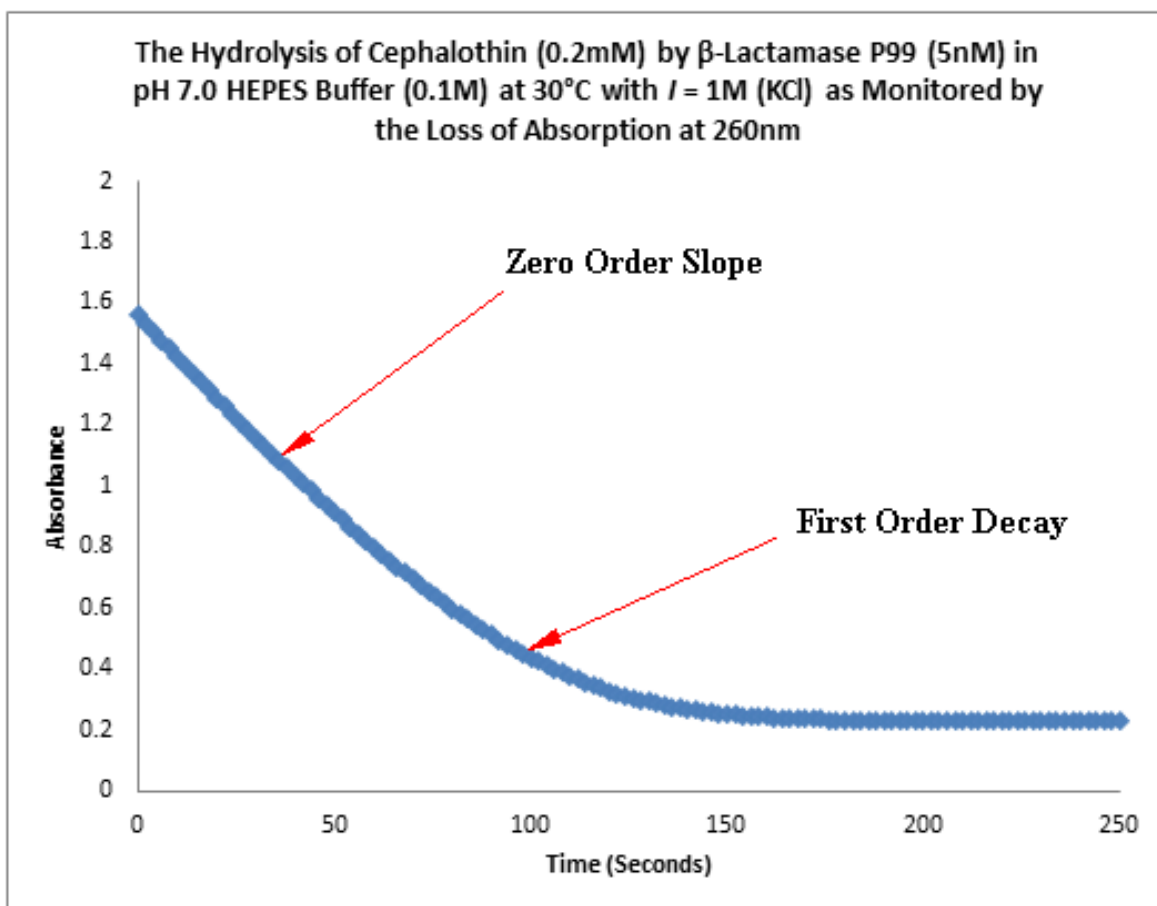
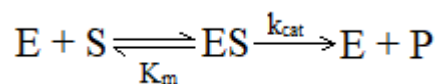


Figure 3.6: Hydrolysis of cephalothin by SBL P99, showing initial rate (zero order slope) and first order decay.

The zero-order slope corresponds to the saturation of the enzyme and the rate of reaction is independent of the concentration of substrate. These straight line slopes are proportional to enzyme concentration and hence are a simple and accurate way to measure enzyme activity.

The experiments measured the rate of hydrolysis of a substrate antibiotic by a selected SBL enzyme, using the loss of absorbance as a tool to deduce the concentration of the active enzyme. An overview of this reaction can be seen in the following Michaelis—Menten kinetics scheme:



$$Rate = \frac{k_{cat} [E][S]}{K_m + [S]}$$

When [S] is greater than  $K_m$ , the rate is equal to:

$$Rate = k_{cat}[E]$$

Saturation kinetics are zero order with respect to the substrate and are independent of the concentration of substrate. However, when [S] is less than  $K_m$ , the rate equation changes to the following:

$$Rate = \frac{k_{cat}}{K_m} [E][S]$$

The reaction is first order with respect to the substrate:

$$k_{obs} = \frac{Rate}{[S]} = \frac{k_{cat}}{K_m} [E]$$

and the rate (change in concentration of substrate divided by change in time) changes with the concentration of substrate.

A time dependent UV method was designed to monitor for inhibition of SBLs. The rate of decrease in absorbance of cephalothin, a  $\beta$ -lactam antibiotic, in the presence of a  $\beta$ -lactamase is measured. All assays were performed in 0.1 M pH 7.0 HEPES buffer with ionic strength ( $I$ ) = 1 M with KCl, prepared using ultra-pure water (UPW) from a Millipore Milli-Q Gradient device. The pH of the buffer was checked using a calibrated Mettler Toledo Inlab Routine Pro pH Measurement instrument with a FE20/FG2 probe.

A cephalothin stock solution was made by dissolving 16.74 mg into 1 ml of pH 7.0 HEPES buffer (0.1 M). 10  $\mu$ l of this stock solution was transferred to the 2ml test solution in the cuvette to give a final test concentration of 0.2 mM. The inhibitor stocks were made fresh on the day of experiments and were kept in melting ice when not kept refrigerated. For the MA carbamate, 29.61 mg was dissolved in 1 ml pH 7.0 HEPES buffer (0.1 M) to create a 100 mM stock. For the TA carbamate, 3.64 mg was dissolved into the same buffer to create a 10 mM stock for use in further experiments. For the HFIP carbamate, 6.48 mg was dissolved in 100 ml of the same buffer to create a 150  $\mu$ M stock. For the HFA carbamate, 6.71 mg was dissolved in 100 ml of the same buffer to create a 150  $\mu$ M stock. Finally, for avibactam 3.96 mg was dissolved in 100 ml of the same buffer to create a 150  $\mu$ M stock.

SBLs were provided in frozen form from the University of Oxford Schofield group, in  $\mu$ M concentration stocks. Upon receipt, the enzymes were diluted and aliquoted appropriately in pH 7.0 HEPES buffer (0.1 M) and stored at -20 °C until needed. Further information regarding enzyme production can be found in chapter six.

In each experiment, a 2 ml quartz cuvette was used containing 5 nM enzyme and 0.2 mM cephalothin and varying concentrations of the inhibitor. These concentrations provided a reasonable absorbance change and so were deemed suitable. A scan of the entire wavelength (190 nm - 800 nm) was collected for the hydrolysis of cephalothin using the Scan application, and 260 nm was deemed a suitable wavelength to monitor the hydrolysis (loss) of cephalothin. The system was blanked using a solution containing everything except the analyte (cephalothin) and reactions were commenced by the addition of cephalothin to the solution containing the inhibitor and enzyme. The initial rate of the loss of absorption at 260 nm was used as a measurement of the concentration of active enzyme and so as a tool to determine the rate of inhibition. The faster the loss of enzyme activity the faster the rate of inhibition. Time dependent inhibition experiments were performed by creating a 20 ml stock

solution of enzyme, to which an inhibitor was added and a stopwatch started. Samples were taken periodically to which cephalothin was added, to allow the monitoring of hydrolysis. The enzyme and inhibitor were incubated at room temperature for varying amounts of time to see if the reaction between the enzyme and inhibitor could be time dependent. An example of the data obtained from the time dependent inhibition experiments can be seen in figure 3.7 below.

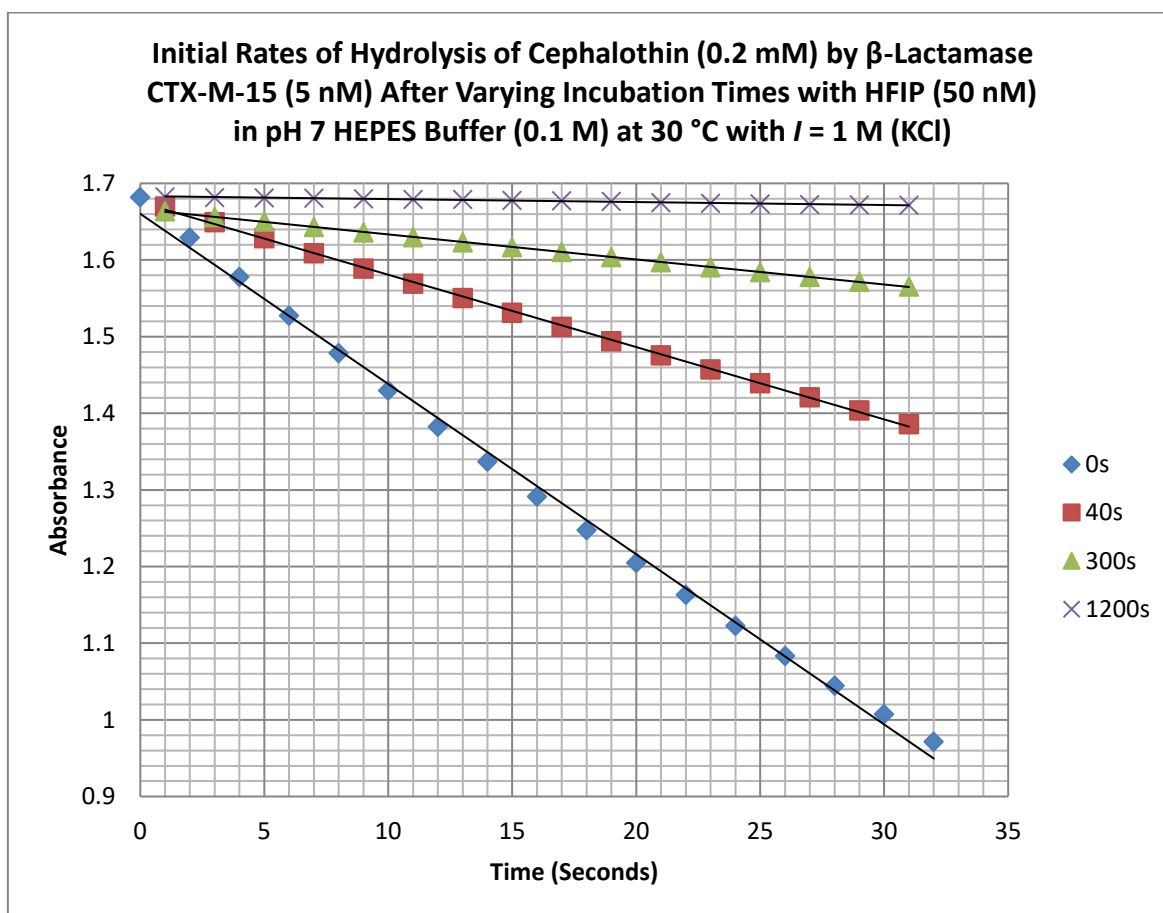


Figure 3.7: Example of data from the time dependent inhibition experiments.

As native enzyme is inhibited, its concentration as an active catalyst decreases and so the rate of the enzyme catalysed hydrolysis of cephalothin decreases. The initial slopes of enzyme with inhibited samples over time can be compared against the initial rate of the

control sample (antibiotic and enzyme with the absence of inhibitor) and plots of these slopes against time give the rate of inactivation of the enzyme.

### **3.3.4: pH Dependence of the Rate of Inactivation Inhibition of SBLs by the Carbamate Inhibitors and pH Dependence of the Rates of Hydrolysis of Substrates by SBLs**

The pH dependence of the rate of inhibition of the enzymes by the carbamate inhibitors was compared to that for the hydrolysis of the substrates by SBLs was investigated. This was accomplished by following the method described previously, but carrying out the inhibition/hydrolysis experiments in different pH buffers. All buffers were made to 0.1 M with ionic strength made constant to 1 M maintained by KCl. Formic acid ( $pK_a$  3.75) was used as the buffer for pH levels between 3-4.5, 2-(N-morpholino)ethanesulfonic acid ( $pK_a$  6.21) (MES) was used as the buffer for pH levels between 5-6.5, HEPES was employed as the buffer for pH levels between 7-8.0, and tris(hydroxymethyl)methylamino]propanesulfonic acid ( $pK_a$  = 8.51 (TAPS) was used as the buffer for pH levels between 8.5-9. Kinetic data were interpreted using GraphPad Prism 7 and Microsoft Excel.

### **3.3.5: Triple Quadrupole Analysis of Carbamate Inhibitors**

An Agilent Technologies 1260 high pressure liquid chromatography system coupled to an Agilent Technologies 6495 Triple Quadrupole (QqQ) Mass Spectrometer was utilised to probe for any avibactam present to ensure it was not the cause of inactivation. Samples were made up to 10 nM along with a 10 nM avibactam standard. The mobile phase on line A was

LCMS water 0.1 % formic acid, and the line B mobile phase was LCMS ACN 0.1 % formic acid. The composition of the mobile phase was 50/50, with a flow rate of 0.4 ml/min. A zero dead volume was used instead of a column. The instrument was set up to monitor for the negative adduct of avibactam, with a single ion monitoring (SIM) of 264.1. The parameters for the QqQ were as follows: gas temperature, 300 °C; gas flow, 5 L/min; fragmentor voltage, 135 V in negative polarity mode.

### **3.3.6: Gas Chromatography Mass Spectrometry Monitoring for Loss of Alcohol**

To further the evidence that it was not any residual avibactam remaining in the carbamates which is responsible for the inhibition, a gas chromatography mass spectrometry (GCMS) experiment was designed to monitor for the loss of alcohol, after inactivation of the enzyme. It was anticipated that the production of alcohol would result from the covalent acylation of the active serine site of the enzymes, giving rise to inactivation. To monitor for the loss of alcohol, an experiment was designed which would allow for the time dependent inhibition of the enzyme, and the production of alcohol. 100  $\mu$ M of inhibitor was added to 1  $\mu$ M enzyme and allowed to react for 30 minutes. Appropriate blanks were taken against which the amount of alcohol in the experimental sample could be compared. Butanol was used to extract the alcohol for GCMS analysis. An Agilent Technologies single quadrupole GCMS system was used. 1  $\mu$ L of sample was injected onto a HP5 column. The initial oven temperature was 35 °C with a 5 °C/minute ramp to 80 °C held for 1 minute.

### 3.4: Results and Discussion

#### 3.4.1: LCMS Analysis of Carbamates

The samples were run on a LCMS instrument as described in the methods section. Appropriate blanks were run and the expected mass for each compound was extracted from the total ion chromatogram (TIC) to indicate whether or not the correct compound had been synthesised.

The extracted ion chromatogram (EIC) for the predicted MW of each compound was extracted from the TIC from each sample. Each sample was run in positive and negative ionisation mode, with negative ionisation mode providing the best response for each sample. Unfortunately, it was not possible to fully characterise the hexafluoroacetone hydrate analogue compound via LCMS, and further work is required for this sample to fully elucidate its structure.

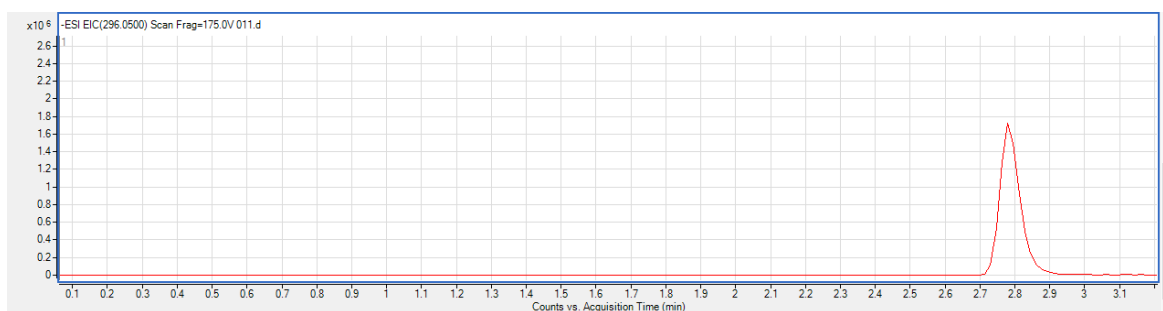


Figure 3.8: EIC of 296.0561 for MA.

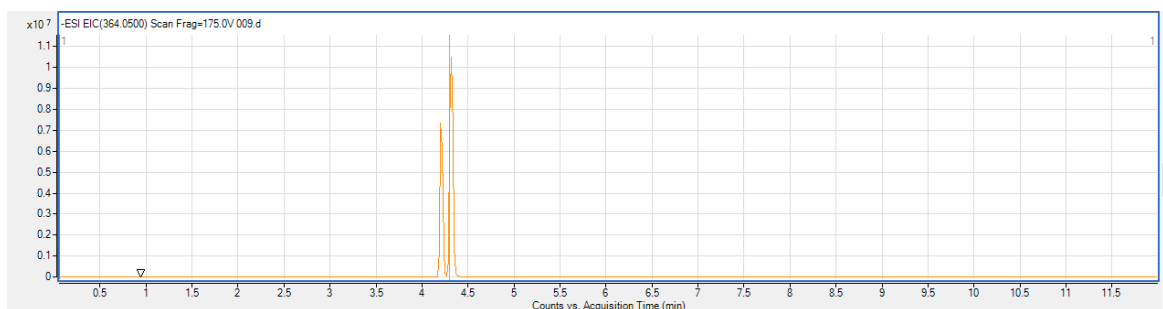


Figure 3.9: EIC of 364.0439 for TA.

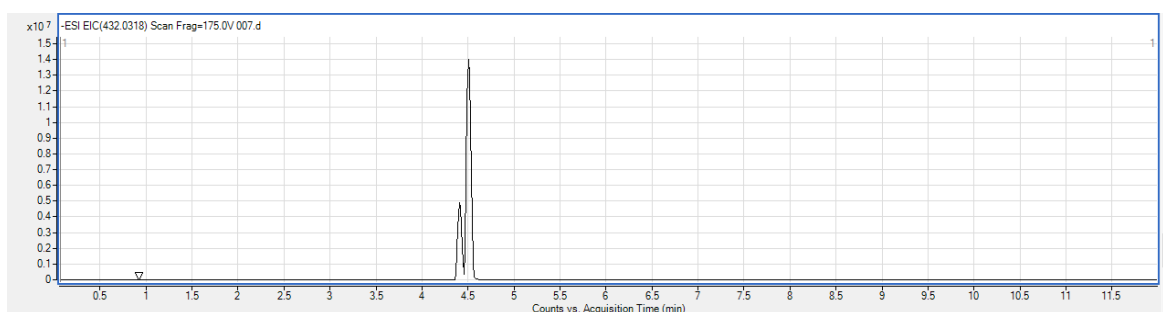


Figure 3.10: EIC of 432.0318 for HFIP analogue.

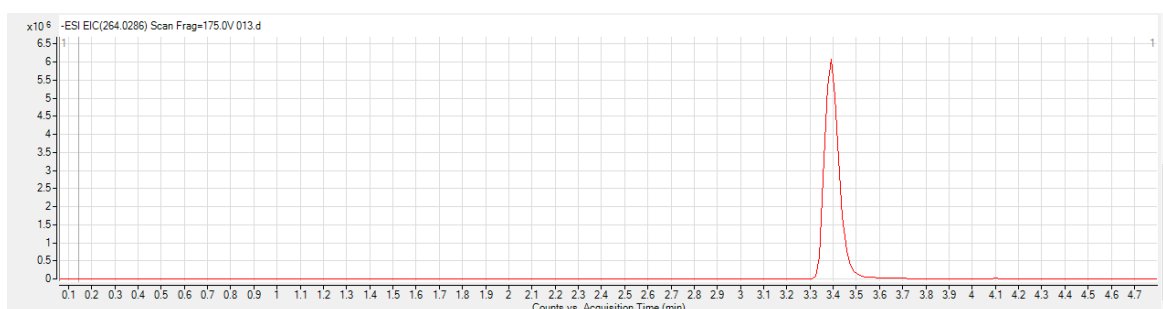


Figure 3.11: EIC of 264.0294 for avibactam.

In figures 3.9 and 3.10 there were two peaks present. This is a common occurrence in HPLC and LCMS and is known as peak splitting; causes can range from poor method design to instrument issues (such as HPLC pump issues), to issues with sample preparation. In the case of this experiment, it was due to the sample being too concentrated, which was confirmed by the instrument indicating that the ion detector was overloaded due to the column being saturated with sample, resulting in an irregular peak shape. The samples in

the above figures were made to a high concentration (10  $\mu$ M) in order to search for any trace evidence of remaining avibactam starting material. Despite being unable to find the mass of 447.03 for the hexafluoroacetone hydrate analogue, the sample showed very effective inhibition of SBLs (which will be discussed later). Avibactam's M/Z was searched for in the TIC and no avibactam was found. The QToF instrument was capable of identifying avibactam with a 1  $\mu$ L injection of a 10 nM standard. This means that if there was any avibactam in the sample, it must be considerably less than the 10 nM standard. This result, along with further experiments to be discussed shortly, suggest that there is no avibactam in the synthesised compounds, meaning that the inhibition must be due to the synthesised compounds.

Further work is required to fully characterise these compounds, and future experiments could include QqQ analysis. QqQ analysis essentially fragments the compounds using an electronic voltage and then looks for the pieces of the compounds remaining. The software then 'pieces' the remaining structures together to collate a fingerprint of the molecule. The masses of the daughter ions provided from fragmenting the molecule and the way in which the structure fragments are used to identify the structure of the compound.

### **3.4.2: QqQ Analysis of Synthesised Compounds for Avibactam Detection**

As mentioned, it was important to ensure that the inhibition seen with the synthesised compounds was due to them, and not due to any remaining avibactam from the synthesis reaction. The LCMS QToF samples looked relatively clean and to contain just the synthesised compounds. Another way to check for the presence of avibactam was to check

using QqQ; the results of which are seen below, and will be discussed further in the discussion.

Figure 3.12 below shows the TIC for the avibactam standard.

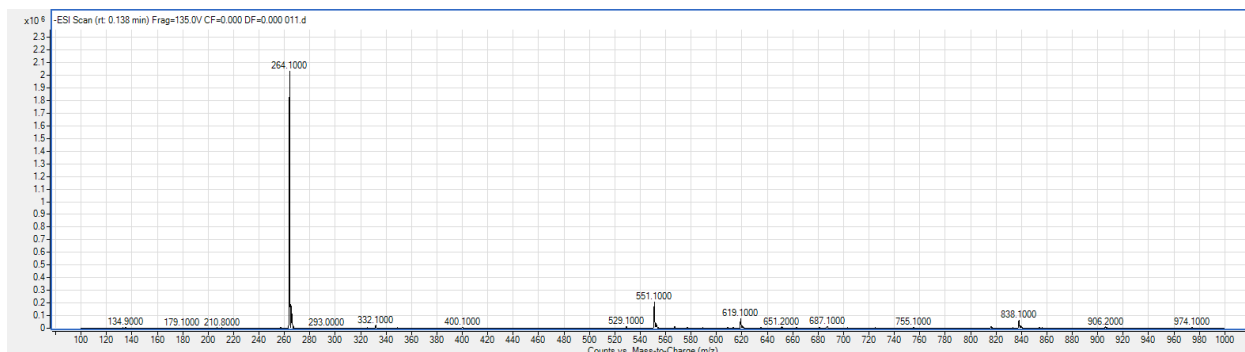


Figure 3.12: TIC of avibactam standard on QqQ, showing a clearly abundant ion of 264.1.

This m/z of 264.1 was then searched for in the two derivatives of avibactam. Using single ion monitoring (SIM) of the QqQ, a higher sensitivity can be achieved in comparison to other LCMS instruments, including the Q-TOF. Figure 3.13 below shows the TIC for 264.1 in the two derivatives made up to 500  $\mu$ M, and a water/ACN blank.

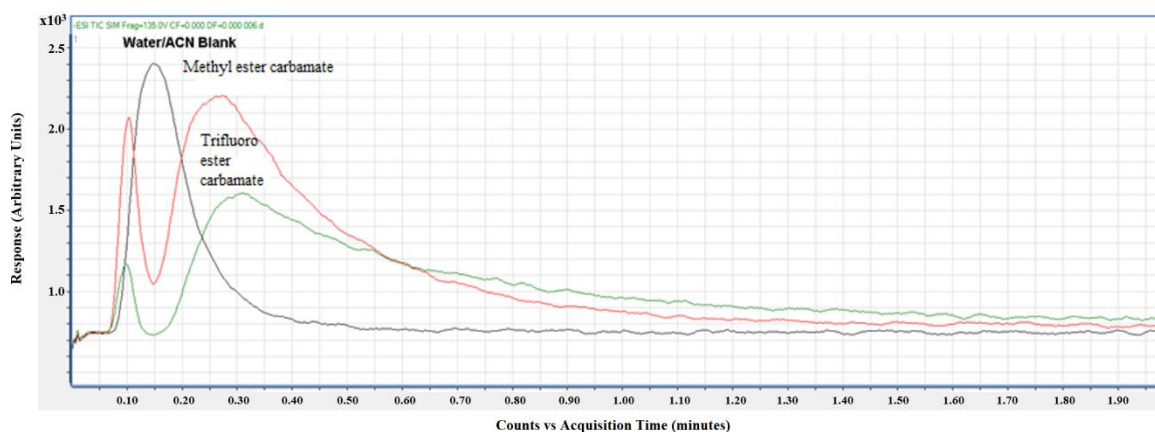


Figure 3.13: TIC of SIM of 264.1 in the two derivatives and a water/ACN blank, showing an instrument response of  $10^3$ .

The three samples shown in figure 3.13 above are a water/ACN blank, the MA sample and the TA sample. The SIM analysis of these three samples gave a response of  $10^3$  on the QqQ instrument. For comparison, the TIC of SIM of 264.1 of 10 nM avibactam is shown below in figure 3.14.

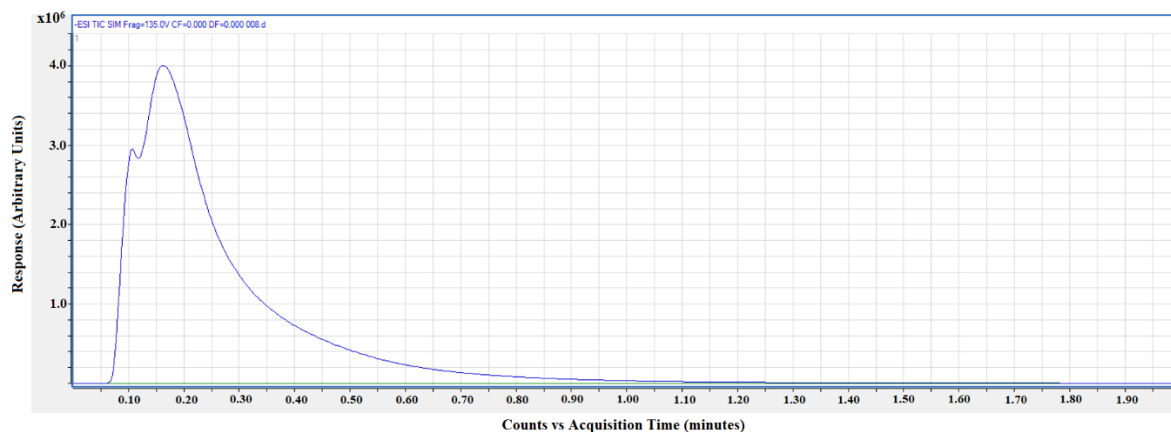


Figure 3.14: TIC of SIM of 264.1 of 10 nM avibactam, showing an instrument response of  $10^6$ .

The results for the SIM analysis of avibactam's  $M/Z$  in a 10 nM avibactam standard gave a response of  $10^6$  on the QqQ instrument. Clearly from the results, 10 nM of avibactam contains much more avibactam than either of the 500  $\mu$ M synthesised compounds. The peaks of the TA and MA samples appear as a flat line on the avibactam sample. This is further proof that there is no avibactam in the synthesised samples. In the experiments, it has clearly been shown that there is no detectable avibactam present in the carbamate inhibitors, as shown by the QqQ and LCMS experiments. This therefore can only mean that it cannot be avibactam that is inhibiting the enzymes, and must be the synthesised carbamates.

### 3.4.3: Liberation of Alcohol

Another theory to support the observation that it is the synthesised carbamates inhibiting the SBLs rather than any remaining avibactam is whether or not the ROH is produced after the synthesised compounds were incubated with the enzyme. If the ROH was detected, then it confirms that the predicted reaction between the carbamate and the enzyme had taken place and the ROH was liberated as predicted. As a control, the same experiment as above was carried out under exactly the same conditions but with no enzyme present.

To investigate this, the TA inhibitor (100  $\mu$ M) was incubated with SBL CTX-M-15 (1  $\mu$ M) for 20 minutes. The alcohol (if present) was then extracted into butanol and ran on GCMS.

First, a blank of butanol and a TA spike were run as described in the methods section.

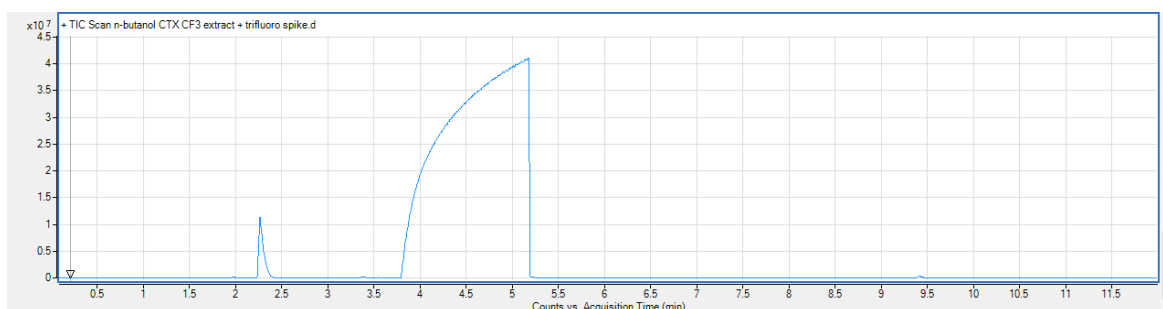


Figure 3.15: Trifluoroethanol (1 mM) spike in butanol (10 cm<sup>3</sup>)

The first peak at 2.27 minutes gave the following prominent ions.

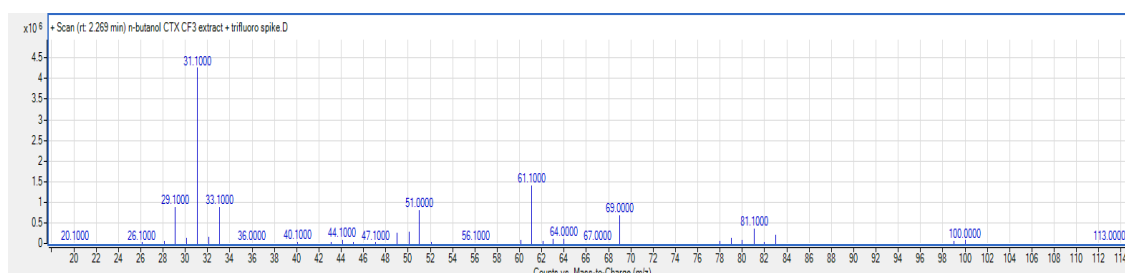


Figure 3.16: Prominent ions for peak at 2.27 minutes.

These spectral parameters were ran against the National Institute of Standards and Technology Mass Spectral database tool and identified trifluoroethanol with a strong match, as can be seen in figure 3.17 below.

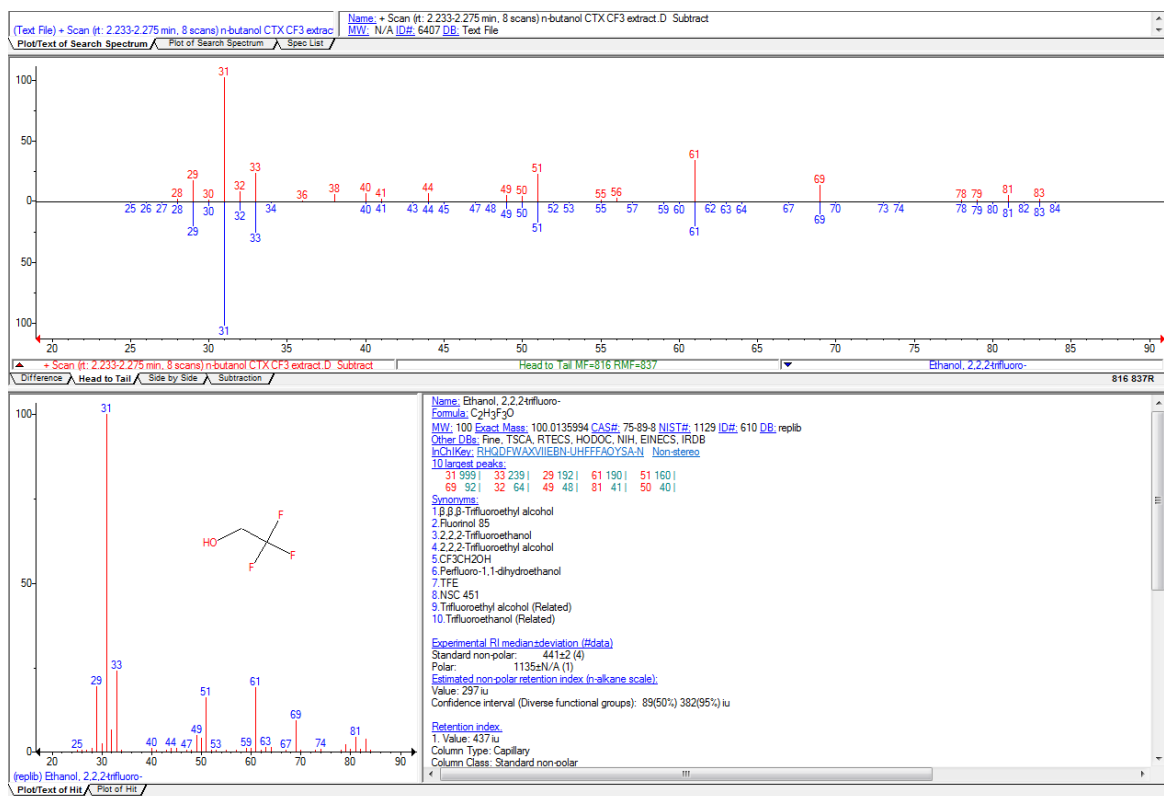


Figure 3.17: Strong match for trifluoroethanol.

The peak at 2.27 minutes was therefore confirmed as trifluoroethanol. A 500  $\mu$ M solution of the trifluoroethanol carbamate derivative was prepared in 0.1 M HEPES buffer at pH 7. The sample was extracted with butanol and this blank sample was run on GCMS. It was important to detect whether any free trifluoroethanol was detected in a blank sample consisting of just the carbamate in the absence of enzyme under the same conditions for 20 minutes. The TIC of this sample can be seen below.

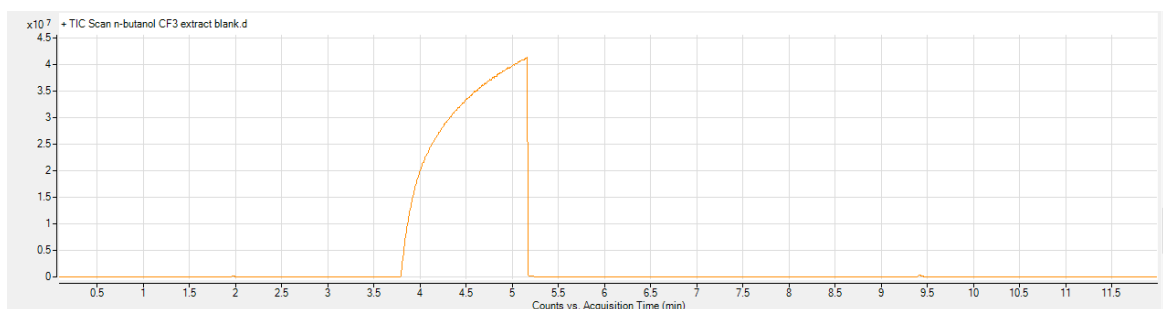


Figure 3.18: Overview of TIC for the blank inhibitor sample.

If the area corresponding to the known retention time of trifluoroethanol is expanded (around 2.27 minutes as from figure 3.15 above), one can clearly see that there is no trifluoroethanol present in this blank sample (see figure 3.19 below, confirming no trifluoroethanol present in the blank inhibitor sample). Therefore, there is no ring closure of the carbamate to generate avibactam and alcohol under these reaction conditions.

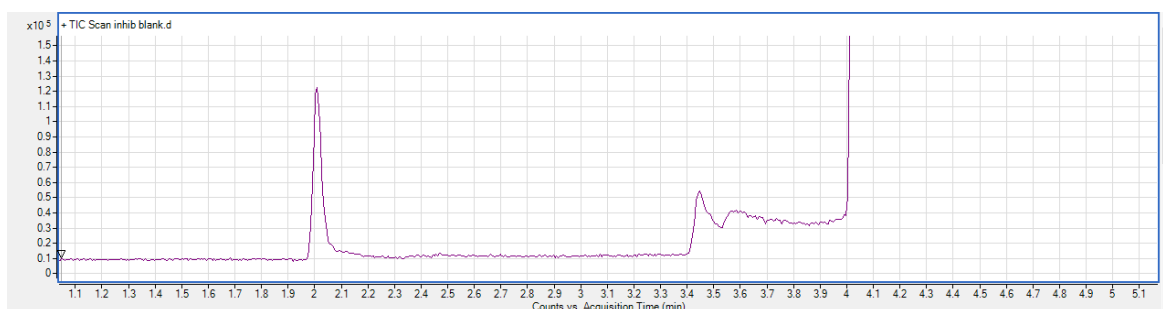


Figure 3.19: Expanded area of TIC of inhibitor blank, showing noticeable lack of peaks around 2.27 minutes, indicating no trifluoroethanol was present in the control reaction.

CTX-M-15 was added to make a final solution of 500  $\mu$ M TA and 5  $\mu$ M CTX-M-15 in 0.1 M HEPES buffer at pH 7.0. The enzyme and inhibitor were incubated together for 20 minutes, and the sample was extracted with butanol and ran on GCMS.

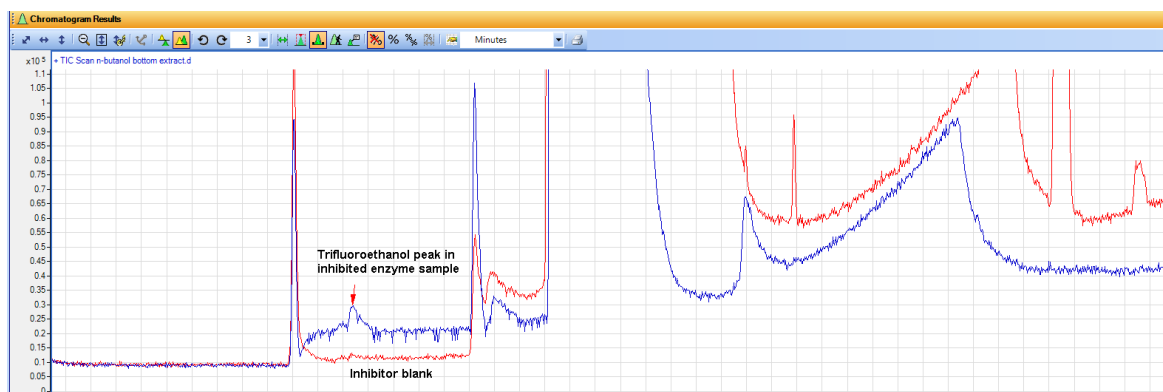


Figure 3.20: Incubated TA and inhibitor samples.

Looking at figure 3.20 above, one can clearly see there is a noticeable peak present in the incubated TA/enzyme sample; the same peak is clearly not present in the control reaction. This indicates that trifluoroethanol is liberated after the reaction between the inhibitor and enzyme commences, which suggests that it is the synthesised inhibitor responsible for the noticed inhibition.

Furthermore, this was confirmed by spiking the same sample with trifluoroethanol, which resulted in the trifluoroethanol peak seen in the inhibited enzyme sample having a much higher response on the GCMS.

The fact that there was no trifluoroethanol detected in the TA control sample, but there was a noticeable peak for trifluoroethanol noticed in the presence of the enzyme/TA sample indicates that trifluoroethanol must be being liberated due to a reaction with the enzyme. The logical conclusion is that the trifluoroethanol is liberated from the TA when the inhibition of the enzyme commences. This is further proof that the inhibition is due to the carbamate, and not because of any avibactam that may be present in the sample.

The GCMS experiment worked well to show that there was no reformation of avibactam (due to the fact there was no liberation of alcohol in the blank inhibitor sample) in the time frames relevant to the inhibition experiments and also showed that alcohol was liberated

from the inhibitor upon the inhibition reaction with the enzyme. However, GCMS as an analytical technique is not as sensitive as LCMS, and a high concentration of enzyme was required in the reaction to facilitate the liberation of enough alcohol to facilitate a response via GCMS. Knowing that the inhibitors probably followed the same reaction mechanism, it was deemed unnecessary to sacrifice more enzyme to test this same reaction on the other inhibitors.

#### **3.4.4: Detection of Avibactam via LCMS in the Carbamate Derivatives**

Further work was carried out to demonstrate the lack of avibactam starting material in the synthesised inhibitors. The kinetic data (which will be discussed shortly), indicated that there was a very fast reaction between the carbamates and the SBL enzymes they inhibited, with the vast majority of inhibition taking place within the first 5 minutes of the reaction commencing. If it could be shown that there was no avibactam reformation in this time frame, then it would be further proof that it was the carbamates responsible for inhibition, and not any left-over avibactam from the synthesis reaction, or recyclisation of the inhibitors to reform avibactam.

It was first deemed necessary to deduce the limit of detection for avibactam for the instrument being used. The work was carried out on an Agilent Technologies 1200 LC system coupled to an Agilent Technologies 6210 Time of Flight (TOF) Mass Spectrometer. A series of avibactam standards were made with set concentrations down to 0.1 nM. A 50 nM avibactam standard was used to give the m/z for avibactam on the TOF instrument. The response for this concentration can be seen below in figure 3.21.

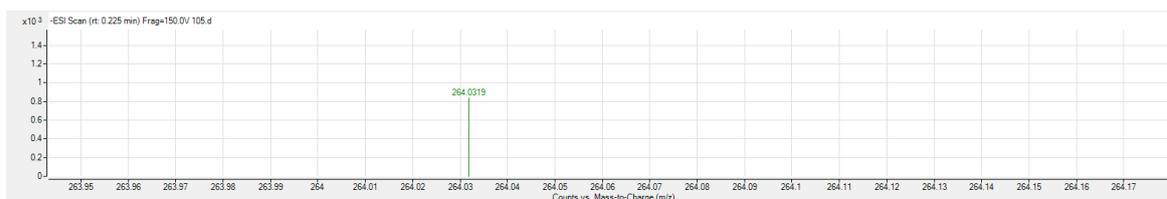


Figure 3.21: TOF Response for 50 nM Avibactam standard.

The system provided a small, but noticeable peak which correlated with the expected m/z of avibactam in negative ionisation mode. This peak was not present in an ultra-pure water (UPW) blank.

Lower concentrations were run down to 0.1 nM and a response for avibactam could still be seen down to the 1 nM level, so if no avibactam could be seen in the synthesised inhibitor samples, then any avibactam present must be below this figure.

Next, a 10  $\mu$ M sample for the HFIP carbamate analogue was prepared and run using the same method and conditions. At this concentration, the instrument detected a response for the EIC of the m/z of the HFIP analogue, but detected absolutely no response for the EIC of the m/z of avibactam. This means that if there was any avibactam present in the synthesised compound, it must be below 1 nM. It is important to take into consideration the fact that the HFIP and HFA carbamates were used at a maximum concentration of 50 nM in the enzyme kinetic experiments (which will be discussed shortly). If no avibactam was detected in the 10  $\mu$ M sample of the synthesised inhibitor, then there will certainly be no avibactam in the 50 nM sample of the inhibitor. This is further proof that it is the carbamate derivatives which are responsible for inhibition. It is also worth noting that, in any case, the concentration of any avibactam present must also be lower than the enzyme concentration used in the experiments; which is further proof that it is the carbamate derivatives responsible for inhibition, not any residual avibactam.

After determining the limits of detection for the instrument with regards to avibactam, attention turned to proving that there was no recyclisation of the carbamate compounds to form avibactam. A 50 nM solution of the HFIP derivative was prepared in a 0.1 M pH 7 HEPES buffer solution at 25 °C, the same experimental conditions that the kinetics experiments were performed. Samples were taken after 30 minutes to monitor for the presence of avibactam. The instrument response from this experiment can be seen in figure 3.22 below.



Figure 3.22: TIC of 30 minute HFIP sample.

The  $m/z$  for avibactam and HFIP were extracted from the TIC. The instrument found no avibactam, and HFIP still had a detectable response, as seen below in figure 3.23.

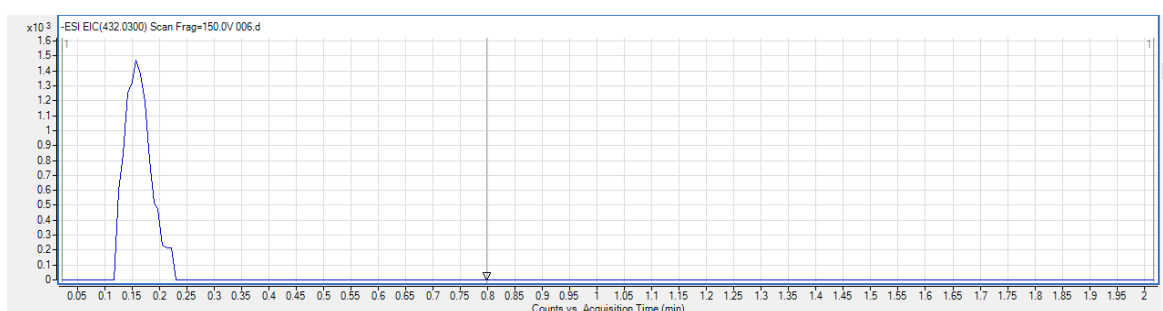


Figure 3.23: EIC for the  $m/z$  of HFIP in the 50 nM sample after incubation for 30 minutes.

This confirmed that there was no detectable recyclisation of avibactam from the carbamates in the time frame for which inhibition was seen in the kinetic experiments. This is further proof that inhibition must be due to the synthesised inhibitors and not due to avibactam.

In summary, there is no avibactam present from the synthesis of the inhibitors, as seen from the clean LCMS traces and the QqQ data. It is also confirmed that the inhibition of the enzyme occurs concurrent with the expulsion of the alcohol leaving group in the inhibitors, as seen from the GCMS data showing the liberation of trifluoroethanol after incubation of the inhibitor with CTX-M-15. Finally, it is shown that there is no recyclisation of avibactam, as seen from the timed LCMS experiment with the HFIP sample stored in 0.1 M HEPES buffer at 25 °C for 30 minutes. After this period, no avibactam was found within the detectable limits of the instrument. It can therefore be concluded that the synthesised carbamates provide a novel inhibition of the SBLs.

### **3.4.5: Kinetics of Hydrolysis of Substrate by SBLs and Inhibition and pH Dependence**

The four synthesised carbamates were tested for their inhibition against common SBLs from classes A and C. The enzymes tested for inhibition from class A were TEM-1, and the classes from class C were AmpC, P99 and CTX-M-15. Also, three of the synthesised carbamates were subjected to hydrolysis in pH 14 NaOH to elucidate their hydroxide rate constant. This could be compared to the  $pK_a$  of their alcohol leaving group to give more information of their effectiveness as inhibitors.

#### ***3.4.5.1: Kinetics of Hydrolysis of Carbamate Inhibitors***

The hydrolysis of the carbamate inhibitors in 1 M pH 14 NaOH at 25 °C was deduced as monitored by the loss of absorbance at certain wavelengths, as discussed in the methods

section. The change in absorbance was recorded over a period of time and the natural logarithm of the absorbance infinity value – absorbance time value gave a straight line corresponding to the observed pseudo first-order rate constant. As these kinetic runs were performed in 1 M NaOH these rate constants also give the second-order values. Figure 3.24 below shows the Bronsted plot for the second-order rate constants ( $M^{-1}s^{-1}$ ) for the hydroxide ion catalysed hydrolysis for three of the carbamates (MA, TA and HFIP) against the  $pK_a$  of the leaving group alcohol.

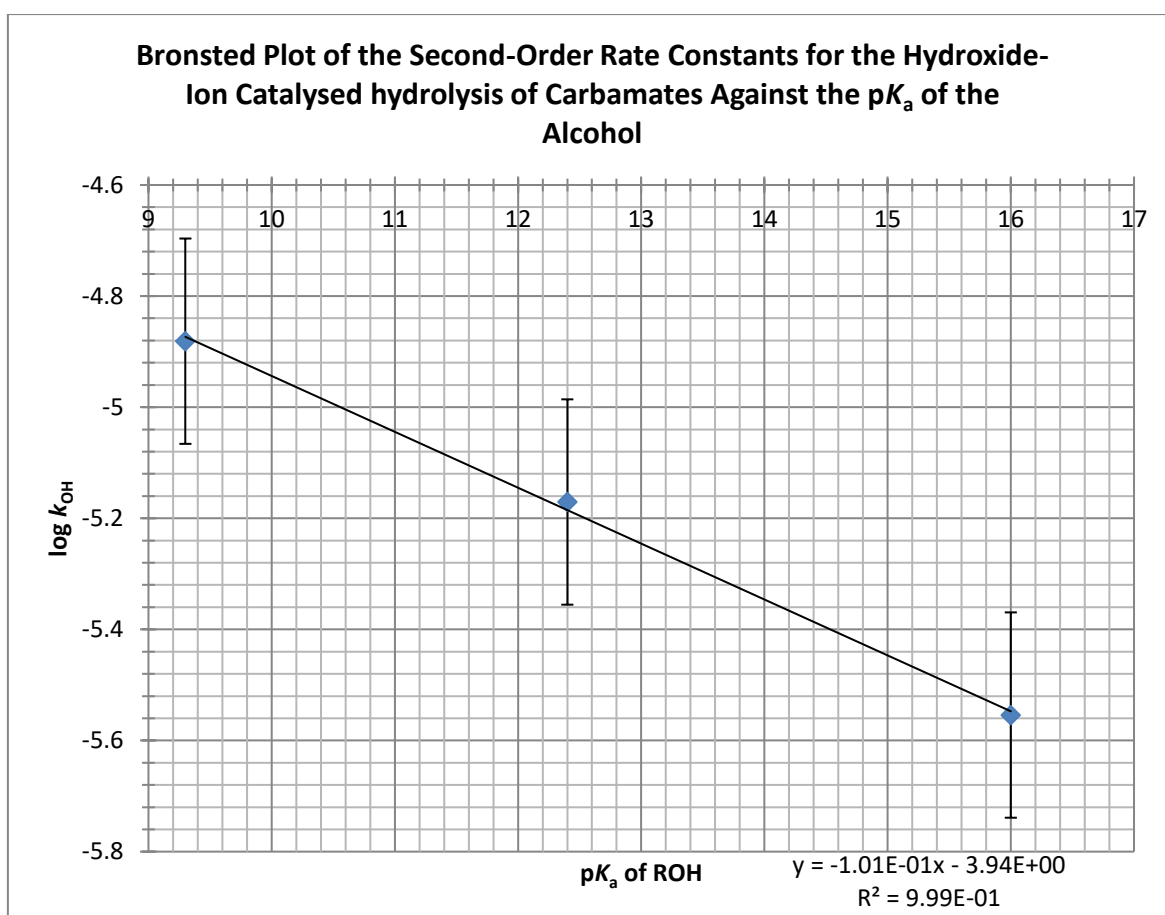


Figure 3.24: Bronsted Plot of the second-order rate constants for the hydroxide-ion catalysed hydrolysis of carbamates against the  $pK_a$  of the alcohol.

As can be seen from figure 3.24 above, as the acidity of the alcohol increased, the hydroxide ion rate constant for hydrolysis is also increased. This gives an indicator to the effectiveness

of the carbamates as an inhibitor. It was confirmed that the more effective inhibitors had higher hydroxide rate constants. Unfortunately, due to time constraints, the hydroxide rate constant of the HFA carbamate was unable to be confirmed. However, it has the lowest  $pK_a$  of the carbamates, so it is predicted that it would have an even greater hydroxide rate constant than the other inhibitors.

The slope of the line in fig 3.24 gives the Bronsted  $\beta_{lg}$  value which in this case is -0.1. This is a surprisingly low value. For comparison the  $\beta_{lg}$  hydroxide-ion catalysed hydrolysis of esters  $\text{PhCH}_2\text{CO}_2\text{R}$  is -0.4. The effective charge on the alcohol oxygen in carbamates is +0.8 and so the observed  $\beta_{lg}$  for alkaline hydrolysis is compatible with rate-limiting breakdown of the tetrahedral intermediate as seen in figure 3.25 below:

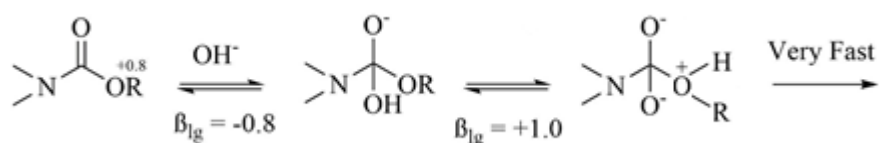


Figure 3.25: Alkaline hydrolysis of carbamates showing rate-limiting step of the breakdown of the tetrahedral intermediate.

### 3.4.6: Kinetics of Inhibition of AmpC, P99, TEM-1 and CTX-M-15 by Methyl ester carbamate and Trifluoroethyl ester Carbamate Derivatives

The MA and TA only provided modest inhibition as compared to the more acidic alcohol derivatives, containing leaving groups with lower  $pK_a$ s. As such, the results of the kinetics data for the MA and TA derivatives will only be discussed briefly, with the results of the more acidic alcohols being explained in more detail.

To determine the kinetics of inhibition, blank samples consisting of enzyme and substrate (cephalothin) were performed using changes in the UV spectra as described in the methods section. Samples were taken at specified time intervals and the initial slopes of each sample were recorded. These samples served as blank determinations, and would be used to compare against the inhibition initial slopes. This ratio of active enzyme to inactive enzyme gives the percentage of active enzyme remaining after times incubated with the inhibitor. The percentage active enzyme remaining figures were plotted against the incubation time to give a graph displaying pseudo first order kinetics.

The percentage active enzyme remaining were converted to concentration of enzyme remaining, and the natural logarithm of these values were plotted against incubation time to give a straight line graph, as shown in figure 3.26 below.

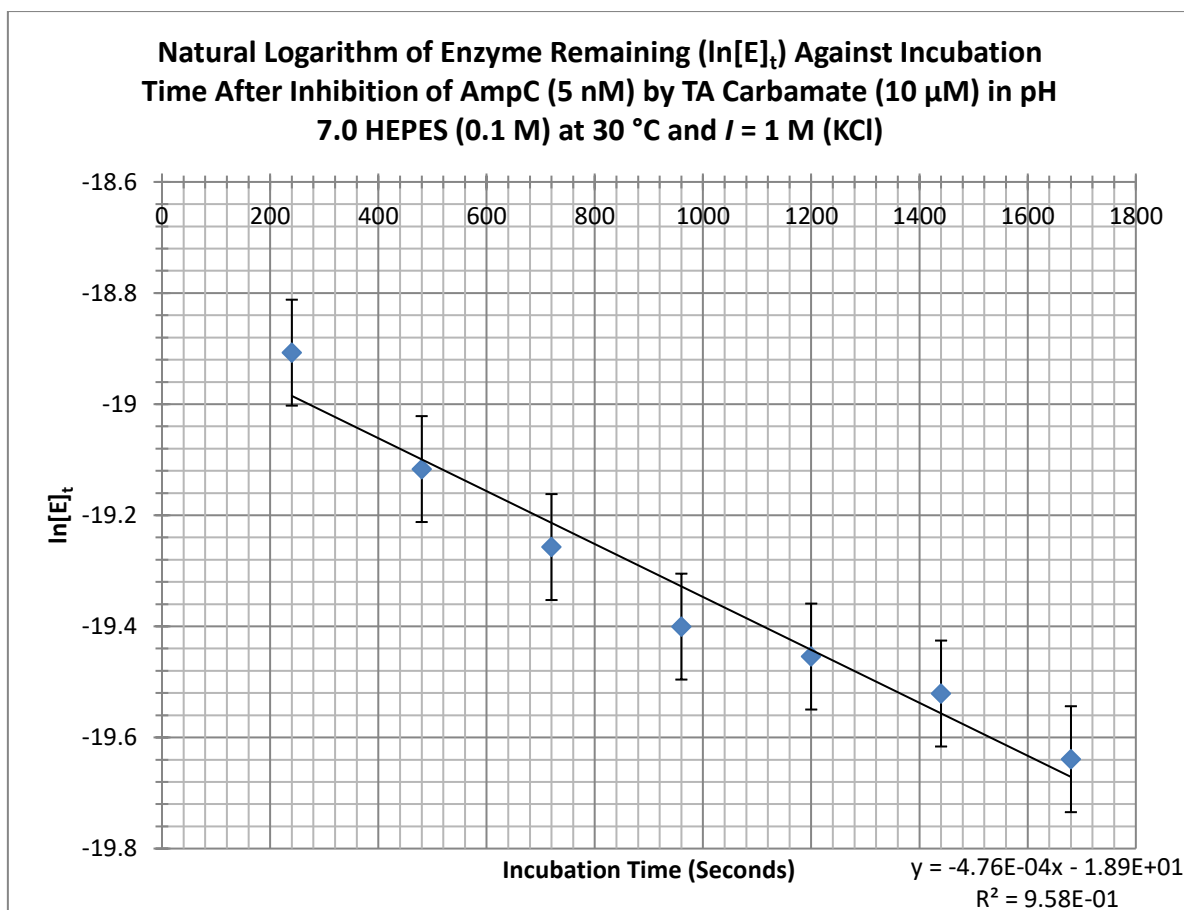


Figure 3.26: Natural logarithm of concentration of active enzyme remaining against incubation time for inhibition of AmpC (5 nM) by the TA carbamate (10  $\mu$ M).

The slope of the graph above in figure 3.26 can be interpreted as the observed pseudo first-order rate constant for the inhibition ( $k_{obs}$ ). This was repeated for each experiment between the enzyme and carbamates, with different concentration of carbamates used. These  $k_{obs}$  values were then plotted against carbamate concentration the slope of which gives the second-order rate constant ( $M^{-1}s^{-1}$ ) for inhibition, as seen below in figure 3.27.

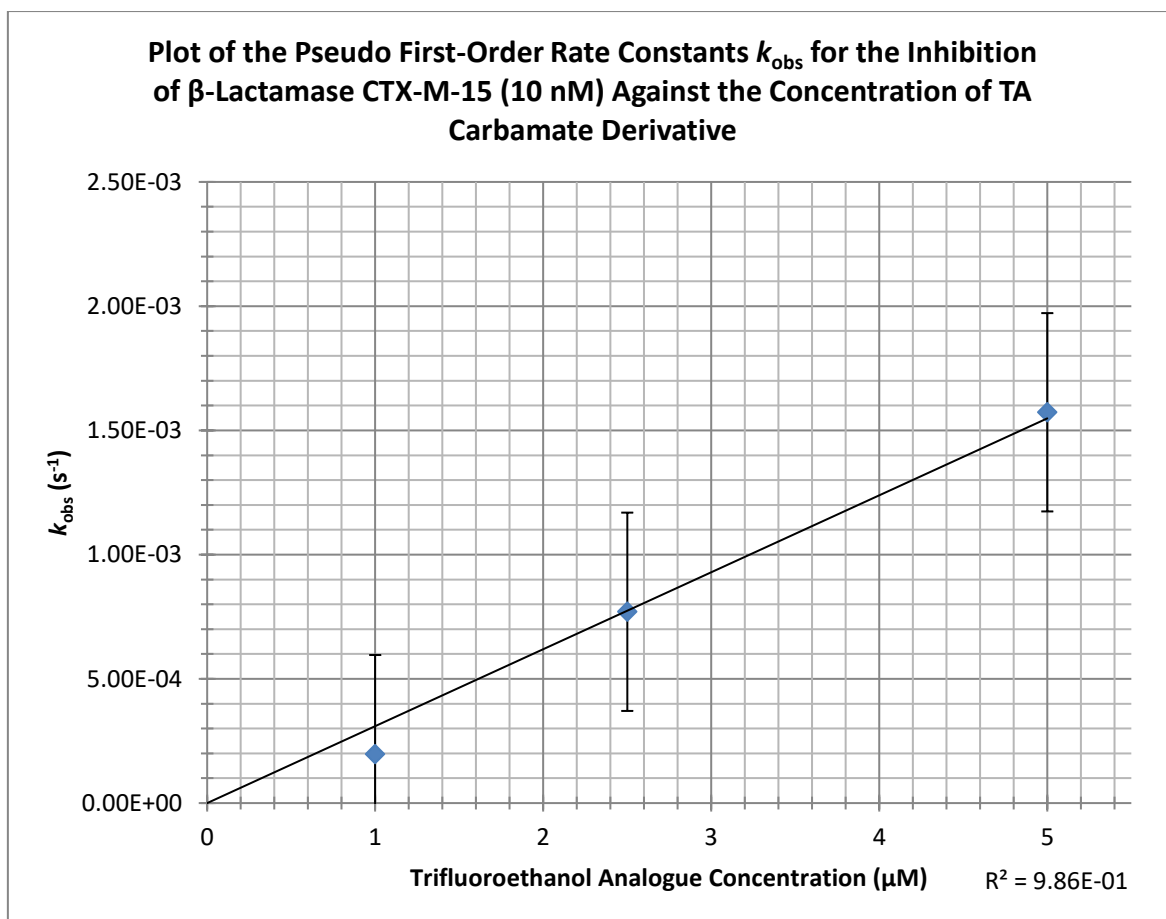


Figure 3.27: Observed pseudo first-order rate constants,  $k_{\text{obs}}$ , for the inhibition of CTX-M-15 (10 nM) by trifluoroethanol analogue (TA) at varying inhibitor concentrations.

This method of data collection/analysis was repeated for different inhibitors and enzyme combinations, the results of which are shown below in table 3.2.

Table 3.2: Kinetic results of inhibition of SBLs by MA and TA carbamate derivatives.

Enzyme	Carbamate Derivative	Concentration (μM)	$k_{obs}$ (s <sup>-1</sup> )	$k_i$ (M <sup>-1</sup> s <sup>-1</sup> )
TEM-1	MA	25	$3.13 \times 10^{-4}$	14.32
		50	$7.16 \times 10^{-4}$	
		100	$9.90 \times 10^{-4}$	
		150	$1.13 \times 10^{-3}$	
		250	$2.72 \times 10^{-3}$	
	TA	0.5	$3.41 \times 10^{-4}$	1016.48
		1	$5.39 \times 10^{-4}$	
		1.5	$6.84 \times 10^{-4}$	
		2.5	$1.83 \times 10^{-3}$	
		3.75	$3.07 \times 10^{-3}$	
AmpC	MA	250	$2.51 \times 10^{-4}$	2.01
		500	$5.58 \times 10^{-4}$	
		1000	$1.19 \times 10^{-3}$	
		1500	$3.02 \times 10^{-3}$	
	TA	5	$1.51 \times 10^{-4}$	36.6
		8	$2.93 \times 10^{-4}$	
		10	$4.76 \times 10^{-4}$	
CTX-M-15	MA	500	$9.5 \times 10^{-4}$	3
		1000	$3 \times 10^{-3}$	
		1250	$3.49 \times 10^{-3}$	
	TA	1	$1.97 \times 10^{-4}$	314.6
		5	$1.57 \times 10^{-3}$	
P99	MA	250	$2.41 \times 10^{-4}$	0.96
		500	$4.54 \times 10^{-4}$	
		1000	$9.84 \times 10^{-4}$	
	TA	1	$1.03 \times 10^{-4}$	105.45
		5	$4.46 \times 10^{-4}$	
		10	$1.05 \times 10^{-3}$	

The synthesised TA and MA samples were tested for their inhibition of TEM-1 AmpC, CTX-M-15 and P99.

For inhibition of AmpC, the data showed modest inhibitory effects, with  $k_i$  of the MA analogue being  $2 \text{ M}^{-1}\text{s}^{-1}$ , but the TA had a higher  $k_i$  in the region of  $40 \text{ M}^{-1}\text{s}^{-1}$ , making it a more effective inhibitor. AmpC SBLs are produced by many of the *Enterobacteriaceae*, so producing novel inhibitors of these enzymes is of great clinical interest.

The data for the inhibition of P99 by MA and TA showed similar kinetics to the inhibition of AmpC. This was to be expected, as AmpC and P99 are both class C SBLs, and MA and TA are predicted to inhibit the enzymes in the same way. However, it was encouraging to see that inhibition was observed with a different enzyme. This suggested that the two inhibitors were novel inhibitors of SBLs. To further confirm this, it was decided to test the two inhibitors against an SBL from a different class. Class A SBL TEM-1 was acquired and similar inhibition testing took place.

With regards to TEM-1, only modest rates of inhibition were noticed by the synthesised inhibitors. However, it was noticed that TEM-1 had relatively high rates of inhibition as compared to the other enzymes, with  $k_i$  being in the region of  $10^3 \text{ M}^{-1}\text{s}^{-1}$  for the TA carbamate.

Finally, for CTX-M-15, modest inhibition was noticed with the TA/MA synthesised inhibitors.

Now that inhibition had been observed across different classes of SBLs, work commenced in trying to improve the modest inhibitory effects of the TA and MA. The effectiveness of the MA and TA carbamates was limited by the  $pK_a$  of the alcohol leaving groups. MeOH has a  $pK_a$  of 16, which showed the lowest activity of any synthesised inhibitor. The  $pK_a$  of

$\text{CF}_3\text{CH}_2\text{OH}$  was lower, at 12.4, and was seen to be a more effective inhibitor. Therefore, alcohols with lower  $\text{p}K_{\text{a}}$ s were identified, and used to synthesise two further compounds: Hexafluoroisopropanol (HFIP) with a  $\text{p}K_{\text{a}}$  of 9.3 and hexafluoroacetone hydrate (HFA) with a  $\text{p}K_{\text{a}}$  of 6.58. It was predicted that these alcohols having lower  $\text{p}K_{\text{a}}$ s would serve as better leaving groups, and therefore act as better inhibitors of SBLs. HFIP and HFA inhibitors were prepared as described in the methods section and were screened for their effectiveness against CTX-M-15.

### 3.4.7 Kinetics of Inhibition of CTX-M-15 by Hexafluoroisopropanol and Hexafluoroacetone Hydrate Carbamate Derivatives

The two carbamates synthesised with the more acidic alcohols (hence providing leaving groups with lower  $pK_{as}$ ) were also tested for their inhibition against SBL CTX-M-15. As will be seen shortly, the inhibition of CTX-M-15 by these enzymes was much more efficient than with either of the MA or TA carbamates. Their results will be discussed in more detail, as their results are of much more clinical relevance.

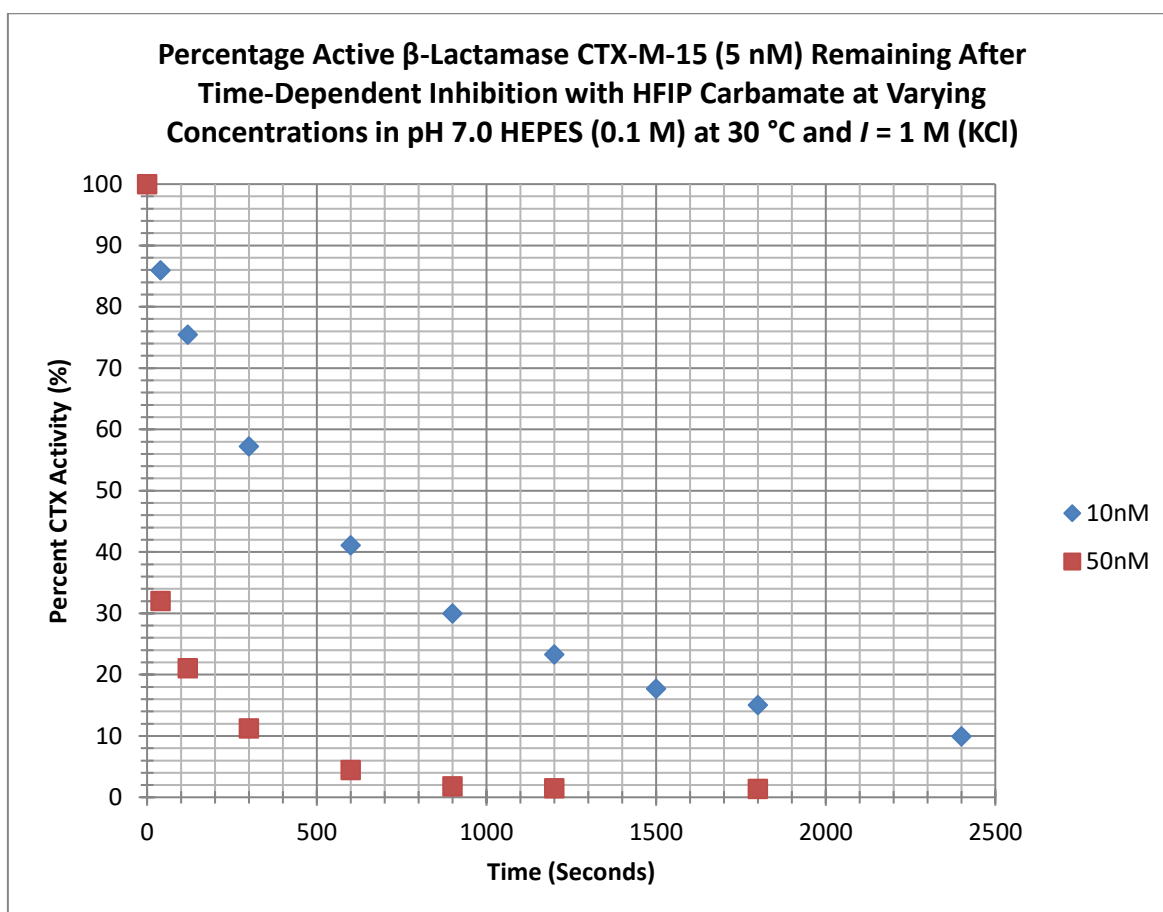


Figure 3.28: Percentage active  $\beta$ -lactamase CTX-M-15 remaining after incubation with HFIP carbamate at 10:1 (50 nM) and 1:1 (10 nM) concentration with enzyme.

It was noted immediately from figure 3.28 that HFIP was a much more effective inhibitor than either of the two previously tested inhibitors. This is thought to be due to the lower  $pK_a$  of the alcohol leaving group, making the HFIP a more efficient inhibitor. As for the previous inhibition experiments with the less acidic alcohol leaving groups, the experiments were conducted in 20 ml pH 7.0 HEPES buffer (0.1M) using 0.2 mM cephalothin as a substrate for hydrolysis. For the 50 nM experiment, 6.67  $\mu$ l was taken from the 150  $\mu$ M HFIP stock solution and added to the 20 ml test solution containing 5 nM CTX-M-15 to create a 50 nM test concentration where as for the 10 nM experiment, 1.33  $\mu$ l was taken and added to the 20 ml test solution to create a final 10 nM concentration.

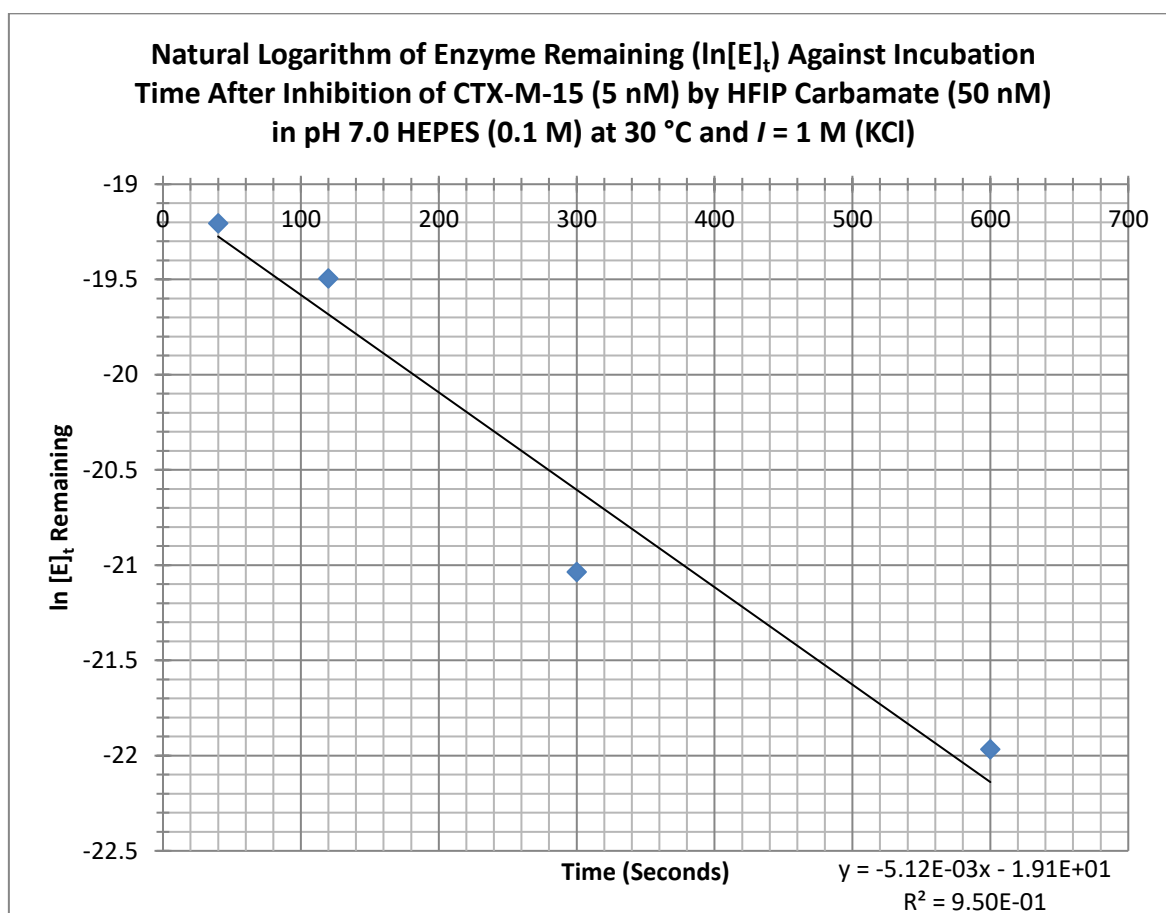


Figure 3.29: Natural logarithm of concentration active enzyme remaining against incubation time for inhibition of CTX-M-15 (5 nM) by the hexafluoroisopropanol analogue (50 nM) at 10:1 concentration with enzyme.

The pseudo first-order rate constant for this inhibition as seen from figure 3.29 was  $5.12 \times 10^{-3} \text{ s}^{-1}$  corresponding to a second-order rate constant  $k_i$  of  $1.02 \times 10^5 \text{ M}^{-1} \text{ s}^{-1}$ . It was noted that the HFIP carbamate derivative was an extremely good inhibitor of CTX-M-15. The experiment was therefore repeated at a lower concentration of inhibitor, with 1:1 concentration with enzyme in what would be a second-order reaction process.

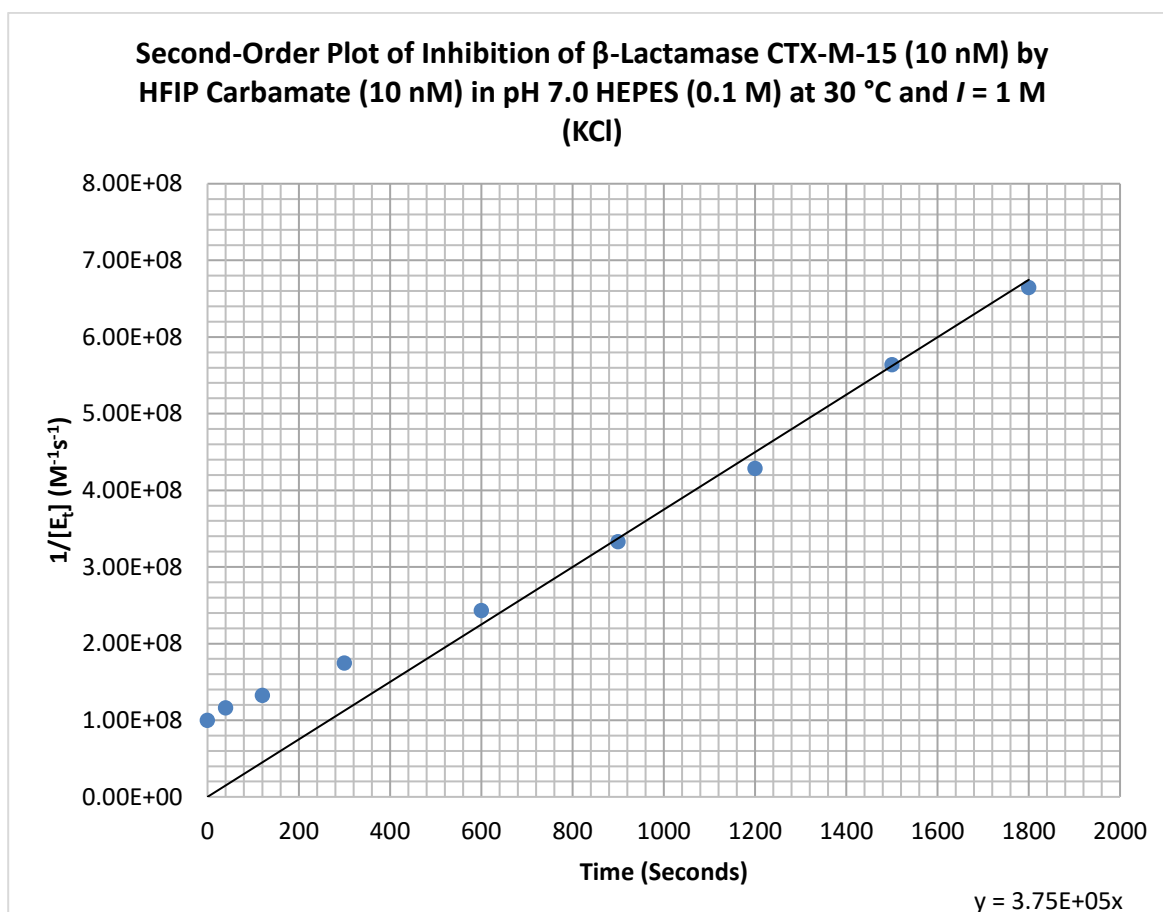


Figure 3.30: Second-order plot for inhibition of CTX-M-15 (10 nM) by HFIP carbamate (10 nM) at 1:1 concentration with enzyme.

The  $k_i$  from the HFIP reaction with CTX-M-15 under second-order conditions where the concentration of the reactants A and B were equal gives  $k_i = 3.75 \times 10^5 \text{ M}^{-1} \text{ s}^{-1}$ , as seen from figure 3.30 above. This makes the HFIP inhibitor an extremely effective inhibitor of CTX. The line of best fit was forced through the origin, as this point (no inhibitor present would

result in no inhibition) was known. The early readings deviate from the line of best fit somewhat. This is likely due to the inhibition reaction happening so quickly, that with the current method design it was difficult to accurately capture data at these early points of the reaction. A stopped flow experiment would be a way to overcome this difficulty for future work. This is unlikely to be of any mechanistic significance, as data from the LCMS inhibitor experiments suggested the compounds were pure and there was no recyclisation/further reactions to form other compounds. The next analogue to try was the HFA inhibitor, which was synthesised with the lowest  $pK_a$  alcohol of all the inhibitors.

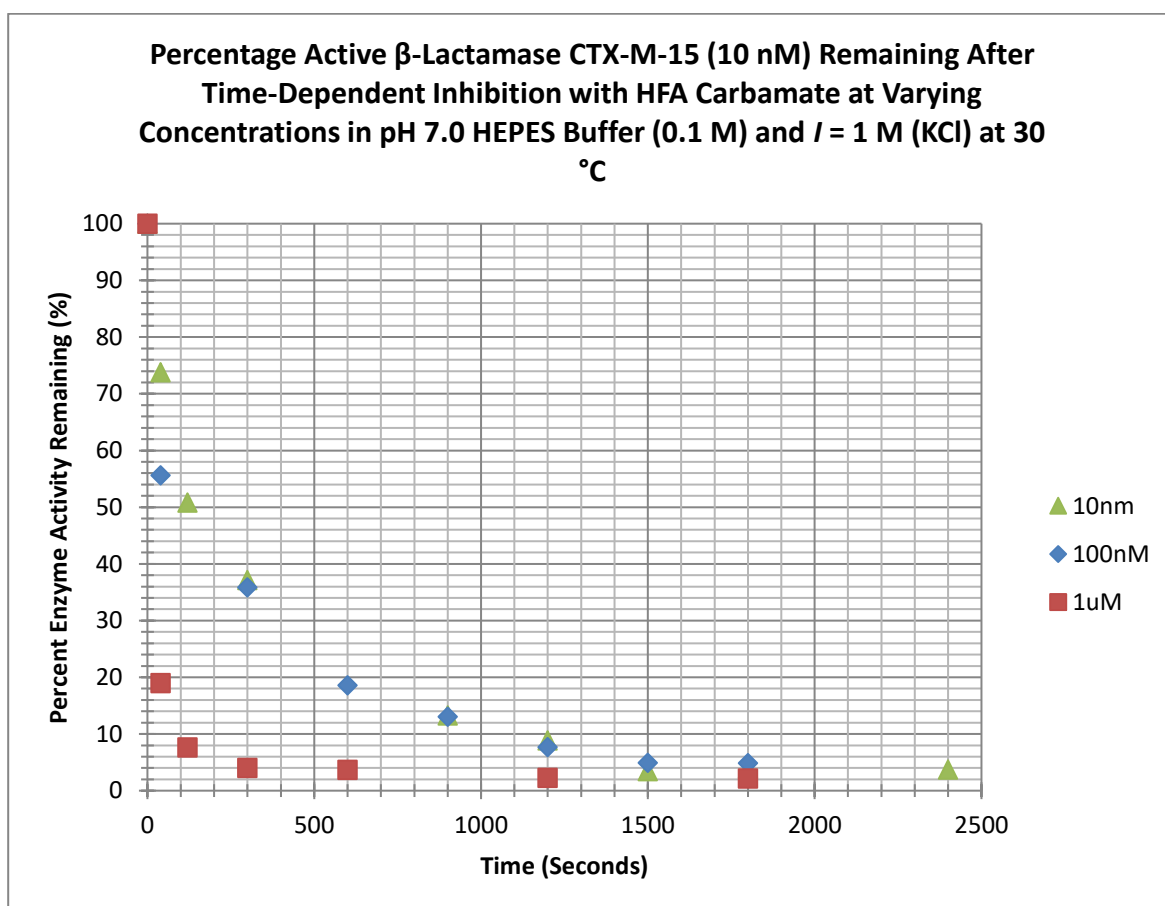


Figure 3.31: Percentage active CTX-M-15 remaining after incubation with HFA carbamate at 100:1 (1  $\mu$ M), 10:1 (100 nM) and 1:1 (10 nM) concentration with enzyme.

As can be seen from figure 3.31 above, the percentage activity remaining for CTX-M-15 after inhibition with low concentrations of the HFA carbamate dropped to 0 % very quickly

as compared to the original inhibitors with higher  $pK_a$  alcohol leaving groups. As for the previous inhibition experiments with the less acidic alcohol leaving groups, the experiments were conducted in 20 ml pH 7.0 HEPES buffer (0.1M) using 0.2 mM cephalothin as a substrate for hydrolysis. For the 1  $\mu$ M experiment, 133.33  $\mu$ l was taken from the 150  $\mu$ M HFA stock solution and added to the 20 ml test solution containing 10 nM CTX-M-15 to create a 1  $\mu$ M test concentration where as for the 100 nM experiment, 13.33  $\mu$ l was taken and added to the 20 ml test solution to create a final 10 nM concentration and finally for the 10 nM experiment, 1.33  $\mu$ l was added to the 20 ml test solution to give a final inhibitor concentration of 10 nM.

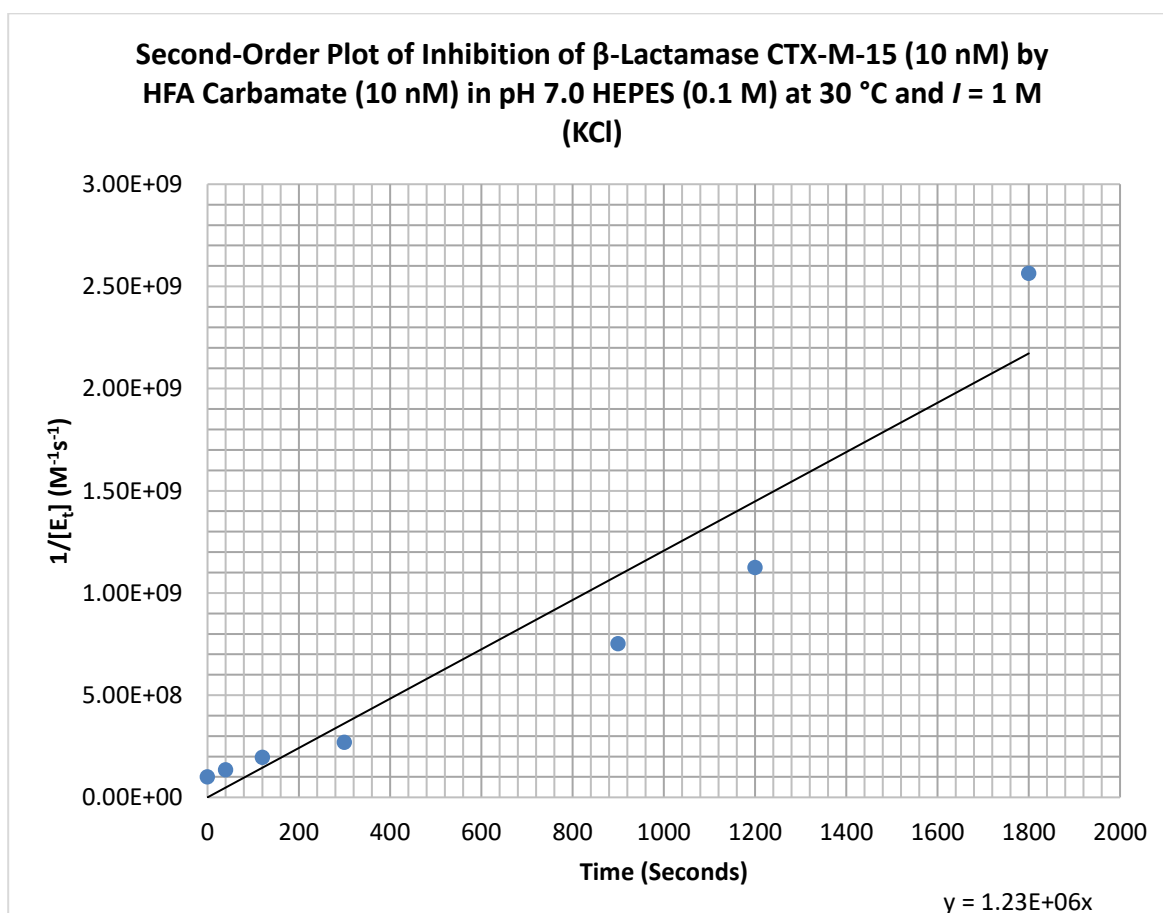


Figure 3.32: Second-order plot for inhibition of CTX-M-15 (10 nM) by HFA carbamate (10 nM) at 1:1 concentration with enzyme.

The data from the inhibition experiments with HFA indicate that HFA had a  $k_i = 1.23 \times 10^6 \text{ M}^{-1}\text{s}^{-1}$ , as seen from figure 3.32 above. This shows that HFA is the most effective inhibitor of the SBLs out of all the compounds synthesised. There was a slight offset result at 1800 seconds which may increase the slope slightly, but clearly HFA was the most effective inhibitor tested. This is in line with figure 3.33 below, the Bronsted Plot showing the  $\text{p}K_a$  of the leaving group against the  $k_i$  calculated from the inhibition experiments for the inhibition of CTX-M-15, where there is clearly a correlation between the  $\text{p}K_a$  of the alcohol leaving group decreasing and  $\log k_i$  increasing.

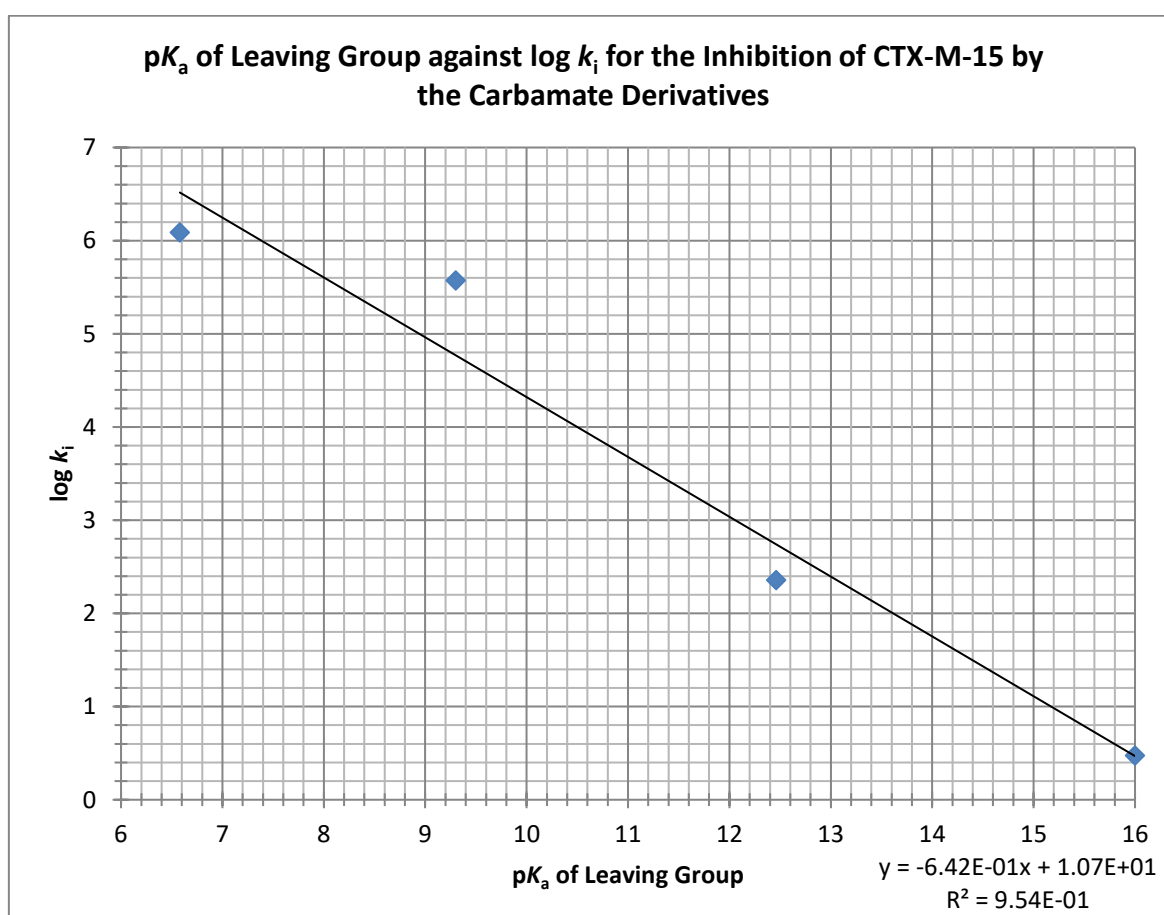


Figure 3.33: Bronsted plot for the carbamate inhibitors and the inhibition of CTX-M-15.

The Bronsted plot in figure 3.33 above shows that as  $\text{p}K_a$  of the leaving group alcohol was decreased, the rate constant for inactivation of the enzyme is increased. i.e. the effective the

inhibitor. The corresponding  $\beta_{lg} = 0.64$ , which is much greater than that of 0.1, which is observed for the alkaline hydrolysis of the carbamates.

Carbamates are much less reactive than esters. The second order rate constants for the alkaline hydrolysis of carbamates are generally very low, for example, for the rate constant for simple carbamates is  $4.5 \times 10^{-6} \text{ M}^{-1}\text{s}^{-1}$  giving a half-life of about 50,000 years at pH 7 (Adams & Baron, 1965). Therefore, the reaction of the avibactam carbamate derivatives with the  $\beta$ -lactamases must be enzyme catalysed.

The effective charge on the alkoxy oxygen of carbamates is +0.8 due to resonance, as seen in figure 3.34 below:

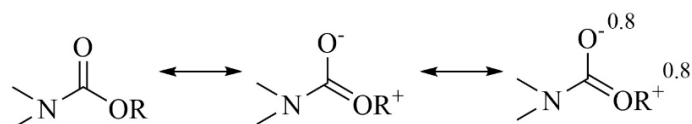


Figure 3.34: Charge of the alkoxy oxygen of carbamates.

The slope of the Bronsted plot gives a  $\beta_{lg} = 0.64$  which indicates rate-limiting formation of the tetrahedral intermediate, as seen in figure 3.35 below:

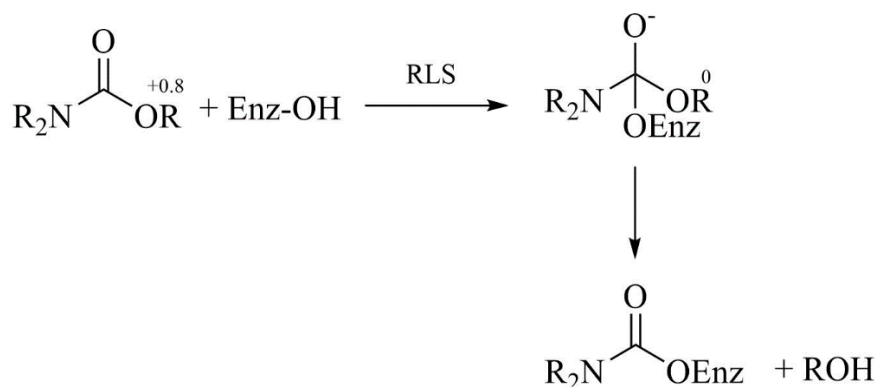


Figure 3.35: Rate-limiting formation of the tetrahedral intermediate between the carbamate and enzyme.

The Bronsted  $\beta_{lg}$  for the alkaline hydrolysis of esters is  $-0.4$ , which has been interpreted as rate-limiting attack of hydroxide-ion upon the carbonyl carbon (Barton, Laws & Page, 1994).

The HFA derivative was such an effective inhibitor, the  $k_i$  for avibactam was determined to see if the HFA inhibitor was a more effective inhibitor than the current market leader.

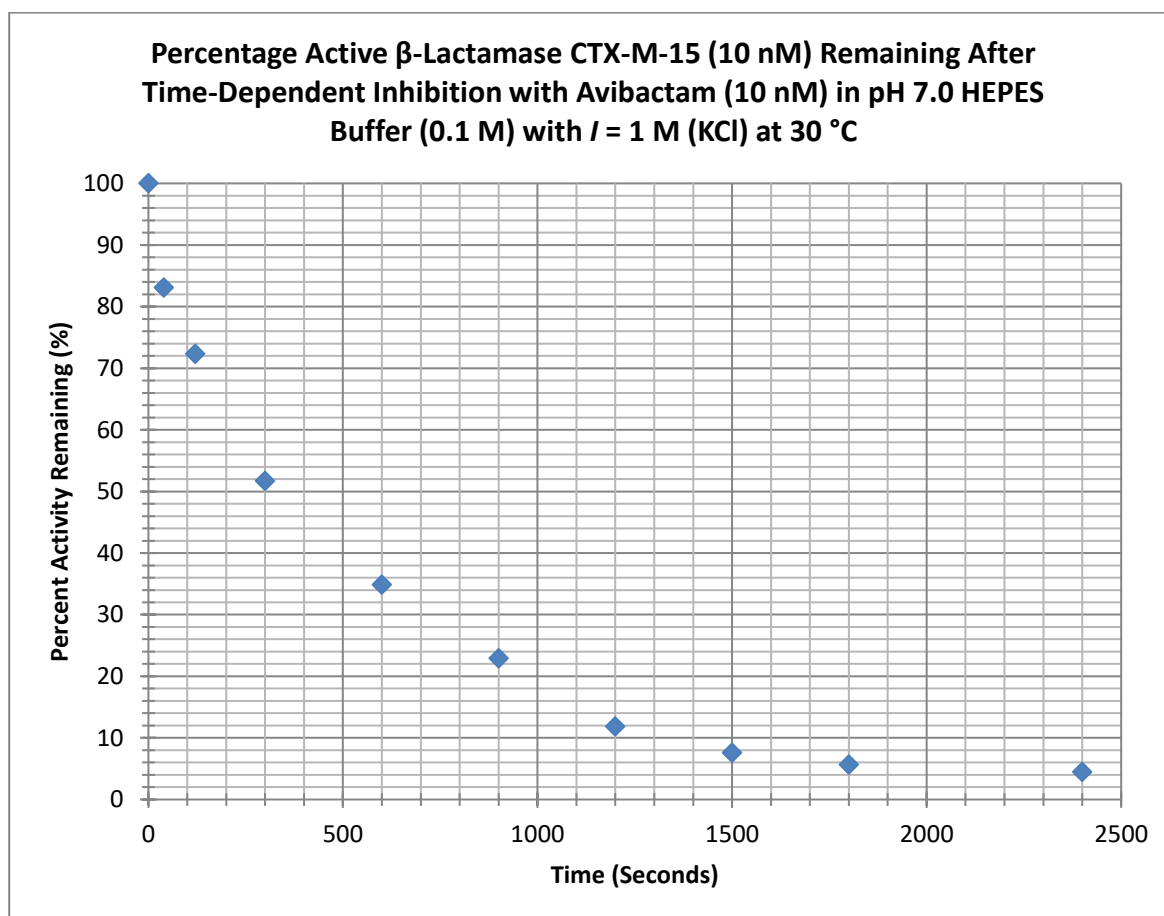


Figure 3.36: Percentage active CTX-M-15 (10 nM) remaining after incubation with avibactam (10 nM) at 1:1 concentration with enzyme.

As can be seen from figure 3.36 above, avibactam showed similar inhibitory action to the two more acidic inhibitors that were synthesised. As for the previous inhibition experiments, the experiment took place in 20 ml pH 7.0 HEPES buffer (0.1 M), using 0.2 mM cephalothin

as the substrate. 1.33  $\mu$ l of the 150  $\mu$ M avibactam stock solution was added to the 20 ml test sample to give an inhibitor concentration of 10 nM.

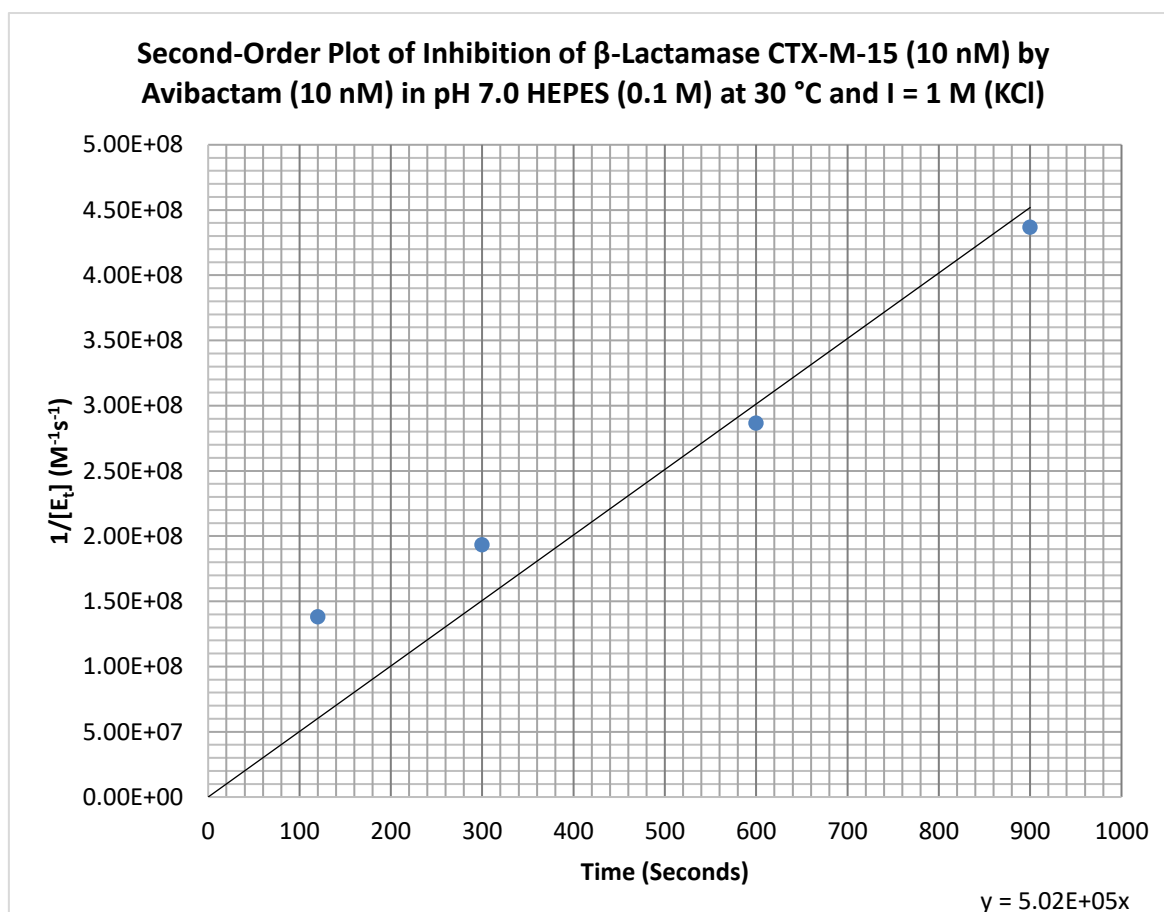


Figure 3.37: Second-order plot for inhibition of CTX-M-15 (10 nM) by avibactam (10 nM) at 1:1 concentration with enzyme.

The  $k_i$  of the inhibition of CTX-M-15 by avibactam was  $5.02 \times 10^5 \text{ M}^{-1}\text{s}^{-1}$ , as seen in figure 3.37 above. Not only does this mean that our HFIP carbamate derivative is a comparable inhibitor to avibactam (with a  $k_i$  of  $3.75 \times 10^5 \text{ M}^{-1}\text{s}^{-1}$ ), but the HFA derivative (with a  $k_i$  of  $1.23 \times 10^6 \text{ M}^{-1}\text{s}^{-1}$ ) surpasses the performance of avibactam at inhibiting CTX-M-15. If, as expected, the mechanism of inhibition is observed amongst different classes of SBLs, the data suggest that a novel inhibitor has been synthesised that is of superior performance to the current market leader, avibactam. The line of best fit in figure 3.32 can be subject to

some scrutiny owing to the result at 1800 seconds, but even if this result is removed, the HFA inhibitor is in the region of a two fold better inhibitor than avibactam. The work detailed here lays the foundations of future work, where a number of similar analogues could be synthesised and screened for their inhibition against emerging important SBLs. Furthermore, the fact that the HFA carbamate derivative is a noticeably better inhibitor of CTX-M-15 than avibactam suggests, once more, that it is indeed the synthesised compounds that are responsible for inhibiting the enzymes, and not residual avibactam left over from the synthesis reaction.

Table 3.3 below summarises the relevant results of the inhibition work carried out with HFIP, HFA and avibactam.

Table 3.3: Summary of the relevant  $k_i$  data of the results of the inhibition of CTX-M-15 by HFIP, HFA and avibactam.

<b>Inhibitor</b>	<b>Concentration (nM)</b>	<b><math>k_i</math> (<math>M^{-1}s^{-1}</math>)</b>
<b>Hexafluoroisopropanol</b>	10	$3.75 \times 10^5$
<b>Carbamate (HFIP)</b>		
<b>Hexafluoroacetone Hydrate</b>	10	$1.23 \times 10^6$
<b>Carbamate (HFA)</b>		
<b>Avibactam</b>	10	$5.02 \times 10^5$

### 3.4.8: Kinetics of Hydrolysis of Substrates by SBLs and pH Dependence

To further investigate the mechanism of inhibition and catalysis of hydrolysis of  $\beta$ -lactams by SBLs, the effect of pH on both the catalysed hydrolysis and inhibition was investigated to see whether they were similar or different.

The pH profiles for hydrolysis were ascertained by using three SBLs (P99, CTX-M-15 and AmpC) at set pH levels to catalyse the hydrolysis of cephalothin and monitoring the hydrolysis via changes in the UV at 260 nm. The solutions were buffered at set pH with the ionic strength (*I*) maintained by KCl. The reaction was allowed to go to completion at each pH to for each enzyme. A representative example will be shown for each enzyme to show how the pH profiles were obtained.

#### *3.4.8.1: pH Dependence of the Hydrolysis of Cephalothin Catalysed by P99*

An example of the P99 catalysed hydrolysis of cephalothin can be seen in figure 3.38 below.

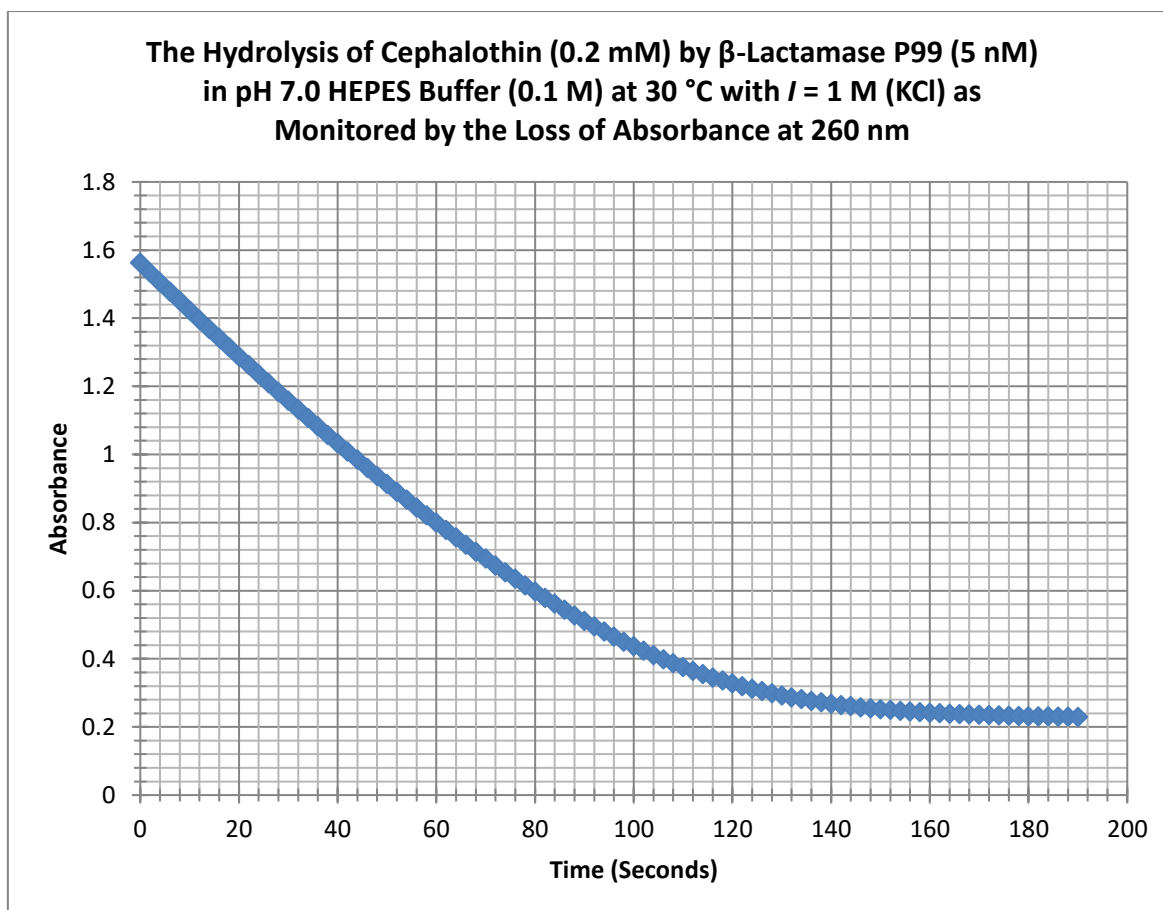


Figure 3.38: P99 (5 nM) catalysed hydrolysis of cephalothin (0.2 mM) at pH 7.0 in HEPES Buffer (0.1 M)

From these hydrolysis graphs (which were repeated for each enzyme at 0.5 pH intervals, which can be seen in the general methods section), one can obtain a variety of information regarding the kinetics of the reaction between the enzyme and substrate. The total change in absorbance divided by the substrate concentration gives  $\Delta\epsilon$ . The slope of the initial straight line portion of the zero order section of the graph can be divided by  $(\Delta\epsilon \times [E])$  to give  $k_{\text{cat}}$  ( $\text{s}^{-1}$ ). This information will be summarised in tables for each enzyme shortly.

The latter part of the hydrolysis reaction corresponds to enzyme catalysis below saturation and follows first order kinetics. This portion of the graph can be imported into GraphPad

Prism (GraphPad Software, California USA) and curve fit against a first order decay equation to give  $k_{\text{obs}}$ , an example of which is seen below in figure 3.39.

**Fit of the Hydrolysis of Cephalothin (0.2 mM) by P99 (5 nM) at pH 7.0 at 30 °C and  $I = 1\text{M}$  (KCl)**

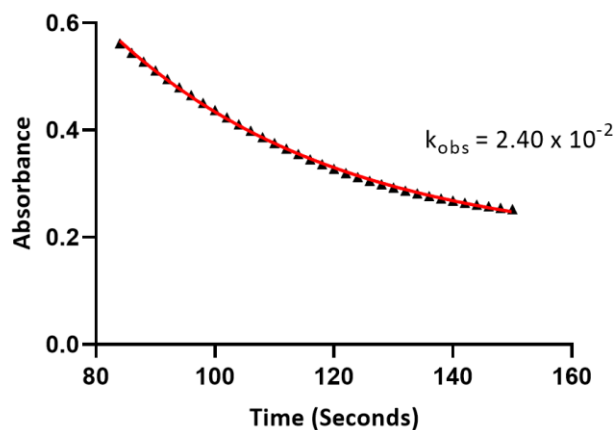


Figure 3.39: First order curve fit of the hydrolysis of cephalothin (0.2 mM) by P99 (5 nM) in pH 7.0 HEPES buffer (0.1 M).

In figure 3.39 above, the black triangles represent the experimental data obtained in the hydrolysis experiments and the red line is the curve fit obtained from GraphPad Prism. This curve fit gave  $k_{\text{obs}}$ . This was repeated for every hydrolysis reaction (the results of which can be seen in the methods section). The  $k_{\text{obs}}$  value can be divided by the enzyme concentration to give  $k_{\text{cat}}/K_{\text{m}}$  ( $\text{M}^{-1}\text{s}^{-1}$ ).

Using the data analysis methods described previously, various kinetic parameters were deduced from the hydrolysis graphs for the enzyme catalysed hydrolysis of cephalothin over various pH by P99 which can be seen in table 3.4 below.

Table 3.4: Kinetic parameters of the hydrolysis of cephalothin (0.2 mM) over various pH at 30 °C with  $I = 1$  M (KCl) by  $\beta$ -lactamase P99 (5 nM).

pH	[E] (nM)	$\frac{\Delta\text{Absorbance}}{\text{[Substrate]}}$		From GraphPad	Zero Order Slope	$\frac{k_{\text{obs}}}{[E]}$	$\frac{(k_{\text{cat}} \times [E])}{k_{\text{obs}}}$
		Zero Order Slope	$\Delta\epsilon$	$k_{\text{obs}} (\text{s}^{-1})$	$\Delta\epsilon \times [E]$	$k_{\text{cat}} (\text{s}^{-1})$	$k_{\text{cat}}/K_m (\text{M}^{-1}\text{s}^{-1})$
5.5	5	$1.88 \times 10^{-3}$	$7.19 \times 10^3$	$2.31 \times 10^{-4}$	52.29	$4.62 \times 10^4$	$1.13 \times 10^{-3}$
6.0	5	$4.65 \times 10^{-3}$	$7.16 \times 10^3$	$7.75 \times 10^{-3}$	129.89	$1.55 \times 10^6$	$8.38 \times 10^{-5}$
6.5	5	$4.87 \times 10^{-3}$	$7.03 \times 10^3$	$1.42 \times 10^{-2}$	138.55	$2.84 \times 10^6$	$4.88 \times 10^{-5}$
7.0	5	$1.35 \times 10^{-2}$	$6.68 \times 10^3$	$2.40 \times 10^{-2}$	404.19	$4.8 \times 10^6$	$8.42 \times 10^{-5}$
7.5	5	$1.08 \times 10^{-2}$	$6.82 \times 10^3$	$2.64 \times 10^{-2}$	316.72	$5.28 \times 10^6$	$6.00 \times 10^{-5}$
8.0	5	$7.73 \times 10^{-3}$	$6.87 \times 10^3$	$2.57 \times 10^{-2}$	225.04	$5.14 \times 10^6$	$4.38 \times 10^{-5}$
8.5	5	$7.10 \times 10^{-3}$	$6.85 \times 10^3$	$2.07 \times 10^{-2}$	207.30	$4.14 \times 10^6$	$5.01 \times 10^{-5}$
9.0	5	$4.67 \times 10^{-3}$	$7.08 \times 10^3$	$1.32 \times 10^{-2}$	131.92	$2.64 \times 10^6$	$5.00 \times 10^{-5}$

The  $k_{\text{cat}}/K_m$  was plotted against pH to give the following graph.

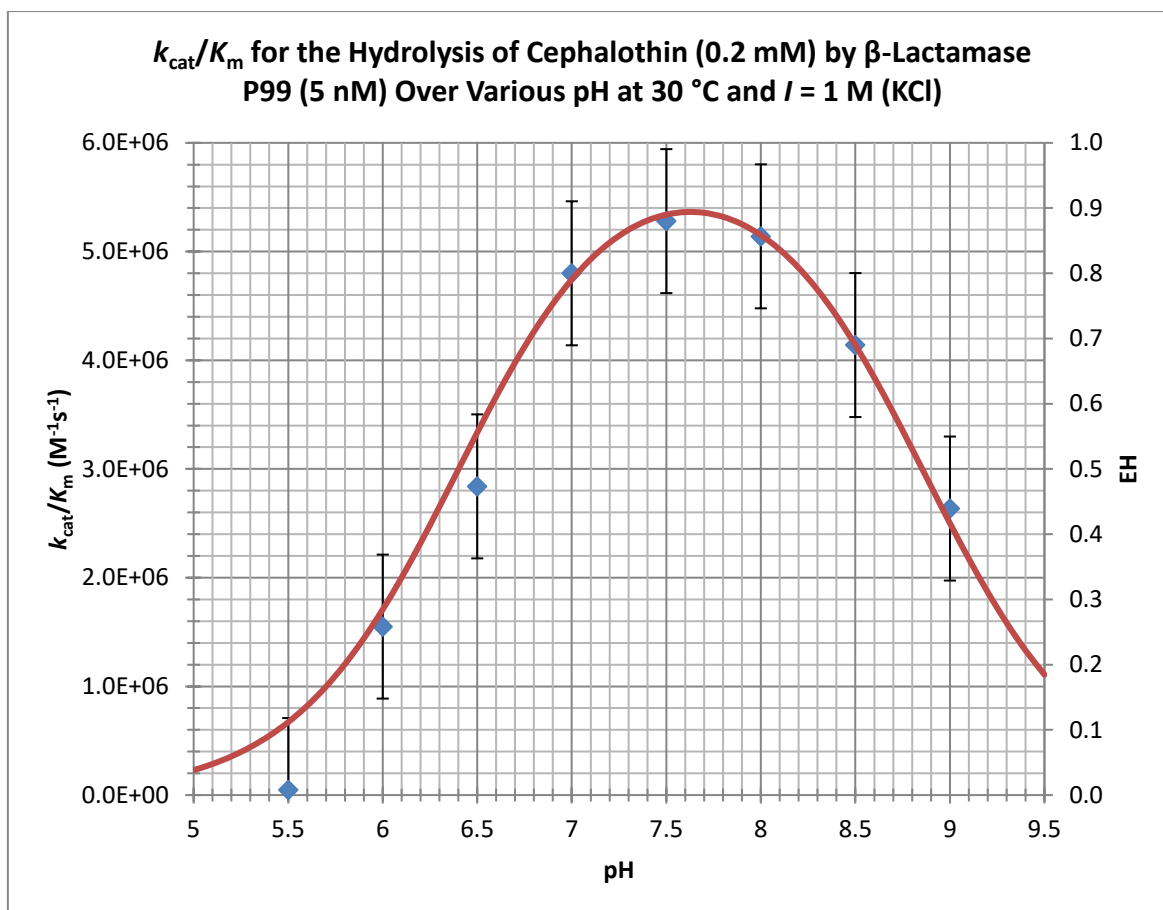


Figure 3.40:  $k_{\text{cat}}/K_m$  for the hydrolysis of cephalothin (0.2 mM) by P99 (5 nM) at various pH.

The P99 β-lactamase catalysed hydrolysis of cephalothin as seen above in figure 3.40 shows the typical bell-shaped pH-rate profile indicative of two important ionisable groups on the enzyme controlling activity. One of these must be ionised for maximal activity and the other unionised as per the scheme below:



From figure 3.40 above,  $\text{p}K_a^1$  is 6.40 and  $\text{p}K_a^2$  is 8.85. For this class C β-lactamase the low  $\text{p}K_a$  is thought to be due to Tyr-150 which is H-bonded to Lys-315 and Lys-67 acting as a

general base (Page, Vilanova & Layland, 1995). The accepted hydrolysis scheme for class C  $\beta$ -lactamases can be seen below in figure 3.41:

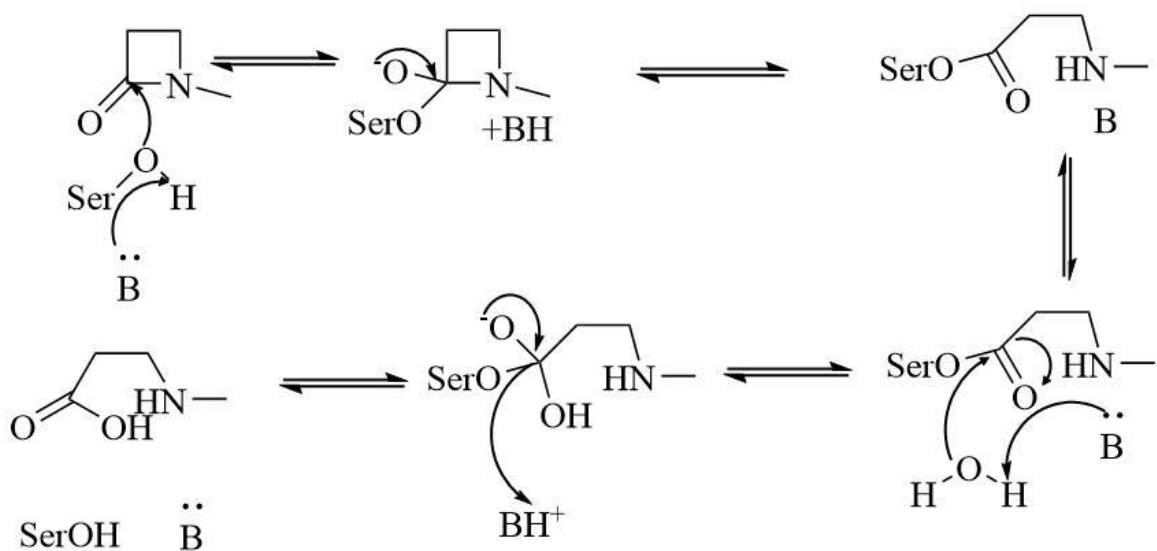


Figure 3.41: Accepted hydrolysis scheme for class C  $\beta$ -lactamases.

#### 3.4.5.4.2: CTX-M-15 pH Dependence of Hydrolysis of Cephalothin

These pH rate profiles for the hydrolysis of  $\beta$ -lactams by  $\beta$ -lactamase enzymes were repeated for other classes of  $\beta$ -lactamases; additional data (such as the absorbance graphs and  $k_{\text{obs}}$  curve fits) can be seen in section 6.10 in the general methods section. The kinetic data for CTX-M-15 can be seen in table 3.5 below. A representative example will be shown and briefly discussed for CTX-M-15. The CTX-M-15 catalysed hydrolysis of cephalothin at pH 5.5 is shown below in figure 3.42.

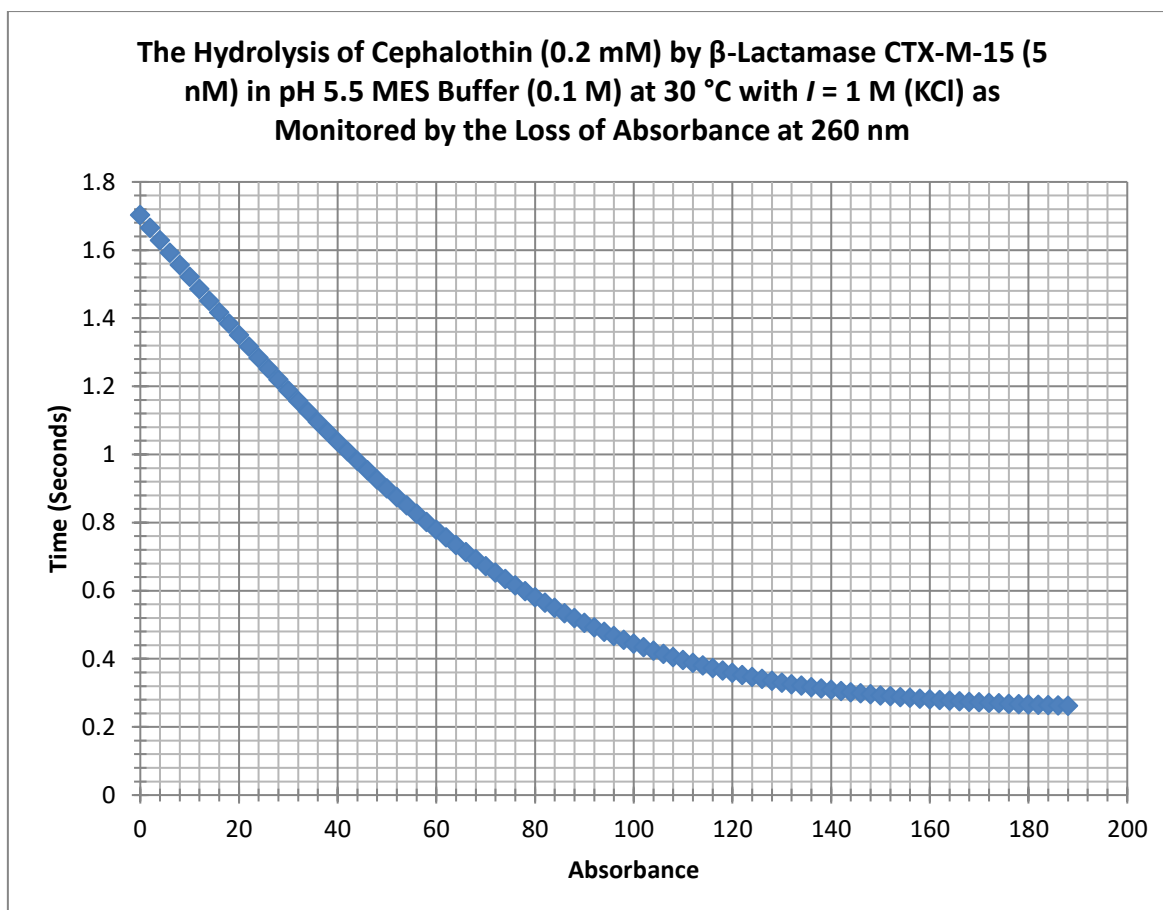


Figure 3.42: CTX-M-15 (5 nM) catalysed hydrolysis of cephalothin (0.2 mM) at pH 5.5 in MES Buffer (0.1 M)

The first order portion of the graph was imported into GraphPad Prism to allow curve fitting against a first order decay equation and  $k_{\text{obs}}$  to be obtained, as shown below in figure 3.43 below.

**Fit of the Hydrolysis of Cephalothin (0.2 mM) by CTX-M-15 (5 nM) at pH 5.5 at 30 °C and  $I = 1$  M (KCl)**

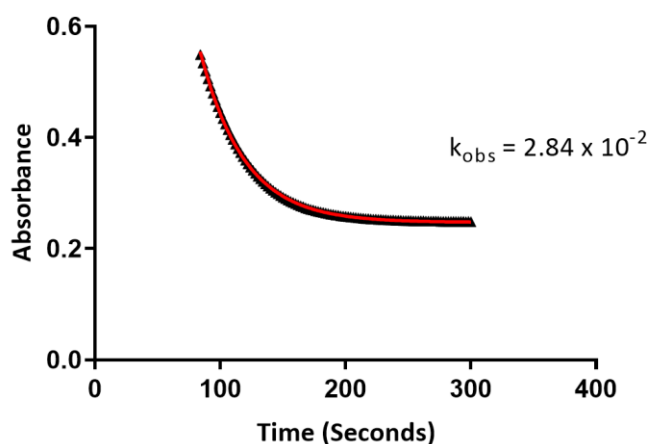


Figure 3.43: First order curve fit of the hydrolysis of cephalothin (0.2 mM) by CTX-M-15 (5 nM) in pH 5.5 MES buffer (0.1 M).

This process was repeated at 0.5 pH intervals from pH 4.0 to 9.0 for CTX-M-15. Using the data analysis methods described previously, various kinetic parameters were deduced from the hydrolysis graphs for the enzyme catalysed hydrolysis of cephalothin over various pH by CTX-M-15 which can be seen in table 3.5 below.

Table 3.5: Kinetic parameters of the hydrolysis of cephalothin (0.2 mM) over various pH at 30 °C with  $I = 1$  M (KCl) by  $\beta$ -lactamase CTX-M-15 (5 nM).

<b>pH</b>	<b>[E] (nM)</b>	<b>Zero Order Slope</b>	<b><math>\Delta\epsilon</math></b>	<b><math>k_{obs}</math> (s<sup>-1</sup>)</b>	<b><math>k_{cat}</math> (s<sup>-1</sup>)</b>	<b><math>k_{cat}/K_m</math> (M<sup>-1</sup>s<sup>-1</sup>)</b>	<b><math>K_m</math> (M)</b>
<b>4.0</b>	5	$3.34 \times 10^{-3}$	$7.21 \times 10^3$	$1.13 \times 10^{-3}$	92.65	$2.26 \times 10^5$	$4.10 \times 10^{-4}$
<b>4.5</b>	5	$1.09 \times 10^{-2}$	$7.72 \times 10^3$	$1.23 \times 10^{-2}$	282.38	$2.46 \times 10^6$	$1.15 \times 10^{-4}$
<b>5.0</b>	5	$1.72 \times 10^{-2}$	$7.52 \times 10^3$	$2.23 \times 10^{-2}$	457.45	$4.46 \times 10^6$	$1.03 \times 10^{-4}$
<b>5.5</b>	5	$1.77 \times 10^{-2}$	$7.69 \times 10^3$	$2.84 \times 10^{-2}$	460.34	$5.68 \times 10^6$	$8.10 \times 10^{-5}$
<b>6.0</b>	5	$1.78 \times 10^{-2}$	$7.38 \times 10^3$	$3.10 \times 10^{-2}$	482.34	$6.20 \times 10^6$	$7.78 \times 10^{-5}$
<b>6.5</b>	5	$1.94 \times 10^{-2}$	$7.56 \times 10^3$	$3.32 \times 10^{-2}$	513.23	$6.64 \times 10^6$	$7.73 \times 10^{-5}$
<b>7.0</b>	5	$1.94 \times 10^{-2}$	$7.28 \times 10^3$	$3.33 \times 10^{-2}$	532.97	$6.66 \times 10^6$	$8.00 \times 10^{-5}$
<b>7.5</b>	5	$1.67 \times 10^{-2}$	$7.19 \times 10^3$	$3.25 \times 10^{-2}$	464.53	$6.50 \times 10^6$	$7.14 \times 10^{-5}$
<b>8.0</b>	5	$1.24 \times 10^{-2}$	$7.72 \times 10^3$	$3.08 \times 10^{-2}$	321.24	$6.16 \times 10^6$	$5.21 \times 10^{-5}$
<b>8.5</b>	5	$7.98 \times 10^{-3}$	$7.40 \times 10^3$	$2.37 \times 10^{-2}$	215.68	$4.74 \times 10^6$	$4.55 \times 10^{-5}$
<b>9.0</b>	5	$5.00 \times 10^{-3}$	$7.80 \times 10^3$	$1.58 \times 10^{-2}$	128.21	$3.16 \times 10^6$	$4.06 \times 10^{-5}$

Much like for P99, the  $k_{cat}/K_m$  was obtained using the  $k_{obs}$  from the hydrolysis experiments and plotted against pH to give the following pH profile.

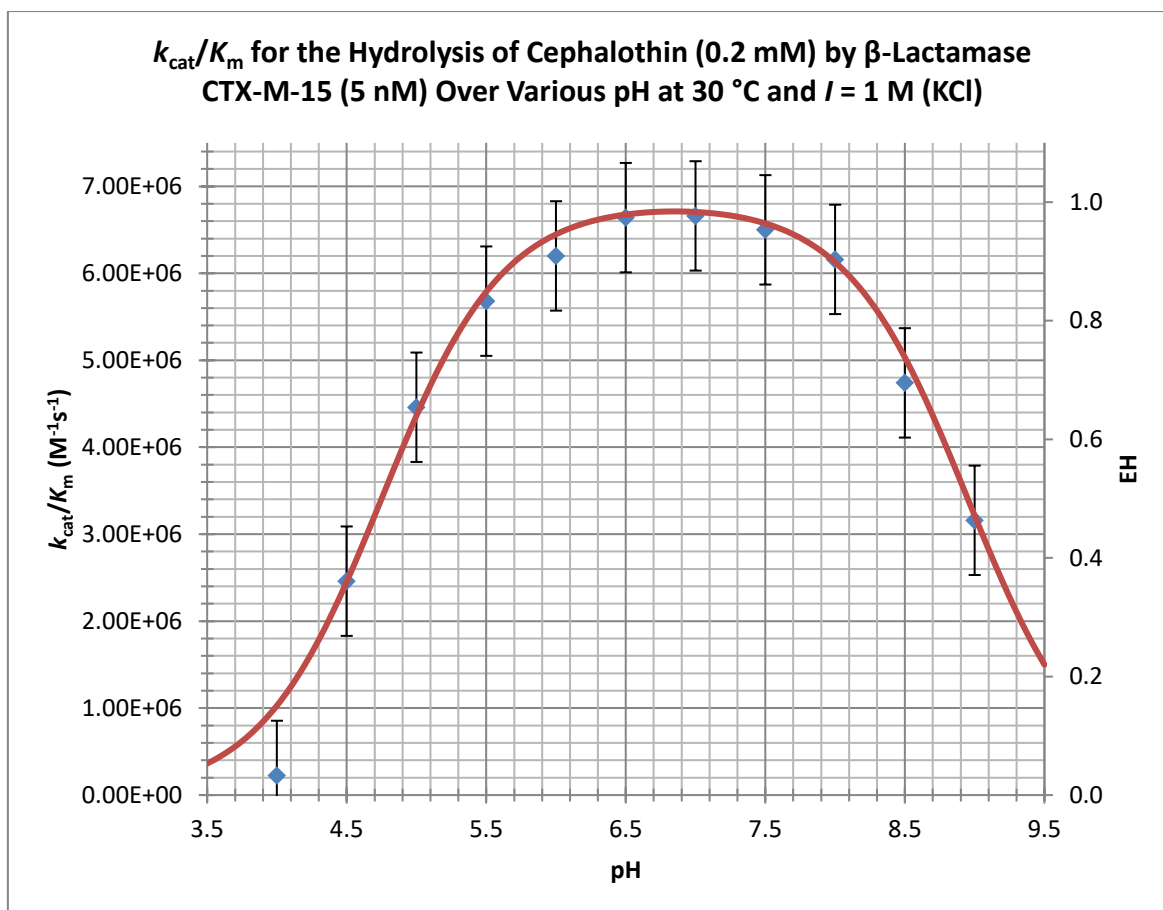


Figure 3.44:  $k_{\text{cat}}/K_m$  for the hydrolysis of cephalothin (0.2 mM) by CTX-M-15 (5 nM) at various pH.

For CTX-M-15  $\beta$ -lactamase the pH profile as seen above in figure 3.44 for hydrolysis of cephalothin again shows the typical bell-shaped profile. For this enzyme  $\text{p}K_{\text{a}}^1$  and  $\text{p}K_{\text{a}}^2$  are 4.75 and 8.95 respectively determined from the hydrolysis reaction.

### 3.4.8.2: AmpC pH Dependence of Hydrolysis of Cephalothin

The pH profile experiments were repeated for AmpC. As before, a representative example of how the kinetic data were obtained will be shown. Figure 3.45 below shows the AmpC catalysed hydrolysis of cephalothin at pH 6.0.

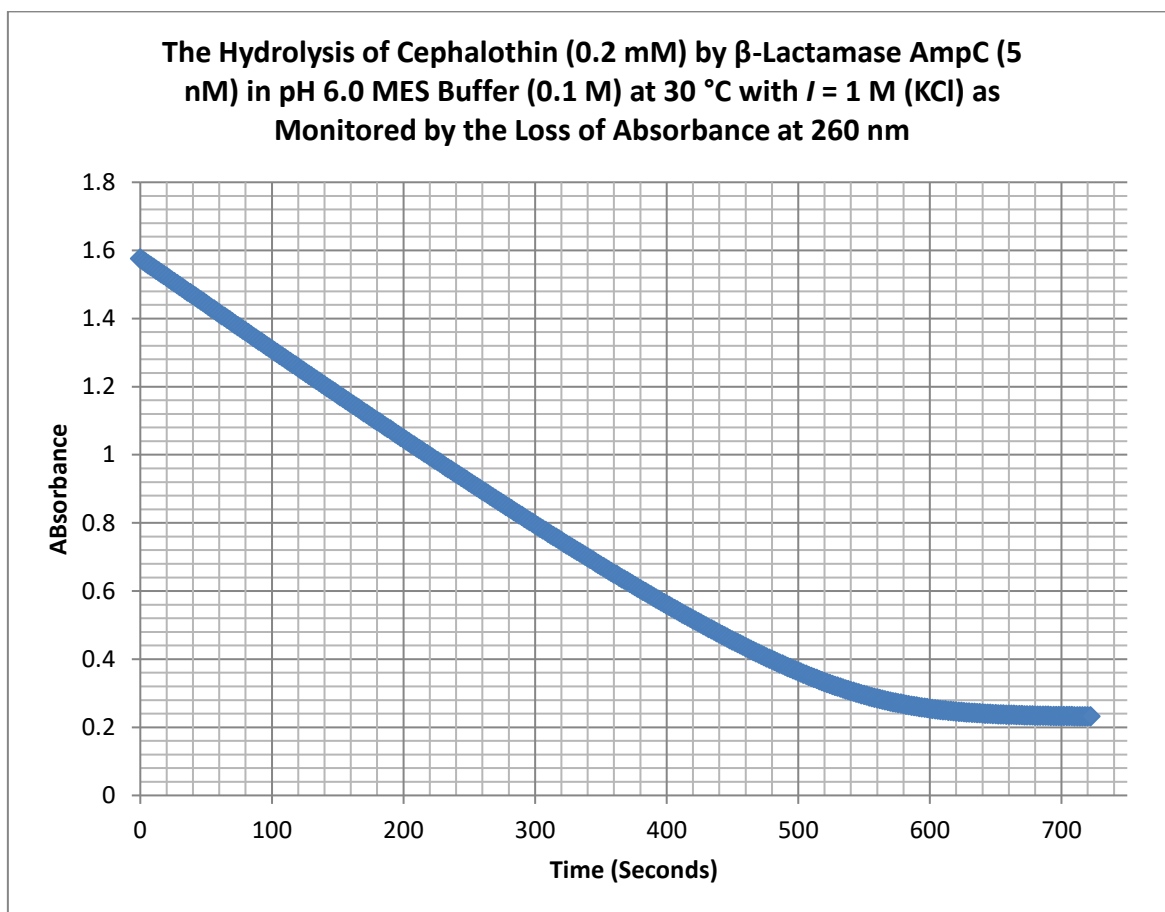


Figure 3.45: AmpC (5 nM) catalysed hydrolysis of cephalothin (0.2 mM) at pH 6.0 in MES Buffer (0.1 M)

The first order portion of the graph was imported into GraphPad Prism to allow curve fitting against a first order decay equation and  $k_{\text{obs}}$  to be obtained, as shown below in figure 3.46 below.

**Fit of the Hydrolysis of Cephalothin (0.2 mM) by AmpC (5 nM) at pH 6.0 at 30 °C and  $I = 1$  M (KCl)**

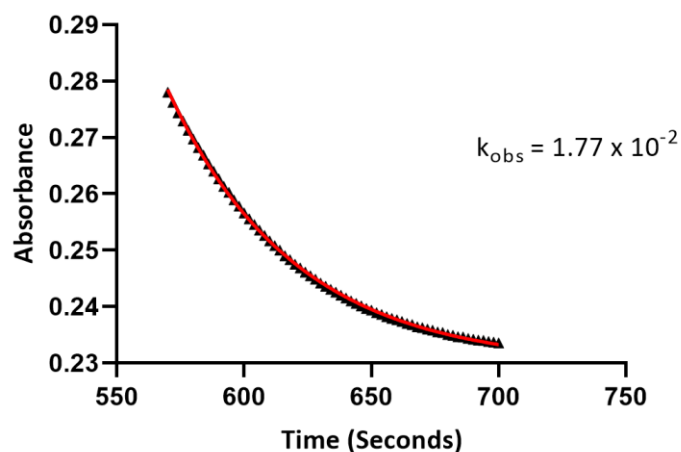


Figure 3.46: First order curve fit of the hydrolysis of cephalothin (0.2 mM) by AmpC (5 nM) in pH 6.0 MES buffer (0.1 M).

This process was repeated at 0.5 pH intervals from pH 5.5 to 8.5 for AmpC. Using the data analysis methods described previously, various kinetic parameters were deduced from the hydrolysis graphs for the enzyme catalysed hydrolysis of cephalothin over various pH by AmpC which can be seen in table 3.6 below.

Table 3.6: Kinetic parameters of the hydrolysis of cephalothin (0.2 mM) over various pH at 30 °C with  $I = 1$  M (KCl) by  $\beta$ -lactamase AmpC (5 nM).

pH	[E] (nM)	Zero Order Slope	$\Delta\epsilon$	$k_{\text{obs}}$ (s <sup>-1</sup> )	$k_{\text{cat}}$ (s <sup>-1</sup> )	$k_{\text{cat}}/K_{\text{m}}$	$K_{\text{m}}$
5.5	5	$2.44 \times 10^{-3}$	$6.51 \times 10^3$	$8.96 \times 10^{-3}$	74.96	$1.79 \times 10^6$	$4.18 \times 10^{-5}$
6.0	5	$2.67 \times 10^{-3}$	$6.94 \times 10^3$	$1.77 \times 10^{-2}$	76.95	$3.54 \times 10^6$	$2.17 \times 10^{-5}$
6.5	5	$3.12 \times 10^{-3}$	$6.97 \times 10^3$	$2.68 \times 10^{-2}$	89.53	$5.36 \times 10^6$	$1.67 \times 10^{-5}$
7.0	5	$3.64 \times 10^{-3}$	$6.71 \times 10^3$	$3.62 \times 10^{-2}$	108.49	$7.24 \times 10^6$	$1.50 \times 10^{-5}$
7.5	5	$4.44 \times 10^{-3}$	$7.02 \times 10^3$	$4.91 \times 10^{-2}$	126.50	$9.82 \times 10^6$	$1.29 \times 10^{-5}$
8.0	5	$3.30 \times 10^{-3}$	$6.83 \times 10^3$	$8.39 \times 10^{-2}$	96.63	$1.68 \times 10^7$	$5.76 \times 10^{-6}$
8.5	5	$3.35 \times 10^{-3}$	$6.67 \times 10^3$	$3.6 \times 10^{-2}$	100.45	$7.2 \times 10^6$	$1.4 \times 10^{-5}$

As for P99 and CTX-M-15, the absorbance and curve fit graphs from which the kinetic data above was deduced can be seen in section 6.10 of the general methods section.  $k_{\text{cat}}/K_{\text{m}}$  was plotted against pH to give the following pH profile.

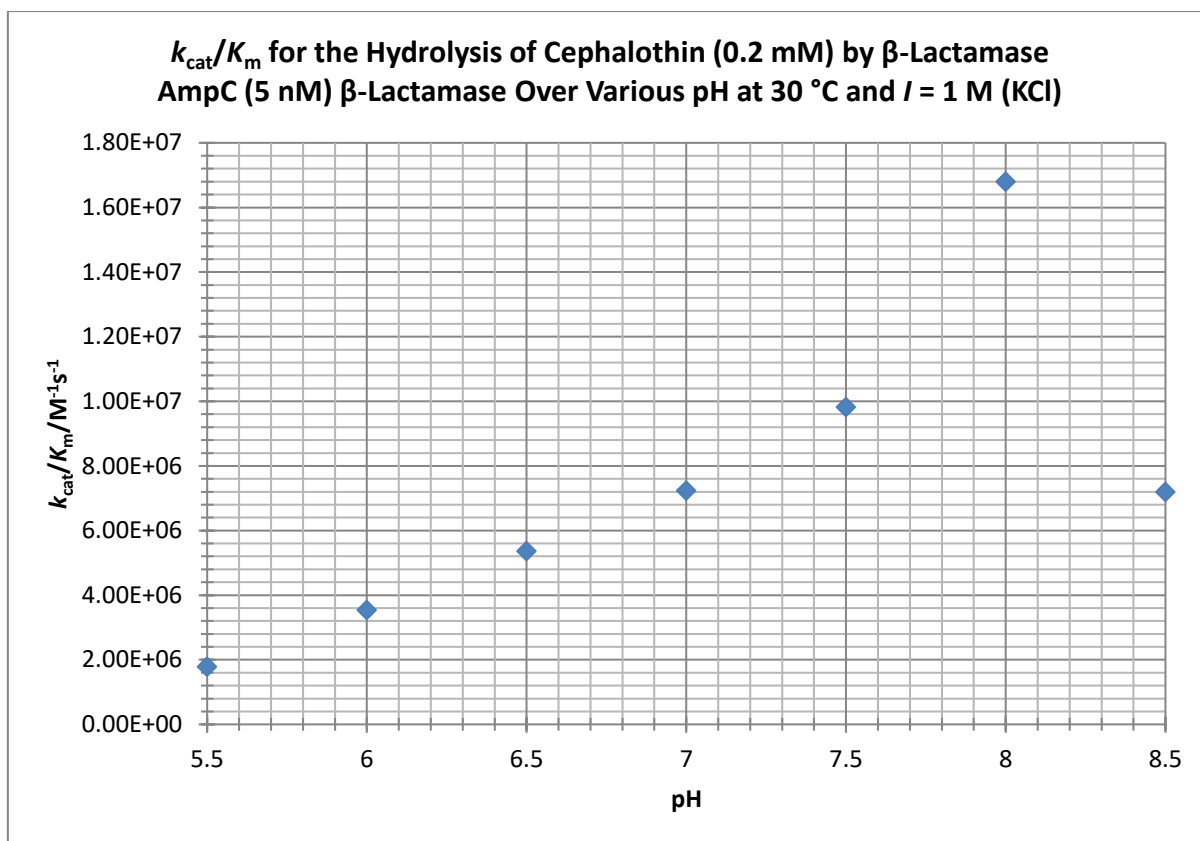


Figure 3.47:  $k_{cat}/K_m$  for the hydrolysis of cephalothin (0.2 mM) by AmpC (5 nM) at various pH.

AmpC has a rather strange pH profile as seen above in figure 3.47, which was confirmed by repeat experiments. It was perhaps that the stock of enzyme used may have been compromised in some way, giving unexpected results. These results were then compared with the dependence of the  $k_i$  by the carbamates  $k_i$  to give some insight into the mechanisms of catalysis/inhibition

### 3.4.9: pH Dependence of Inhibition of SBLs

The effect of pH on the inhibition of the SBLs was also investigated in a similar manner to the pH dependent hydrolysis experiments. As for the pH dependence of the hydrolysis of substrates by  $\beta$ -lactamases, a representative example of how the data was obtained for each enzyme will be shown. For all experiments, the same concentration stock solutions as described previously were used. Blanks were recorded over a period of time relevant for the inhibition experiments for each enzyme and a negligible loss of enzyme activity was recorded (<5%).

#### *3.4.9.1: pH Dependence of Inhibition of P99 by TA Carbamate and Avibactam*

As with the inhibition experiments, the first step was to obtain a blank sample at a set pH where no inhibitor was present, against which inhibition could be compared. In this sample, there was only the  $\beta$ -lactamase P99 (5 nM) and the substrate cephalothin (0.2 mM). This would serve as a reference against which inhibited samples could be compared against to measure remaining enzyme activity. An example of one of the blank reactions (at pH 8.5) is shown in figure 3.48 below.

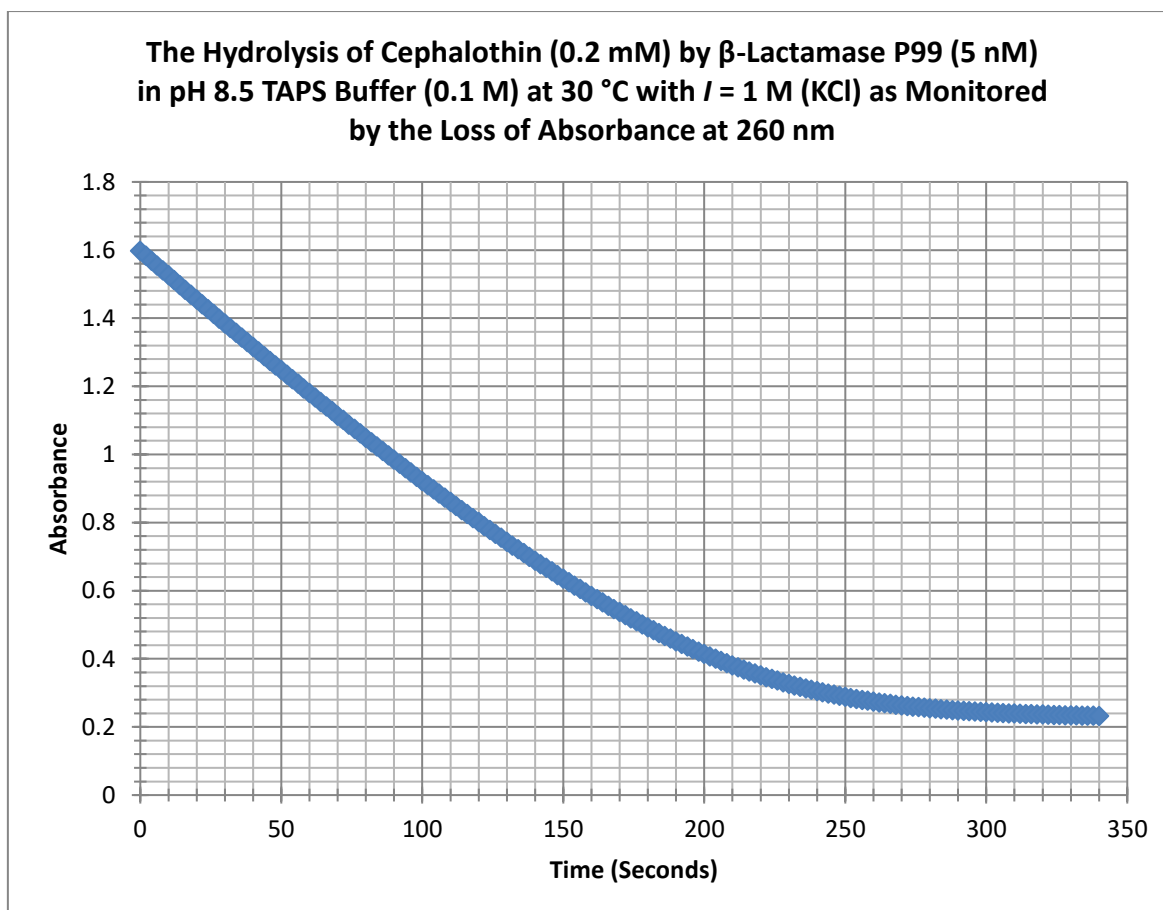


Figure 3.48: P99 catalysed hydrolysis of cephalothin at pH 8.5 without inhibitor present.

The slope of the zero order portion of the graph in figure 3.48 above serves as a reference point, against which inhibition rates can be compared (as in chapter 3.4.6) and can be seen in figure 3.49 below.

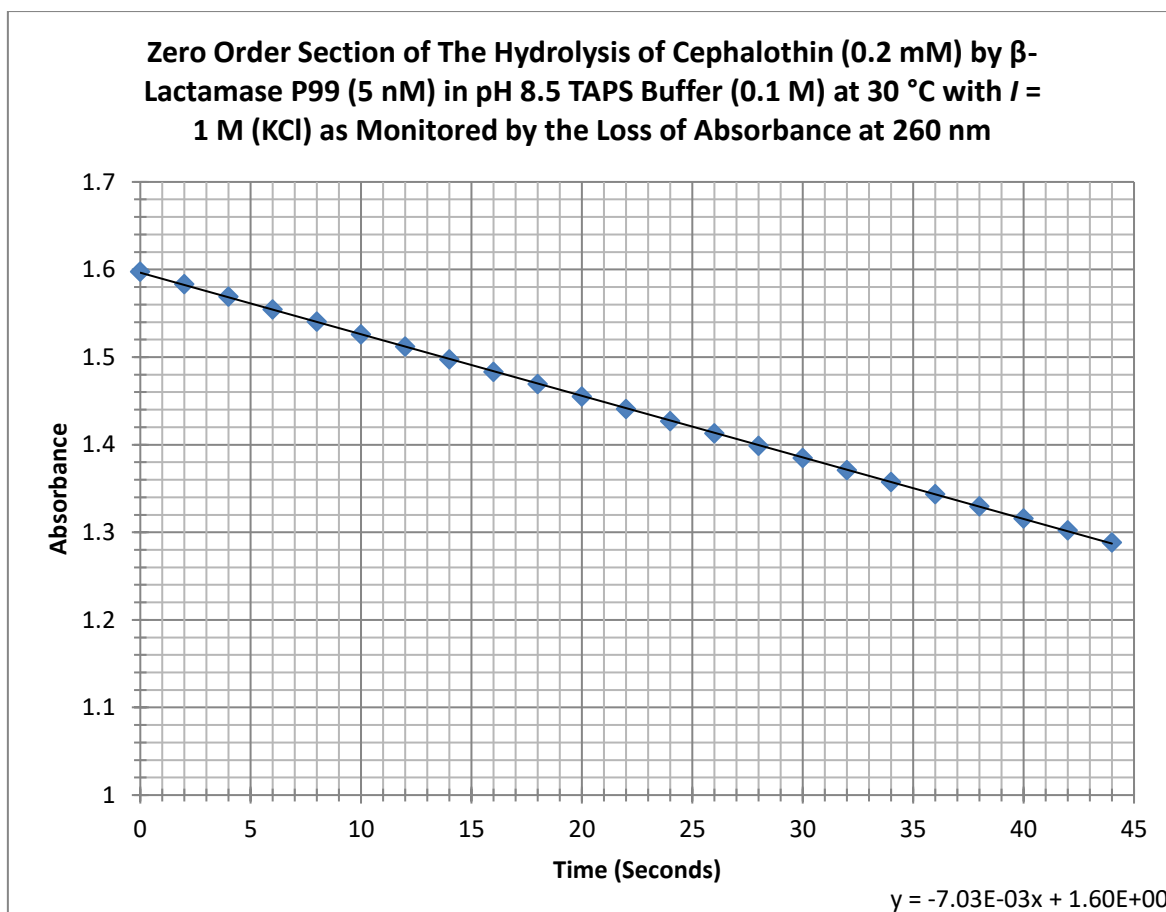


Figure 3.49: Zero order section of the graph in figure 3.48, giving a zero order slope of  $7.03 \times 10^{-3}$

The zero order slope of the blank sample (where no inhibitor was present, only  $\beta$ -lactamase P99 and antibiotic substrate cephalothin) was  $7.03 \times 10^{-3}$  and served as a reference against which inhibited samples can be compared to offer an insight into enzyme activity. The zero order slopes of inhibited samples were compared against the “blank” zero order slope (where there was no inhibition as no inhibitor was present), from which the amount of inhibited enzyme can be calculated.

The inhibitor (TA) was added to the  $\beta$ -lactamase P99 in  $20 \text{ cm}^3$  pH 8.5 TAPS buffer to give final concentrations of TA ( $10 \mu\text{M}$ ) and P99 ( $5 \text{ nM}$ ) and a timer was started. At specified time intervals, a sample was taken and cephalothin was added ( $100 \mu\text{L}$  from a  $40 \text{ mM}$  stock

solution to give a final cephalothin concentration of 0.2 mM) and the hydrolysis of cephalothin was measured. The rate of hydrolysis as compared to the blank sample where there was no inhibitor added gave an indication to the rate of inhibition and the total uninhibited enzyme remaining. The percentage active enzyme remaining was deduced by dividing the zero order slope of the inhibited sample by the zero order slope of the blank sample. For example, the hydrolysis graph of the inhibition sample at 20 minutes (1200 seconds) inhibition time gave the following absorbance graph as shown in figure 3.50 below.

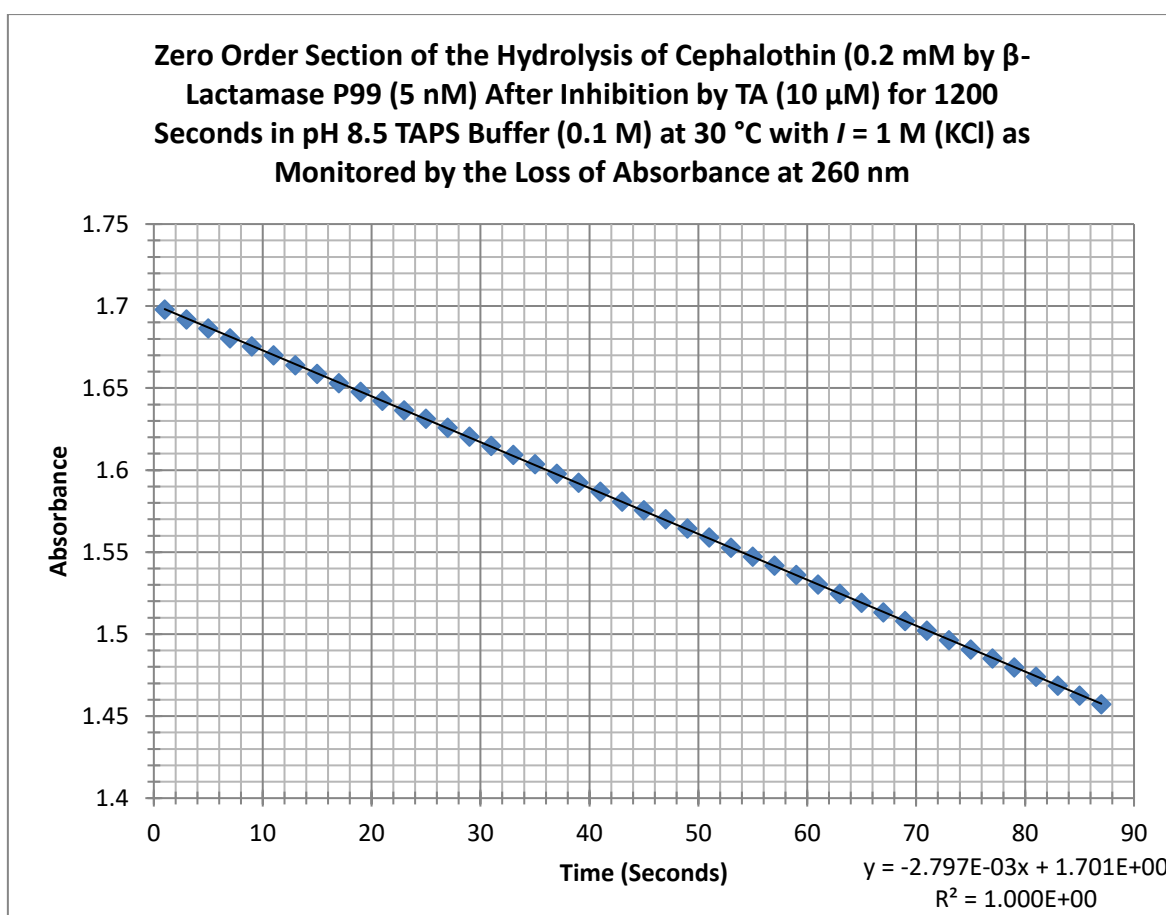


Figure 3.50: Zero order section of the P99 catalysed cephalothin hydrolysis after inhibition by TA after 1200 seconds incubation time at pH 8.5.

Figure 3.50 above gave a zero order slope of  $2.797 \times 10^{-3}$ . When this is divided by the blank zero order slope of  $7.03 \times 10^{-3}$ , it gives a result of 0.3979, indicating 39.79% enzyme activity

was remaining. This corresponded to an enzyme concentration of  $1.99 \times 10^{-9}$  M. This process was repeated at various time points until there was minimal enzyme activity remaining. The concentration enzyme remaining at the recorded time points were then converted to their natural logarithm and plotted against time in seconds. This gave a straight line graph as seen below in figure 3.51.

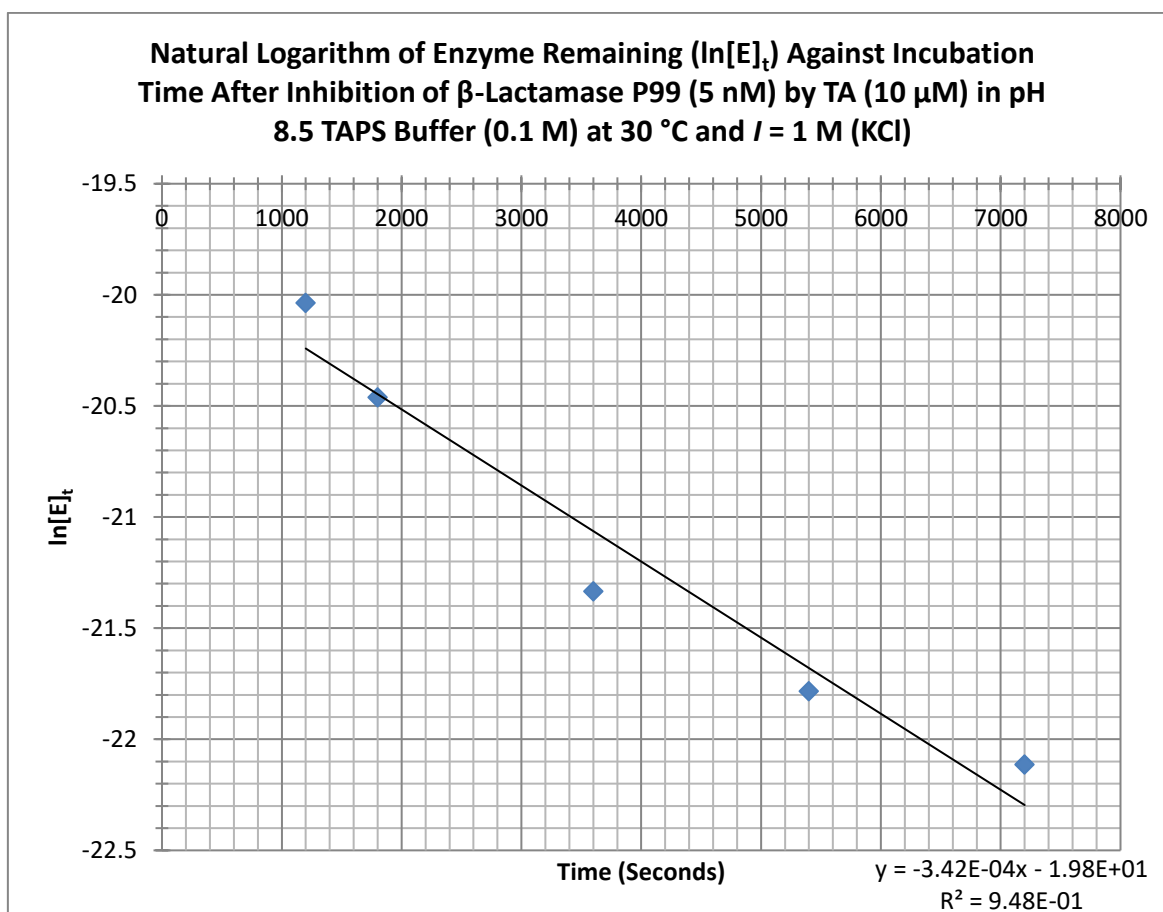


Figure 3.51: Natural logarithm of concentration of active enzyme remaining against incubation time for inhibition of P99 (5 nM) by TA (10  $\mu$ M).

The slope of the graph above in figure 3.51 ( $3.42 \times 10^{-4} \text{ s}^{-1}$ ) can be interpreted as the observed pseudo first-order rate constant for the inhibition ( $k_{\text{obs}}$ ). This result can be divided by the inhibitor concentration (10  $\mu$ M) to give the second order rate constant of  $34.2 \text{ M}^{-1} \text{ s}^{-1}$ .

This process was repeated at 0.5 pH intervals from pH 5.5 to pH 9 to create the following pH profile as seen in figure 3.52 below.

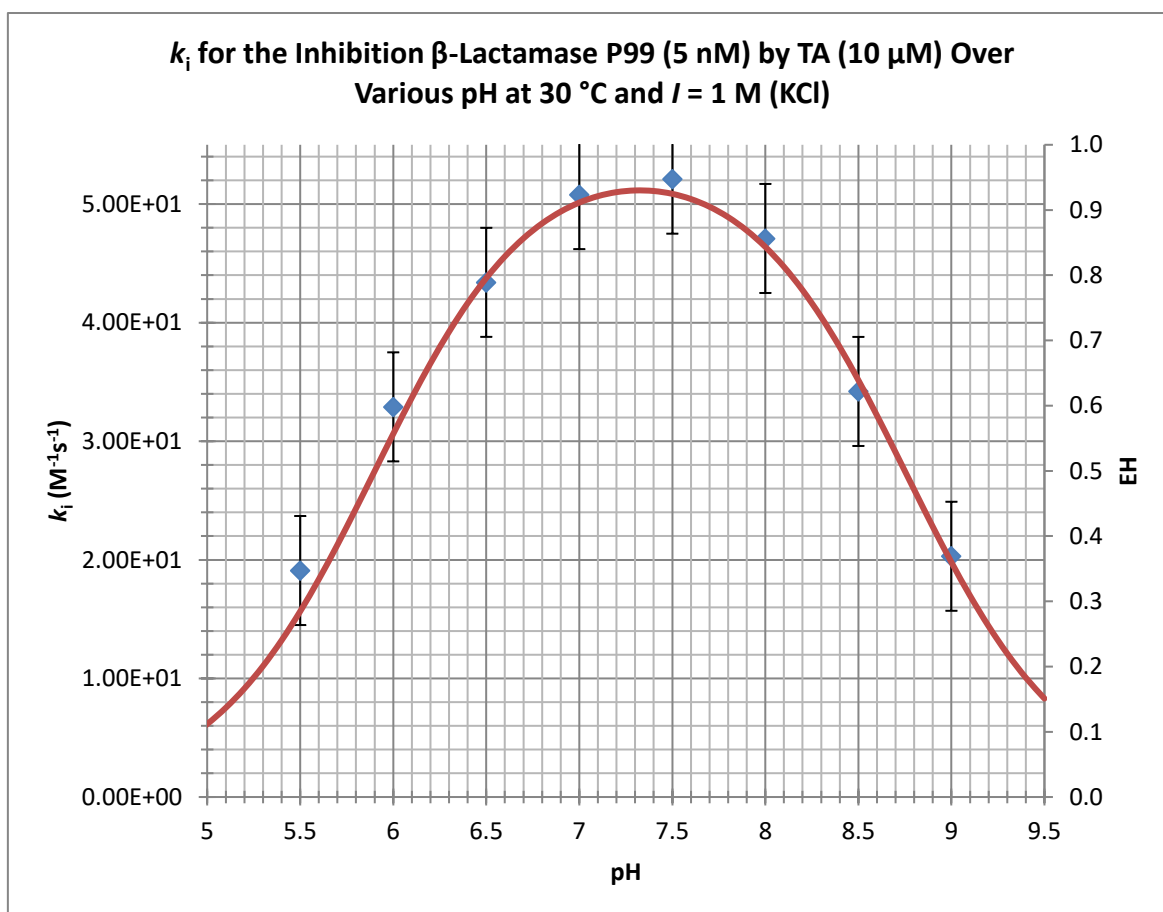


Figure 3.52:  $k_i$  for the inhibition of P99 (5 nM) by TA (10  $\mu$ M) at various pH.

This process was repeated but avibactam was used as the inhibitor instead of TA, as seen in figure 3.53 below. The pH-rate profiles for the inhibition of P99  $\beta$ -lactamase by the carbamate derivatives (figure 3.52 above) and avibactam (figure 3.53 below) are almost identical to that for hydrolysis of  $\beta$ -lactams. The  $pK_a^1$ s of the two important ionisable groups are 5.90 and 6.05 for TA carbamate and avibactam respectively; where-as the  $pK_a^2$  values are 8.75 and 8.30 respectively.

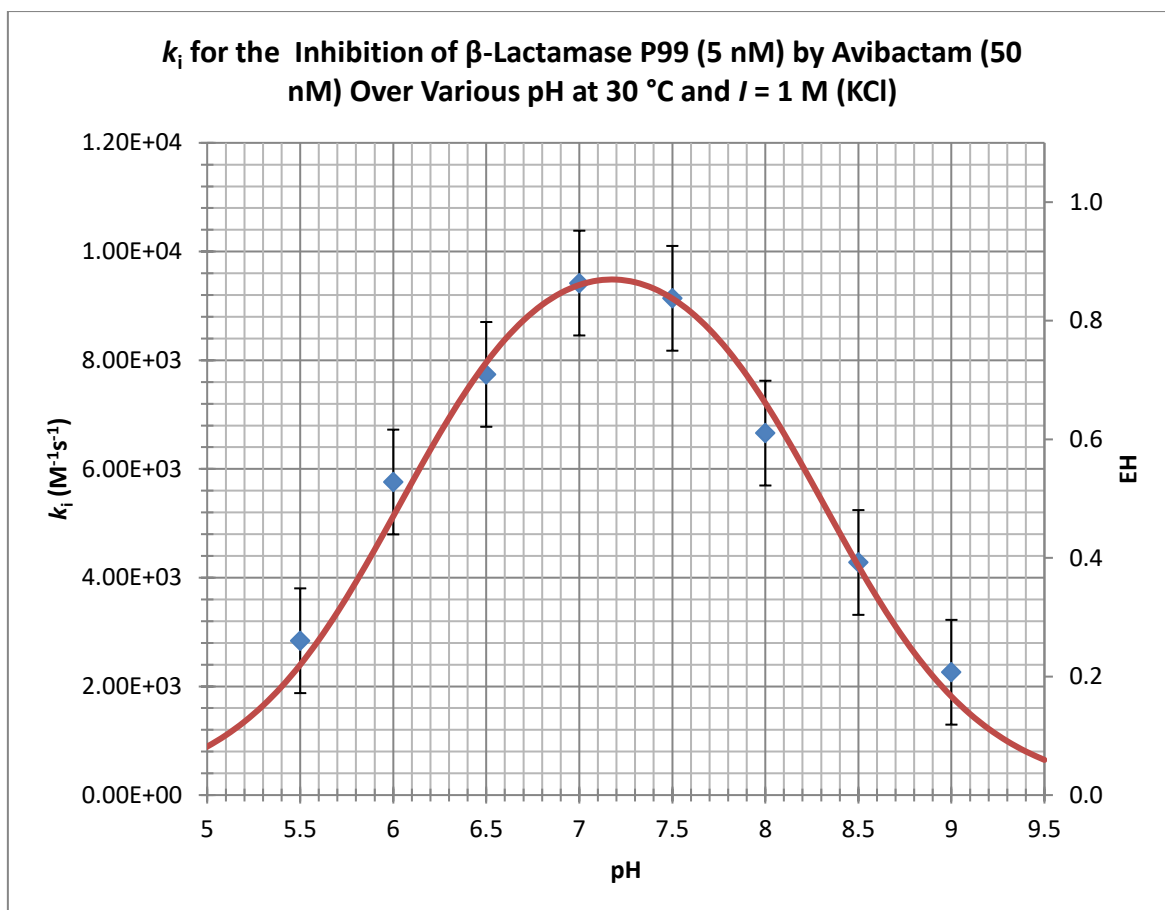


Figure 3.53:  $k_i$  for the inhibition of P99 (5 nM) by avibactam (50 nM) at various pH.

The predicted scheme for the inactivation of SBLs by avibactam and our carbamate inhibitors is shown below in figure 3.54:

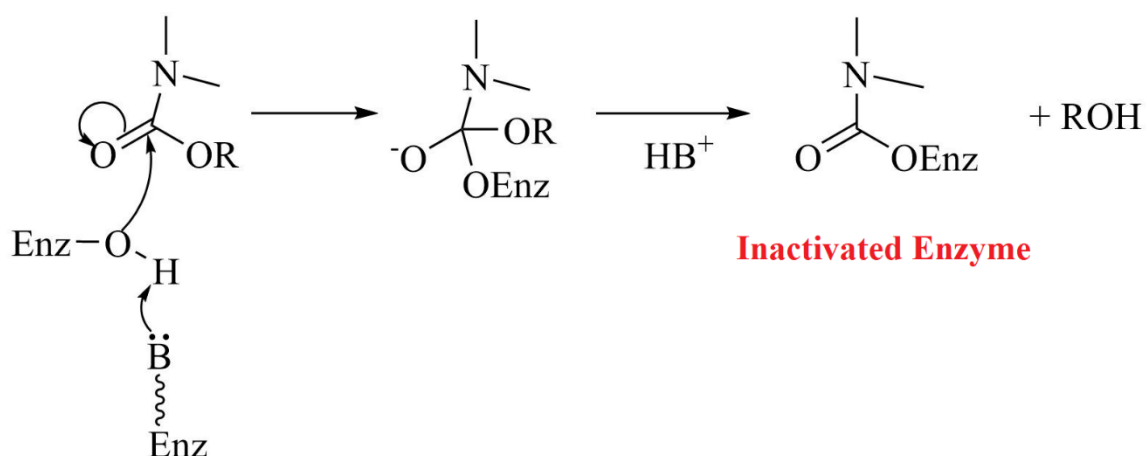


Figure 3.54: Predicted inactivation of SBLs by avibactam and our carbamate inhibitors.

### 3.4.9.2: pH Dependence of Inhibition of CTX-M-15 by TA Carbamate and Avibactam

The process for testing the pH dependent inhibition of P99 with our TA carbamate and avibactam was repeated with other SBL enzymes. As before, a representative example will be shown and briefly explained to show how the data for the pH profiles was obtained.

As for P99, the first step was to obtain a blank sample without inhibitor present, against which inhibited samples could be compared, as seen in figure 3.55 below.

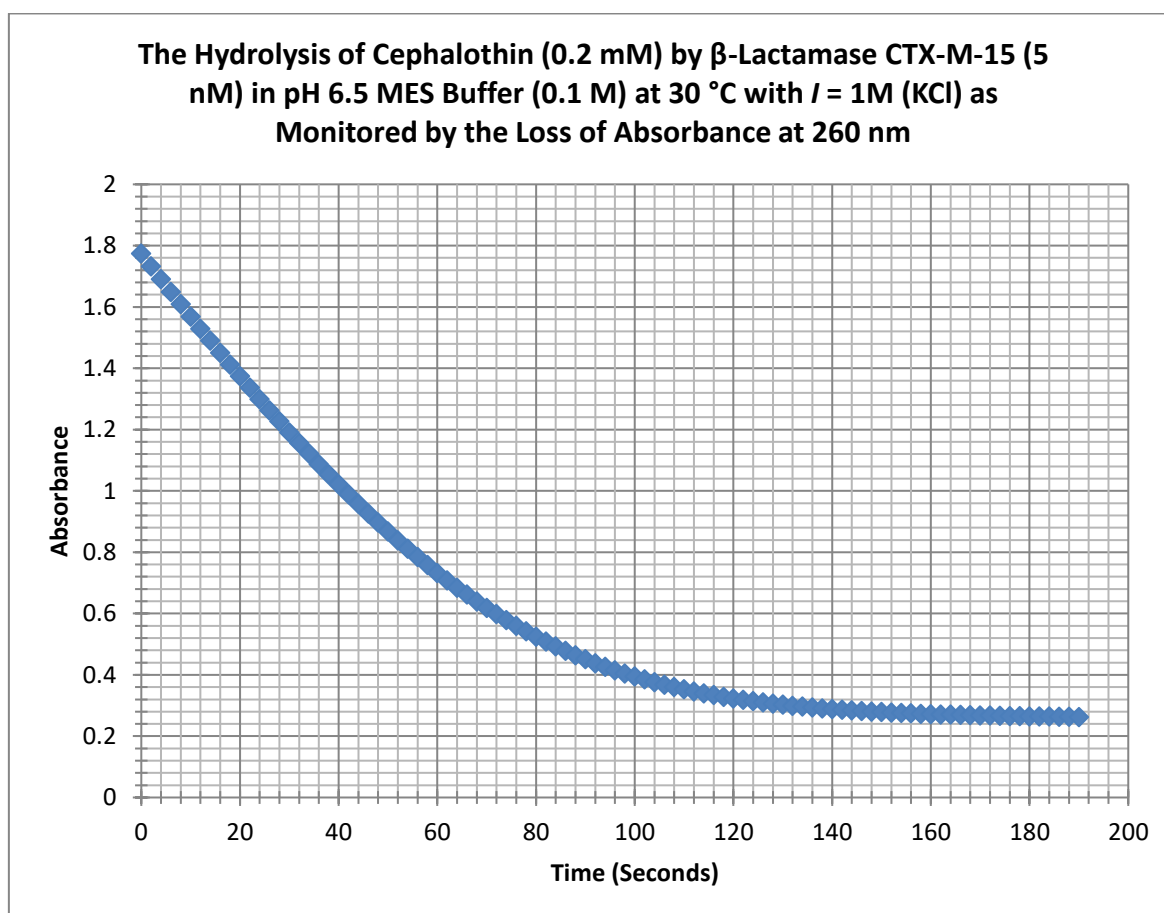


Figure 3.55: CTX-M-15 catalysed hydrolysis of cephalothin at pH 6.5 without inhibitor present.

The zero order slope of the above graph in figure 3.55 serves as a reference against which inhibited samples can be compared to give an insight into the amount of inhibited enzyme.

The zero order slope can be seen below in figure 3.56.

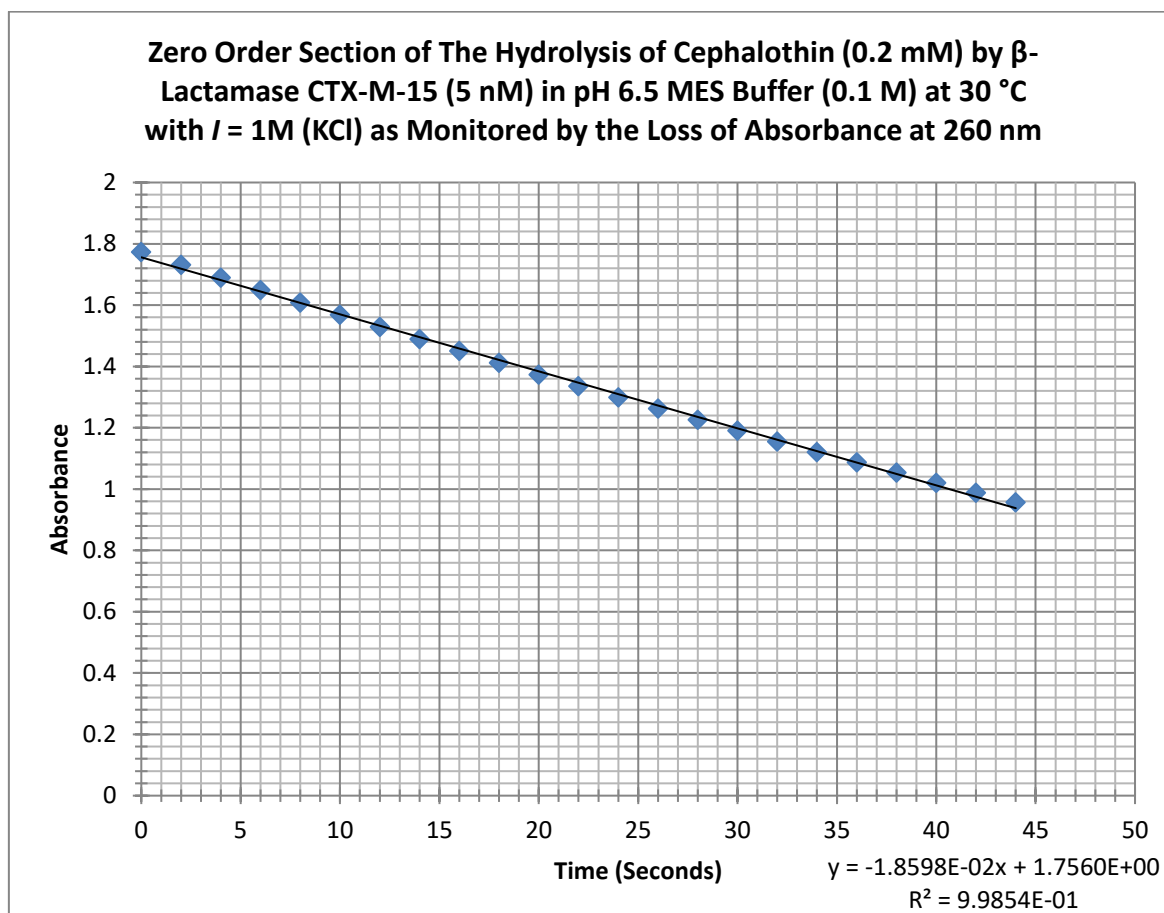


Figure 3.56: Zero order section of the graph in figure 3.55, giving a zero order slope of  $1.8598 \times 10^{-2}$ .

As before, the inhibitor was added to the enzyme and a timer was started. Cephalothin was added at various time points and the hydrolysis was monitored. The rate of hydrolysis in the inhibited samples was compared to the blank sample and the amount of inhibited enzyme was calculated. An example of CTX-M-15 inhibition by TA after 900 seconds can be seen in figure 3.57 below.

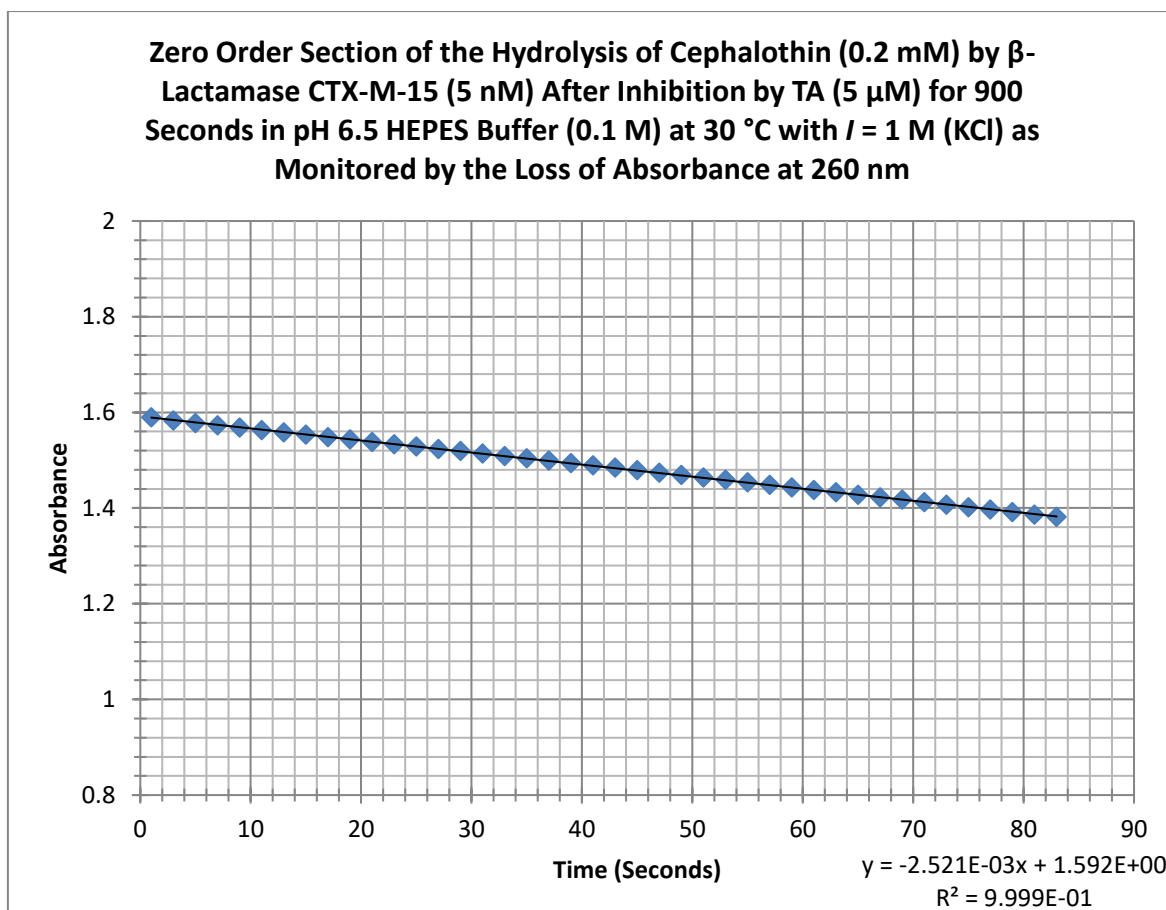


Figure 3.57: Zero order section of the CTX-M-15 catalysed cephalothin hydrolysis after inhibition by TA after 900 seconds incubation time at pH 8.5.

Figure 3.57 gave a zero order slope of  $2.521 \times 10^{-3}$ . When this was divided by the blank zero order slope of  $1.8598 \times 10^{-2}$ , it gave a result of 0.1356, indicating 13.56% enzyme activity was remaining. This corresponded to an enzyme concentration of  $6.78 \times 10^{-10}$  M. This process was repeated at various time points until there was minimal enzyme activity remaining. The concentration enzyme remaining at the recorded time points were then converted to their natural logarithm and plotted against time in seconds. This gave a straight line graph as seen below in figure 3.58.

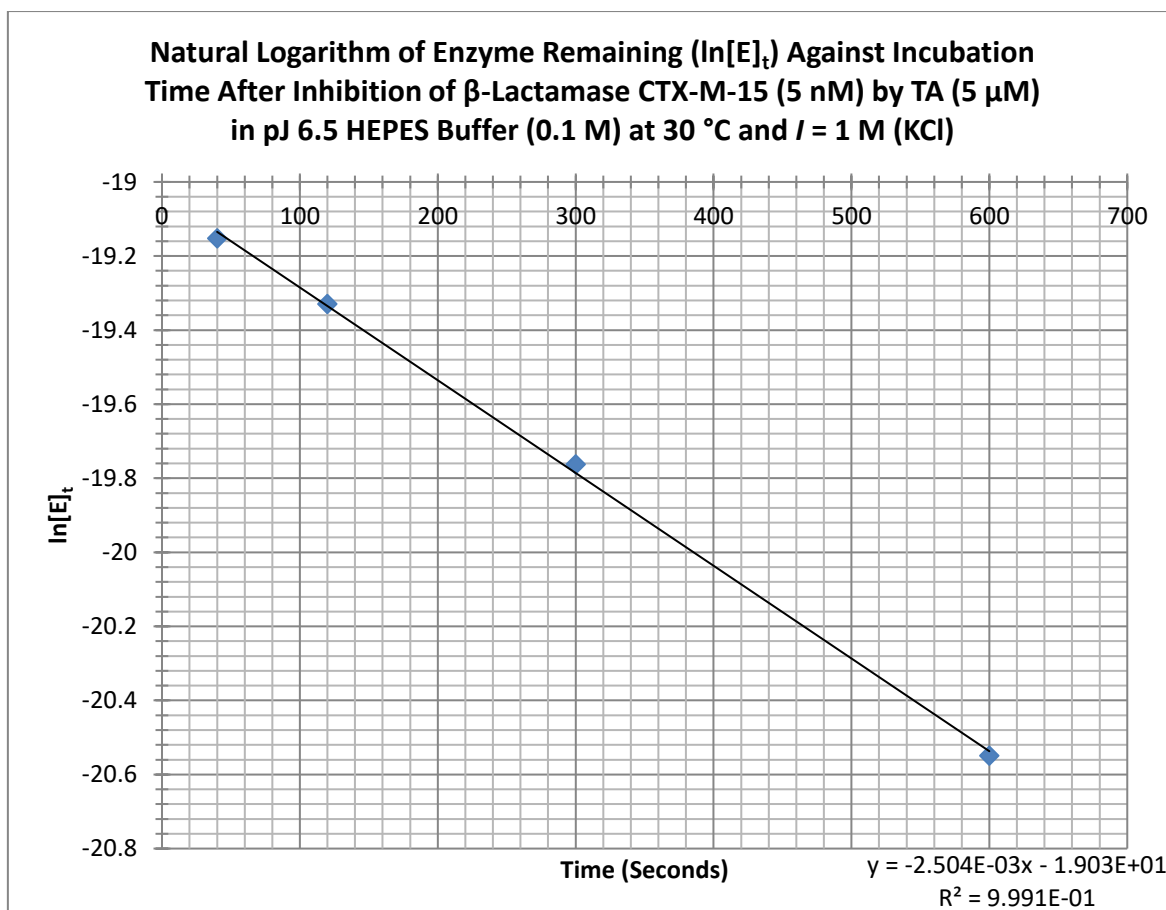


Figure 3.58: Natural logarithm of concentration of active enzyme remaining against incubation time for inhibition of CTX-M-15 (5 nM) by TA (5  $\mu$ M).

As with P99, the slope of the graph above in figure 3.58 ( $2.504 \times 10^{-3} \text{ s}^{-1}$ ) can be interpreted as the observed pseudo first-order rate constant for the inhibition ( $k_{\text{obs}}$ ). This result can be divided by the inhibitor concentration (5  $\mu$ M) to give the second order rate constant of 500.8  $\text{M}^{-1}\text{s}^{-1}$ .

This process was repeated at 0.5 pH intervals from pH 4.0 to pH 9.0 to create the following pH profile as seen in figure 3.59 below.

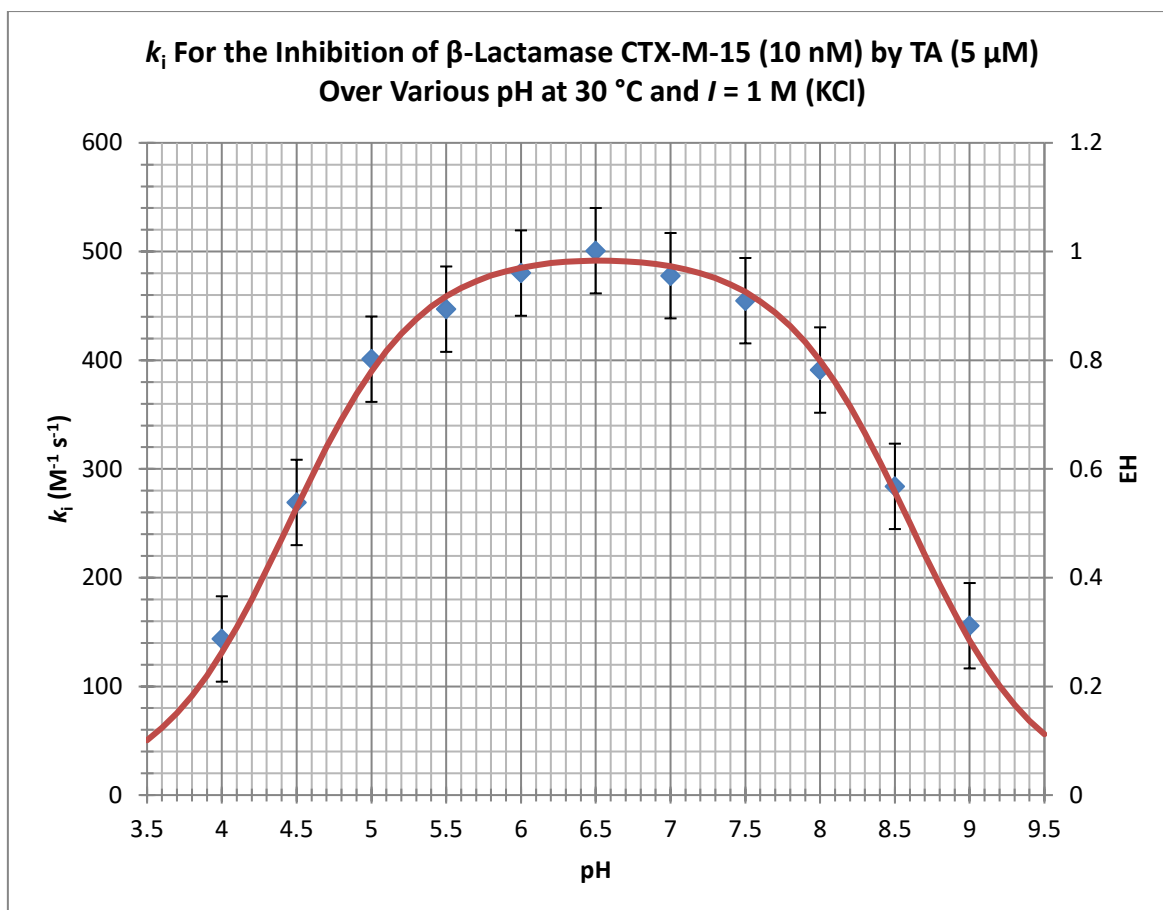


Figure 3.59:  $k_i$  for the inhibition of CTX-M-15 (10 nM) by TA (5  $\mu$ M) at various pH.

This process was repeated with avibactam as the inhibitor.

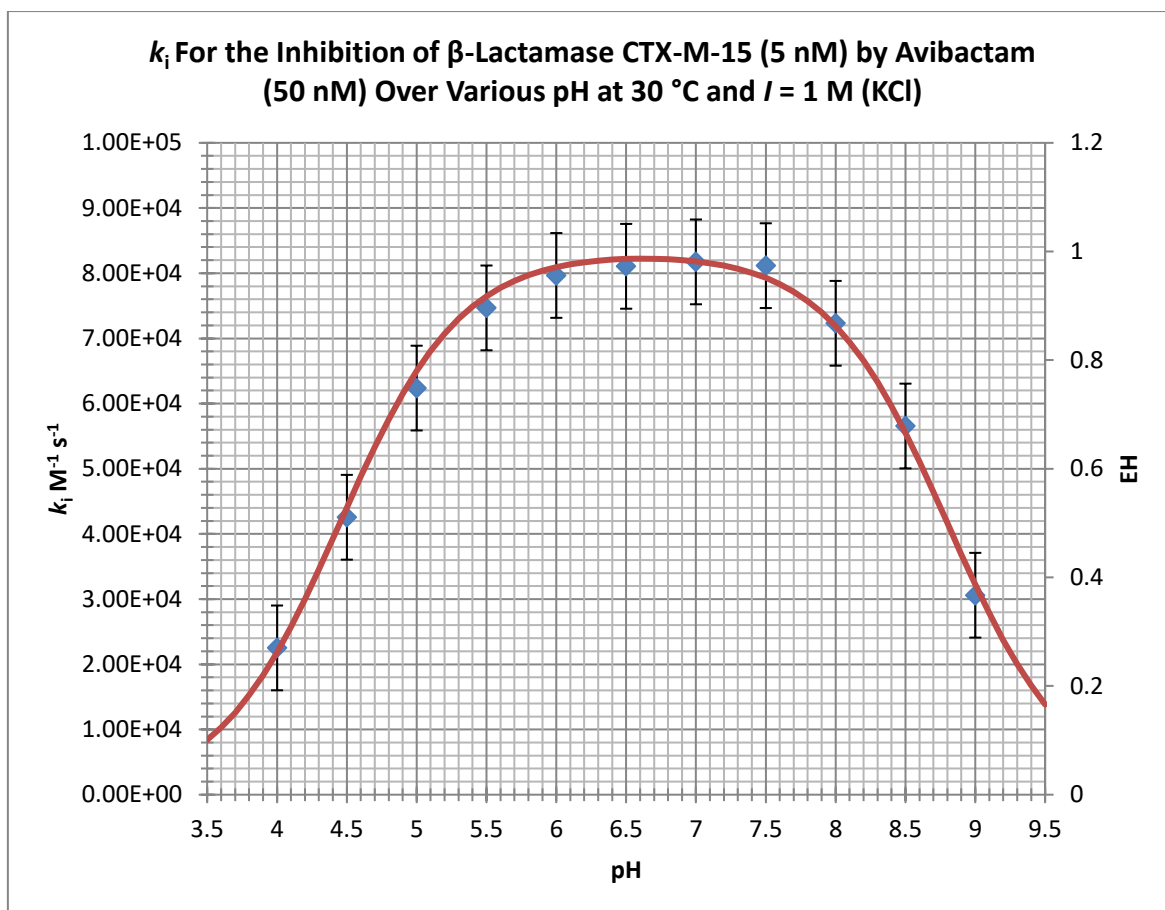


Figure 3.60:  $k_i$  for the inhibition of CTX-M-15 (5 nM) by avibactam (50 nM) at various pH.

The typical bell-shaped profile of the hydrolysis of cephalothin by CTX-M-15 is mirrored in those for inhibition of the enzyme by the TA carbamate (figure 3.59 above) and avibactam (figure 3.60 above). For this enzyme, the  $pK_a^1$ s are both 4.45, and for  $pK_a^2$ s they are 8.65 and 8.80 for the TA carbamate and avibactam respectively. For hydrolysis of cephalothin  $pK_a^1 = 4.75$  and  $pK_a^2 = 8.95$ .

So again, for the inhibition of CTX-M-15 it appears that the same catalytic machinery is used for both hydrolysis and inhibition. The general base is probably Glu-166 (Po, Chan & Chen, 2017), (Delmas, Chen, Prati, Robin, Shoichet & Bonnet, 2008).

### 3.4.9.3: pH Dependence of Inhibition of AmpC by TA Carbamate

As with P99 and CTX-M-15, the pH dependence of inhibition was investigated with the TA carbamate. A representative example will be briefly explained here before the pH profile is explained in further detail.

First, a blank sample consisting of just the enzyme and substrate was obtained, as in figure 3.61 below.

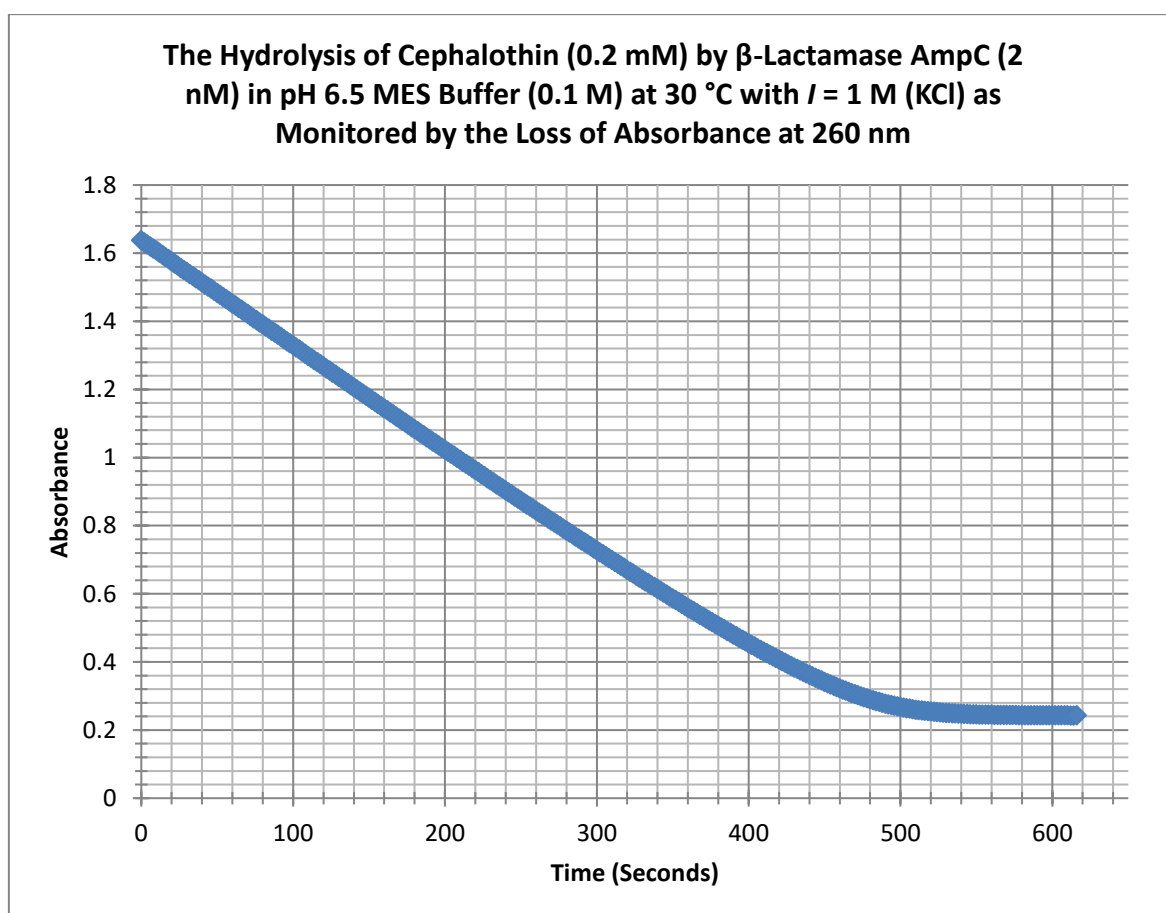


Figure 3.61: AmpC catalysed hydrolysis of cephalothin in pH 6.5 MES buffer.

The zero order portion of figure 3.61 above serves as a blank reference, against which inhibition rates can be deduced.

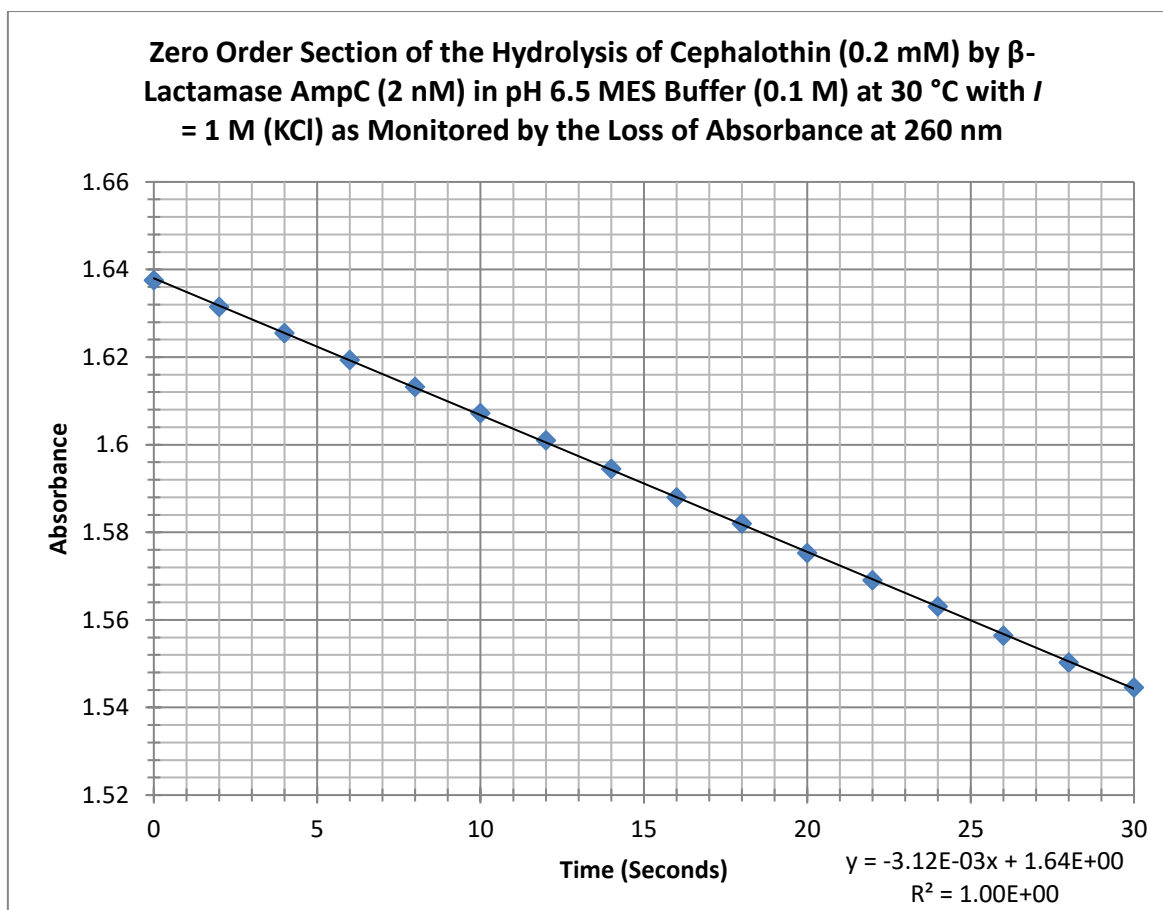


Figure 3.62: Zero order section of AmpC catalysed hydrolysis of cephalothin in pH 6.5 MES buffer.

Figure 3.62 above gives a zero order slope of  $3.12 \times 10^{-3}$ , which can be used as a reference to compare enzyme activity, or amount of inhibition. As before, the inhibitor (in this case, TA carbamate in  $10 \mu\text{M}$  final concentration) was added to the enzyme sample (AmpC with a final concentration of  $5 \text{ nM}$ ) and a timer was started. Samples were taken at various time points and the zero order slopes were recorded and compared against the blank zero order slope (cephalothin and enzyme only) to give an indication to the amount of enzyme activity, and therefore the amount of enzyme which is inhibited.

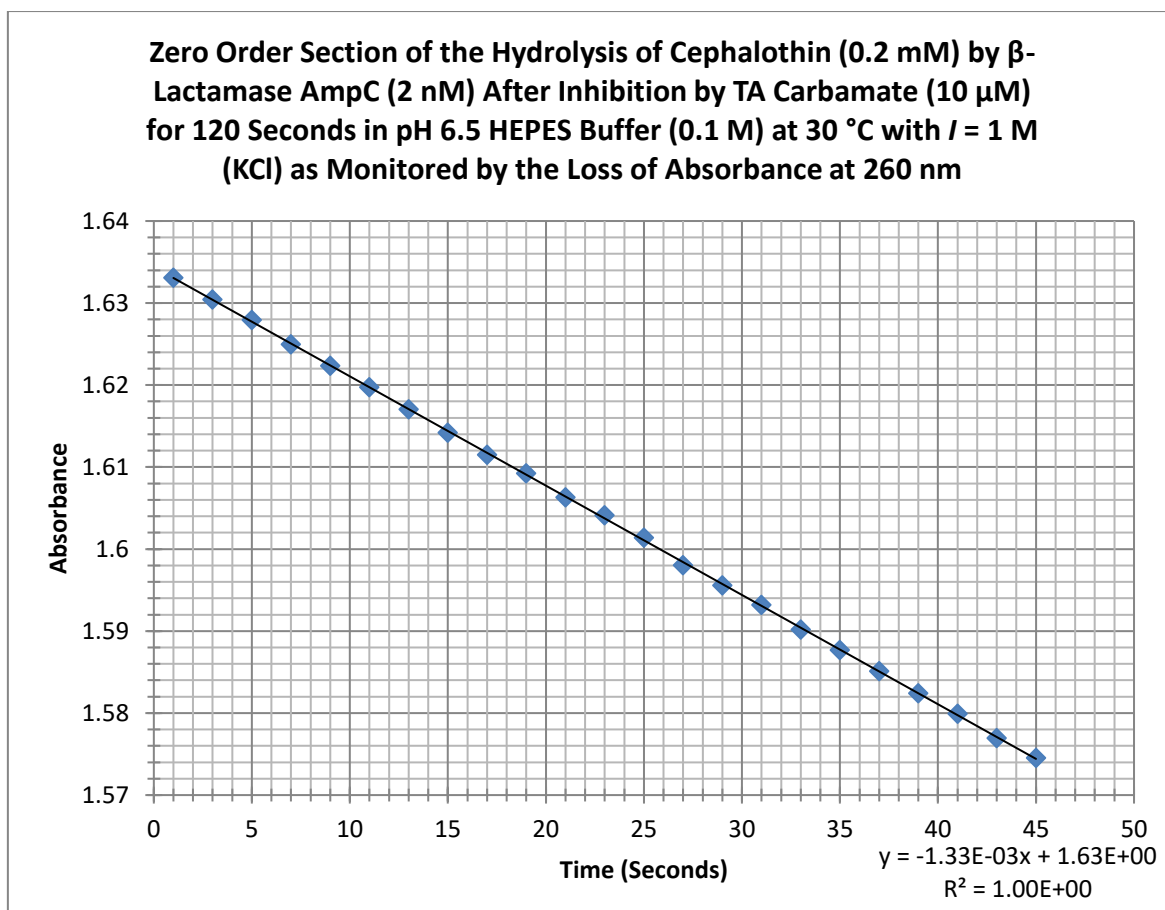


Figure 3.63: Zero order section of the AmpC catalysed cephalothin hydrolysis after inhibition by TA carbamate after 120 seconds at pH 6.5.

Figure 3.63 gave a zero order slope of  $1.33 \times 10^{-3}$ . When this was divided by the blank zero order slope of  $3.12 \times 10^{-3}$ , it gave a result of 0.4263, indicating 42.63% enzyme activity was remaining. This corresponded to an enzyme concentration of  $8.53 \times 10^{-10}$  M. This process was repeated for various time points until there was minimal enzyme activity remaining. The concentration enzyme remaining were then converted to their natural logarithm and plotted against time in seconds. This gave a straight line graph as seen below in figure 3.64.

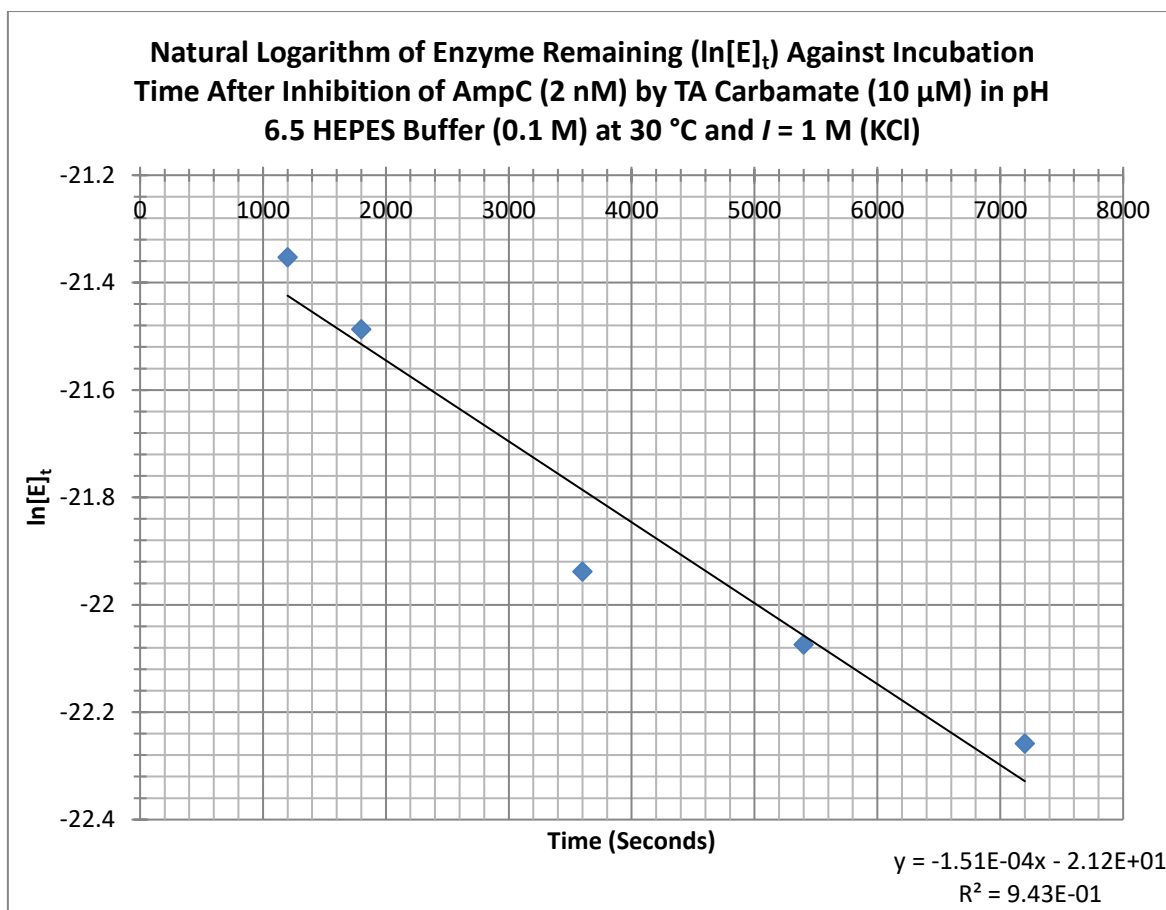


Figure 3.64: Natural logarithm of concentration enzyme remaining (AmpC) after inhibition by TA carbamate.

The slope of the graph above in figure 3.64 ( $1.51 \times 10^{-4} \text{ s}^{-1}$ ) can be interpreted as the observed pseudo first-order rate constant for the inhibition ( $k_{\text{obs}}$ ). This result can be divided by the inhibitor concentration (10  $\mu$ M) to give the second order rate constant of  $15.10 \text{ M}^{-1}\text{s}^{-1}$ .

This process was repeated at 0.5 pH intervals from pH 5.5 to pH 9 to create the following pH profile as seen in figure 3.65 below.

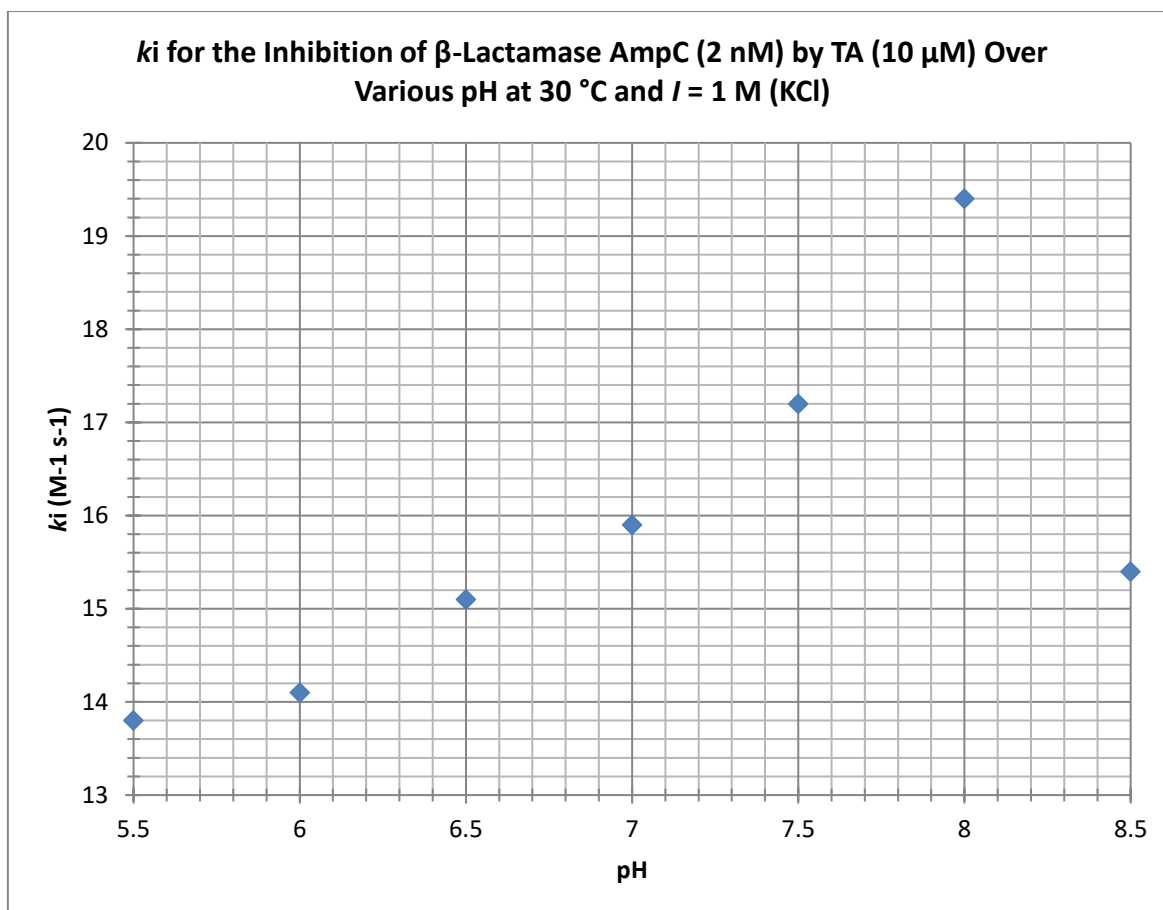


Figure 3.65:  $k_i$  for the inhibition of AmpC (2 nM) by TA (10  $\mu$ M) at various pH.

As can be seen from figure 3.65 above,  $k_{cat}/K_m$  and  $k_i$  for pH dependent hydrolysis of cephalothin and the inhibition of AmpC correlate with each other on their dependence upon pH. This suggests that there is active-site directed inhibition. The close similarity between the  $k_{cat}/K_m$  for the hydrolysis of cephalothin by AmpC and the inhibition of AmpC by TA suggests that the catalytic apparatus used for hydrolysis of  $\beta$ -lactams is the same for inhibition of the enzyme by the TA carbamate derivative.

### 3.4.10: Hydrolysis and Inhibition Conclusions

The carbamate derivatives are good time-dependent inhibitors of classes of serine  $\beta$ -lactamases. There is a good relationship between the second order rate constants for inhibition and the  $pK_a$  of the leaving group alcohol generating a Bronsted  $\beta_{lg}$  value = 0.59, consistent with rate limiting formation of a tetrahedral intermediate. The carbamate with the best leaving group, hexafluoroacetone hydrate (HFA), is a better inhibitor than avibactam itself. The pH-rate profiles for hydrolysis and inhibition by the carbamates and avibactam are all similar, indicating that the same catalytic machinery is used for these different processes. The  $pK_a$ s for the hydrolysis and inhibition for each experiment are shown below in table 3.7.

Table 3.7:  $pK_a$ s for the hydrolysis and inhibition for each pH dependent experiment in chapter 3.

Enzyme	Hydrolysis $pK_a^1$	Inhibition $pK_a^1$ TA	Inhibition $pK_a^1$ Avi	Hydrolysis $pK_a^2$	Inhibition $pK_a^2$ TA	Inhibition $pK_a^2$ Avi
<b>P99</b>	6.40	5.90	6.05	8.85	8.75	8.30
<b>CTX-M-15</b>	4.75	4.45	4.45	8.95	8.65	8.80

### 3.5: Chapter Three References

Adams, P. & Baron, F.A. (1965). Esters of Carbamic Acid. *Chemical Reviews*, 65 (5), 567-602. doi: 10.1021/cr60237a002.

Ayllon, M.S.G., Small, D.H., Avila, J., & Valero, J.S. (2011). Revisiting the Role of Acetylcholinesterase in Alzheimer's Disease: Cross-Talk with P-tau and  $\beta$ -Amyloid. *Frontiers in Molecular Neuroscience*, 4 (22), 1-9. Retrieved from <https://www.ncbi.nlm.nih.gov/pmc/articles/PMC3171929/pdf/fnmol-04-00022.pdf>.

Bajda, M., Latka, K., Hebda, M., Jonczyk, J., & Malawska, B. (2018). Novel carbamate derivatives as selective butyrylcholinesterase inhibitors. *Bioorganic Chemistry*, 78 (1), 29-38. doi: 10.1016/j.bioorg.2018.03.003.

Barton, P., Laws, A.P., & Page, M.I. (1994). Structure-Activity Relationships in the Esterase-Catalysed Hydrolysis and Transesterification of Esters and Lactones. *Journal of the Chemical Society*, 0 (4), 2021-2029. doi: 10.1039/P29940002021.

Beaudoin, M.E. & Gangl, E.T. (2016). Bioanalytical method validation for the simultaneous determination of ceftazidime and avibactam in rat plasma. *Bioanalysis*, 8 (2), 111-122. doi: 10.4155/bio.15.233.

Bonomo, R.A. & Rice, L.B. (1999). Inhibitor resistant class A beta-lactamases. *Frontiers in Bioscience*, 15 (4), 34-41. Retrieved from <https://www.ncbi.nlm.nih.gov/pubmed/10331993>.

Chaibi, E.B., Sirot, D., Paul, G., & Labia, R. (1999). Inhibitor-resistant TEM beta-lactamases: phenotypic, genetic and biochemical characteristics. *Journal of Antimicrobial*

*Chemotherapy*, 43 (4), 447-458. Retrieved from <https://www.ncbi.nlm.nih.gov/pubmed/10350372>.

Chiou, S.Y., Huang, C.F., Hwang, M.T., & Lin, G. (2009). Comparison of Active Sites of Butyrylcholinesterase and Acetylcholinesterase Based on Inhibition by Geometric Isomers of Benzene-di-N- Substituted Carbamates. *Journal of Biochemistry and Molecular Toxicology*, 23 (5), 303-308. doi: 10.1002/jbt.

Colovic, M.B., Krstic, D.Z., Pasti, T.D.L., Bondzic, A.M., & Vasic, V.M. (2013). Acetylcholinesterase Inhibitors: Pharmacology and Toxicology. *Current Neuropharmacology*, 11 (3), 315-335. doi: 10.2174/1570159X11311030006.

Delmas, J., Prati, F., Robin, F., Shoichet, B.K., & Bonnet, R. (2008). Structure and dynamics of CTX-M enzymes reveal insights into substrate accommodation by extended spectrum beta-lactamases. *Journal of Molecular Biology*, 375 (1), 192-201. doi: 0.1016/j.jmb.2007.10.026.

Dvir, H., Silman, I., Harel, M., Rosenberry, T.L., & Sussman, J.L. (2010). Acetylcholinesterase: From 3D Structure to Function. *Chemico-Biological Interactions*, 187 (1), 10-22. doi: 10.1016/j.cbi.2010.01.042.

Hecker, S.J., Reddy, K.R., Totrov, M., Hirst, G.C., Lomovskaya, O., Griffith, D.C. ... Dudley, M.N. (2015). Discovery of a Cyclic Boronic Acid B-Lactamase Inhibitor (RPX7009) With Utility vs Class A Serine Carbapenemases. *Journal of Medicinal Chemistry*, 58 (9), 3682-3692. doi: 10.1021/acs.jmedchem.5b00127.

Johnson, J.L., Cusack, B., Highes, T.F., McCullough, E.H., Fauq, A., Romanovskis, P. ... Rosenberry, T.L. (2003). Inhibitors Tethered Near the Acetylcholinesterase Active Site

Serve as Molecular Rulers of the Peripheral and Acylation Sites. *Journal of Biological Chemistry*, 278 (40), 38948-38955. doi: 10.1074/jbc.M304797200.

Jones, R.N., Barry, A.L., Thornsberry, C., & Wilson, H.W. (1985). The cefoperazone-sulbactam combination. In vitro qualities including beta-lactamase stability, antimicrobial activity, and interpretive criteria for disk diffusion tests.. *American Journal of Clinical Pathology*, 84 (4), 496-504. Retrieved from <https://www.ncbi.nlm.nih.gov/pubmed/2994461>.

Kiener, P.A. & Waley, S.G. (1978). Reversible Inhibitors of Penicillinases. *Biochemical Journal*, 169 (1), 197-204. Retrieved from <https://www.ncbi.nlm.nih.gov/pmc/articles/PMC1184209/>.

Martinez, J.L., Vicente, M.F., Delgado-Iribarren, A., Perez-Diaz, J.C., & Baquero, F. (1989). Small Plasmids are Involved in Amoxicillin-Clavulanate Resistance in *Escherichia coli*. *Antimicrobial Agents and Chemotherapy*, 33(4), 595-595. Retrieved from <https://www.ncbi.nlm.nih.gov/pmc/articles/PMC172490/>.

McGleenon, B.M., Dynan, K.B., & Passmore, A.P. (1999). Acetylcholinesterase inhibitors in Alzheimer's disease. *British Journal of Clinical Pharmacology*, 48 (4), 471-480. doi: 10.1046/j.1365-2125.1999.00026.x.

McHardy, S.F., Wang, H.Y.L., McCowen, S.V., & Valdez, M.C. (2017). Recent advances in acetylcholinesterase inhibitors and reactivators: an update on the patent literature (2012-2015). *Expert Opinion on Therapeutic Patents*, 27 (4), 455-476. doi: 10.1080/13543776.2017.1272571.

Mehta, M., Adem, A., & Sabbagh, M. (2012). New Acetylcholinesterase Inhibitors for Alzheimer's Disease. *International Journal of Alzheimer's Disease*, 1 (2012), 1-8. doi: 0.1155/2012/728983.

Mosley, J.F., Smith, L.L., Parke, C.K., Brown, J.A., Wilson, A.L., & Gibbs, L.V. (2016). Ceftazidime-Avibactam (Avycaz) For the Treatment of Complicated Intra-Abdominal and Urinary Tract Infections. *Pharmacy and Therapeutics*, 41 (8), 479-483. Retrieved from <https://www.ncbi.nlm.nih.gov/pmc/articles/PMC4959616/>.

Nicolas-Chanoine, M.H. (1997). Inhibitor-resistant B-lactamases. *Journal of Antimicrobial Chemotherapy*, 40(1), 1-3. Retrieved from [209](https://watermark.silverchair.com/400001.pdf?token=AQECAHi208BE49Ooan9kkhW_Er cy7Dm3ZL_9Cf3qfKAc485ysgAAAcIwggG-BgkqhkiG9w0BBwagggGvMIIBqwIBADCCAaQGCSqGSIB3DQEHATAeBgIghkgBZQ MEAS4wEQQMYvhX_pOS0C5idZH0AgEQgIIBdYBTUA5Jvui0LYr4RReqWDnV1Uf Nu1Ap7gET20lsb-dH3dPVf8EId2GlmHNTCNQtxFLPDxoYI-VI3qRYQu4AYCaN7LiINX9DwnudpgXY_7sz3T7YUU4F8K_voXhAw1TnfWB8mUoor -Lz2oBSUXu5iiZ0D_Ge-7poAjvvKDY2KxIBd9prJrN3WHqMKP6SShJz8Ce0T8DJUXDsPPaBPshSRaej9wRNSn UjNGsjNPoEcNgq2FzerDkpN_uQBKC_BGNwbigUTANx-T4O_AbStQyTqx1X86OwBqM70NnjAZvi155oOd3EwMEHrt8NcQqa1JtZBFK2UCu047 KsO64AR7Zmb264swde-LilFyy1OpYvf46t3A0hhj4zlFvkoaWaB8GkfQNynuyqIR1TEtB5x5F5WTingXwmtq2xOF isWifJW_tKGSD_jXkM76gSxM9mlhCLM-uHm4KDbTU4AGkRKv4zGIeSrGc2F2c5TV36SScBHCngr7e_vJM.</a></p></div><div data-bbox=)

Page, M.I., Vilanova, B., & Leyland, N.J. (1995). pH Dependence of and Kinetic Solvent Isotope Effects on the Methanolysis and Hydrolysis of B-Lactams Catalyzed by Class C B-Lactamase. *Journal of the American Chemical Society*, 117 (49), 12092-12095. doi: 0.1021/ja00154a009.

Po, K.H.L., Chan, E.W.C., & Chen, S. (2017). Functional Characterization of CTX-M-14 and CTX-M-15  $\beta$ -Lactamases by In Vitro DNA Shuffling. *Antimicrobial Agents and Chemotherapy*, 61 (12), 1-10. doi: 10.1128/AAC .00891-17.

Queensland Department of Health. (2002). *Carbamate Insecticides*. Retrieved from [https://www.health.qld.gov.au/\\_\\_data/assets/pdf\\_file/0027/422298/4174.pdf](https://www.health.qld.gov.au/__data/assets/pdf_file/0027/422298/4174.pdf).

Reading, C. & Cole, M. (1977). Clavulanic Acid: a Beta-Lactamase-Inhibiting Beta-Lactam from *Streptomyces clavuligerus*. *Antimicrobial Agents and Chemotherapy*, 11 (5), 852-857. Retrieved from <https://www.ncbi.nlm.nih.gov/pmc/articles/PMC352086/pdf/aac00299-0090.pdf>.

Reguera, J.A., Baquero, F., Perez-Diaz, J.C., & Martinez, J.L. (1991). Factors determining resistance to B-lactam combined with B-lactamase inhibitors in *Escherichia coli*. *Journal of Antimicrobial Chemotherapy*, 27 (1), 559-575. Retrieved from [569.pdf?token=AQECAHi208BE49Ooan9kkhW\\_Ercy7Dm3ZL\\_9Cf3qfKAc485ysgAAaA0wggGpBqkqhkiG9w0BBwagggGaMIIBlgIBADCCAY8GCSqGSIB3DQEHATAeBgIghkgBZQMEAS4wEQQMMuGWuCIQ28depcXnAgEQgIIBYHm5K6LVP1Oti65h1a4PALoWyTodbLr9EyNp2p\\_Z41aeE0uquJkGfD0bNC1Cdqny7cKvOUtw4s1Hi-VgAFhVEdEO0quL33PvpceVIuGHKx0zDFDKk\\_hBb7bsEnCX\\_AV\\_DwcnPoifRn7A\\_G9SqyF5FYyrY\\_p3kh9IUy-BhYZII4GEBflCvrA5n1ZB3cfZ6CqIDNfQgImAAAnmo8ygbzv5O2S9iBtypuSZpJpYS8FyzIH-](https://watermark.silverchair.com/27-5-569.pdf?token=AQECAHi208BE49Ooan9kkhW_Ercy7Dm3ZL_9Cf3qfKAc485ysgAAaA0wggGpBqkqhkiG9w0BBwagggGaMIIBlgIBADCCAY8GCSqGSIB3DQEHATAeBgIghkgBZQMEAS4wEQQMMuGWuCIQ28depcXnAgEQgIIBYHm5K6LVP1Oti65h1a4PALoWyTodbLr9EyNp2p_Z41aeE0uquJkGfD0bNC1Cdqny7cKvOUtw4s1Hi-VgAFhVEdEO0quL33PvpceVIuGHKx0zDFDKk_hBb7bsEnCX_AV_DwcnPoifRn7A_G9SqyF5FYyrY_p3kh9IUy-BhYZII4GEBflCvrA5n1ZB3cfZ6CqIDNfQgImAAAnmo8ygbzv5O2S9iBtypuSZpJpYS8FyzIH-</a></p></div><div data-bbox=)

BGMpic\_KDJFPhYMNSm4PQsJGpfKGY2UenuPR-

0g5EXaWW37t4BsvosWOVJ2HvTIyF0kAkdUzRb9oMdVZys\_pBmX8mwn1hTJ-

dK34iyrl15bQQngHUW6HQSlfV5C7\_jFiF6vvkBDhTXj27uOgGIW8r68KtDssSwDqwyc

6COTC-J9vnzeno09YC-D-

BPjnspNBPrmXnxTLJJLOHMuP\_mJV9DQ9QulCNPsc8jqDN4dOsw.

Risher, J.F., Mink, F.L., & Stara, J.F. (1987). The toxicologic effects of the carbamate insecticide aldicarb in mammals: a review. *Environmental Health Perspectives*, 72 (1), 267-281. doi: 10.1289/ehp.8772267.

Shields, R.K., Nguyen, M.H., Press, E.G., Cheng, L., Kreiswirth, B.N., & Clancy, C.J. (2017). Emergence of Ceftazidime-Avibactam Resistance and Restoration of Carbapenem Susceptibility in *Klebsiella pneumoniae* Carbapenemase-Producing *K pneumoniae*: A Case Report and Review of Literature. *Open Forum Infectious Diseases*, 4 (3), 1-4. Retrieved from <https://www.ncbi.nlm.nih.gov/pmc/articles/PMC5493938/pdf/ofx101.pdf>.

Struger, J., Grabuski, J., Cagampan, S., Sverko, E., & Marvin, C. (2016). Occurrence and Distribution of Carbamate Pesticides and Metalaxyl in Southern Ontario Surface Waters 2007-2010. *Bulletin of Environmental Contamination and Toxicology*, 96 (1), 423-431. doi: 10.1007/s00128-015-1719-x.

Tabet, N. (2006). Acetylcholinesterase inhibitors for Alzheimer's disease: anti-inflammatories in acetylcholine clothing! *Age and Ageing*, 35 (4), 336-338. doi: 10.1093/ageing/afl027.

Toussaint, K.A. & Gallagher, J.C. (2015).  $\beta$ -Lactam/ $\beta$ -Lactamase Inhibitor Combinations: From Then to Now. *Annals of Pharmacotherapy*, 49 (1), 86-98. doi: 10.1177/1060028014556652.

Titus, A.M., Revest, P., & Shortland, P. (2010). *The Nervous System* (2nd ed.). London: Churchill Livingstone.

Wang, D.Y., Abboud, M.I., Markoulides, M.S., Brem, J., & Schofield, C.J. (2016). The road to avibactam: the first clinically useful non-B-lactam working somewhat like a B-lactam. *Future Medicinal Chemistry*, 8 (10), 1063-1084. doi: 10.4155/fmc-2016-0078.

Wu, P.J., Shannon, K., & Phillips, I. (1994). Effect of hyper-production of TEM-1 beta-lactamase on in vitro susceptibility of *Escherichia coli* to beta-lactam antibiotics. *Antimicrobial Agents and Chemotherapy*, 38 (3), 494-498. Retrieved from <https://www.ncbi.nlm.nih.gov/pmc/articles/PMC284486/>.

Wu, P.J., Shannon, K., & Phillips, I. (1995). Mechanisms of hyperproduction of TEM-1 beta-lactamase by clinical isolates of *Escherichia coli*. *Journal of Antimicrobial Chemotherapy*, 36 (6), 927-939. Retrieved from <https://www.ncbi.nlm.nih.gov/pubmed/8821592>.

Yanovsky, E., Groner, E.F., Zaikin, A., Lerman, L., Shalom, H., Zeeli, S. ... Weinstock, M. (2012). Carbamate derivatives of indolines as cholinesterase inhibitors and antioxidants for the treatment of Alzheimer's disease. *Journal of Medicinal Chemistry*, 55 (23), 10700-10715. doi: 10.1021/jm301411.

## Chapter Four: Other Novel $\beta$ -Lactamase Inhibitors

### 4.1: Introduction

#### 4.1.1: Ellagic Acid

Ellagic acid is a polyphenolic phytochemical (Vattem & Shetty, 2005) present in various fruits and vegetables (Corbett, Daniel, Drayton, Field, Steinhardt & Garrett, 2010), with pomegranate juice being a traditional rich source of this polyphenol (Usta, Ozdemir, Schiariti & Puddu, 2013). Ellagic acid is a highly symmetrical molecule which contains a fused four ring system, with four phenolic groups (Priyadarsini, Khopde, Kumar & Mohan, 2002). Polyphenols are naturally derived products, produced as secondary metabolites by plants, and play an essential role in plant physiology (Beart, Lilley & Haslam, 1985), and also assist in the prevention of infection from plant pathogens (Daglia, 2012). Ellagic acid contains a  $\delta$ -lactone as a possible acylating residue and an acidic phenol thus possessing the two fundamental requirements of an inhibitor of serine  $\beta$ -lactamases. However, before discussing those aspects, it is worth reviewing their general biological activities.

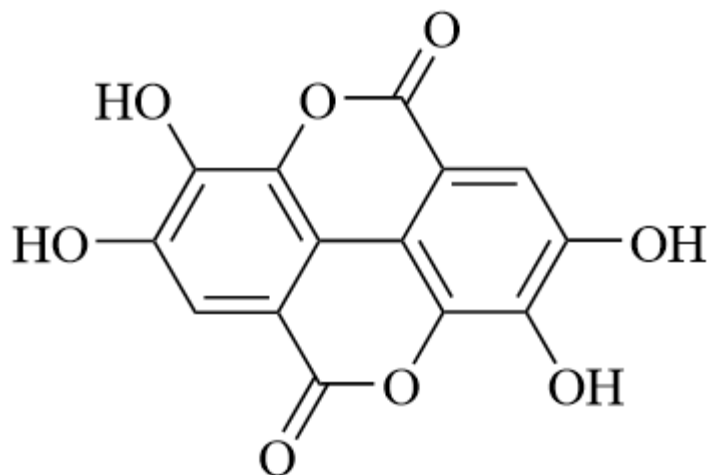


Figure 4.1: Structure of ellagic acid

Ellagic acid (as seen above in figure 4.1) has long been a molecule of biological and pharmaceutical interest due to its antioxidant properties (Talcott, Talcott & Percival, 2003). In chemical terms, antioxidants are compounds capable of reacting and “neutralising” free radicals, by acting almost as an electron “sponge”. Free radicals are reactive oxygen and nitrogen species that have an unpaired electron in their outer shell, making them highly reactive (Lobo, Patil, Phatak & Chandra, 2010). Antioxidants such as phenols are capable of transferring H atoms (via electron and proton transfer) to the active free radical to generate a neutral species and a stabilised phenol radical:



Free radicals are capable of causing cell damage by reacting indiscriminately with cell components. Free radicals are capable of oxidising many compounds, including components of human cells. Whilst this can lead to cell damage, a key concern of free radicals is that they may ultimately lead to cell mutations, and possibly cancer (Thyagarajan & Sahu, 2017). Antioxidants therefore spare cells from damage, by undergoing oxidation by free radicals themselves, saving cells from being potentially damaged. Ellagic acid and similar

compounds are important components of a healthy diet, and have been shown to be stable under physiological conditions, and are therefore capable of reaching various parts of the digestive system intact (Usta et al., 2013).

Furthermore, ellagic acid has been shown to have anti-inflammatory effects (Favarin et al., 2013). Inflammation occurs when the immune system responds to threats, such as foreign pathogens which may be introduced from wounds. Inflammation also occurs where there has been damage to tissue, such as a blow to a joint and has familiar characteristics, such as pain, redness, swelling and heat. Inflammation encourages healing by promoting blood flow to the source of the injury, allowing white blood cells and other immune responses to reach the damaged area and promote healing (Koh & DiPietro, 2011). Whilst inflammation has been shown to be essential for healing (Landen, Li & Stahle, 2016), immune system responses can sometimes incorrectly trigger inflammation where there is no threat posed by an invading pathogen, in what is referred to as chronic inflammation. Chronic inflammation is typically brought on by a combination of host factors (for example, the specific health of the individual) including age and genetic predisposition to inflammation and lifestyle factors such as smoking, poor diet and a sedentary lifestyle (Garn et al., 2016). In chronic inflammation, the immune system continues producing an immune response (the traditional redness, swelling and pain etc.) even after the immune threat has been eliminated, or even in the complete absence of a threat to the immune system. Unrestrained, the immune system continues to produce macrophages and other white blood cells which, in the absence of a foreign pathogen, begin to attack surrounding healthy tissue and organs. This chronic inflammatory response can be a prerequisite to some of the most notorious challenges of our age, including cancer, diabetes and arthritis (Chang & Yang, 2016). The protective activity afforded to ellagic acid and other polyphenols has generally been attributed to their antioxidant, free radical scavenger and metal chelator properties. Also, polyphenols have

been shown to be capable of inhibiting physiologically important enzymes such as digestive enzymes including  $\alpha$ -glucosidase and pancreatic  $\alpha$ -amylase, helping to decrease blood sugar levels (McDougall & Stewart, 2005), (Gu, Hurst, Stuart & Lambert, 2011) and also pancreatic lipase, reducing the amount of fat absorbed during digestion (Glisan, Sae-Tan, Grove, Yennawar & Lambert, 2014).

Additionally, naturally occurring polyphenols (including ellagic acid) have been investigated for their antibacterial properties (Daglia, 2012), (Coppo & Marchese, 2014), (Sanhuenza, Melo, Montero, Maisey, Mendoza, Wilkens & 2017). Flavan-3-ols, flavanols and tannins have received the most attention from the scientific community due to their wider spectrum of activity and antibacterial potency, and the fact they are able to operate synergistically with antibiotics to improve their potency as evidenced by a decrease in minimum inhibitory concentrations (MICs) for  $\beta$ -lactam antibiotics combatting clinically important strains of *Enterobacteriaceae*, including *Escherichia coli* and *Staphylococcus aureus* (Haghjoo, Lee, Habiba, Tahir, Olabi & Chu, 2013). Figure 4.2 below shows some common polyphenols and their applications as antimicrobial agents.

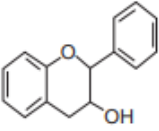
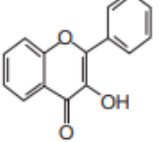
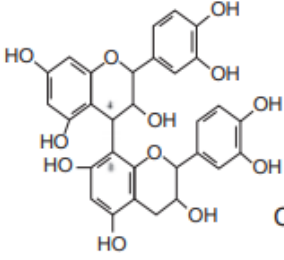
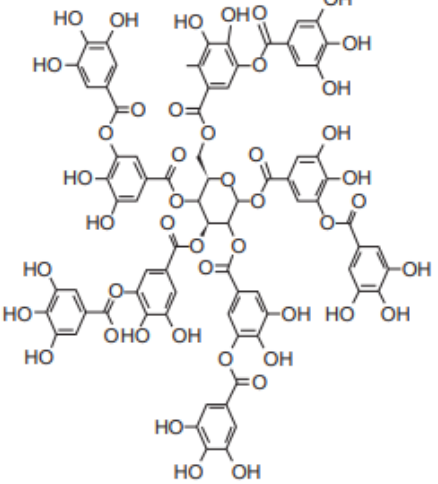
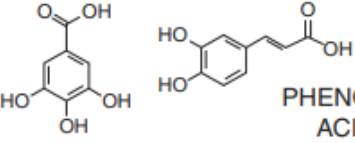
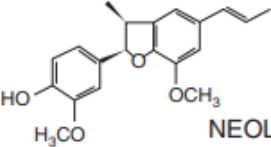
 <p style="text-align: center;"><b>FLAVAN-3-OL</b></p>	<p style="text-align: center;">ANTIBACTERIAL</p> <p style="text-align: center;">ANTIVIRAL</p> <p style="text-align: center;">ANTIFUNGAL</p>	<p><i>V.cholerae</i> - <i>S.mutans</i> - <i>C.jejuni</i>  <i>C.perfringes</i> - <i>E.coli</i> - <i>B.Cereus</i>  <i>H.pylori</i> - <i>S.aureus</i> - <i>L.acidophilus</i>  <i>A.naeslundii</i> - <i>P.oralis</i> - <i>P.gingivalis</i>  <i>P.melaninogenica</i> - <i>F.nucleatum</i> -  <i>C.pneumonia</i></p> <p>Adenovirus– Enterovirus –Flu virus</p> <p><i>Candida albicans</i>  <i>Microsporium gypseum</i>  <i>Trichophyton mentagrophytes</i>  <i>Trichophyton rubrum</i></p>
 <p style="text-align: center;"><b>FLAVONOL</b></p>		<p><i>S.mutans</i>  <i>E.coli</i>  <i>S.aureus</i></p> <p>influenza A virus  type -1 herpes simplex virus (HSV)</p>
 <p style="text-align: center;"><b>CONDENSED TANNIN</b></p>	<p style="text-align: center;">ANTIBACTERIAL</p> <p style="text-align: center;">ANTIVIRAL</p>	<p><i>S.mutans</i>  <i>E.coli</i>  <i>S.aureus</i></p> <p>influenza A virus  type -1 herpes simplex virus (HSV)</p>
 <p style="text-align: center;"><b>HYDROLYSABLE TANNIS</b></p>	<p style="text-align: center;">ANTIBACTERIAL</p> <p style="text-align: center;">ANTIVIRAL</p> <p style="text-align: center;">ANTIFUNGAL</p>	<p>Different strains of :  <i>Salmonella</i> - <i>Staphylococcus</i>  <i>Helicobacter</i> - <i>E.coli</i> - <i>Bacillus</i>  <i>Clostridium</i> - <i>Campylobacter</i>  <i>Lysteria</i></p> <p>Epstein-Barr virus  Herpes virus  HSV -1 and HSV -2,</p> <p><i>Candida parapsilosis</i></p>
 <p style="text-align: center;"><b>PHENOLIC ACID</b></p>	<p style="text-align: center;">ANTIBACTERIAL</p>	<p><i>S.aureus</i> - <i>L.monocytogenes</i>  <i>E.coli</i> - <i>Paeruginosa</i></p>
 <p style="text-align: center;"><b>NEOLIGNAN</b></p>	<p style="text-align: center;">ANTIBACTERIAL</p>	<p>Different strains of :  <i>Mycobacterium tuberculosis</i></p>

Figure 4.2: classes of polyphenols and their typical applications as antimicrobial agents (Daglia, 2012).

Ellagic acid is a derivative of tannins and is produced biosynthetically by the hydrolysis of tannins (Zhang, Wang & Xu, 2014). Indeed, the effectiveness of polyphenols as antibacterial agents has prompted research into their suitability as natural preservatives for food products, owing to the strong public demand to reduce the amount of synthetic materials used in food production and storage (Vaguero, Fernandez, Nadra & Saad, 2010) and also as novel antibiotics owing to the prevalence of resistance to conventional therapies (Jayaraman, Sakharkar, Lim, Tang & Sakharkar, 2010), (Saavedra, Borges, Dias, Aires, Bennett, Rosa & Simoes, 2010).

Mechanisms of action for polyphenols as antibacterial agents are not fully understood. It is thought that owing to the structural similarity with some existing antibiotics that they will operate in mechanistically similar circumstances. For example, it has been suggested that some polyphenols are able to interfere with cell membrane and wall production, resulting in destabilisation of the membrane and eventual cell death, showing a similar mechanism of action to existing  $\beta$ -lactam antibiotics (Heinonen, 2007). Additionally, polyphenols have been shown to act as chelating agents, being capable of binding metal ions including iron and zinc. Metal depletion causes severe limitations to bacterial growth, resulting in bacterial cells being unable to reproduce and grow (Dixon, Xie & Sharma, 2005). Also, it has been shown that polyphenols are able to inhibit extracellular enzymes essential for normal bacterial cell function and growth, leading to cell death (Pimia, 2004). Finally, polyphenols have been shown to have activity against not only bacteria, but fungi and viruses also, including herpes, influenza and flu viruses (Ho, Cheng, Weng, Leu & Chiu, 2009). Susceptible strains of fungi to polyphenols include *Candida albicans*, *Candida parapsilosis* and *Microsporium gypseum* (Hirasawa & Takada, 2004). An example of the mechanism of action for viral inhibition is by preventing the attachment of viral particles to their target receptor cells, preventing transmission of the virus to host cells (Nakayama, Suzuki, Toda,

Okubo, Hara & Shimamura, 1993) and also by modification to the membrane of the viral particles, resulting in a decrease of viral activity (Song, Lee & Seong, 2005). The mechanism of action of antifungal polyphenols is not fully understood and is in area of developing research as more and more polyphenols are screened for their antimicrobial properties, but it is thought that polyphenols can disrupt healthy spore formation, and interruptions of cell membrane permeability, resulting in the lack of reproduction of fungal cells and lysis of the cell due to altered membrane permeability (Yang & Jiang, 2015).

As analytical tools and extraction methods improve, the number of identified and characterised polyphenols has increased, with over 8,000 phenolic compounds identified (Dai & Mumper, 2010) and over 4,000 flavonoids described (Tsao, 2010). There is a rich opportunity for the investigation of these compounds and into their potential benefits as use for novel therapies concerned with the previously mentioned health ailments. Ellagic acid has only relatively recently been recognised as having biologically relevant activities and as such investigation into its potential uses as a pharmaceutical agent is beginning to increase.

Ellagic acid has not been subject to much research within the field of microbial chemotherapy, with interest only slowly accumulating in the compound since 2010. A 2010 study by Ghudhaib, Hanna & Jawad explored the use of ellagic acid as an antimicrobial agent. Their research concluded that ellagic acid provided lower MICs than the existing antibiotics gentamycin and streptomycin for important pathogenic strains of bacteria, including the Gram-negative  $\beta$ -lactamase producing pathogen *Klebsiella pneumoniae*. Another study by Panichayupakaranant, Tewtrakul & Yuenyongsawad (2010) tested the antibiotic activities of pomegranate rind, containing 13 % v/v ellagic acid. They found the MIC of ellagic acid against *Staphylococcus aureus* to be in the range of around 10  $\mu$ g, which is in a similar region to existing antibiotics including the BLBLIC amoxicillin/clavulanate, which has an MIC of 8  $\mu$ g (Rubin, Ball & Trejo, 2011). Finally, a more recent study by De

and colleagues (2018), investigated the use of ellagic acid as an antibacterial agent against the problematic stomach ulcer causing Gram-negative pathogen *Helicobacter pylori*. *H. pylori* is a troublesome pathogen, capable of producing  $\beta$ -lactamases (Tseng et al., 2009) and therefore possibly resistant to many existing antibiotics dependent upon the strain. The results from this study showed that ellagic acid was capable of inhibiting all the strains of *H. pylori* infected, with MICs in the range of 5-30 mg/ml. Whilst this range is higher than the classic antibiotic used in *H. pylori* suspected infections (amoxicillin) with MICs of around 1  $\mu$ g/ml (Kim, Kim, Jung, Kim, Kim & Song, 2004), it is still interesting that ellagic acid was capable of inhibiting all strains with modest MICs. Furthermore, ellagic acid aided in the healing and restitution of gastric mucosal damage caused by *H. pylori*. These studies show that ellagic acid has a huge potential for development as a novel antimicrobial product.

Clearly, a naturally occurring compound that is shown to reduce the occurrence of chronic inflammation with anti-oxidant and antibacterial properties is of significant interest to the pharmaceutical community. Indeed, ellagic acid has been labelled as a super-nutrient owing to these properties. However, the question of whether ellagic acid is capable of inhibiting  $\beta$ -lactamases has so far not been investigated. Ellagic acid is a potential acylating agent and a metal-ion chelator. Therefore, there is a potential for ellagic acid to be an SBL inhibitor, and perhaps also an MBL inhibitor. Investigations into the antibacterial activity of ellagic acid have shown its potential to be a future novel antimicrobial agent. If this molecule also possessed a  $\beta$ -lactamase inhibiting ability, it would make it an ideal candidate for investigations and development as a dual action novel antimicrobial and  $\beta$ -lactamase inhibiting agent, perhaps making it a resistance proof antibiotic. It could also be used in a synergistic fashion with other existing  $\beta$ -lactams, as has been shown with other polyphenols; the ellagic acid could exhibit modest antimicrobial capability, but then also act as a protector of the  $\beta$ -lactam antibiotic by inhibiting  $\beta$ -lactamases produced by the target bacteria. This

co-administration could help lower MICs, as shown with other polyphenols. In this chapter, the MBL and SBL capability of ellagic acid will be investigated, along-side other interesting molecules, including another plant derived compound (urolithin A), and an existing lipase inhibitor (orlistat).

#### 4.1.2: Urolithin A

Urolithin A is also a plant based metabolite (Zhao, Shi, Guo, Zhao, Song & Yang, 2018), similar to ellagic acid, and is found from similar sources including fruits and nuts (Paivarinta, Pajari, Torronen & Mutanen, 2009). Like ellagic acid, it contains a  $\delta$ -lactone and acidic phenolic groups. Urolithins are formed after elagitannins are hydrolysed to ellagic acid under physiological conditions *in vivo*, and ellagic acid is then gradually metabolised by the intestinal microbiota to produce different types of urolithins (Landete, 2011). When unabsorbed elagitannins and ellagic acid reach the colon in the latter part of the digestive system, they are metabolised by gut microbiota to yield a variety of urolithins (Villalba, Beltran, Espin, Selma, Barberan, 2013). There are four main types of urolithin: urolithin A, B, C and D (Espin, Larrosa, Teresa & Barberan (2013). The subject of this chapter will be urolithin A. Urolithin D is produced from ellagic acid upon the opening of a lactone ring and removal of a carboxyl group. Urolithin D then loses 1, 2 or 3 hydroxyl groups via dihydroxylation to form urolithin C, urolithin A and urolithin B respectively (Kang, Buckner, Shay, Gu & Chung, 2016).

In terms of its chemical nature, urolithin A is a benzocoumarin, being a combination of coumarin and isocoumarin, as seen in figure 4.3 below.

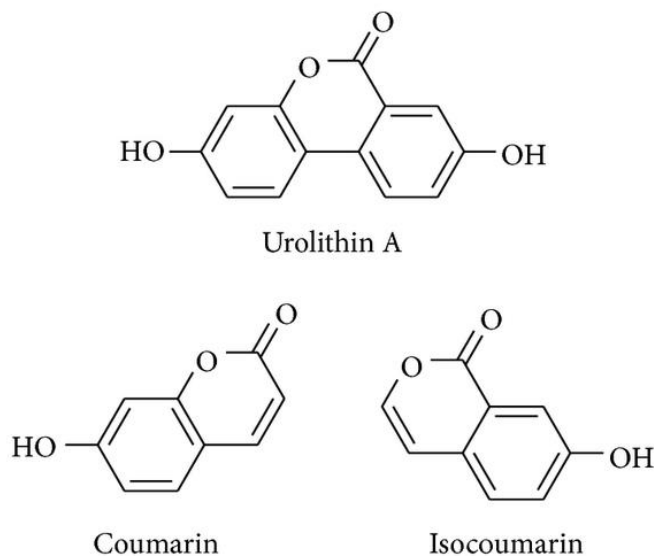


Figure 4.3: Structure of urolithin A, showing similarities between coumarin and isocoumarin (Espin, Larrosa, Conesa & Barberan, 2013).

As urolithin A is a metabolite of ellagic acid, it is perhaps unsurprising that the associated health benefits of both molecules are fairly similar. Urolithin A has been shown to have antioxidant properties, although it is not as capable an antioxidant as other polyphenols such as ellagic acid (Biolonska, Kasimsetty, Khan & Ferreira, 2009). Additionally, urolithin A has been shown to have anti-inflammatory properties, also similar to ellagic acid. In a study by Gimenez-Bastida et al., (2012), urolithin A at relevant physiological concentrations ( $\mu\text{M}$  range) was shown to exhibit anti-inflammatory activity in the progression of atherosclerosis (an inflammatory disease affecting the arteries [Fana & Montagnana, 2018]), moderately inhibiting monocyte adhesion to endothelial cells, thereby preventing the progression of the disease.

Furthermore, urolithin A has been shown to exhibit anticarcinogenic effects, which has been one of the most heavily investigated health effects of this compound (Heber, 2008). Conventional cancer therapies are associated with severe side effects, which can often be

debilitating, such as pain, diarrhoea, and often infection brought about by a weakened immune system for those patients undergoing chemotherapy (Pearce, Haas, Vuney, Pearson, Haywood, Brown & Ward, 2017). Therefore, the demand for alternative therapies that avoids these side effects is of great interest to the scientific community. Urolithin A has been shown to inhibit cancer related enzymes and modulate certain genes associated with cancer. For example, Zhang et al., (2016) found that urolithin A modulated ER alpha-dependent gene expression, which resulted in the inhibition of endometrial cancer proliferation. Also, in a study probing the effects of urolithins on bladder cancer cells, Liberal, Carmo, Gomes, Cruz and Batista (2017) found that urolithin A impaired the proliferation of bladder cancer cells, and induced apoptosis (cell death) of cancer cells. An important aspect of this study is that urolithin A had selective effects against cancer cells, and did not interfere with the growth of normal, healthy cells. Furthermore, urolithin A has been shown to be effective at inhibiting the growth of cancer cells in the colon, which is perhaps of greater relevance than cancer of other areas, as it is in the colon where ellagic acid is metabolised to form urolithin A, and can reach bioactive concentrations (Espin et al., 2013). Urolithin A alongside ellagic acid and urolithin B, were shown to prevent the cell cycle of caco-2 cancer cells in the colon through gene modulation of those genes involved in cell cycle regulation (Sarrias, Espin, Barberan & Conesa, 2009). Finally, many studies have shown urolithin A to be capable of controlling prostate cancer tumour growth (Gonzalez, Ciudad, Pulido & Noe, 2016), (Stanislawska, Piwowarski, Granica & Kiss, 2018), (Poudel, Vadhanam & Burliston, 2014), (Vicinanza, Zhang, Henning & Heber, 2013), (Stanislawska, Granica & Kiss, 2015) making it a promising candidate for a future chemopreventative agent for prostate cancer. The typical mechanisms of action for urolithin as an anti-prostate cancer agent included: modulating genes involved with cancerous cell growth and inducing apoptosis of cancer cells.

It is understood that intestinal absorption of elagitannins and ellagic acid is quite low, which results in an abundant source of elagitannins and ellagic acid for biosynthesis of urolithins, which have a much higher bioavailability for absorption in the intestine (Cerdeira, Llorach, Ceron, Espin, Barberan, 2003). This suggests that it is the urolithins which may be the actual bioactive molecules and the source of the health benefits from polyphenols as discussed in the previous sub chapter, and the health benefits rely on the effect of the metabolites produced by the gut microbiota.

#### 4.1.3: Orlistat

Orlistat is an approved gastric and pancreatic lipase inhibitor drug developed by Roche, marketed under the trade name Xenical in the United States and Alli in the United Kingdom (Drew, Dixon & Dixon, 2007). Dietary fat must be broken down into smaller fatty acid chains and glycerol by digestive lipase, before being capable of absorption in the digestive tract. Orlistat's intended mechanism of action is to inhibit digestive lipase enzymes by binding covalently to the active site, resulting in a reduction in activity of lipase enzymes, thereby decreasing the amount of dietary fat absorbed in the intestinal tract; ultimately leading to a reduction in the amount of calories consumed (Heck, Yanovski & Calis, 2012). Lipase enzymes in the digestive system rely on a catalytic triad of serine, histidine and an aspartic acid residue to catalyse the hydrolysis of dietary fat (Brumlik & Buckley, 1996). In terms of its chemistry, orlistat is a diastereomeric molecule with four chiral centres, containing a  $\beta$ -lactone group (Heck, Yanovski & Calis, 2012). Orlistat's structure can be seen in figure 4.4 below.

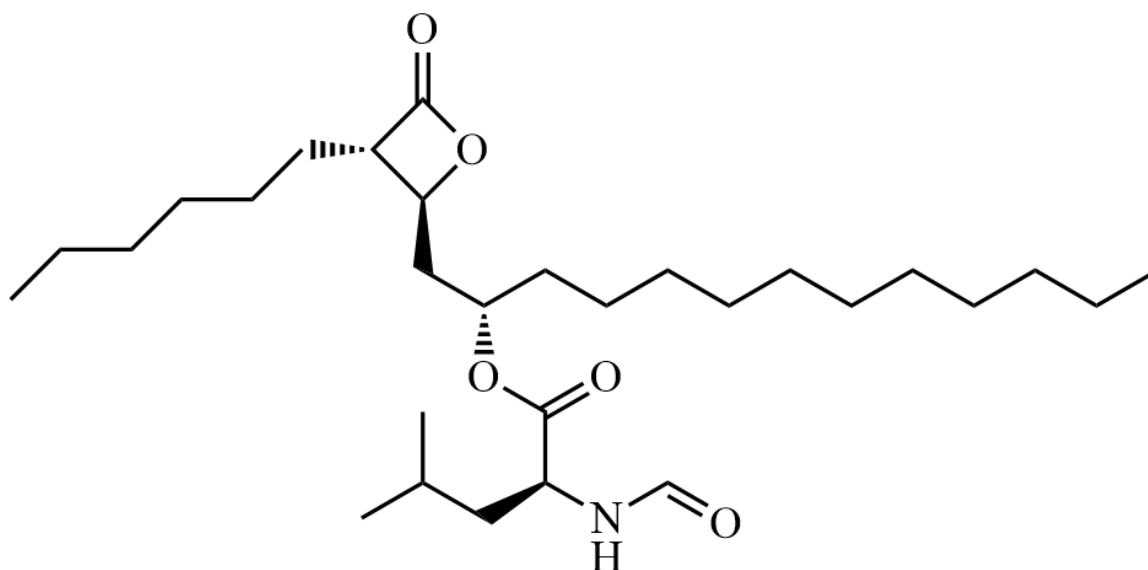


Figure 4.4: Chemical structure of orlistat.

Interestingly, although the main focus of orlistat has been its capability as a digestive lipase inhibitor, it has also been shown to be an effective inhibitor of the fatty acid synthase enzyme. This enzyme is associated with tumour progression in prostate cancer (Kridel, Axelrod, Rozenkrantz & Smith, 2004).

Kinetic data show that orlistat is the most effective lipase inhibitor currently on the market, with  $IC_{50}$  values lower than other polyphenol natural products with known lipase inhibiting activity, as shown in a study by Gonzalez et al., (2017).  $IC_{50}$  (also known as the half maximal inhibitory concentration), is a measure of the effectiveness of an inhibitor binding to an enzyme. The lower an  $IC_{50}$ , the more potent is the inhibitor and it is the most commonly used metric as a measure of an inhibitor's effectiveness (Kalliokoski, Kramer, Vulpetti & Gedeck, 2013).

Despite their similarity to  $\beta$ -lactams, there has been little research into the use of lactones as  $\beta$ -lactamase inhibitors. The work of Gal et al., (2000) describes the activity of a  $\gamma$ -lactone acting as a  $\beta$ -lactamase inhibitor.  $\gamma$ -Lactones are structurally similar to  $\beta$ -lactones, with the

only difference being that the oxygen is part of a five member ring in gamma lactones, as opposed to a four member ring in  $\beta$ -lactones. A literature review found no references to  $\beta$ -lactones being employed as  $\beta$ -lactamase inhibitors.

It is hypothesised, that owing to the fact that orlistat is an efficient inhibitor of digestive lipases, and the fact that these enzymes have a serine in their active site, and also the fact that previous work has shown gamma lactones to be capable of inhibiting  $\beta$ -lactamases, that orlistat may perhaps show inhibitory activity against SBLs. It is known that  $\beta$ -lactones can act as both acylating and alkylating agents, as seen below in figure 4.5:

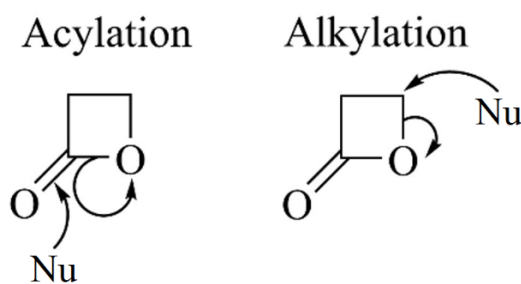


Figure 4.5:  $\beta$ -lactones acting as acylating and alkylating agents.

#### 4.1.4: Chapter Four Aims

As discussed, three potential novel  $\beta$ -lactamase inhibitors have been identified and will be assessed for their suitability as inhibitors and for their antibiotic capability. Furthermore, as ellagic acid has 4 ionisable groups, the effect of pH on the activity of potential  $\beta$ -lactamase inhibition by ellagic acid will also be determined.

## 4.2: Methods

### 4.2.1: UV Methods

The UV methods for detection of inhibition were much the same as the methods used in chapter three. Briefly, stock solutions of the potential inhibitors were created in MeOH for ellagic acid and ACN for orlistat and urolithin A. A 1 mM ellagic acid stock solution was created in MeOH by dissolving 3.02 mg of ellagic acid in 1 ml MeOH and sonicating for 20 minutes. The inhibition experiments for ellagic acid were conducted in the usual buffers for the respective pH but supplemented with 10 % MeOH to aid solubility of ellagic acid. For example, for the inhibition experiments with ellagic acid at pH 8.5, the buffer would be 20 ml pH 8.5 TAPS buffer (0.1 M) with 10 % MeOH (18 ml aqueous TAPS buffer and 2 ml MeOH) with ionic strength maintained to 1 M with KCl. Similarly, for orlistat and urolithin A, a different solvent composition was required. 4.96 mg of orlistat was dissolved in 1 ml ACN to create a 10 mM stock solution. For urolithin A, 2.28 mg was dissolved in 1 ml ACN to create a 10 mM stock solution. For both of these inhibitors, the inhibition experiments were conducted in pH 7.0 HEPES buffer (0.1 M) with 10 % ACN (18 ml pH 7.0 HEPES buffer and 2 ml ACN) maintained to 1 M ionic strength with KCl.

Appropriate blanks containing the same concentrations of solvent (10% MeOH/ACN) were taken to see if they had any effect on the activity of the enzyme and much like for the other time dependent blanks, enzyme activity loss was negligible (<5%). The hydrolysis of the antibiotic cephalothin was used as a tool to measure the concentration of the enzyme through inhibition/hydrolysis rates of the enzyme.

The enzyme was thawed slowly in melting ice and was added to the stock solution of the potential inhibitors and a stopwatch was started. Samples were taken at intermittent intervals after incubation of the potential inhibitor with various  $\beta$ -lactamases and pipetted into a 1 cm<sup>3</sup> cuvette. The cuvette was then placed in a UV cell thermostatted to 30 °C, and the instrument was then blanked at 260 nm (a good wavelength for cephalothin) with the contents of the UV cell (buffer, solvent, inhibitor and enzyme). Cephalothin solution was added and the instrument began recording the absorbance at 260 nm. The rates of hydrolysis were determined from the initial slopes of absorbance against time. These initial slopes gave the percentage of active enzyme remaining and were converted to concentration values. A graph of the natural logarithm of the concentration of active enzyme remaining against incubation time in seconds, gave a straight line graph, the slope of which was  $k_{\text{obs}}$  for the inhibition reaction.

The stability of the enzyme over the time periods used for the inhibition studies was determined from observing the initial slopes of the change in absorbance in the hydrolysis of cephalothin. This was to ensure that any change in the rate of hydrolysis reflects inhibition of the enzyme and not any 'natural' loss of activity of the enzyme.

For the pH dependent analysis of ellagic acid, the method was much the same except the pH and the buffer used was altered dependent upon the requirements of the pH levels. The following buffers were used depending upon the pH required: pH 4-5: acetic acid, pH 5.5-6.5: 2-(*N*-morpholino)ethanesulfonic acid, pH 7.0-8.0: HEPES, pH 8.5-9.0 TAPS.

### 4.2.2: Microbiological Methods

The antibiotic potential of the three compounds was qualitatively tested. Tryptone soya agar (TSA) plates were prepared and maximum recovery diluent (MRD) solutions containing different antibiotic resistant strains of bacteria were spread over the surface of the agar using a sterile plate spreader and were placed in a sterile laminar flow hood until the surfaces were dry. Six wells were created in the agar plates by using a sterile 10 mm cork borer. A 10  $\mu$ M solution of each of the compounds was prepared and 50  $\mu$ L was pipetted into each well and allowed to diffuse through the agar before being placed in an incubator at 37 °C. Appropriate blanks containing the diluent (MeOH/ACN) were also prepared to ensure the concentration of solvent used had no effect on microbial growth.

### 4.3: Results and Discussion

#### 4.3.1: Inhibition Results

All of the compounds tested showed inhibition with differing degrees of effectiveness.

##### 4.3.1.1: Ellagic Acid $\beta$ -Lactamase Inhibition and Microbial Inhibition Results

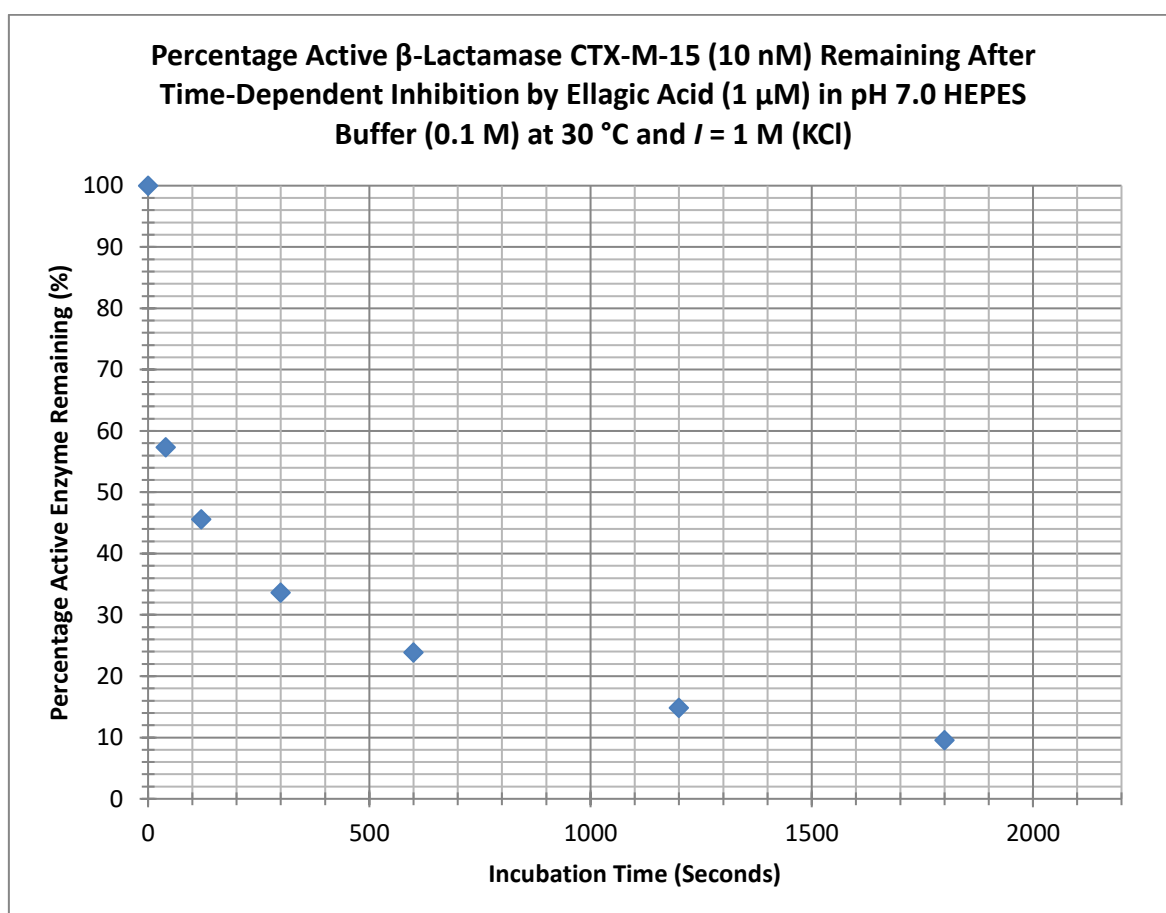


Figure 4.6: Percentage active CTX-M-15 (10 nM) remaining after incubation with ellagic acid (1  $\mu$ M).

Figure 4.6 above shows a dramatic decrease in the activity of CTX-M-15 when inhibited with 1  $\mu\text{M}$  of ellagic acid, with the activity exponentially decreasing to a negligible amount.

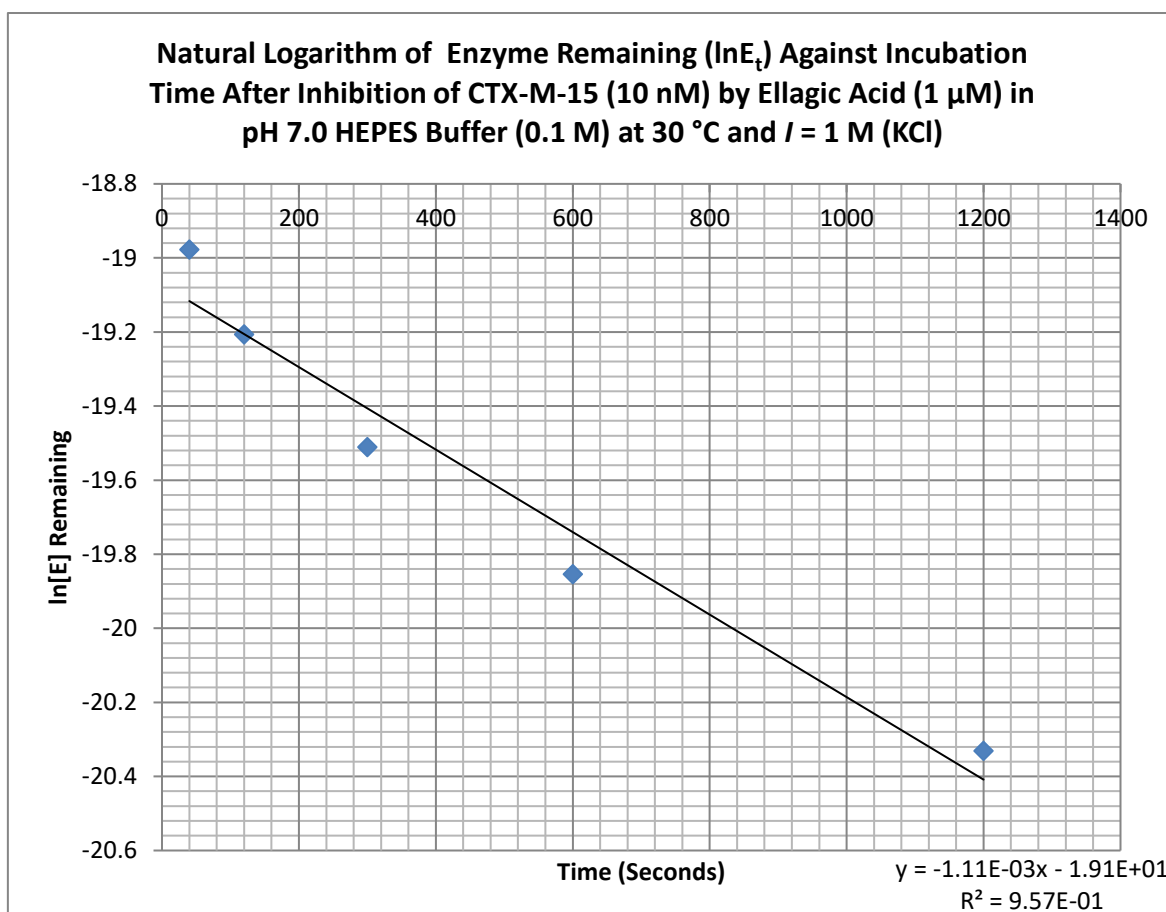


Figure 4.7: Natural logarithm of concentration of active CTX-M-15 (10 nM) enzyme remaining after inhibition with ellagic acid (1  $\mu\text{M}$ ).

Clearly, as seen from figure 4.7 above, ellagic acid has an inhibitory effect on the CTX enzyme with a  $k_{\text{obs}}$  of  $1.11 \times 10^{-3} \text{ M}^{-1}\text{s}^{-1}$ , giving a second order rate constant  $k_i = 1.11 \times 10^3 \text{ M}^{-1}\text{s}^{-1}$ . An experiment with 10-fold less ellagic acid was undertaken, with the concentration of ellagic acid being 100 nM, only 10 x the concentration of the enzyme.

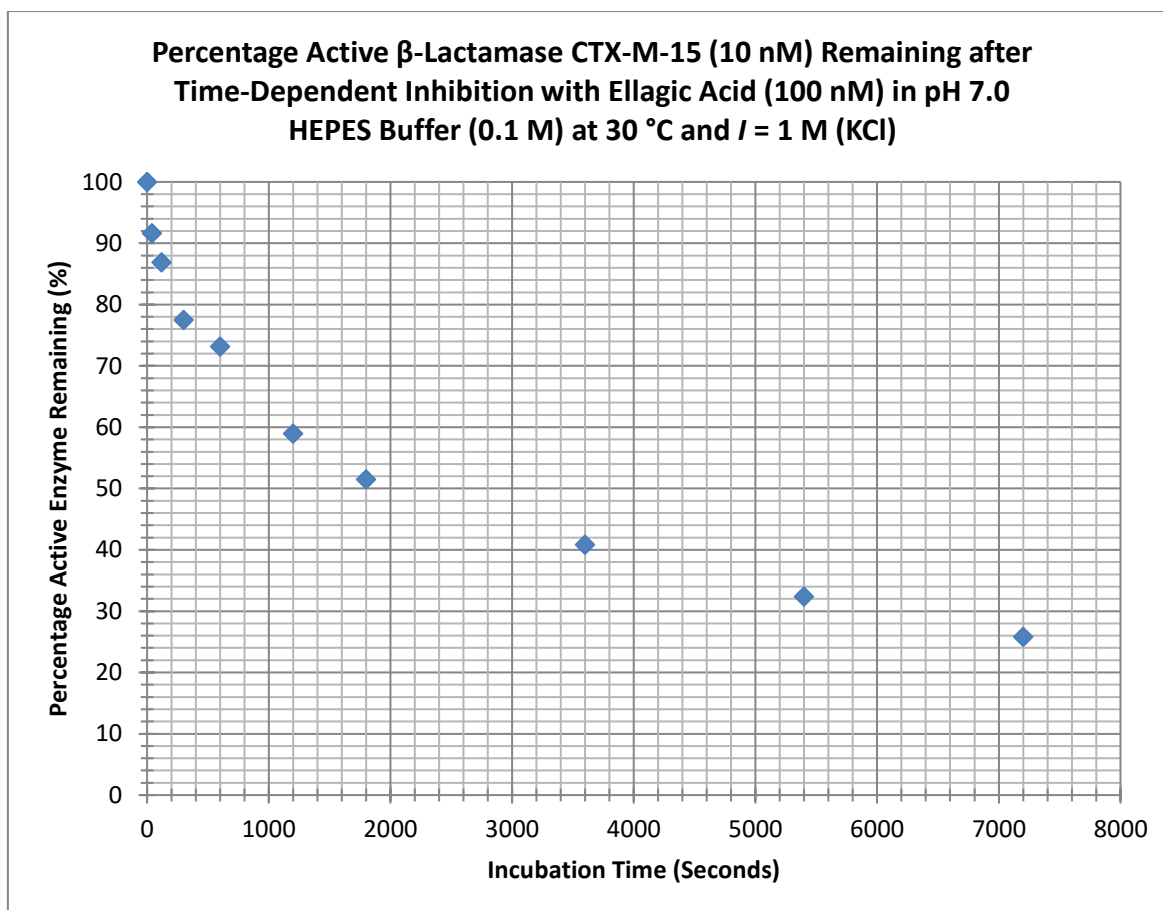


Figure 4.8: Percentage active CTX-M-15 (10 nM) remaining after incubation with ellagic acid (100 nM) at 1:10 concentration with enzyme.

Figure 4.8 above shows the activity decrease of CTX-M-15 after incubation with ellagic acid in a 1:10 concentration ratio of enzyme to inhibitor. Clearly, there is time-dependent inhibition occurring. However, the activity of the enzyme does not appear to go to zero which is perhaps indicative of an equilibrium process. The concentration of ellagic acid is 100-fold less than in the previous 10  $\mu$ M experiment.

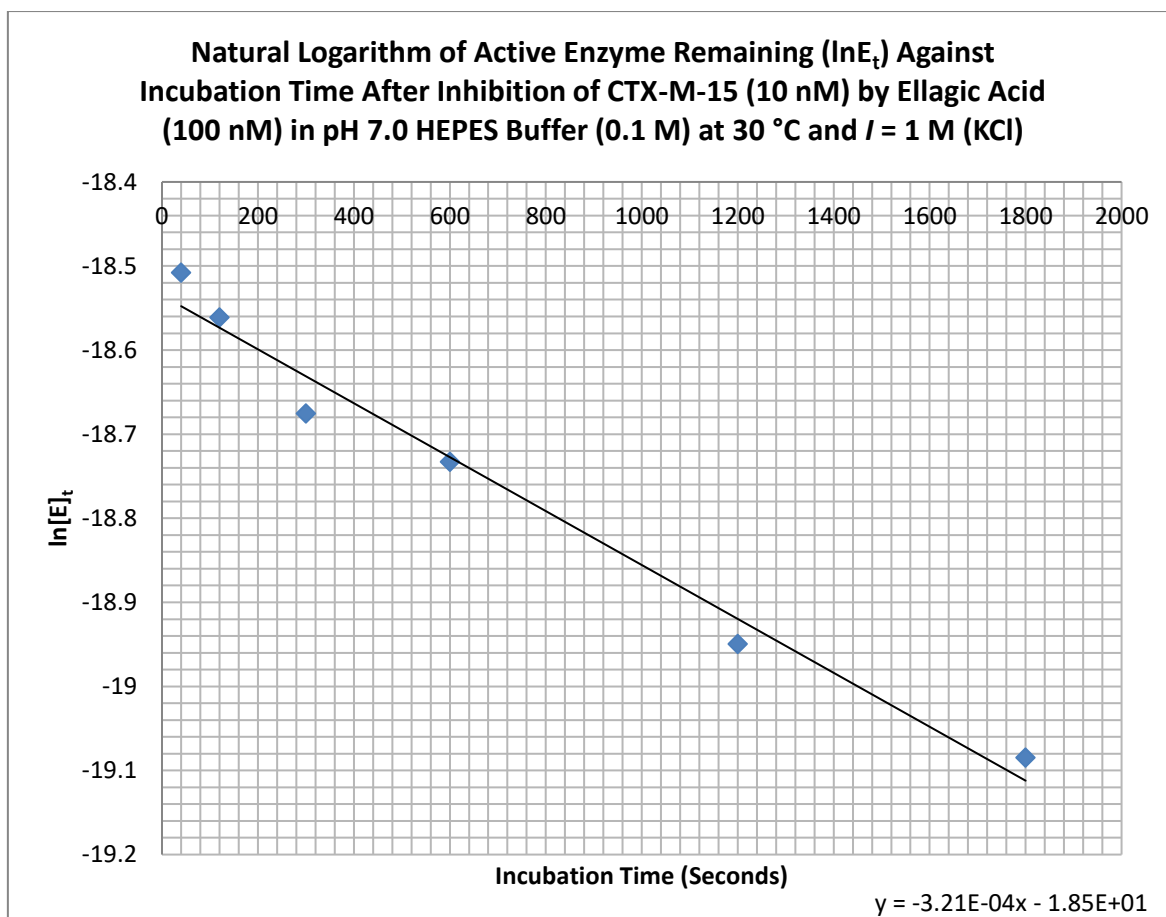


Figure 4.9: Natural logarithm of concentration active enzyme remaining against incubation time for inhibition of CTX-M-15 (10 nM) by ellagic acid (100 nM).

The loss of enzyme activity by ellagic acid gives a pseudo first-order rate  $k_{\text{obs}}$  of  $3.21 \times 10^{-4} \text{ M}^{-1}\text{s}^{-1}$ , corresponding to a second-order rate constant for inhibition  $k_i = 3.21 \times 10^3 \text{ M}^{-1}\text{s}^{-1}$ , as seen from figure 4.9 above.

At this point, appropriate enzyme blanks were ran over a similar amount of time as the inhibition experiments to ensure that it wasn't simply the CTX-M-15 losing activity over the time period of the experiment. These experiments confirmed that CTX-M-15 remained active over this time period, with a negligible loss of activity (<5 %). This showed that the enzyme activity decrease with ellagic acid must be due to the inhibitory action of ellagic acid, and not any natural loss of enzyme activity.

Finally, another way to investigate if the ellagic acid is indeed inhibiting the enzyme through a chemical reaction is to investigate the UV profile of the reaction between the ellagic acid and the enzyme. The CTX—M-15 enzyme was used at a concentration of 800 nM and ellagic acid inhibitor at a concentration of 8  $\mu$ M were incubated over a two-hour period and repeated UV scans took place. If there was a difference in the UV profile of the incubated enzyme and inhibitor over time, it was further proof that some sort of reaction was taking place.

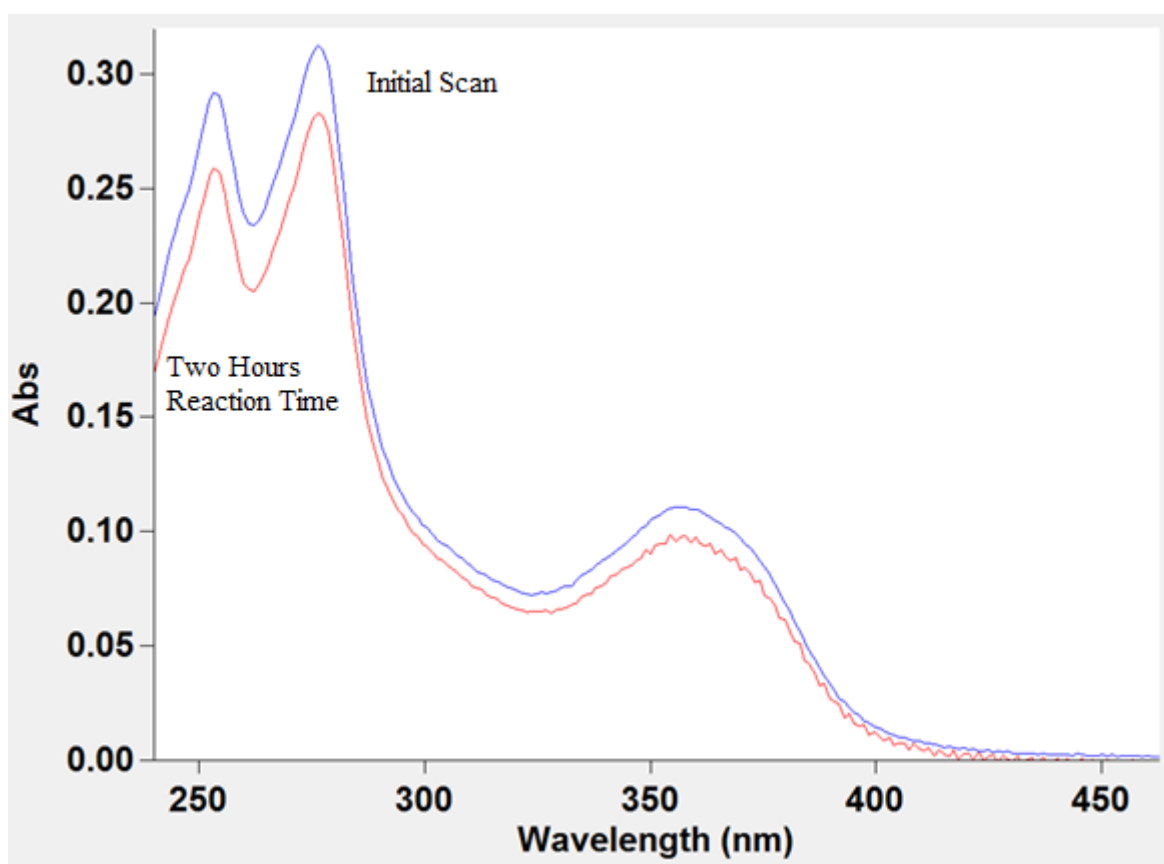


Figure 4.10: UV scans of CTX-M-15 (800 nM) and ellagic acid (8  $\mu$ M) in pH 7.0 HEPES (0.1 M) at 30  $^{\circ}$ C with  $I = 1$  M (KCl).

In figure 4.10 above, the blue spectra are the first scan of 8  $\mu$ M ellagic acid incubated with 800 nM CTX-M-15 in 0.1 M HEPES buffer with 10 % MeOH at 30  $^{\circ}$ C, and the red line is a scan after 16 hours. As can be seen, the UV profile clearly changes after this time,

indicating that some sort of reaction is taking place. At 275 nm the absorbance is roughly 0.3112, and it decreases to 0.281 after 2 hours, roughly representing a 10 % drop. The amount of enzyme compared to ellagic acid (800 nM compared to 8  $\mu$ M) is also a 1:10 ratio, so this corroborates the theory that most of the enzyme present is reacting with the ellagic acid. This is further evidence that it is the ellagic acid reacting with the enzyme in an inhibition reaction, causing the UV profile to change.

This experiment was repeated with a different SBL enzyme, TEM-1, but the concentrations of ellagic acid to enzyme were present in a 1:1 ratio.

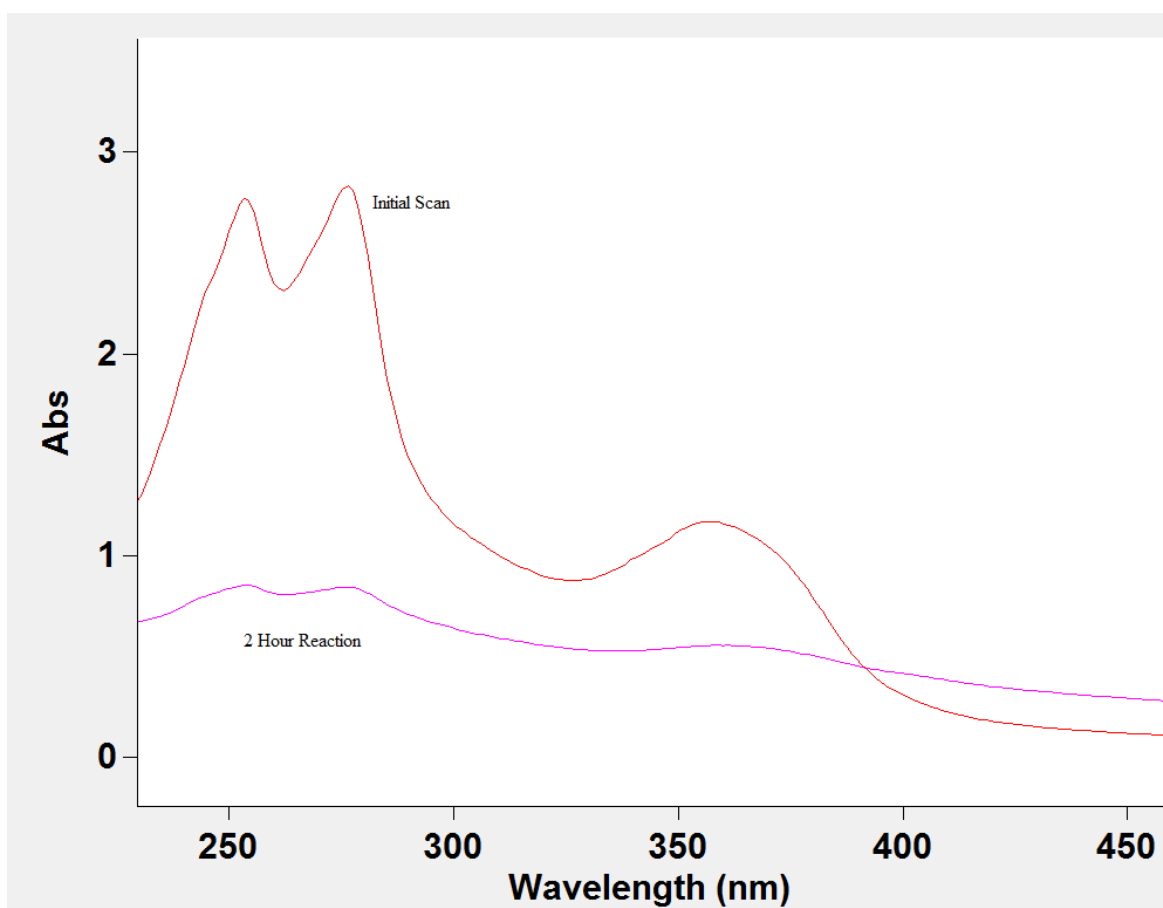


Figure 4.11: UV scans of TEM-1 (70  $\mu$ M) and ellagic acid (70  $\mu$ M) in pH 7.0 HEPES (0.1 M) at 30  $^{\circ}$ C with  $I = 1$  M (KCl).

In figure 4.11 above, the red spectrum is the initial scan and the pink spectrum is a UV scan after 2 hours reaction time. One can clearly see there is a lot more of reaction between the ellagic acid and enzyme. This is because there is a lot more enzyme present, so one would expect there to be a more dramatic change in the UV profile as more ellagic acid is reacted with by the higher concentration of enzyme. The fact that an increase in the amount of enzyme increases the change seen in the two UV spectra confirms that there is a reaction taking place between the enzyme and the ellagic acid. When taking into consideration the other inhibition results, it is beyond doubt that the ellagic acid is inhibiting the SBLs it has been tested against.

#### *4.3.1.2: Inhibition Studies with a Metallo- $\beta$ -Lactamase*

After establishing that ellagic acid showed potential as an SBL inhibitor, it was possible that it may act as an MBL inhibitor, owing to its ability to act as a chelating agent for metal ions. Ellagic acid was examined for any inhibitory activity against NDM-1 MBL up to a concentration of 10 mM, but no inhibition was recorded.

#### *4.3.1.3: pH Dependence of Inactivation of CTX-M-15 by Ellagic Acid*

The effect of pH on the inhibitory action of ellagic acid on CTX-M-15 was investigated, similar to pH dependent inhibition experiments in chapter 3. Ellagic acid has 4 ionisable groups; therefore it was necessary to establish how many of the 5 forms of ellagic acid showed inhibitory activity. Appropriate buffer solutions were prepared at various pH levels

using a calibrated pH probe, and the inhibition experiments for ellagic acid and CTX-M-15 were repeated at different pH levels over physiologically relevant levels.

The literature revealed the 4  $pK_a$ s of ellagic acid as: 6.5, 7.45, 9.61 and 11.50 (United States National Library of Medicine, 2008). Using these values, a graph showing the speciation plot of ellagic acid was constructed.

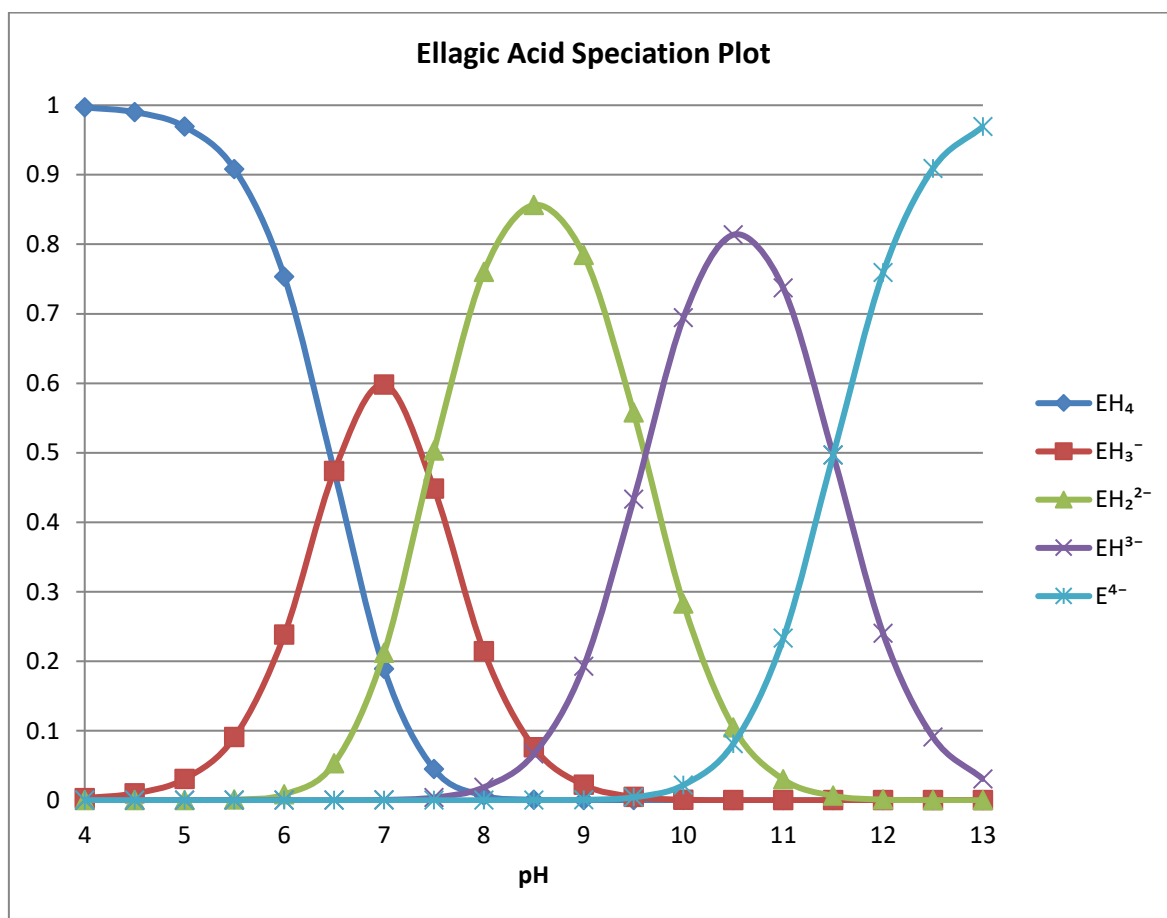


Figure 4.12: Speciation plot of ellagic acid,  $EH_4$  is the undissociated species,  $EH_3^-$ ,  $EH_2^{2-}$ ,  $EH^{3-}$  and  $E^{4-}$  are the mono-, di-, tri- and tetra-anions respectively.

The speciation plot in figure 4.12 above shows the abundance of each of the 4 ionisable forms of ellagic acid at various pH levels. The obtained  $k_i$  for the inhibition of CTX-M-15 by ellagic acid at various pH levels can be seen in figure 4.13 below.

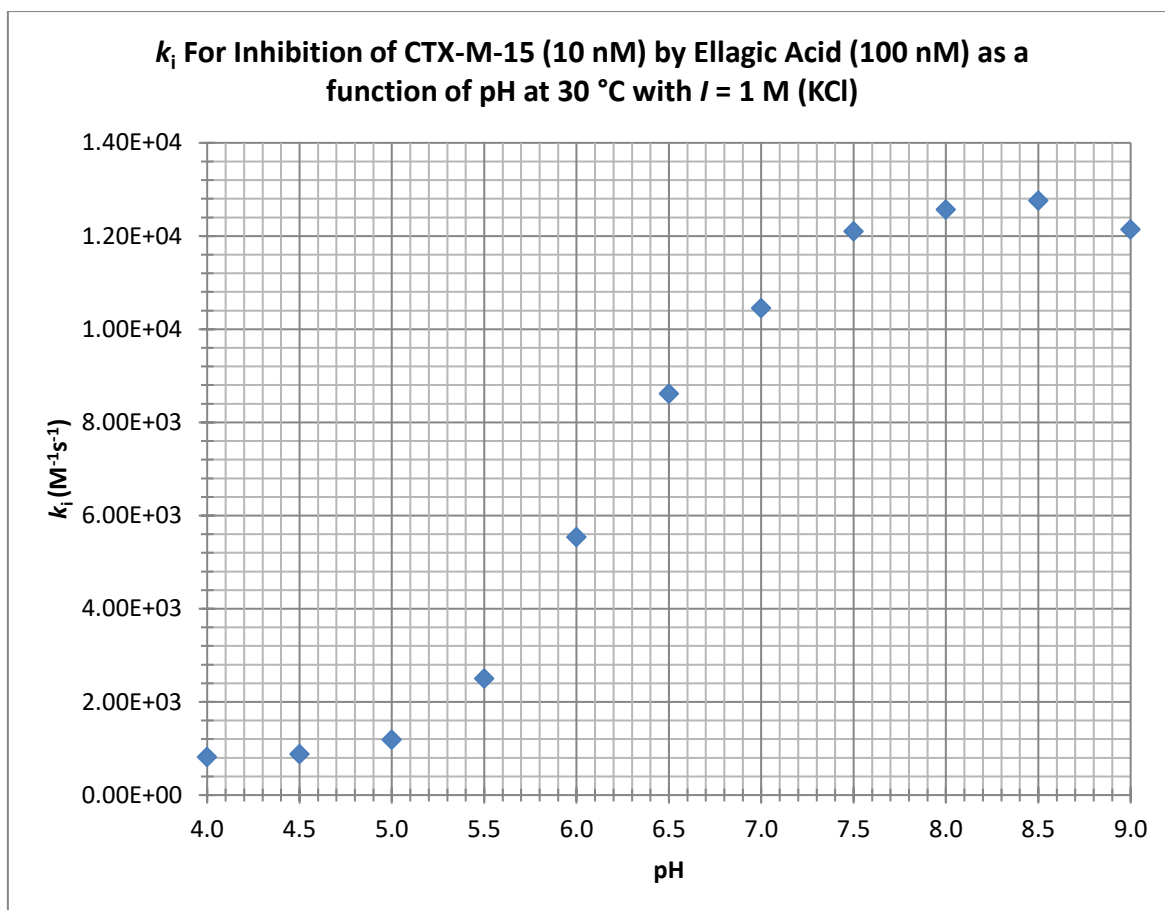


Figure 4.13:  $k_i$  for the inhibition of CTX-M-15 (10 nM) by ellagic acid (100 nM) over various pH.

This can then be superimposed over the speciation plot for ellagic acid to give an indication of the ionised forms of ellagic acid responsible for the inhibition, as seen below in figure 4.14.

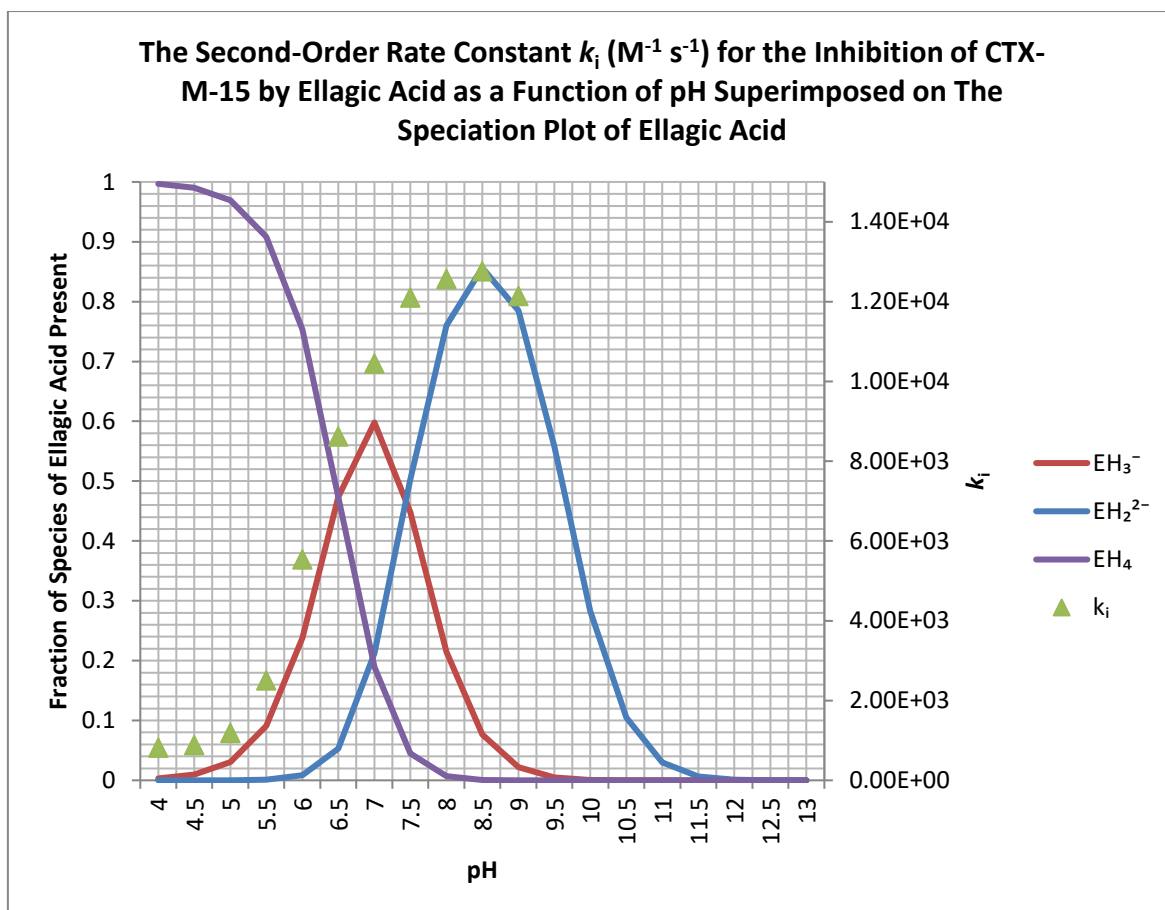


Figure 4.14: Speciation plot of ellagic acid superimposed with  $k_i$  over physiologically relevant pH levels.

The  $k_i$ s for the inhibition of CTX-M-15 by ellagic acid were recorded over physiologically relevant pH levels. It was initially intended to go above pH 9.0, but unfortunately the enzyme does not operate at these relatively extreme pH levels. As can be seen from figure 4.14 above, the  $k_i$  for the inhibition of CTX-M-15 by ellagic acid follows the emergence of the mono- and di-anions forms of ellagic acid. This indicates that ellagic acid is active as an inhibitor when it has these negative charges, and some deprotonation of the molecule is required for it to be able to inhibit with the serine active site of CTX-M-15. The requirement for a negative charge on the inhibitor is compatible with that for substrates and reflects the interaction with a positively charged residue (Lys-240) on the enzyme.

Using the fundamentals of the Henderson-Hasselbach equation and the data available in the speciation plot, one can determine the fraction of the specific ion of ellagic acid present at a specific pH. For example, at pH 6.0, the following is true for  $\text{EH}_3^-$ :

$$\frac{Ka}{H^+ + Ka} \frac{10^{-6.5}}{10^{-6.0} + 10^{-6.5}} = \frac{0.316 \times 10^{-6}}{1.316 \times 10^{-6}} = 0.24 \times 100 = 24 \%$$

Therefore, at pH 6.0 the amount of ellagic acid present is 24 % in the  $\text{EH}_3^-$  form. This calculation can be repeated for the other ionic forms at other pH levels.

The approximate values of the second-order rate constants for the anionic species can be estimated from:

$$k_i^{\text{tot}} = k_i^{\text{EH}_3^-} + k_i^{\text{EH}_2^{2-}}$$

At pH 6.0 there is 'no'  $\text{EH}_2^{2-}$  but 24 %  $\text{EH}_3^-$ :

$$k_i^{\text{tot}} = 5.6 \times 10^3 = 0.24 k_i^{\text{EH}_3^-}$$

Therefore,  $k_i^{\text{EH}_3^-} = 2.33 \times 10^4 \text{ M}^{-1}\text{s}^{-1}$

At pH 7.5  $k_i^{\text{tot}} = 1.20 \times 10^4 \text{ M}^{-1}\text{s}^{-1}$  and the fraction of  $\text{EH}_2^{2-}$  present is 0.5 (50 %) whilst the fraction of  $\text{EH}_3^-$  present is 0.45 (45 %).

$$k_i^{\text{tot}} = 1.20 \times 10^4 = 0.45 \times 2.33 \times 10^4 + 0.5 k_i^{\text{EH}_2^{2-}}$$

$$1.20 \times 10^4 - 1.05 \times 10^4 = 0.5 k_i^{\text{EH}_2^{2-}}$$

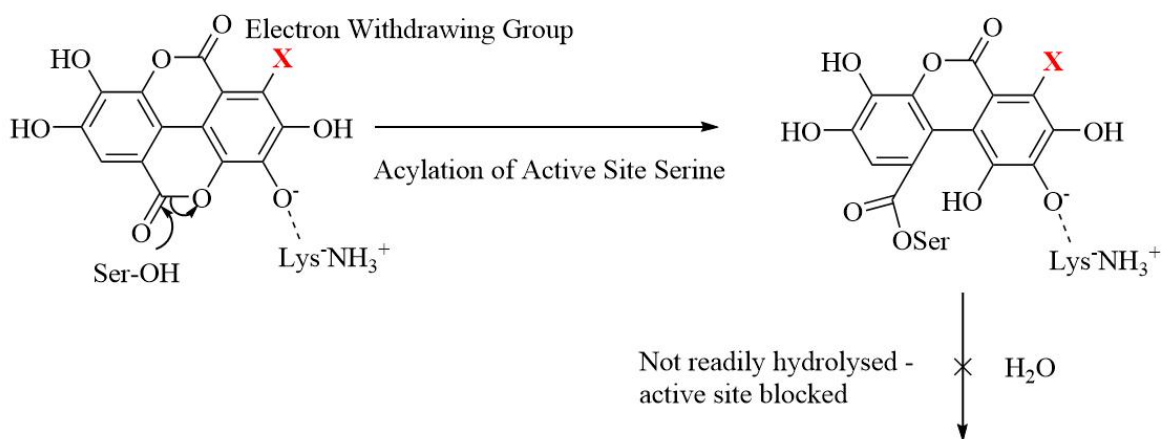
$$k_i^{\text{EH}_2^{2-}} = 0.30 \times 10^4 \text{ M}^{-1}\text{s}^{-1}$$

$$k_i^{\text{EH}_2^{2-}} = 3.0 \times 10^3 \text{ M}^{-1}\text{s}^{-1}$$

Therefore, the mono-anionic species is almost 10-fold a better inhibitor than the di-anionic ellagic acid.

It appears that both the mono and di-anionic species of ellagic acid are effective inhibitors.

It would be useful to study the effectiveness of ellagic acid with an electron-withdrawing group para to the departing phenol group to improve the rate of acylation:



Possible electron withdrawing groups could be -NO<sub>2</sub> or -F.

#### 4.3.1.4 Urolithin A Inhibition Results

Urolithin A was tested for any  $\beta$ -lactamase inhibitory activity. As can be seen from figure 4.15 below, Urolithin A only had very modest inhibitory activity against CTX-M-15, and as such does not represent a good candidate for future novel inhibitor development.

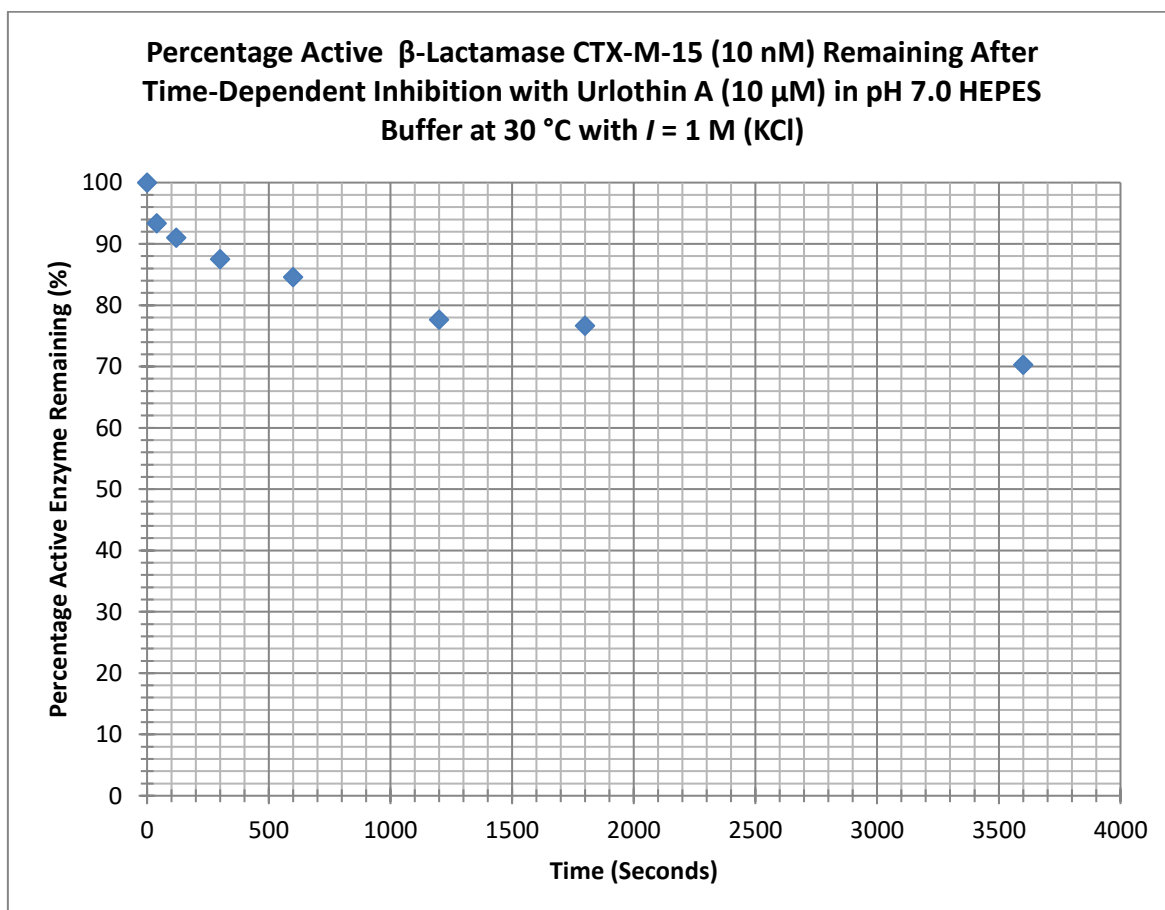


Figure 4.15: Percentage active CTX-M-15 (10 nM) remaining after incubation with urolithin A (10  $\mu$ M).

When one considers the structure of urolithin A (as seen again in figure 4.16 below), it is perhaps unsurprising that it has a lower inhibitory activity than that of ellagic acid. Specifically, the  $pK_a$  of the phenols will give ellagic acid a higher value than that of urolithin A, which also means that the phenols will not be ionised, meaning that inhibition will be less likely to occur. Also, there is not the correct geometrical relationship between the

carbonyl group and the phenol to bind well to the active site of the  $\beta$ -lactamase enzyme, which means you will not be able to achieve the same binding shown by ellagic acid.

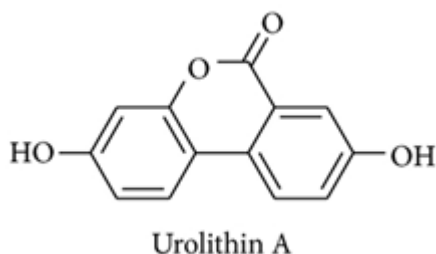


Figure 4.16: Structure of urolithin A.

#### *4.3.1.5: Orlistat Inhibition Results*

The inhibitory effects of orlistat against SBL CTX-M-15 were investigated, in much the same way as ellagic acid. Orlistat (as seen in figure 4.17 below) is a lipophilic molecule with limited solubility however the solubility of orlistat was determined and was found to be soluble in a 10 % solution of ACN in pH 7.0 HEPES (0.1 M) buffer solution. Appropriate blanks were run with CTX-M-15 in this solution to ensure the added ACN had no effect on enzyme activity.

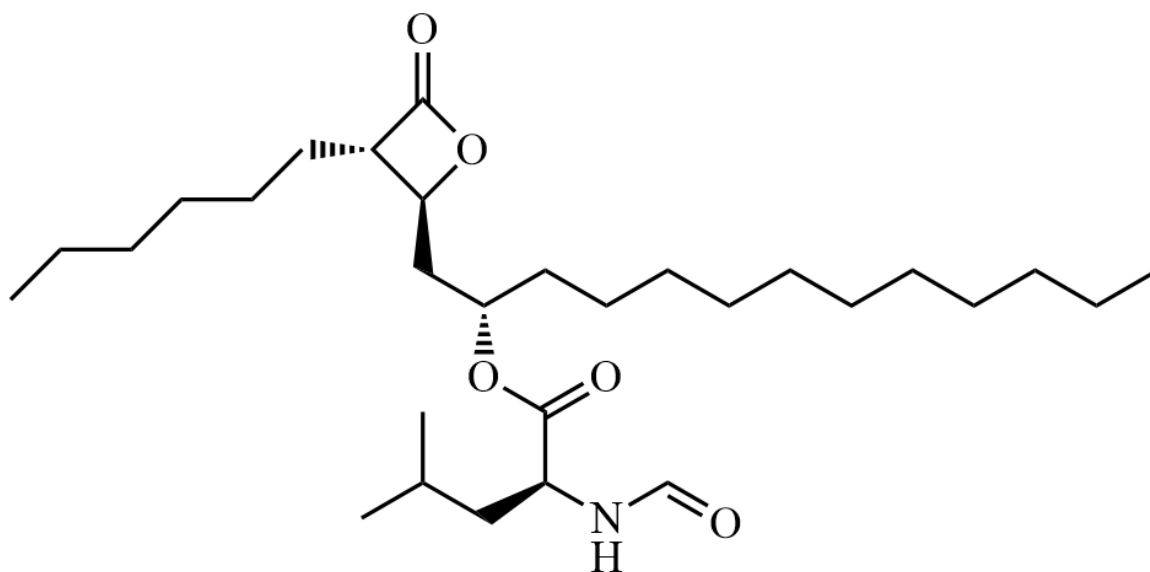


Figure 4.17: Chemical structure of orlistat.

There was negligible loss in enzyme activity over 30 minutes for CTX-M-15 in the 10 % ACN buffer solution. This means that any loss of activity in the actual experiments must be due to the actions of orlistat behaving as an inhibitor. Orlistat was found to be a weak inhibitor of CTX-M-15, as can be seen in figure 4.18 below.

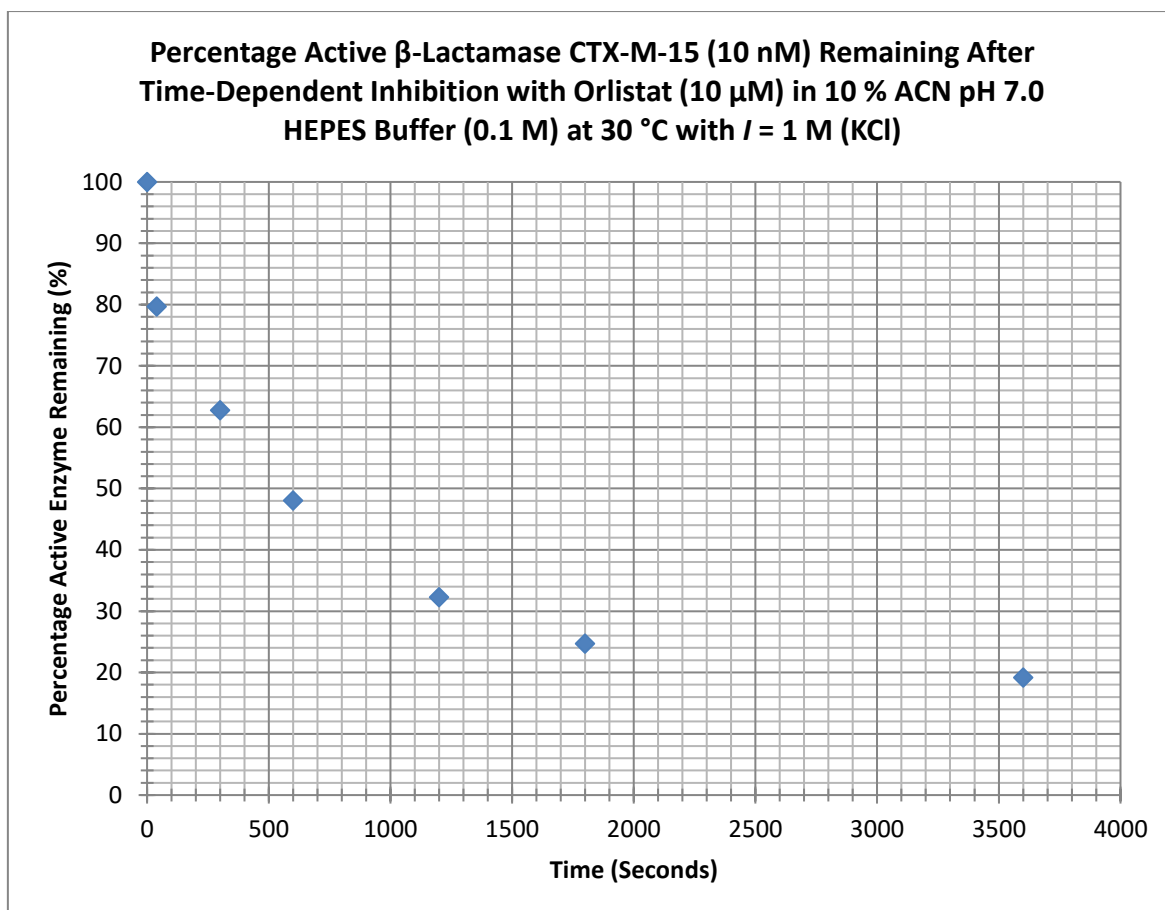


Figure 4.18: Percentage active CTX-M-15 (10 nM) remaining after incubation with orlistat (10  $\mu$ M).

10  $\mu$ M was the lowest concentration at which a reasonable amount of inhibition was noticed, making orlistat a weak inhibitor of CTX-M-15. The pseudo first-order rate constant from figure 4.18 was  $k_{\text{obs}} 7.73 \times 10^{-4} \text{s}^{-1}$  corresponding to a second-order rate constant of  $77.3 \text{ M}^{-1} \text{s}^{-1}$ .

To help confirm that orlistat was indeed acting as an inhibitor, the experiments were repeated but with a much higher concentration of orlistat. If orlistat was acting as an inhibitor, there should be a lower amount of active enzyme over the same time period as in the 10  $\mu$ M experiment.

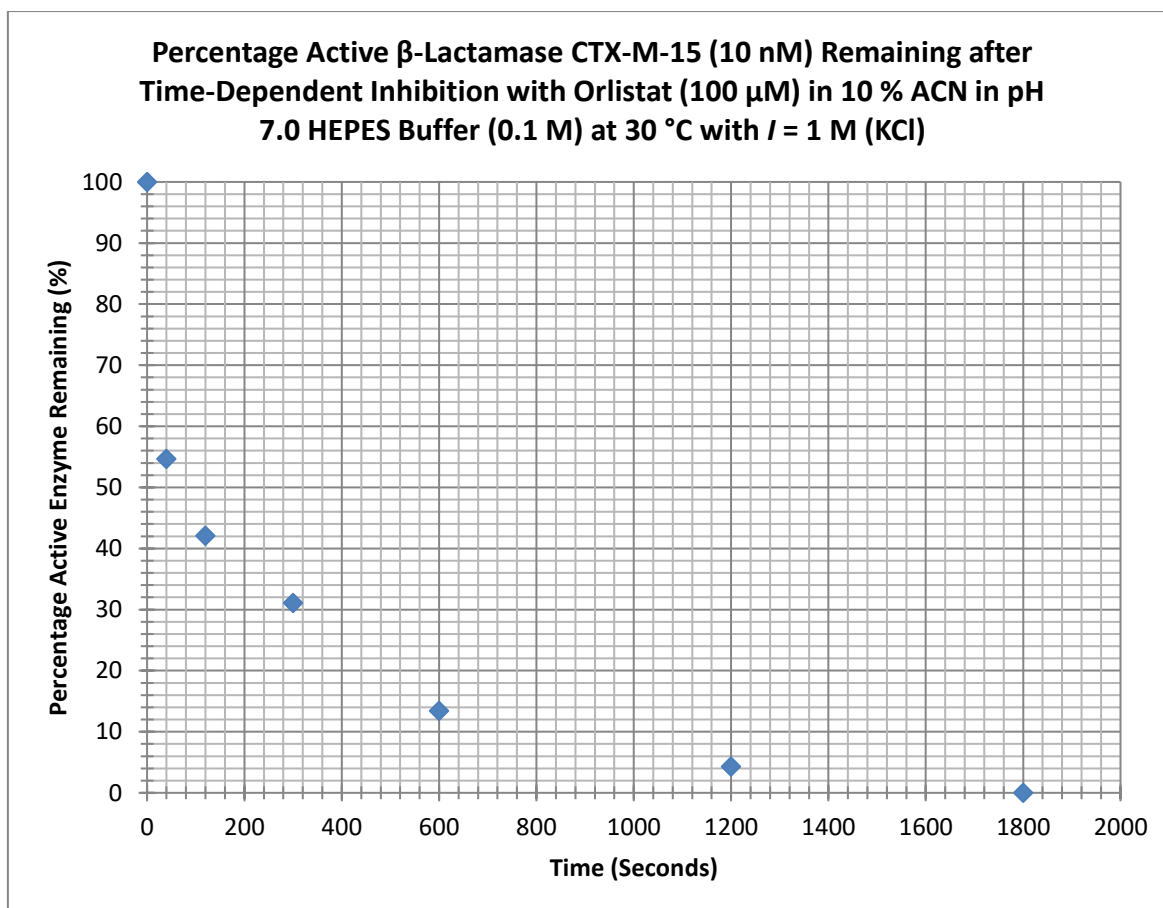


Figure 4.19: Percentage active CTX-M-15 (10 nM) remaining after incubation with orlistat (100  $\mu$ M).

As can be seen from figure 4.19 above, there is much more inhibition than the 10  $\mu$ M sample, this data gives a  $k_{\text{obs}} = 5.35 \times 10^{-3} \text{ s}^{-1}$ , corresponding to a second-order rate constant = 53.5  $\text{M}^{-1} \text{ s}^{-1}$ , which is in reasonably good agreement with 10  $\mu$ M data and confirmed the inhibition was due to orlistat.

### 4.3.2: Microbial Inhibition by Ellagic Acid

As discussed in the introduction to this chapter, polyphenols and ellagic acid in particular have received attention owing to their ability to inhibit microbial pathogens. To qualitatively investigate this, various plates of pathogenic bacteria, some capable of producing  $\beta$ -lactamases, were prepared according to the methods section. The results can be seen in figures 4.20-4.22 below.

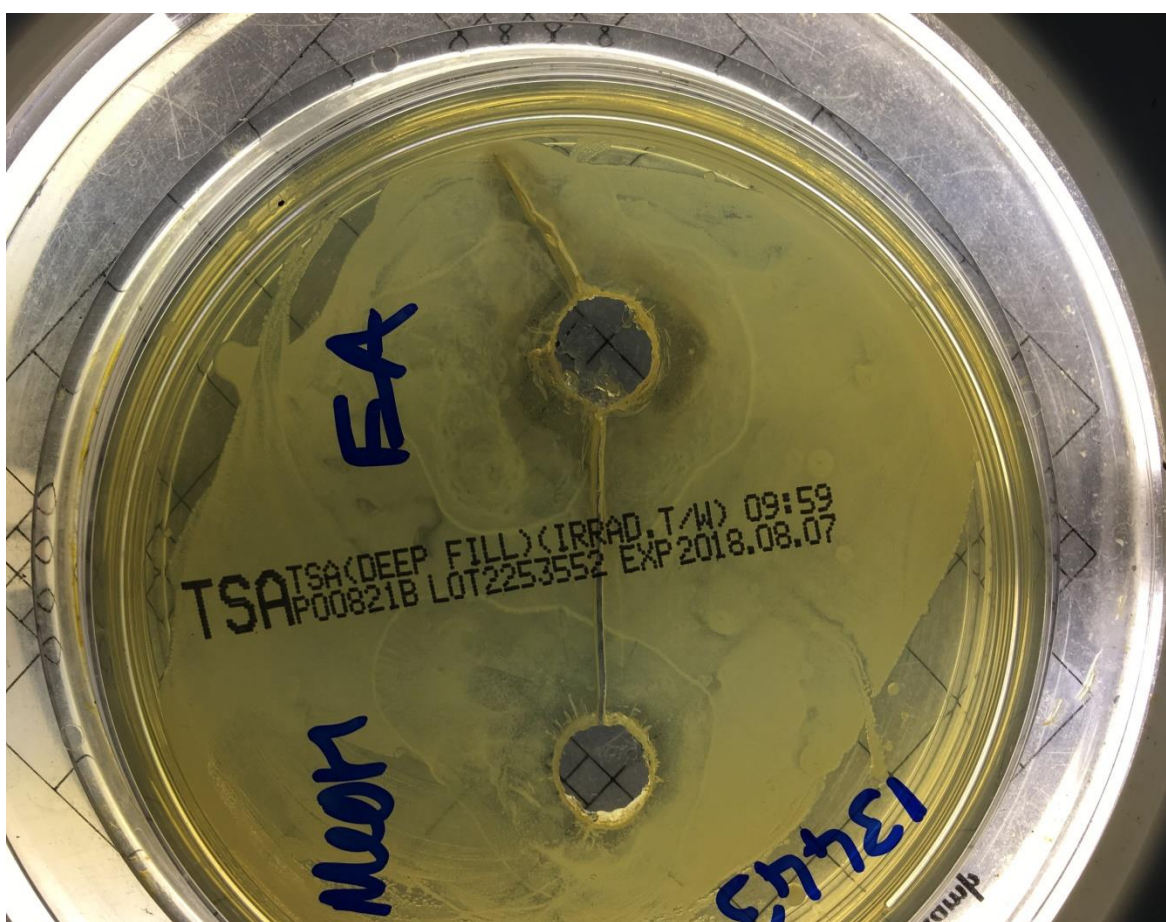


Figure 4.20: Inhibition of *Klebsiella pneumoniae* NCTC 13443 by ellagic acid with a MeOH blank.

As can be seen from figure 4.20 above, there is a clear inhibition zone around the ellagic acid (EA) well. *Klebsiella pneumoniae* is also an NDM-1 metallo- $\beta$ -lactamase producing

microbe. It is of therefore significant clinical interest if ellagic acid is capable of both SBL enzymes and MBL producing bacteria, perhaps representing a potential future treatment development option for infections SBL/MBL producing microbes.



Figure 4.21: Inhibition of *Escherichia coli* NCTC 13476 by ellagic acid.

As can be seen in figure 4.21 above, there is a clear area of inhibition around the ellagic acid well in the agar plate. *Escherichia coli* NCTC 13476 is also an MBL producing microbe, producing Imipenemase (IMP). The fact that ellagic acid is capable of inhibiting growth of this microbe along with *Klebsiella pneumoniae* 13476 (also an MBL producing microbe) is further proof that ellagic acid is capable of inhibiting growth of problematic Gram negative MBL producing bacteria and warrants further research as a potential treatment of infections caused by MBL producing bacteria.

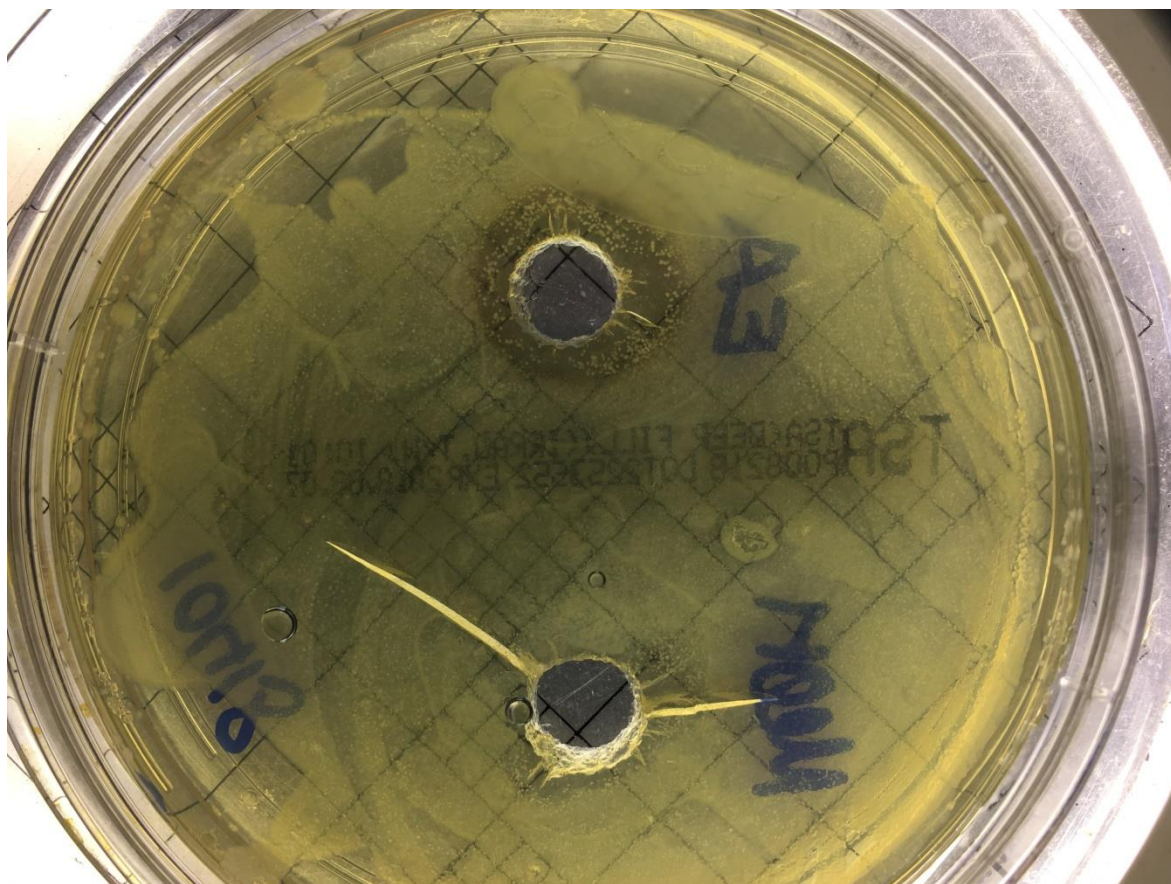


Figure 4.22: Inhibition of *Escherichia coli* NCTC 10418 by ellagic acid.

Finally, ellagic acid was tested for its inhibition against *Escherichia coli* NCTC 10418, which is a non- $\beta$ -lactamase producing bacteria. As can be seen from figure 4.22 above, ellagic acid also had inhibitory activity against this pathogen. Urolithin A and orlistat were also assessed for their microbial inhibitory activity, but unfortunately possessed no antibiotic ability.

#### 4.4: Chapter Four Conclusion

Three novel inhibitors of SBLs have been identified and their effectiveness as inhibitors has been determined. Ellagic acid, a plant polyphenol, urolithin A, a plant metabolite and orlistat, an existing dietary lipase inhibitor used as a weight loss aid. Out of the three novel inhibitors, ellagic acid showed the most promise for future development as a  $\beta$ -lactamase inhibitor. It was shown that the mono-anionic species of ellagic acid was the most effective. Whilst urolithin A and orlistat also showed SBL inhibitory action, urolithin A only exhibited very modest activity, whilst orlistat was a more effective inhibitor. This is perhaps not too surprising, as digestive lipase enzymes are known to have a serine in their active site, as do SBL enzymes (Ranjbar, Zibae & Sendi, 2014), (Rouseel et al., 1999), (Chater, Wilcox, Houghton & Pearson, 2015). Table 4.1 below summarises the inhibitors and the calculated  $k_i$ s.

Table 4.1: Summary of calculated  $k_i$ s for the novel inhibitors discussed in chapter 4.

Inhibitor	$k_i$ ( $M^{-1}s^{-1}$ )
Ellagic Acid Mono-Anion	$2.33 \times 10^4$
Ellagic Acid Di-Anion	$3.00 \times 10^3$
Urolithin A	<20
Orlistat	65.4

Ellagic acid was not only the most effective inhibitor, it also showed effectiveness at inhibiting several problematic Gram-negative pathogens, including MBL producing *Klebsiella pneumoniae* and *Escherichia coli*. *Enterobacteriaceae* such as these pathogens are associated with increased morbidity and mortality worldwide (Zowawi, Balkhy, Walsh

& Paterson, 2013), (Babu, Visweswaraiah & Kumar, 2014). Therefore, ellagic acid represents an interesting, novel antimicrobial agent, which is capable of inhibiting SBLs and also inhibiting MBL producing bacteria.

Further work was concluded on ellagic acid, investigating the effect of pH on the inhibitory actions against CTX-M-15. The outcomes of this work suggest that out of the 4 ionisable forms of ellagic acid, only two are effective as SBL inhibitors. Future work with ellagic acid could include nitrating the molecule to further its effectiveness as an SBL inhibitor.

#### 4.5: Chapter Four References

Babu, K.V.Y., Visweswaraiah, D.S., & Kumar, A. (2014). The influence of Imipenem resistant metallo-beta-lactamase positive and negative *Pseudomonas aeruginosa* nosocomial infections on mortality and morbidity. *Journal of Natural Science, Biology and Medicine*, 5 (2), 345-351. doi: 10.4103/0976-9668.136181.

Beart, J.E., Lilley, T.H., & Haslam, E. (1985). Plant polyphenols - secondary metabolism and chemical defence: Some observations. *Phytochemistry*, 24 (1), 33-38. doi: 10.1016/S0031-9422(00)80802-X.

Biolonska, D., Kasimsetty, S.G., Khan, S.I., & Ferreira, D. (2009). Urolithins, Intestinal Microbial Metabolites of Pomegranate Ellagitannins, Exhibit Potent Antioxidant Activity in a Cell-Based Assay. *Journal of Agricultural and Food Chemistry*, 57 (21), 10181-10186. doi: 10.1021/jf9025794.

Brumlik, M.J. & Buckley, J.T. (1996). Identification of the catalytic triad of the lipase/acetyltransferase from *Aeromonas hydrophila*. *Journal of Bacteriology*, 178 (7), 2060-2064. Retrieved from <https://www.ncbi.nlm.nih.gov/pmc/articles/PMC177905/>.

Cerda, B., Llorach, R., Ceron, J.J., Espin, J.C., & Tomas, F.A. (2003). Evaluation of the bioavailability and metabolism in the rat of punicalagin, an antioxidant polyphenol from pomegranate juice. *European Journal of Nutrition*, 42 (1), 18-28. doi: 10.1007/s00394-003-0396-4.

Chang, S.C. & Yang, W.V. (2016). Hyperglycemia, tumorigenesis, and chronic inflammation. *Critical Reviews in Oncology/Hematology*, 108 (1), 146-153. doi: 10.1016/j.critrevonc.2016.11.003.

Chater, P.I., Wilcox, M.D., Houghton, D., & Pearson, J.P. (2015). The role of seaweed bioactives in the control of digestion: implications for obesity treatments. *Food & Function*, 6 (11), 3420-3427. doi: 10.1039/C5FO00293A.

Coppo, E. & Marchese, A. (2014). Antibacterial Activity of Polyphenols. *Current Pharmaceutical Biotechnology*, 15 (4), 380-390. doi: 10.2174/138920101504140825121142.

Corbett, S., Daniel, J., Drayton, R., Field, M., Steinhardt, R., & Garrett, N. (2010). Evaluation of the Anti-Inflammatory Effects of Ellagic Acid. *American Society of Peri Anesthesia Nurses*, 25 (4), 214-220. doi: 10.1016/j.jopan.2010.05.011.

Daglia, M. (2012). Polyphenols as antimicrobial agents. *Current Opinion in Biotechnology*, 23 (1), 174-181. doi: 10.1016/j.copbio.2011.08.007.

Dai, J. & Mumper, R.J. (2010). Plant Phenolics: Extraction, Analysis and Their Antioxidant and Anticancer Properties. *Molecules*, 1 (10), 7313-7352. doi: 10.3390/molecules15107313.

De, R., Sarkar, A., Ghosh, P., Ganguly, M., Karmakar, B.C., Saha, D.R. ... Mukhopadhyay, A.K. (2018). Antimicrobial activity of ellagic acid against *Helicobacter pylori* isolates from India and during infections in mice. *Journal of Antimicrobial Chemotherapy*, 73 (6), 1595-1603. doi: 10.1093/jac/dky079.

Dixon, R.A., Xie, D.Y., & Sharma, S.B. (2005). Proanthocyanidins - a final frontier in flavonoid research?. *New Phytologist*, 165 (1), 9-28. doi: 10.1111/j.1469-8137.2004.01217.x.

Drew, B.S., Dixon, A.F., & Dixon, J.B. (2007). Obesity management: Update on orlistat. *Vascular Health and Risk Management*, 3 (6), 817-821. Retrieved from <https://www.ncbi.nlm.nih.gov/pmc/articles/PMC2350121/>.

Espin, J.C., Larrosa, M., Conesa, M.T.G., & Barberan, F.T. (2013). Biological Significance of Urolithins, the Gut Microbial Ellagic Acid-Derived Metabolites: The Evidence So Far. *Evidence Based Complementary and Alternative Medicine*, 2013 (1), 1-15. doi: 10.1155/2013/270418.

Fava, C. & Montagnana, M. (2018). Atherosclerosis is and Inflammatory Disease which Lacks a Common Anti-inflammatory Therapy: How Human Genetics Can Help to Solve This Issue. A Narrative Review. *Frontiers in Pharmacology*, 9 (55), 1-9. doi: 10.3389/fphar.2018.00055.

Favarin, D.C., Teixeira, M.M., Andrade, E.L.D., Alves, C.D.F., Chica, J.E.L., Sorgi, C.A. ... Rogerio, A.P. (2013). Anti-Inflammatory of Effects of Ellagic Acid on Acute Lung Injury Induced by Acid in Mice. *Mediators of Inflammation*, 2013 (1), 1-13. doi: 10.1155/2013/164202.

Gal, Z.S., Koncz, A., Szabo, I., Deak, E., Benko, I., Barabas, G.Y. ... Kovacs, P. (2000). A Synthetic  $\gamma$ -Lactone Group with  $\beta$ -Lactamase Inhibitory and Sporulation Initiation Effects. *Journal of Chemotherapy*, 12 (4), 274-279. doi: 10.1179/joc.2000.12.4.274.

Garn, H., Bahn, S., Baune, B.T., Binder, E.B., Bisgaard, H., Chatila, T.A. ... Renz, H. (2016). Current concepts in chronic inflammatory diseases: Interactions between microbes, cellular metabolism and inflammation. *The Journal of Allergy and Clinical Immunology*, 138 (1), 47-56. doi: 10.1016/j.jaci.2016.02.046.

Ghudhaib, K.K., Hanna, E.R., & Jawad, A.H. (2010). Effect of Ellagic Acid on Some Types of Pathogenic Bacteria. *Journal of Al-Nahrain University*, 13 (2), 79-85. Retrieved from <http://www.jnus.org/pdf/1/2010/1/517.pdf>.

Giminez-Bastida, J.A., Gonzalez-Sarrias, A., Larrosa, M., Tomas-Barberan, F., Espin, J.C., & Garcia-Conesa, M.T. (2012). Ellagitannin metabolites, urolithin A glucuronide and its aglycone urolithin A, ameliorate TNF- $\alpha$ -induced inflammation and associated molecular markers in human aortic endothelial cells.. *Molecular Nutrition and Food Research*, 56 (5), 784-796. doi: 10.1002/mnfr.201100677.

Glisan, S., Sae-Tan, S., Grove, K., Yennawar, N., & Lambert, J. (2014). Inhibition of digestive enzymes by tea polyphenols: enzymological and in silico studies. *Federation of American Societies for Experimental Biology*, 28(1), 1-1. Retrieved from [https://www.fasebj.org/doi/abs/10.1096/fasebj.28.1\\_supplement.1045.34](https://www.fasebj.org/doi/abs/10.1096/fasebj.28.1_supplement.1045.34).

Gonzalez, A.I.M., Parrilla, E.A., Sanchez, A.G.D., de la Rosa, L.A., Gastelum, J.A.N., Flores, A.A.V., & Aguilar, G.A.G. (2017). In vitro Inhibition of Pancreatic Lipase by Polyphenols: A Kinetic, Fluorescence Spectroscopy and Molecular Docking Study. *Food Technology and Biotechnology*, 55 (4), 519-530. doi: 10.17113/ftb.55.04.17.5138.

Gonzalez, C.S., Ciudad, C.J., Pulido, M.I., & Noe, V. (2016). Urolithin A causes p21 up-regulation in prostate cancer cells. *European Journal of Nutrition*, 55 (3), 1099-1112. doi: 0.1007/s00394-015-0924-z.

Gu, Y., Hurst, W.J., Stuart, D.A., & Lambert, J.D. (2011). Inhibition of Key Digestive Enzymes by Cocoa Extracts and Procyanidins. *Journal of Agricultural and Food Chemistry*, 59 (10), 5305-5311. doi: 10.1021/jf200180n.

Haghjoo, B., Lee, L.H., Habiba, U., Tahir, H., Olabi, M., & Chu, T.C. (2013). The synergistic effect of green tea polyphenols and antibiotics against potential pathogens. *Scientific Research*, 4 (11), 959-967. doi: 0.4236/abb.2013.411127.

Heber, D. (2008). Multitargeted therapy of cancer by ellagitannins. *Cancer Letters*, 269 (2), 262-268. doi: 10.1016/j.canlet.2008.03.043.

Heck, A.M., Yanovski, J.A., & Calis, K.A. (2012). Orlistat, a new lipase inhibitor for the management of obesity. *Pharmacotherapy*, 20 (3), 270-279. doi: 10.1592/phco.20.4.270.34882.

Heinonen, M. (2007). Antioxidant activity and antimicrobial effect of berry phenolics - a Finnish perspective. *Molecular Nutrition and Food Research*, 51 (1), 684-691. doi: 10.1002/mnfr.200700006.

Hirasawa, M. & Takada, K. (2004). Multiple effects of green tea catechin on the antifungal activity of antimycotics against *Candida albicans*. *Journal of Antimicrobial Chemotherapy*, 53 (2), 225-229. doi: 10.1093/jac/dkh046.

Ho, H.Y., Cheng, M.L., Weng, S.F., Leu, Y.L., & Chiu, D.T.Y. (2009). Antiviral Effect of Epigallocatechin Gallate on Enterovirus 71. *Journal of Agricultural and Food Chemistry*, 57 (14), 6140-6147. doi: 10.1021/jf901128u.

Jayaraman, P., Sakharkar, M.K., Lim, C.S., Tang, T.H., & Sakharkar, K.R. (2010). Activity and interactions of antibiotic and phytochemical combinations against *Pseudomonas aeruginosa* in vitro. *International Journal of Biological Sciences*, 6 (6), 556-568. doi: 10.7150/ijbs.6.556.

Kallioski, T., Kramer, C., Vulpetti, A., & Gedeck, P. (2013). Comparability of Mixed IC50 Data - A Statistical Analysis. *Public Library of Science*, 8 (4), 1-12. doi: 10.1371/journal.pone.0061007.

Kang, I., Buckner, T., Shay, N.F., Gu, L., & Chung, S. (2016). Improvements in Metabolic Health with Consumption of Ellagic Acid and Subsequent Conversion into Urolithins: Evidence and Mechanisms. *Advances in Nutrition*, 7(5), 961-972. doi: 10.3945/an.116.012575.

Kim, J.M., Kim, J.S., Jung, H.C., Kim, N., Kim, Y.J., & Song, I.S. (2004). Distribution of Antibiotic MICs for *Helicobacter Pylori* Strains over a 16-Year Period in Patients from Seoul, South Korea. *Antimicrobial Agents and Chemotherapy*, 48 (12), 4843-4847. doi: 10.1128/AAC.48.12.4843-4847.2004.

Koh, T.J. & DiPietro, L.A. (2011). Inflammation and wound healing: the role of the macrophage. *Expert Reviews in Molecular Medicine*, 13 (23), 1-14. doi: 10.1017/S1462399411001943.

Kridel, S.J., Axelrod, F., Rozenkrantz, N., & Smith, J.W. (2004). Orlistat is a Novel Inhibitor of Fatty Acid Synthase with Antitumor Activity. *Cancer Research*, 64 (1), 2070-2075. Retrieved from <http://cancerres.aacrjournals.org/content/canres/64/6/2070.full.pdf>.

Landen, N.X., Li, D., & Stahle, M. (2016). Transition from inflammation to proliferation: a critical step during wound healing. *Cellular and Molecular Life Sciences*, 73 (20), 3861-3885. doi: 10.1007/s00018-016-2268-0.

Landete, J.M. (2011). Ellagitannins, ellagic acid and their derived metabolites: A review about source, metabolism, functions and health. *Food Research International*, 44 (5), 1150-1160. doi: 10.1016/j.foodres.2011.04.027.

Liberal, J., Carmo, A., Gomes, C., Cruz, M.T., & Batista, M.T. (2017). Urolithins impair cell proliferation, arrest the cell cycle and induce apoptosis in UMUC3 bladder cancer cells. *Investigational New Drugs*, 35 (6), 671-681. Retrieved from <https://link.springer.com/article/10.1007%2Fs10637-017-0483-7>.

Lobo, V., Patil, A., Phatak, A., & Chandra, N. (2010). Free radicals, antioxidants and functional foods: Impact on human health. *Pharmacognosy Review*, 4 (8), 118-126. doi: 10.4103/0973-7847.70902.

McDougall, G.J. & Stewart, D. (2008). The inhibitory effects of berry polyphenols on digestive enzymes. *Biofactors*, 23 (4), 189-195. doi: 10.1002/biof.5520230403 .

Nakayama, M., Suzuki, K., Toda, M., Okubo, S., Hara, Y., & Shimamura, T. (1993). Inhibition of the infectivity of influenza virus by tea polyphenols. *Antiviral Research*, 21 (4), 289-299. doi: 10.1016/0166-3542(93)90008-7.

Paivarinta, E., Pajari, A.M., Torronen, R., & Mutanen, M. (2006). Tumorigenesis in the Min Mouse. *Nutrition and Cancer*, 54 (1), 79-83. doi: 10.1207/s15327914nc5401\_9.

Panichayupakaranant, P., Tewtrakul, S., & Yuenyongsawad, S. (2010). Antibacterial, anti-inflammatory and anti-allergic activities of standardised pomegranate rind extract. *Food Chemistry*, 123 (1), 400-403. doi: 10.1016/j.foodchem.2010.04.054.

Pearce, A., Haas, M., Viney, R., Pearson, S.A., Haywood, P., Brown, C., & Ward, R. (2017). Incidence and severity of self-reported chemotherapy side effects in routine care: A prospective cohort study. *Public Library of Science*, 12 (10), 1-12. doi: 10.1371/journal.pone.0184360.

Poudel, A., Vadhanam, M.V., & Burliston, J. (2014). Efficacy of ellagic acid and its major urolithin metabolites in inhibiting growth of prostate cancer cells. *Cancer Research*, 74 (19), . doi: 10.1158/1538-7445.AM2014-4108.

Priyadarsini, K.I., Khopde, S.M., Kumar, S.S., & Mohan, H. (2002). Free Radical Studies of Ellagic Acid, A Natural Phenolic Antioxidant. *Journal of Agricultural and Food Chemistry*, 50 (7), 2200-2206. doi: 10.1021/jf011275g.

Pumia, R.P. (2005). Bioactive berry compounds - novel tools against human pathogens. *Applied Microbiology and Biotechnology*, 67 (1), 8-18. doi: 10.1007/s00253-004-1817-x.

Ranjbar, M., Zibae, A., & Sendi, J.J. (2015). Purification and characterization of a digestive lipase in the midgut of *Ectomyelois ceratoniae* Zeller (Lepidoptera: Pyralidae). *Frontiers in Life Science*, 1 (8), 64-70. doi: 10.1080/21553769.2014.961616.

Roussel, A., Canaan, S., Egloff, M.P., Riviere, M., Dupuis, L., Verger, R., & Cambillau, C. (1999). Crystal Structure of Human Gastric Lipase and Model of Lysosomal Acid Lipase, Two Lipolytic Enzymes of Medical Interest. *The Journal of Biological Chemistry*, 274 (24), 16995-17002. doi: 10.1074/jbc.274.24.16995.

Rubin, J.E., Ball, K.R., & Trejo, M.C. (2011). Antimicrobial susceptibility of *Staphylococcus aureus* and *Staphylococcus pseudintermedius* isolated from various animals. *Canadian Veterinary Journal*, 52 (2), 153-157. Retrieved from <https://www.ncbi.nlm.nih.gov/pmc/articles/PMC3022451/>.

Saavedra, M.J., Borges, A., Dias, C., Aires, A., Bennett, R.N., Rosa, E.S., & Simoes, M. (2010). Antimicrobial activity of phenolics and glucosinolate hydrolysis products and their synergy with streptomycin against pathogenic bacteria. *Journal of Medicinal Chemistry*, 6 (3), 174-183. doi: 10.2174/1573406411006030174.

Sanhueza, L., Wil, M., Montero, R., Maisey, K., Mendoza, L., & Wilkens, M. (2017). Synergistic interactions between phenolic compounds identified in grape pomace extract with antibiotics of different classes against *Staphylococcus aureus* and *Escherichia coli*. *Public Library of Science*, 12 (2), 1-15. doi: 10.1371/journal.pone.0172273.

Sarrias, A.G., Espin, J.C., Barberan, F.A.T., & Conesa, M.T.G. (2009). Gene expression, cell cycle arrest and MAPK signalling regulation in Caco-2 cells exposed to ellagic acid and its metabolites, urolithins. *Molecular Nutrition & Food Research*, 53 (6), 686-698. doi: 0.1002/mnfr.200800150.

Song, J.M., Lee, K.H., & Seong, B.L. (2005). Antiviral effect of catechins in green tea on influenza virus. *Antiviral Research*, 68 (2), 66-74. doi: 10.1016/j.antiviral.2005.06.010.

Stanislawska, I.J., Piwowarski, J.P., Granica, S., & Kiss, A.K. (2018). The effects of urolithins on the response of prostate cancer cells to non-steroidal antiandrogen bicalutamide. *Phytomedicine*, 46 (1), 176-183. doi: 10.1016/j.phymed.2018.03.054.

Talcott, S.U.M., Talcott, S.T., & Percival, S.S. (2003). Low Concentrations of Quercetin and Ellagic Acid Synergistically Influence Proliferation, Cytotoxicity and Apoptosis in MOLT-4 Human Leukemia Cells. *The Journal of Nutrition*, 133 (8), 2669-2674. doi: 10.1093/jn/133.8.2669.

Thyagarajan, A. & Sahu, R.P. (2017). Potential Contributions of Antioxidants to Cancer Therapy: Immunomodulation and Radiosensitization. *Integrative Cancer Therapies*, 17 (2), 210-216. doi: 10.1177/1534735416681639.

Tsao, R. (2010). Chemistry and Biochemistry of Dietary Polyphenols. *Nutrients*, 2 (12), 1231-1246. doi: 10.3390/nu2121231.

Tseng, Y.S., Wu, D.C., Chang, C.Y., Kuo, C.H., Yang, Y.C., Jan, C.M. ... Chang, L.L. (2009). Amoxicillin resistance with beta-lactamase production in *Helicobacter pylori*. *European Journal of Clinical Investigations*, 39 (9), 807-812. doi: 10.1111/j.1365-2362.2009.02166.x.

United States National Library of Medicine. (2008). Ellagic Acid. Retrieved from <https://toxnet.nlm.nih.gov/cgi-bin/sis/search2/r?dbs+hsdb:@term+@rn+@rel+476-66-4>.

Usta, C., Ozdemir, S., Schiarity, M., & Puddu, P.E. (2013). The pharmacological use of ellagic acid-rich pomegranate fruit. *International Journal of Food Sciences and Nutrition*, 64 (7), 907-913. doi: 10.3109/09637486.2013.798268.

Vaguero, M.J.R., Fernandex, P.A.A., Nadra, M.D.M.C., & Saad, A.M.S.D. (2010). Phenolic compound combinations on *Escherichia coli* viability in a meat system. *Journal of Agricultural Food Chemistry*, 58 (10), 6048-6052. doi: 10.1021/jf903966p.

Vettem, D.A. & Shetty, K. (2005). Biological Functionality of Ellagic Acid: A Review. *Journal of Food Biochemistry*, 29 (3), 234-266. doi: 10.1111/j.1745-4514.2005.00031.x.

Vicianza, R., Zhang, Y., Henning, S.M., & Heber, D. (2013). Pomegranate Juice Metabolites, Ellagic Acid and Urolithin A, Synergistically Inhibit Androgen-Independent Prostate Cancer Cell Growth via Distinct Effects on Cell Cycle Control and Apoptosis.

Evidence Based Complementary and Alternative Medicine, 2013 (1), 1-12. doi: 10.1155/2013/247504.

Villalba, R.G., Beltran, D., Espin, J.C., Selma, M.V., & Barberan, F.A.T. (2013). Time course production of urolithins from ellagic acid by human gut microbiota. *Journal of Agricultural Food Chemistry*, 61 (37), 8797-8806. doi: 10.1021/jf402498b.

Yang, X. & Jiang, X. (2015). Antifungal activity and mechanism of tea polyphenols against *Rhizopus stolonifer*. *Biotechnology Letters*, 37 (7), 1463-1472. doi: 10.1007/s10529-015-1820-6.

Zhang, L., Wang, Y., & Xu, M. (2014). Acid hydrolysis of crude tannins from infructescence of *Platycarya strobilacea* Sieb et Zucc to produce ellagic acid. *Natural Product Research*, 28 (19), 1637-1640. doi: 10.1080/14786419.2014.923998.

Zhang, W., Chen, J.H., Barrantes, I.A., Shiau, C.W., Sheng, X., Wang, L.S. ... Huang, Y.W. (2016). Urolithin A suppresses the proliferation of endometrial cancer cells by mediating estrogen receptor- $\alpha$ -dependent gene expression. *Molecular Nutrition and Food Research*, 60 (11), 2387-2395. doi: 10.1002/mnfr.201600048.

Zhao, W., Shi, F., Guo, Z., Zhao, J., Song, X., & Yang, H. (2018). Metabolite of elagitannins, urolithin A induces autophagy and inhibits metastasis in human sw620 colorectal cancer cells. *Molecular Carcinogenesis*, 57 (2), 193-200. doi: 10.1002/mc.22746.

Zowawi, H.M., Balkhy, H.H., Walsh, T.R., & Paterson, D.L. (2013). B-Lactamase Production in Key Gram-Negative Pathogen Isolates from the Arabian Peninsula. *Clinical Microbiology Reviews*, 26 (3), 361-380. doi: 10.1128/CMR.00096-12.

## Chapter Five: Summary and Concluding Remarks

### 5.1 Introduction

Antibiotic resistance is an unavoidable inevitability owing to the genetic drivers of resistance present in all bacteria, pathogenic and non-pathogenic alike. The greatest contributor to antibiotic resistance is overwhelmingly the capability of bacteria to produce antibiotic cleaving enzymes,  $\beta$ -lactamases.  $\beta$ -Lactamases are capable of efficiently catalysing the hydrolysis of  $\beta$ -lactam antibiotics, thereby rendering them useless in combatting microbial infections.  $\beta$ -Lactam antibiotics are the most widely used and relied upon class of antibiotics by a great deal, owing to their efficacy and limited side effects. The dissemination of  $\beta$ -lactamase encoding genes throughout pathogenic bacteria represent the greatest threat to  $\beta$ -lactam antibiotics, which have long been our weapon of choice in the fight against pathogenic infections. Unfortunately, we have been unable to replicate the success of  $\beta$ -lactam antibiotics into novel classes of antimicrobial treatments. The antibiotic production pipeline has been drying up since the “golden era” of discovery of antibiotics in the 1950-1970s. The goal of developing a completely novel class of resistance-proof synthetic antibiotics has not been achieved. Antibiotics are expensive to research, time consuming to develop, and as they are treatment for acute infections, they do not give a great return relative to the high investment needed to get from concept to approved drug. Pharmaceutical companies have therefore been moving away from novel antibiotic research, instead concentrating resources on developing treatments for more lucrative chronic diseases such as cancers or diabetes. The development of novel antibiotics has therefore been somewhat neglected in recent decades; although there has been a recent rekindling of interest owing to

the disturbing dearth of novel antibiotics. The bleakness of a post-antibiotic reality is becoming a more concerning threat within the scientific community.

The work detailed in this thesis has aimed to go some way to providing insights into ways of culturing bacteria perhaps as a pathway to discover novel antibiotics. Novel  $\beta$ -lactamase inhibitors have also been synthesised and discussed, and the pH dependent nature of hydrolysis of antibiotics by SBLs and their inhibition by novel inhibitors has also been explored. Also, novel compounds acting as SBL inhibitors have been identified, and their applications for future development have also been highlighted.

## 5.2: The Search for Novel Antimicrobials from Microbial Origins

It is well known that the vast majority of microbes will not grow in laboratory conditions. The vast majority of our existing classes of antibiotics have originated from screening platforms investigating the metabolites of bacteria for antibiotic capabilities, mainly spurred on by Fleming's serendipitous discovery of the anti-microbial properties of *Penicillium*. Microbial sources of novel antibiotics have been described as over-mined and long depleted. However, when one considers that around 98 % of bacteria *in situ* are un-culturable *in vitro*, many scientists have explored ways of trying to increase the *in vitro* growth rate in order to explore the metabolites of potentially novel bacteria, doing so would re-vitalise the "Waksman Platform of Discovery" – a method employed during the golden era of antibiotic discovery to identify antimicrobial producing bacteria from environmental samples.

The work in this chapter explored one such method for increasing the *in vitro* growth rate of bacteria. The "iChip" is a multi-welled plastic device traps bacteria in agar plugs for

incubation *in situ* until colonies are well established. After this point, the whole unit is transferred back to the laboratory and disassembled and agar plugs exhibiting growth are incubated. This process identified one such microbe which repeatedly showed inhibition of clinically relevant SBL/MBL producing bacteria. PCR was carried out to identify the strain of the specific microbe, and it was identified as *Pseudomonas baetica*, a little described strain of bacteria whose only noticeable trait was that it was pathogenic to wedge sole – a species of fish popular for consumption in Spain. LCMS analysis took place on a broth of *Pseudomonas baetica* and identified over 400 unique compounds. Clearly, this was far too many to try and realistically quantify with the time and resources available, but it showed that the iChip and LCMS could be used as tools to potentially isolate novel antimicrobial producing bacteria and then to identify the antibiotic using LCMS.

### 5.3: Novel Avibactam Analogues as Novel Inhibitors of Serine Beta Lactamases

In an attempt to combat the greatest threat to  $\beta$ -lactam antibiotics,  $\beta$ -lactamase enzymes, pharmaceutical companies have developed  $\beta$ -lactamase inhibitors (BLIs). BLIs represent a way of inhibiting  $\beta$ -lactamases produced from  $\beta$ -lactamase producing enzymes, thereby preventing hydrolysis of the  $\beta$ -lactam ring present in  $\beta$ -lactam antibiotics to their microbial killing mechanism. BLI's are paired with existing  $\beta$ -lactam antibiotics in an attempt to restore their antimicrobial killing capability. Historically, there has been three clinically approved BLI: tazobactam, sulbactam and clavulanic acid. Owing to the dearth of novel antibiotics, interest has increased in recent years around novel BLIs, in an attempt to extend the life of existing  $\beta$ -lactam antibiotics and help combat infections caused by antibiotic resistant bacteria.

The work in this chapter looked at avibactam, a novel  $\beta$ -lactamase inhibitor and novel carbamate derivatives of avibactam. The work predominantly revolved around 4 carbamate inhibitors which were shown to have inhibitory effects towards SBLs. The work showed that the leaving groups of the carbamate derivatives could be altered to result in more effective inhibition. More acidic alcohols were introduced as leaving groups and it was found that as the  $pK_a$  of the alcohol used as a leaving group decreased, the inhibitory effectiveness of the carbamate derivatives increased. The most effective carbamate derivative, the hexafluoroacetone derivative (HFA) had a higher  $k_i$  than avibactam itself, whilst the second most effective inhibitor (the hexafluoroisopropanol [HFIP]) carbamate derivative had a  $k_i$  comparable to that of avibactam.

The work in this chapter also explored the pH dependency of hydrolysis of antibiotics catalysed by different SBLs and the inhibition of these SBLs. The work concluded that the catalytic machinery used in both the hydrolysis of antibiotics and inhibition of the enzymes were the same, owing to the similar bell shaped curves obtained from these experiments ( $k_{cat}/K_m$  for enzyme catalysed hydrolysis of cephalothin and  $k_i$  for the inhibition of these enzymes by the carbamate inhibitors/avibactam).

#### 5.4: Other Novel $\beta$ -Lactamase Inhibitors

The work in this chapter investigated three potential novel  $\beta$ -lactamase inhibitors, ellagic acid, urolithin A and orlistat. All three were investigated owing to their structural characteristics, as it was predicted that they had the necessary features essential for being able to inhibit SBLs.

Ellagic acid, a polyphenol with supposed health benefits, was found to be the most effective inhibitor out of the three compounds tested. Urolithin A (a plant derived metabolite) and orlistat (a dietary lipase inhibitor). Urolithin A and orlistat had only modest inhibitory effects. Ellagic acid has great potential for future development, as the molecule can be nitrated which will, in theory, improve its ability as an inhibitor of SBL enzymes.

All three of the compounds were also tested for their ability to inhibit microbial pathogens. Out of the three tested, only ellagic acid showed any inhibitory activity against the pathogens tested, which included MBL producing bacteria. Ellagic acid clearly shows potential as a dual microbial pathogen and SBL inhibitor, which could present an interesting future development option.

## Chapter Six: General Methods

### 6.1: Sourcing of Materials

All materials used were obtained from Fisher Scientific, Loughborough, Leicestershire Sigma Aldrich, Gillingham, Dorset or Fluorochem, Hadfield, Derbyshire and were of analytical reagent grade or higher.

Ultra-pure water refers to water purified from a Milli-Q Millipore Gradient ultra-pure water system.

### 6.2: Preparation of Tryptone Soy Agar

Tryptone soy agar powder was obtained from LabM, Heywood, Lancashire, and the typical formulation was as follows:

Table 6.1: Ingredients of tryptone soy agar powder.

Ingredient	Amount (g)
Tryptone	15
Soy peptone	5
Sodium chloride	5
Agar No. 2	12

37 g of powder was weighed into a clean 1 L Schott bottle in a decontaminated laminar flow hood. 1 L of deionised water was added and was swirled to mix with the powder. The bottle was sealed and autoclave tape was placed across the lid and the bottle was then placed into

a Prestige Medical Autoclave Classic 12 litre benchtop autoclave and sterilised at 121 °C at 15 psi for 15 minutes. Once the autoclave cycle had finished, the autoclave tape was inspected and the molten agar was placed in a Precision (Thermo Fisher) water bath at 50 °C and allowed to cool until the bottle was warm to the touch. Once the bottle was cool enough to handle but the agar was still molten, the bottle was transported to a laminar flow hood and 9 cm agar plates were prepared by aseptically pouring the molten agar into the plates and swirling gently to ensure the agar would solidify evenly. The plates were allowed to cool and harden for 30 minutes and were then stored inverted in a sealed bag at 4 °C until needed.

### 6.3: Preparation of Tryptone Soy Broth

Tryptone soy broth powder was obtained from LabM and the ingredients were as follows:

Table 6.2: Ingredients of tryptone soy broth powder.

Ingredient	Amount (g)
Tryptone	17
Soy peptone	3
Sodium chloride	5
Dipotassium phosphate	2.5
Dextrose	2.5

30 g of powder was weighed into a clean 1 L Schott bottle in a decontaminated laminar flow hood. 1 L of deionised water was added and was swirled to mix with the powder. The bottle

was sealed and autoclave tape was placed across the lid and the bottle was then placed into a Prestige Medical Autoclave Classic 12 litre benchtop autoclave and sterilised at 121 °C at 15 psi for 15 minutes. Once the autoclave cycle had finished, the autoclave tape was inspected and the broth was allowed to cool until the bottle was warm to the touch. Once the broth had cooled to room temperature it was ready to use in further experiments or was stored at 4 °C until needed.

## **6.4: Polymerase Chain Reaction**

### **6.4.1: Extraction**

For the extraction of DNA from microbial origins for PCR analysis, a MO-BIO PowerSoil DNA Extraction Kit was used (MO-BIO, Carlsbad, CA, US), as according to the manufacturer's instructions. Several inoculating loops of pure isolate were added to a PowerBeads tube and vortexed. 60 µL of cell lysing solution (C1) was added to the PowerBeads tube and vortexed briefly. The PowerBead tubes containing sample and cell lysing solution were then attached to a MO-BIO horizontal vortex machine and operated at maximum velocity for 10 minutes. The tubes were then centrifuged for 30 seconds at 10,000 g. 400 µl of the supernatant was collected and transferred to a new, clean, 2 ml collection tube. 250 µl of solution C2 was then added to remove non-DNA and other non-essential materials from the sample and was vortexed for 5 seconds to mix with the sample and then incubated for 5 minutes at 4 °C. The sample was centrifuged after incubation for 1 minute at 10,000 g. 600 µl of supernatant was then collected and transferred to a new, clean, 2 ml collection tube, with care being taken to avoid disturbing the pellet. 200 µL of C3 solution

was then added to further remove any non-DNA and other inorganic material from the sample and a further incubation period of 5 minutes at 4 °C. The samples were then centrifuged at room temperature for 1 minute at 10,000 g, with the supernatant being transferred to a new 2 ml collection tube. 1200 µl of solution C4 was added to the sample and then vortexed for 5 seconds. The salt content of C4 solution aids in the aggregation (accumulation and clumping together of) of the DNA, which allows it to be more efficiently loaded onto a spin filter, which acts as a silica membrane column to aid in the purification of the sample – the DNA is collected on the spin filter whilst any non-DNA material is eluted via centrifugation. The sample is centrifuged at 10,000 g for 1 minute through the spin filter and the flow through is discarded each time. This process is repeated at least three times with the rest of the supernatant. 500 µl of solution C5, an ethanol based wash solution is then added to the spin filter and centrifuged, which helps eliminate any non-DNA material from the sample following centrifugation at 10,000 g for 60 seconds. After the C5 solution flow through is discarded, the centrifugation step is repeated to ensure the elimination of any remaining non-DNA material, and the flow through is discarded once more. Now the pure, clean DNA is on the spin filter, it needs to be eluted for further down-stream processing. The spin filter is transferred to a new 2 ml collection tube and 30 µL of C6 solution is added to the spin filter. The sample is centrifuged for 1 minute at 10,000 g which elutes the DNA from the spin filter. The DNA is now in the collection tube, ready for down-stream processing.

#### 6.4.2: Quantification of Nucleic Acids

The concentration of nucleic acids was determined using a spectrophotometer, operating at 260 nm. It is at this wavelength that the extinction coefficient of DNA is  $0.020 \mu\text{g}/\text{mL}^{-1} \text{ cm}^{-1}$

<sup>1</sup> and for RNA the extinction coefficient is  $0.025 \mu\text{g}/\text{ml}^{-1} \text{cm}^{-1}$ . The purity of DNA and RNA can be determined by the ratio of optical densities at 260:280 nm, with a ratio falling between 1.8-2.0 for DNA being considered to be consisting of minimal contamination of a protein source.

### 6.4.3: Polymerase Chain Reaction

Once the amount of DNA present in the isolated sample had been quantified, it could be prepared for PCR. The final sample needed to be made up to 50  $\mu\text{L}$ , with a DNA concentration of no more than 5-10 ng/ml. The sample contained 25  $\mu\text{l}$  *Taq* polymerase from myTaq HS red mix (Bioline, London), 2  $\mu\text{L}$  8F1510R primer mix, the appropriate amount of DNA as calculated from the quantification stage and then made up to 50  $\mu\text{L}$  with DNA/RNA grade DEPC water.

The DNA in the correct concentration with the appropriate polymerase and primers was then transferred to a Techne <sup>3</sup>Prime Thermal Cycler (Stone, Staffordshire) and the reaction was carried out as follows: initial denaturation at 95 °C for 2 minutes, followed by 33 cycles of: denaturing (95 °C for 30 seconds), annealing (55 °C for 30 seconds) and primer extension (72 °C for 30 seconds). This was followed by a final extension step of 72 °C for 7 minutes. To check whether the PCR had been successful, samples were subject to a gel electrophoresis.

#### 6.4.4: Visualisation of PCR Samples by Gel Electrophoresis

PCR products were visualised using gel electrophoresis on 1 % agarose gels prepared in tris-acetate EDTA buffer (TAE). A 50X concentrated solution was prepared by dissolving 242 g TRIS base, 57.1 ml glacial acetic acid and 100 ml 0.5 M Ethylenediaminetetraacetic acid (EDTA) per litre of ultra-pure water (pH 8.0) and diluted when required. The 1 % agarose solution was then completely melted by microwaving (2-3 minutes per 100 ml) before being allowed to cool to ~45 °C, prior to the addition of 1 µL of SYBR safe stain (Life Technologies, Paisley, UK). The gel was then cast and allowed to set. 5 µl of each PCR product was loaded into each gel utilising the dye present in the original PCR master mix, alongside 5 µL of ladder (Hyperladder 1 kb) and electrophoresed for 60 minutes at 100 V. Gels were then visualised under UV light and an image taken using BioDoc-It® 210 imaging system (UVP LLC, Upland, CA, US). Once the presence of DNA had confirmed that the PCR process had been carried out correctly, the PCR samples could be purified prior to being sent to external sequencing.

#### 6.4.5: PCR Product Purification

Following the PCR and the visualisation process, the PCR product needed to be purified before being sent for external sequencing. This was accomplished by using a commercially available PCR purification kit supplied by Qiagen (Surrey, UK), and the manufacturer's instructions were followed. 5 volumes of Buffer PB are added to 1 volume of PCR sample in order to salt the sample, and ensure that the pH is <7.5, which was ensured by the addition of 10 µl of 3 M sodium acetate pH 5.0. The sample is then binded to a silica column by placing the sample onto a spin filter (silica column) and centrifuging for 60 seconds at

10,000 g. The flow through is discarded and the column is washed with 750  $\mu$ l of Buffer PE (buffer containing ethanol) and centrifuged for 60 seconds. The flow through is discarded and the centrifugation step is repeated. The DNA is then eluted by placing the spin filter column into a clean 1.5 ml microcentrifuge tube and adding 50  $\mu$ l of elution buffer (10 mM TRIS-Cl) to the centre of the spin column and letting the sample stand for 60 seconds before centrifuging the sample for 60 seconds. The purified PCR product was then ready to be sent for external sequencing at Eurofins Laboratories, Wolverhampton, where the Sanger sequencing method was used (discussed in more detail in chapter 2).

#### 6.4.6: Sequence Analysis

Sequences were returned from the laboratory in Notepad file format. File formats were prepared for comparative analysis using MEGA 5 for Windows where duplicated sequences or poor data could be eliminated. They could then be uploaded into the US National Library of Medicine's **B**asic **L**ocal **A**lignment **S**earch **T**ool (BLAST) for 16s ribosomal RNA sequences, where the sequence similarity of the samples could be compared to database records for existing species.

#### 6.5: QToF Mass Spectrometry

The QToF was used in the metabolomics experiments and some of the rest of the analytical experiments except those ran on the QqQ and GCMS. Data were collected using an Agilent Technologies 1290 Infinity II LC system coupled to an Agilent Technologies 6545 QToF Mass Spectrometer in negative ionisation mode using an ACE 5 C18-AR (3  $\mu$ M, 50 x 4.6

mm) column, with the column compartment temperature set to 30 °C. The binary pump flow rate was 0.8 ml with an injection volume of 5 µl. The mobile phases used were A: 0.1 % formic acid LCMS grade water and B: 0.1 % formic acid LCMS grade ACN and the gradient was as follows: 3 % B for 1 minute, then a linear increase from 3 to 50 % B in 1.4 minutes, followed by another linear increase from 50 to 99 % B in 1.6 minutes, hold at 99 % B for 0.5 minutes, then a return to 3 % B for 3.5 minutes, followed by an equilibration time of 10 minutes before the next sample was injected. The carrier gas used was nitrogen and the source used was a jet stream electrospray ionisation (JS-ESI) with the following voltages and temperatures used:

Table 6.3: QToF Instrument parameters.

Instrument Parameter	Value
Gas temp (°C)	320
Gas flow (L/min)	8
Nebuliser pressure (psig)	35
Sheath gas temperature (°C)	350
Sheath gas flow (L/min)	11

Table 6.4: QToF source parameters.

Scan Source Parameter	Value
Capillary voltage (V)	4000
Nozzle voltage (V)	1000
Fragmentor (V)	175
Skimmer (V)	65
Octopole RF peak (V)	750

### 6.6: QqQ Mass Spectrometry

The QqQ was used in some of the avibactam detection experiments. Data were collected using an Agilent Technologies 1290 Infinity II LC system coupled to an Agilent Technologies 6470 QqQ Mass Spectrometer in negative ionisation mode using a zero dead volume column, with the column compartment temperature set to 30 °C. The binary pump flow rate was 0.4 ml with an injection volume of 20 µl. The mobile phases used were A: 0.1 % formic acid LCMS grade water and B: 0.1 % formic acid LCMS grade ACN and the method was isocratic, with a 1:1 mobile phase composition. The carrier gas used was nitrogen and the source used was a jet stream electrospray ionisation (JS-ESI) with the following voltages and temperatures used:

Table 6.5: QqQ Instrument parameters.

Instrument Parameter	Value
Gas temp (°C)	300
Gas flow (L/min)	5
Nebuliser pressure (psig)	45
Sheath gas temperature (°C)	250
Sheath gas flow (L/min)	11

Table 6.6: QqQ source parameters.

Scan Source Parameter	Value
Capillary voltage (V)	3500
Fragmentor (V)	135
Collision cell (V)	5

### 6.7: Gas Chromatography Mass Spectrometry

The GCMS was used for the liberation of alcohol experiments. Data were collected using an Agilent Technologies 5975C gas chromatography mass spectrometry (GCMS) system with auto sampler injection, in positive ionisation mode using a HP5 column. The source temperature was set at 230 °C with an injection volume of 1 µL. The oven temperature was set at 35 °C, held for 2 minutes after sample injection and ramped at 10 °C per minute to 80 °C and held for 1 minute.

## 6.8: Synthesis of Carbamate Inhibitors

The synthesis of the inhibitors roughly followed the same synthesis pathway. 500 mg of avibactam was dissolved in 300 ml of solvent (methanol, trifluoroethanol, hexafluoroisopropanol, hexafluoroacetone hydrate) and stirred under reflux until dissolved. One equivalence of triethylamine was added and was stirred under reflux until the reaction was complete as monitored by LCMS. At this point, the reaction was drive using a Heidolph Hei Vap Precision rotary evaporator operating at 20 mbar pressure with a water bath temperature of 40 °C with an RPM of 200. The rotary evaporator was connected to a Huber Mini Chiller 300 OLÉ operating at -10 °C. The instrument was kept under vacuum by an Edwards RV12 vacuum pump.

## 6.9: Reagent Preparations

### 6.9.1: Buffer Preparations

All buffers used were 0.1 M concentration unless otherwise stated within the main chapters of the thesis. All buffers were corrected to 1 M ionic strength using KCl. All buffers used were obtained from Sigma Aldrich (Dorset, UK), and were of reagent grade or higher. Buffers were made in 1 L batches with ultra-pure water using a Millipore Milli-Q system. The weights of buffer used to create 1 L of 0.1 M buffer can be seen in table 6.7 below.

Table 6.7: Details of buffers used and preparation instructions.

Buffer	$pK_a$	Molecular Weight	Weight of Buffer Used to Create 1 L of 0.1 M Buffer
Formic Acid	3.75	46.03	4.603
MES	6.16	206.73	20.673
HEPES	7.55	283.30	28.33
TAPS	8.49	243.37	24.34

### 6.9.2 Experimental Reagent Preparations

All reagents (apart from those synthesised) were purchased from Sigma Aldrich (Dorset, UK) and were of reagent grade or higher unless otherwise stated.

A 40 mM stock solution of cephalothin was made fresh by dissolving 16.74 mg into 1 ml of pH 7.0 HEPES buffer (0.1 M). 10  $\mu$ l of this stock solution was added to 2 ml of test solution to create a final concentration of 0.2 mM in the hydrolysis/inhibition experiments.

The inhibitor stocks were made fresh on the day of experiments and were kept in melting ice when not kept refrigerated. For the MA carbamate, 29.61 mg was dissolved in 1 ml pH 7.0 HEPES buffer (0.1 M) to create a 100 mM stock. For the TA carbamate, 3.64 mg was dissolved into the same buffer to create a 10 mM stock for use in further downstream experiments. For the HFIP carbamate, 6.48 mg was dissolved in 100 ml of the same buffer to create a 150  $\mu$ M stock. For the HFA carbamate, 6.71 mg was dissolved in 100 ml of the same buffer to create a 150  $\mu$ M stock. Finally, for avibactam 3.96 mg was dissolved in 100 ml of the same buffer to create a 150  $\mu$ M stock. For all of these inhibition experiments, the experiments were conducted in 100 % aqueous buffers as described in their relevant chapters.

For ellagic acid, 3.02 mg was dissolved in 10 ml of MeOH to give a 1 mM stock solution and sonicated for 20 minutes to ensure all of the substance was in solution. The inhibition experiments for ellagic acid were conducted in the usual buffers for the respective pH but supplemented with 10 % MeOH to ensure the ellagic acid stayed in solution. For example, for inhibition experiments with ellagic acid at pH 7.0, the buffer sample would be 20 ml pH 7.0 HEPES buffer (0.1 M) with 10 % MeOH (18 ml aqueous HEPES buffer and 2 ml MeOH) with ionic strength maintained to 1 M with KCl.

Similarly, for orlistat and urolithin A, a different solvent composition was required. 4.96 mg of orlistat was dissolved in 1 ml ACN to create a 10 mM stock solution. For urolithin A, 2.28 mg was dissolved in 1 ml ACN to create a 10 mM stock solution. For both of these inhibitors, the inhibition experiments were conducted in pH 7.0 HEPES buffer (0.1 M) with 10 % ACN (18 ml pH 7.0 HEPES buffer and 2 ml ACN) maintained to 1 M ionic strength with KCl.

### **6.10: Kinetic UV Experiments**

All kinetic UV experiments were performed on an Agilent Technologies Cary UV-Vis 4000 instrument in a quartz UV cell with a 1 cm path length, operated with Cary Win UV Kinetics software application. All samples were blanked with all sample components minus antibiotic (cephalothin). The kinetics scan settings for the cephalothin experiments were as follows:

Table 6.8: UV kinetics parameters.

Parameter	Setting
Wavelength (nm)	260
Spectra bandwidth (nm)	1.000
Average time (s)	2.000
Thermostatted (°C)	30

### 6.10.1: P99 Catalysed Cephalothin Hydrolysis Additional Data

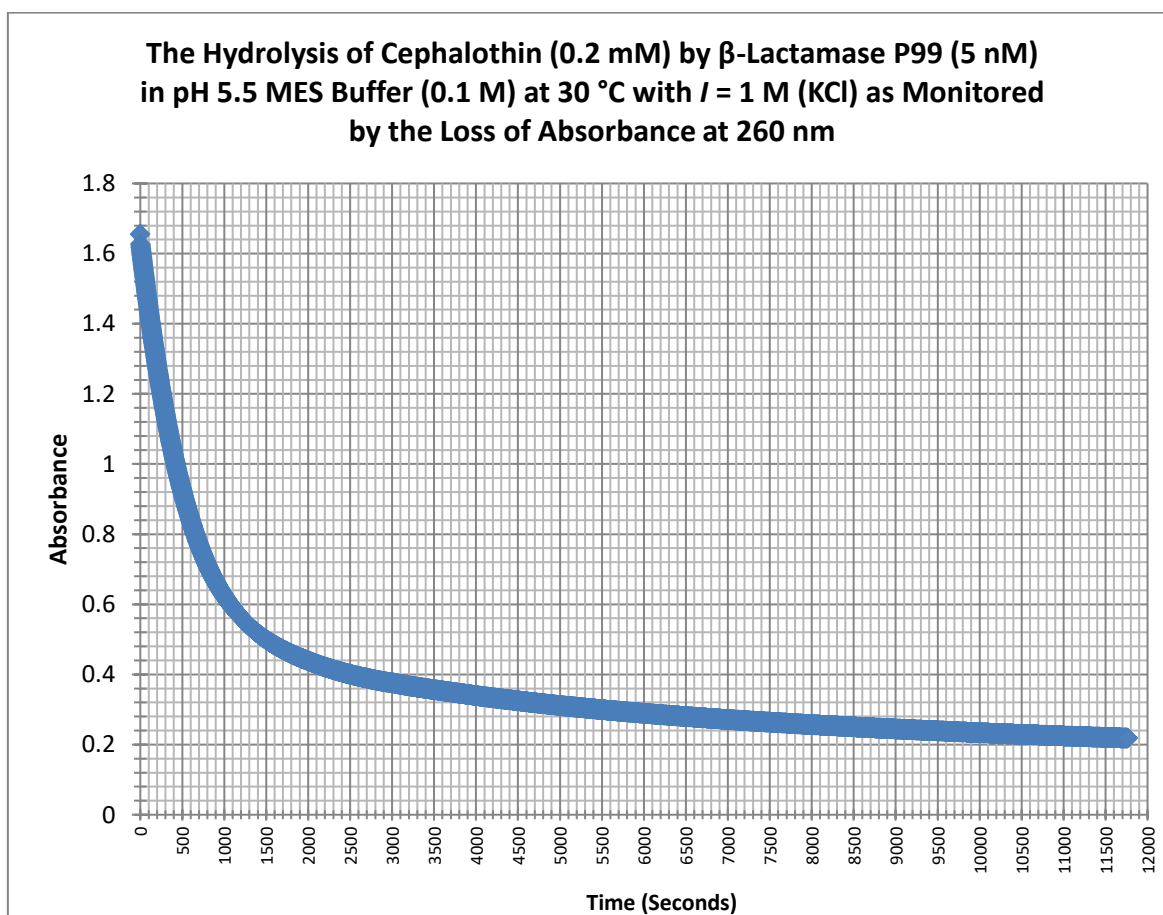


Figure 6.1: P99 (5 nM) catalysed hydrolysis of cephalothin (0.2 mM) at pH 5.5.

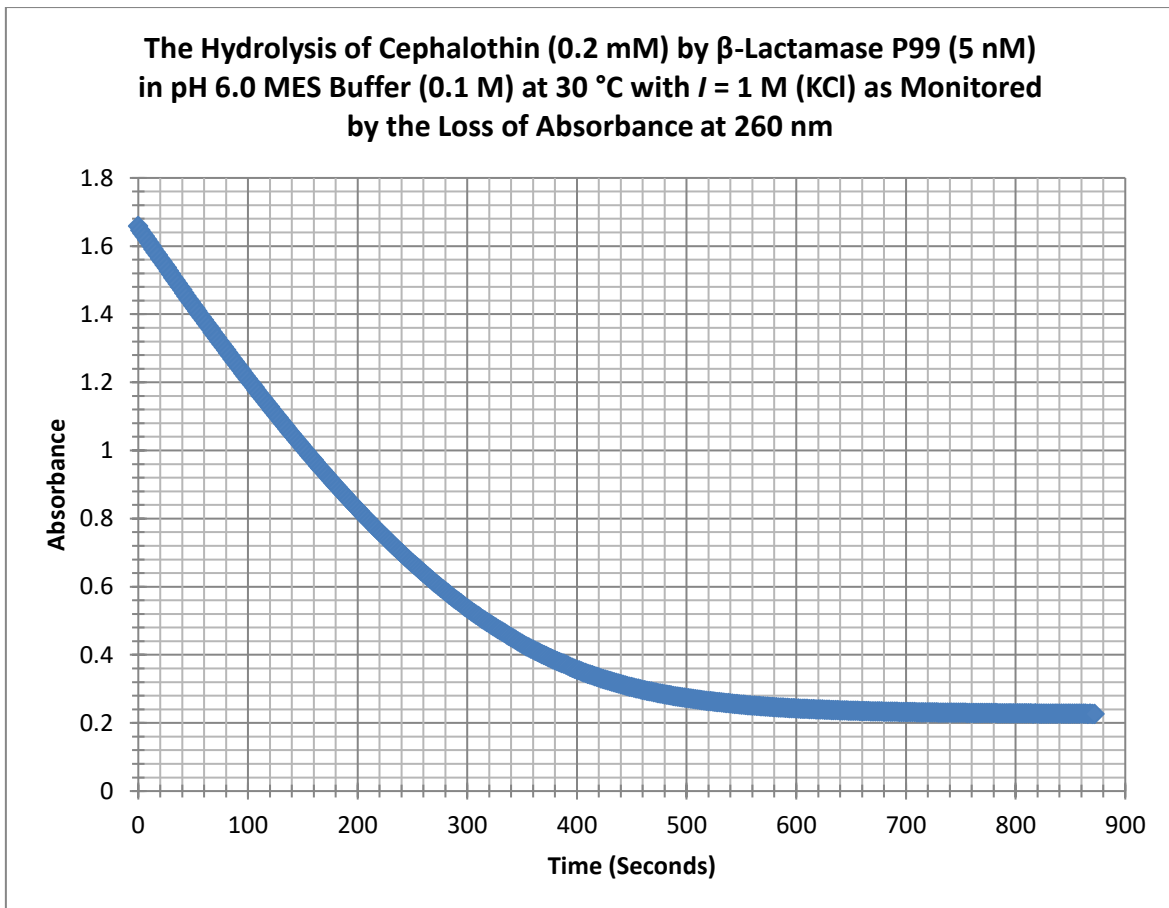


Figure 6.2: P99 (5 nM) catalysed hydrolysis of cephalothin (0.2 mM) at pH 6.0.

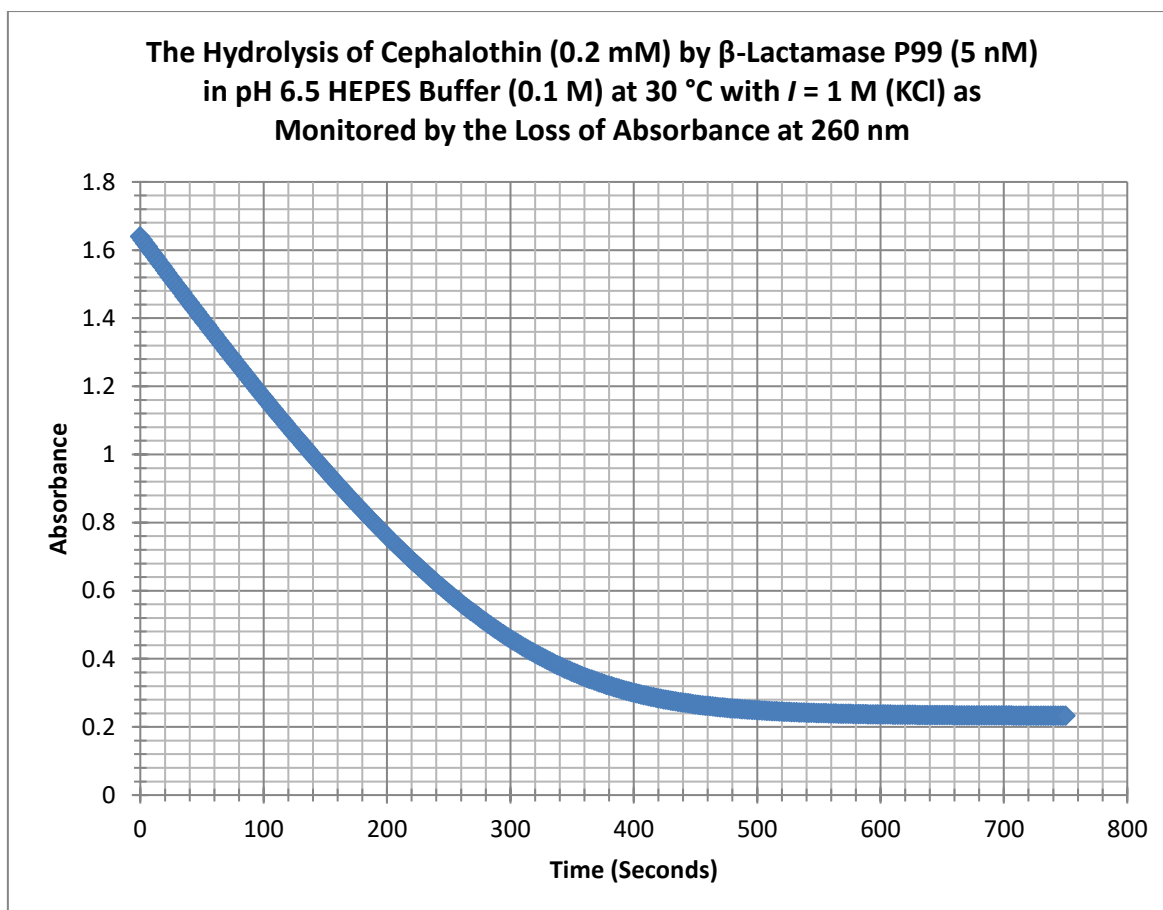


Figure 6.3: P99 (5 nM) catalysed hydrolysis of cephalothin (0.2 mM) at pH 6.5.

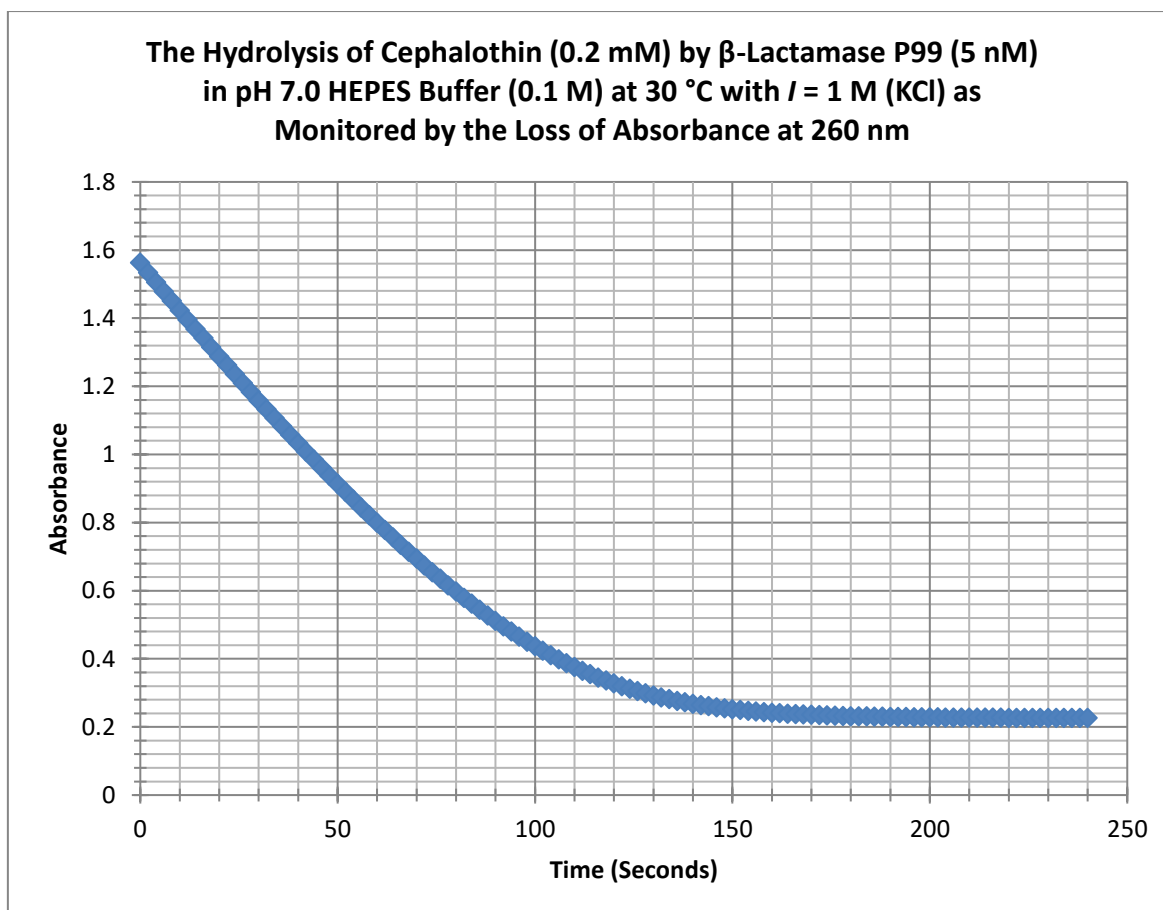


Figure 6.4: P99 (5 nM) catalysed hydrolysis of cephalothin (0.2 mM) at pH 7.0.

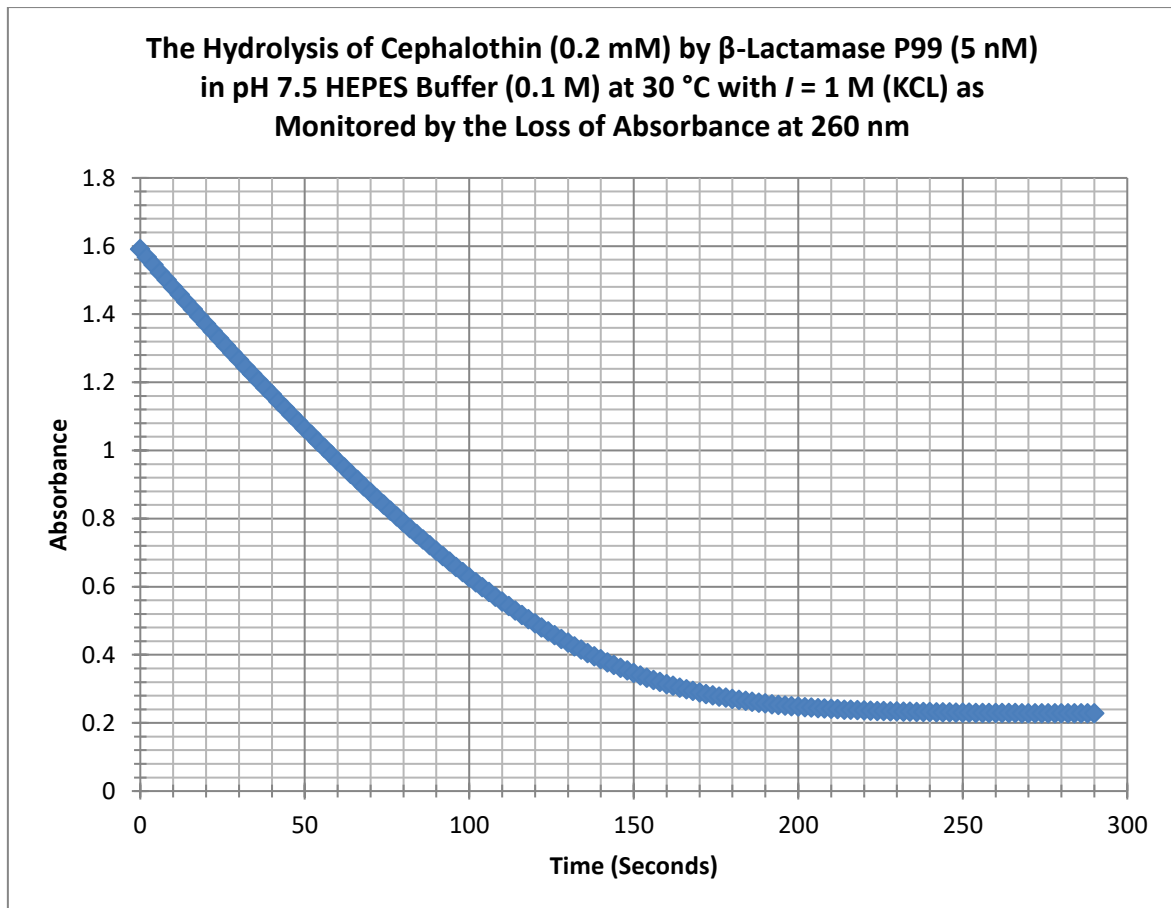


Figure 6.5: P99 (5 nM) catalysed hydrolysis of cephalothin (0.2 mM) at pH 7.5.

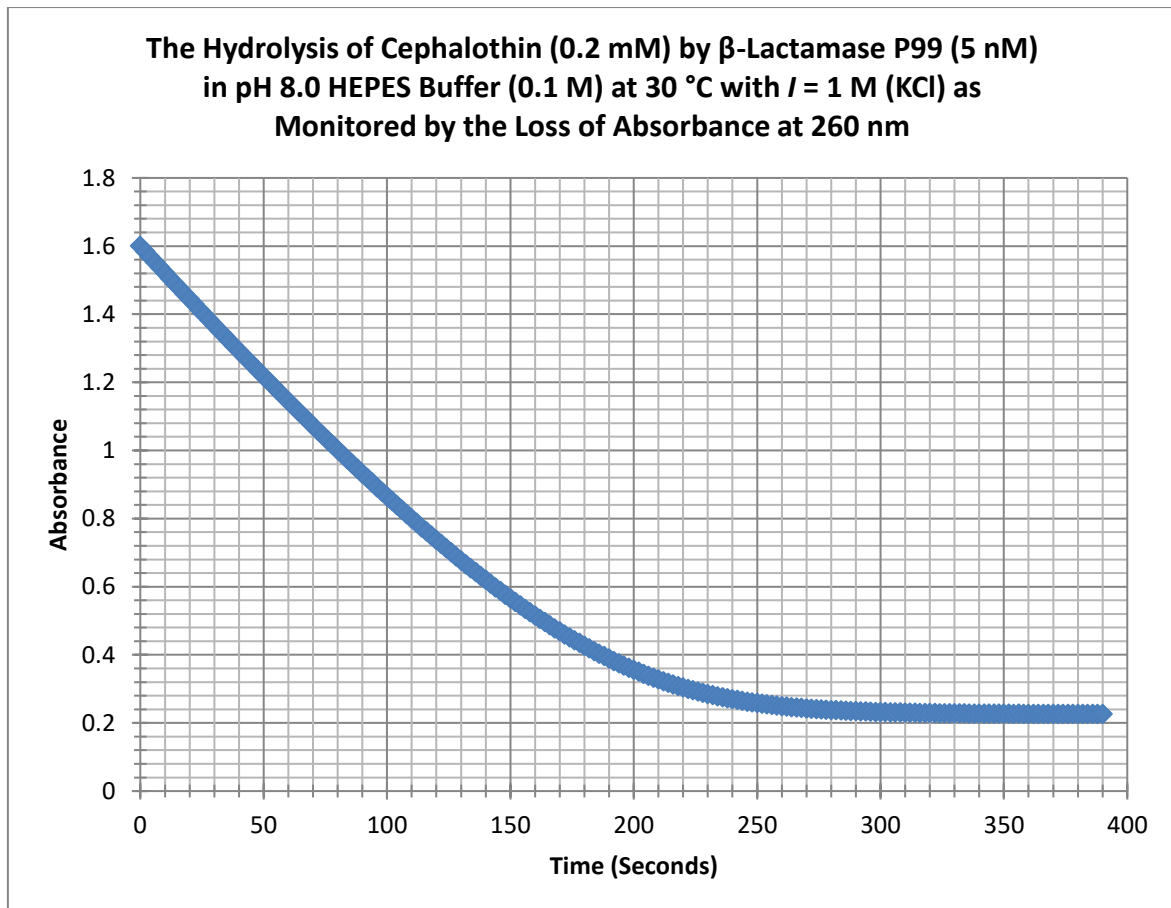


Figure 6.6: P99 (5 nM) catalysed hydrolysis of cephalothin (0.2 mM) at pH 8.0.

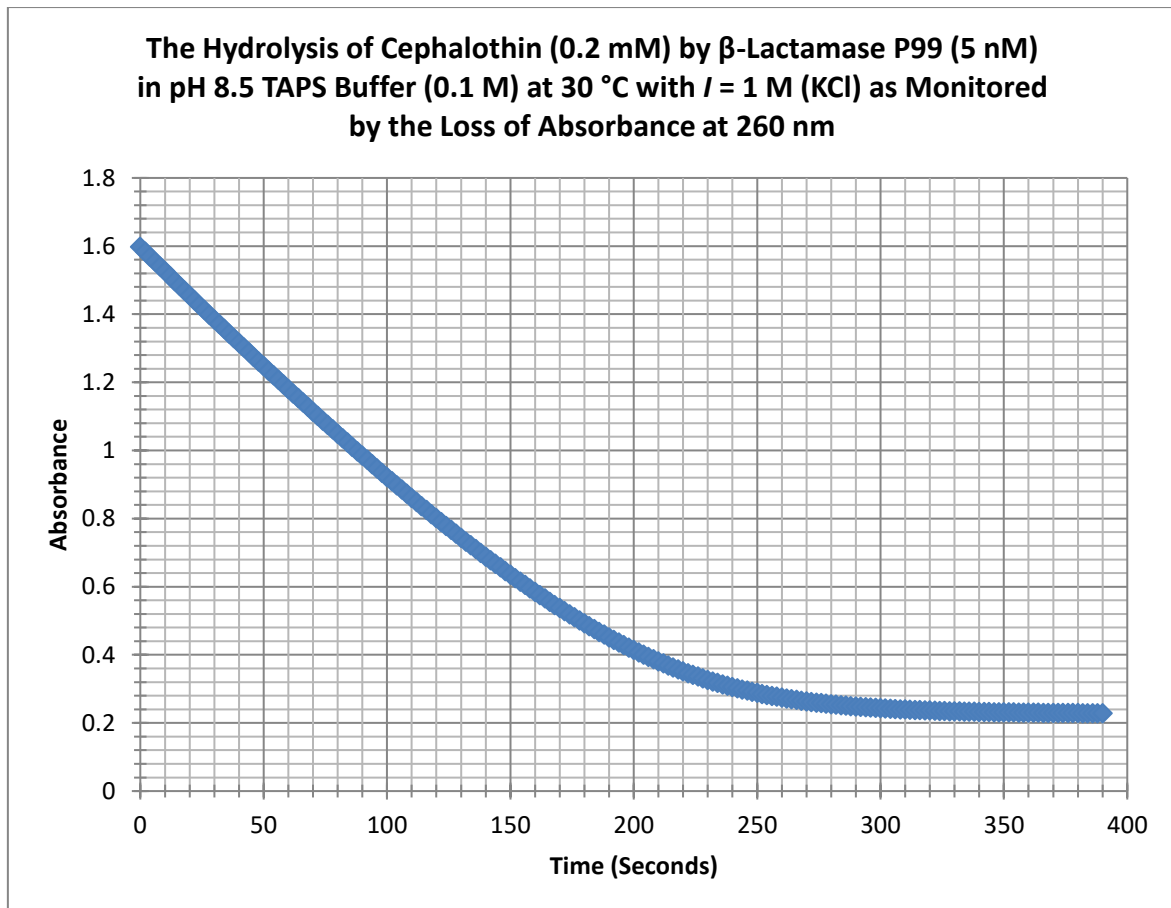


Figure 6.7: P99 (5 nM) catalysed hydrolysis of cephalothin (0.2 mM) at pH 8.5.

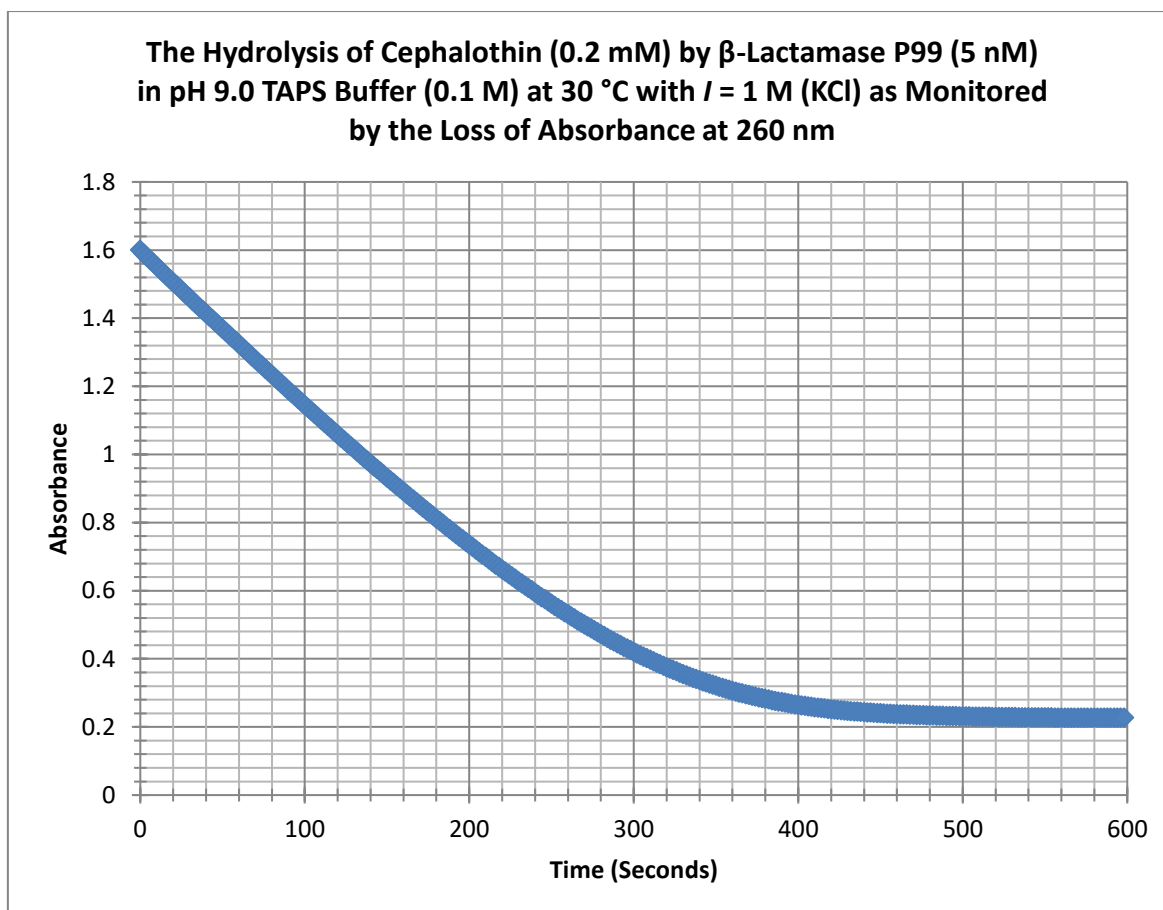


Figure 6.8: P99 (5 nM) catalysed hydrolysis of cephalothin (0.2 mM) at pH 9.0.

**Fit of the Hydrolysis of Cephalothin (0.2 mM) by P99 (5 nM) at pH 5.5 at 30 °C and  $I = 1$  M (KCl)**

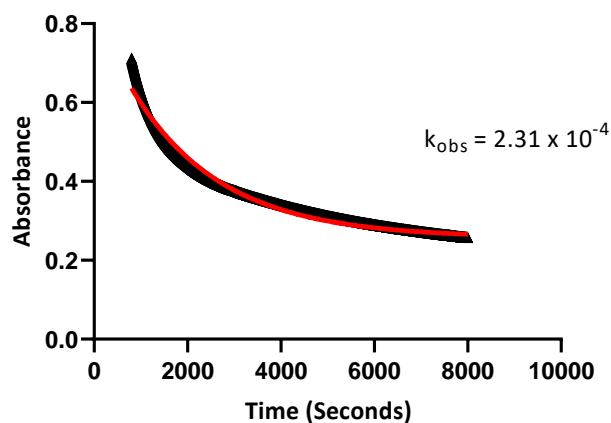


Figure 6.9: Curve fit of the hydrolysis of cephalothin (0.2 mM) catalysed by P99 (5 nM) at pH 5.5 obtained using GraphPad Prism (black triangles = experimental data, red line = curve fit from software).

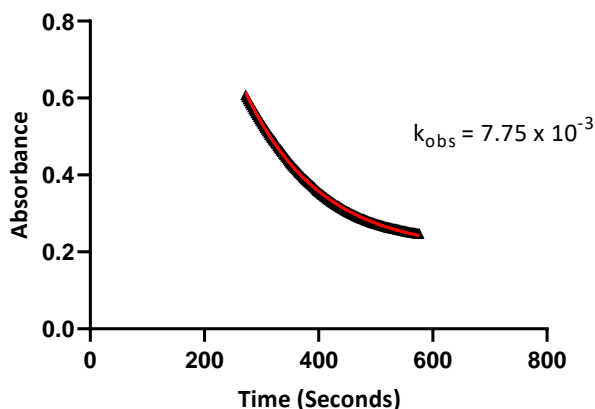
**Fit of the Hydrolysis of Cephalothin (0.2 mM) by P99 (5 nM) at pH 6.0 at 30 °C and  $I = 1M$  (KCl)**

Figure 6.10: Curve fit of the hydrolysis of cephalothin (0.2 mM) catalysed by P99 (5 nM) at pH 6.0 obtained using GraphPad Prism (black triangles = experimental data, red line = curve fit from software).

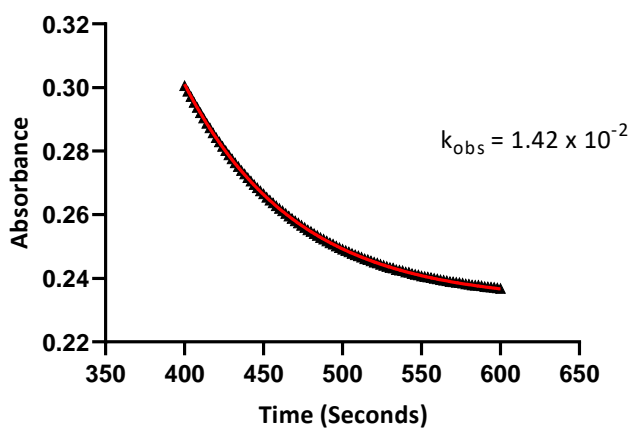
**Fit of the Hydrolysis of Cephalothin (0.2 mM) by P99 (5 nM) at pH 6.5 at 30 °C and  $I = 1M$  (KCl)**

Figure 6.11: Curve fit of the hydrolysis of cephalothin (0.2 mM) catalysed by P99 (5 nM) at pH 6.5 obtained using GraphPad Prism (black triangles = experimental data, red line = curve fit from software).

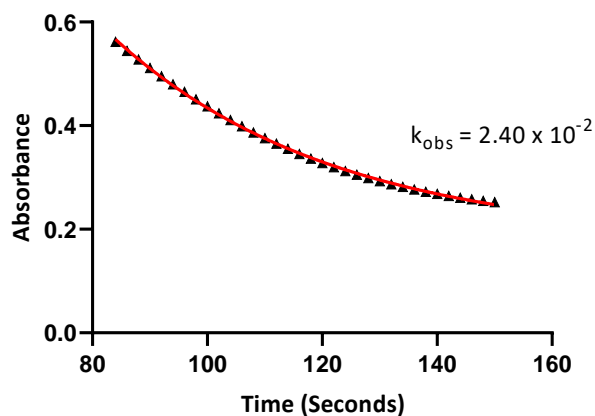
**Fit of the Hydrolysis of Cephalothin (0.2 mM) by P99 (5 nM) at pH 7.0 at 30 °C and  $I = 1M$  (KCl)**

Figure 6.12: Curve fit of the hydrolysis of cephalothin (0.2 mM) catalysed by P99 (5 nM) at pH 7.0 obtained using GraphPad Prism (black triangles = experimental data, red line = curve fit from software).

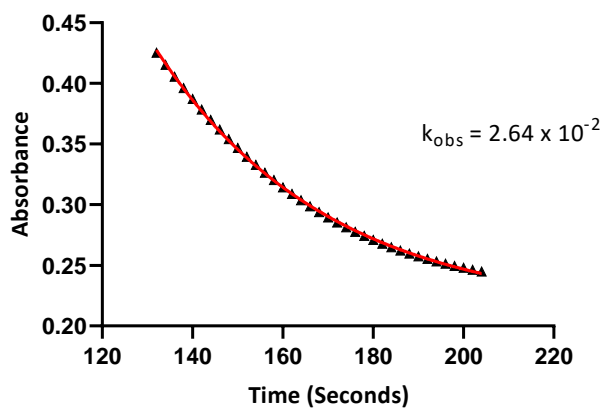
**Fit of the Hydrolysis of Cephalothin (0.2 mM) by P99 (5 nM) at pH 7.5 at 30 °C and  $I = 1M$  (KCl)**

Figure 6.13: Curve fit of the hydrolysis of cephalothin (0.2 mM) catalysed by P99 (5 nM) at pH 7.5 obtained using GraphPad Prism (black triangles = experimental data, red line = curve fit from software).

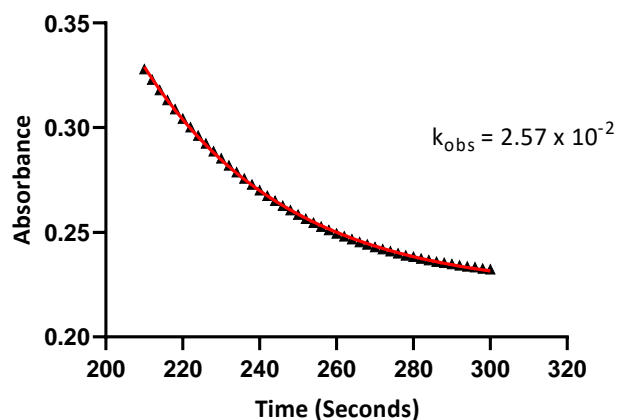
**Fit of the Hydrolysis of Cephalothin (0.2 mM) by P99 (5 nM) at pH 8.0 at 30 °C and  $I = 1M$  (KCl)**

Figure 6.14: Curve fit of the hydrolysis of cephalothin (0.2 mM) catalysed by P99 (5 nM) at pH 8.0 obtained using GraphPad Prism (black triangles = experimental data, red line = curve fit from software).

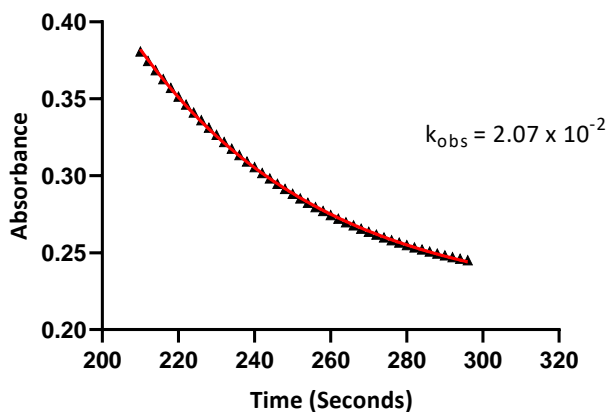
**Fit of the Hydrolysis of Cephalothin (0.2 mM) by P99 (5 nM) at pH 8.5 at 30 °C and  $I = 1M$  (KCl)**

Figure 6.15: Curve fit of the hydrolysis of cephalothin (0.2 mM) catalysed by P99 (5 nM) at pH 8.5 obtained using GraphPad Prism (black triangles = experimental data, red line = curve fit from software).

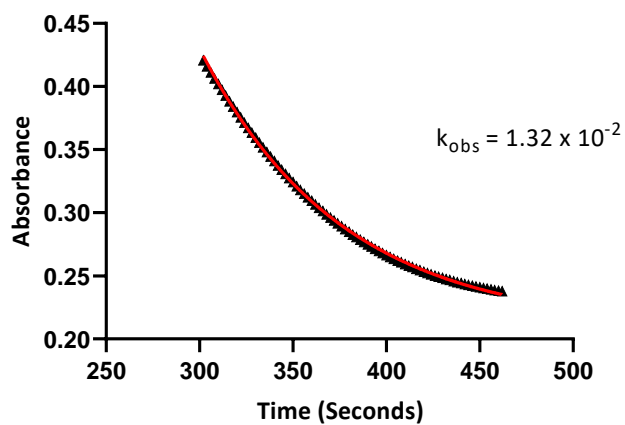
**Fit of the Hydrolysis of Cephalothin (0.2 mM) by P99 (5 nM) at pH 9.0 at 30 °C and  $I = 1M$  (KCl)**

Figure 6.16: Curve fit of the hydrolysis of cephalothin (0.2 mM) catalysed by P99 (5 nM) at pH 9.0 obtained using GraphPad Prism (black triangles = experimental data, red line = curve fit from software).

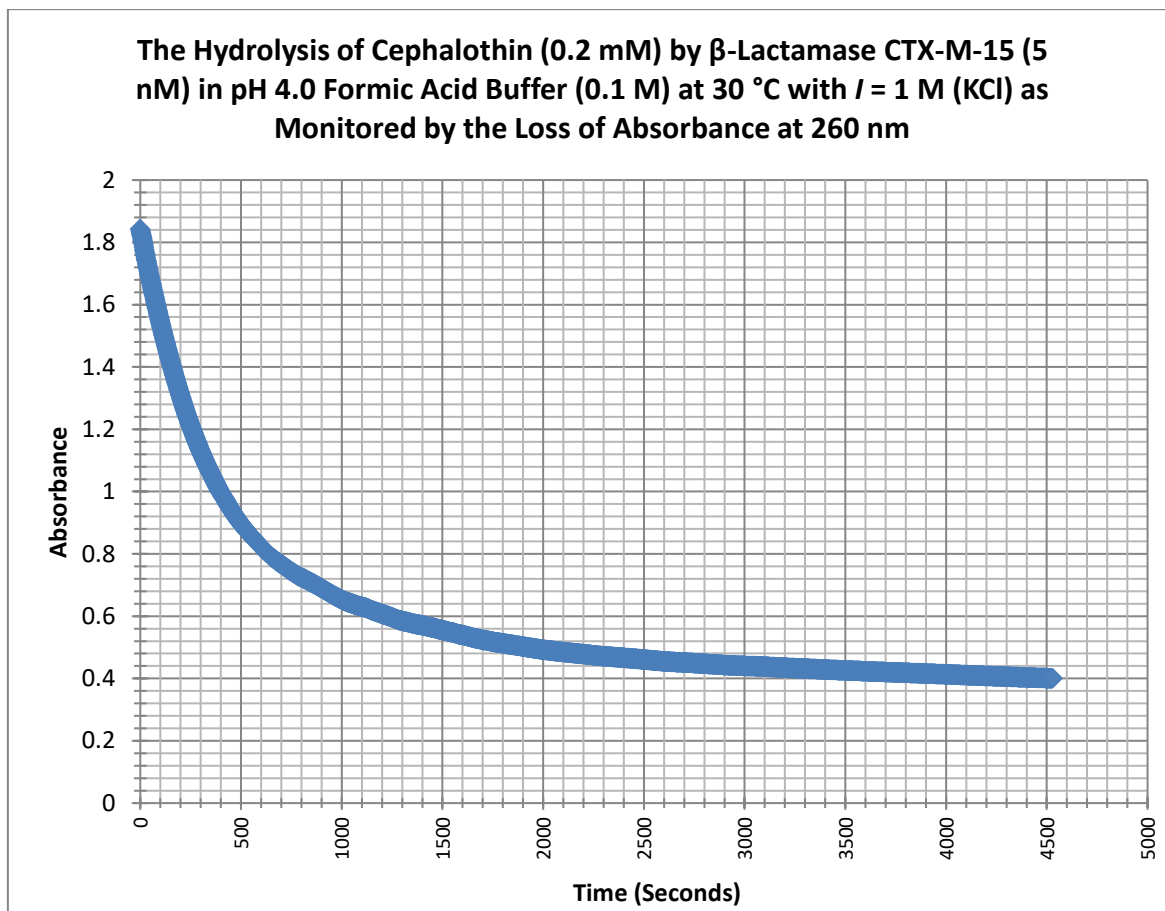
**6.10.2: CTX-M-15 Catalysed Cephalothin Hydrolysis Additional Data**

Figure 6.17: CTX-M-15 (5 nM) catalysed hydrolysis of cephalothin (0.2 mM) at pH 4.0.

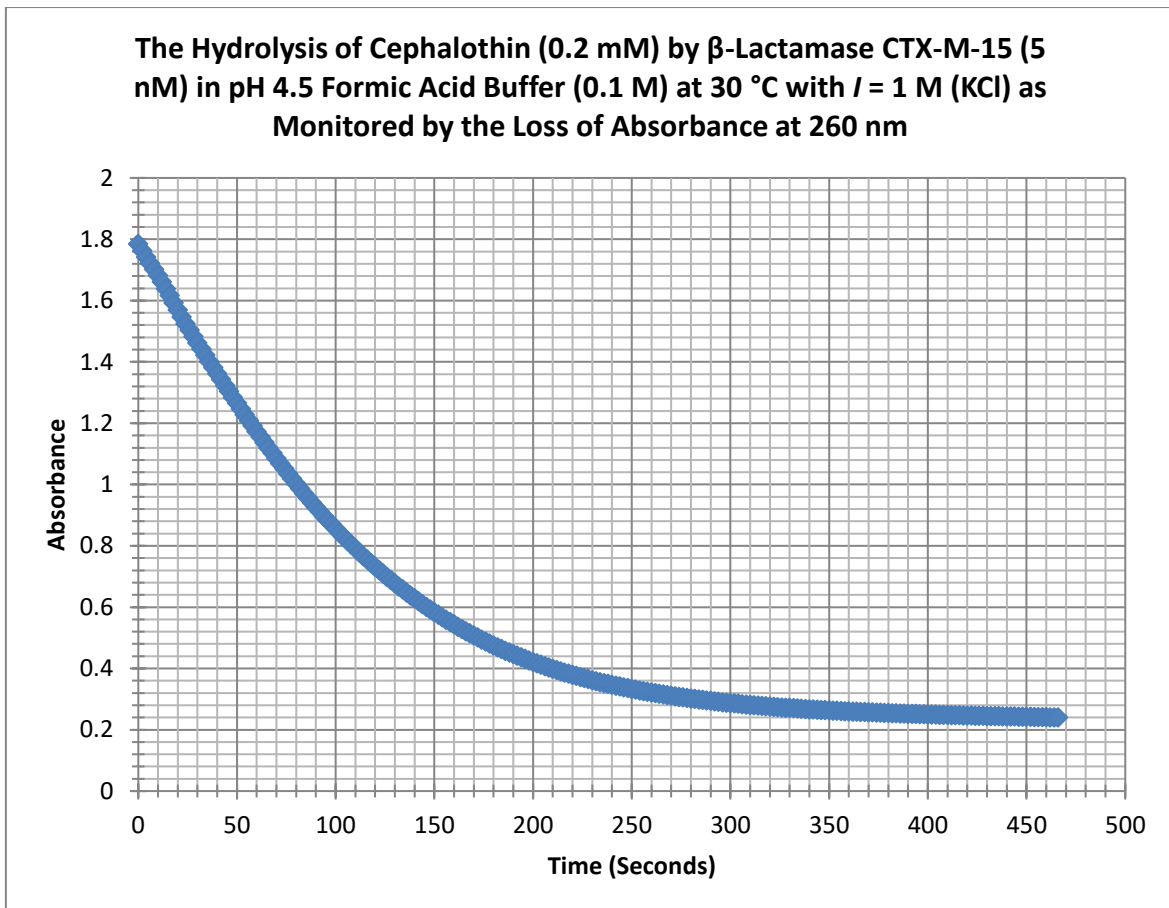


Figure 6.18: CTX-M-15 (5 nM) catalysed hydrolysis of cephalothin (0.2 mM) at pH 4.5.

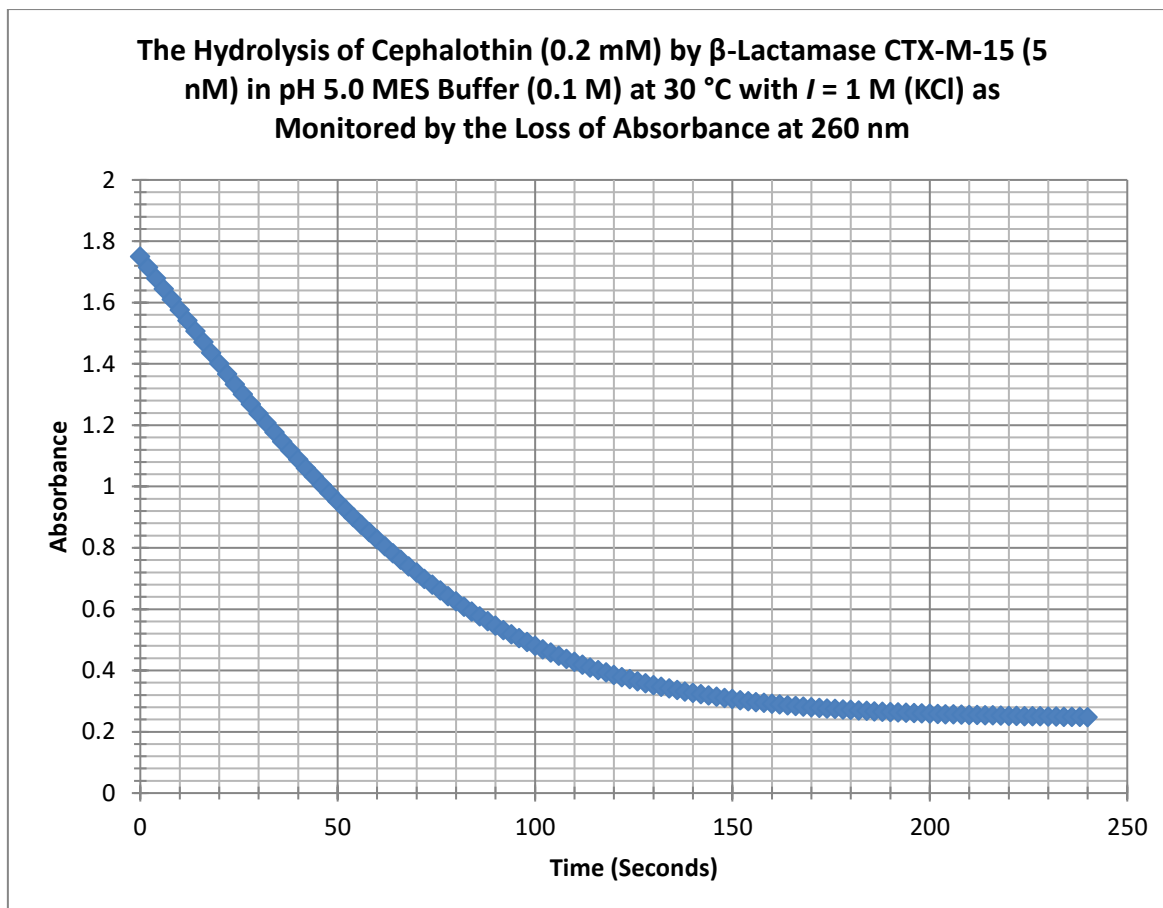


Figure 6.19: CTX-M-15 (5 nM) catalysed hydrolysis of cephalothin (0.2 mM) at pH 5.0.

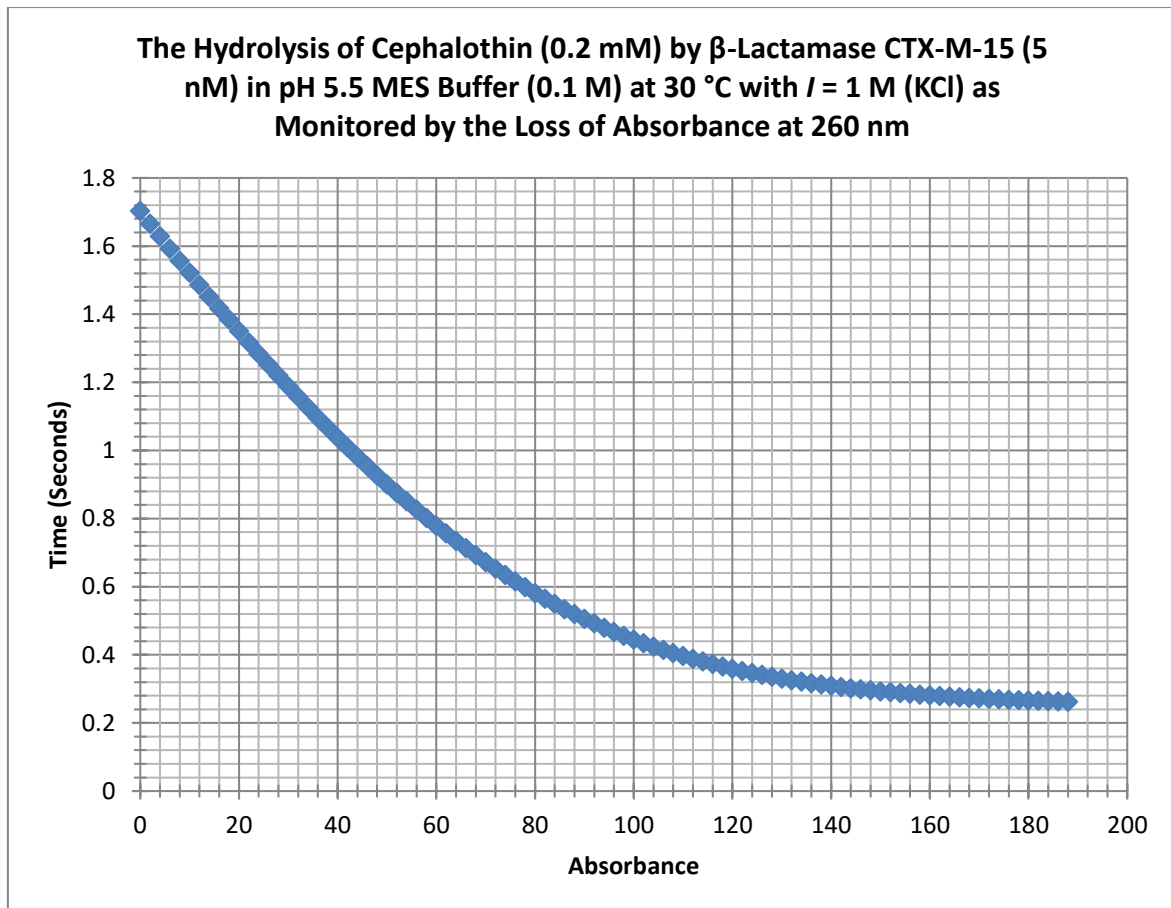


Figure 6.20: CTX-M-15 (5 nM) catalysed hydrolysis of cephalothin (0.2 mM) at pH 5.5.

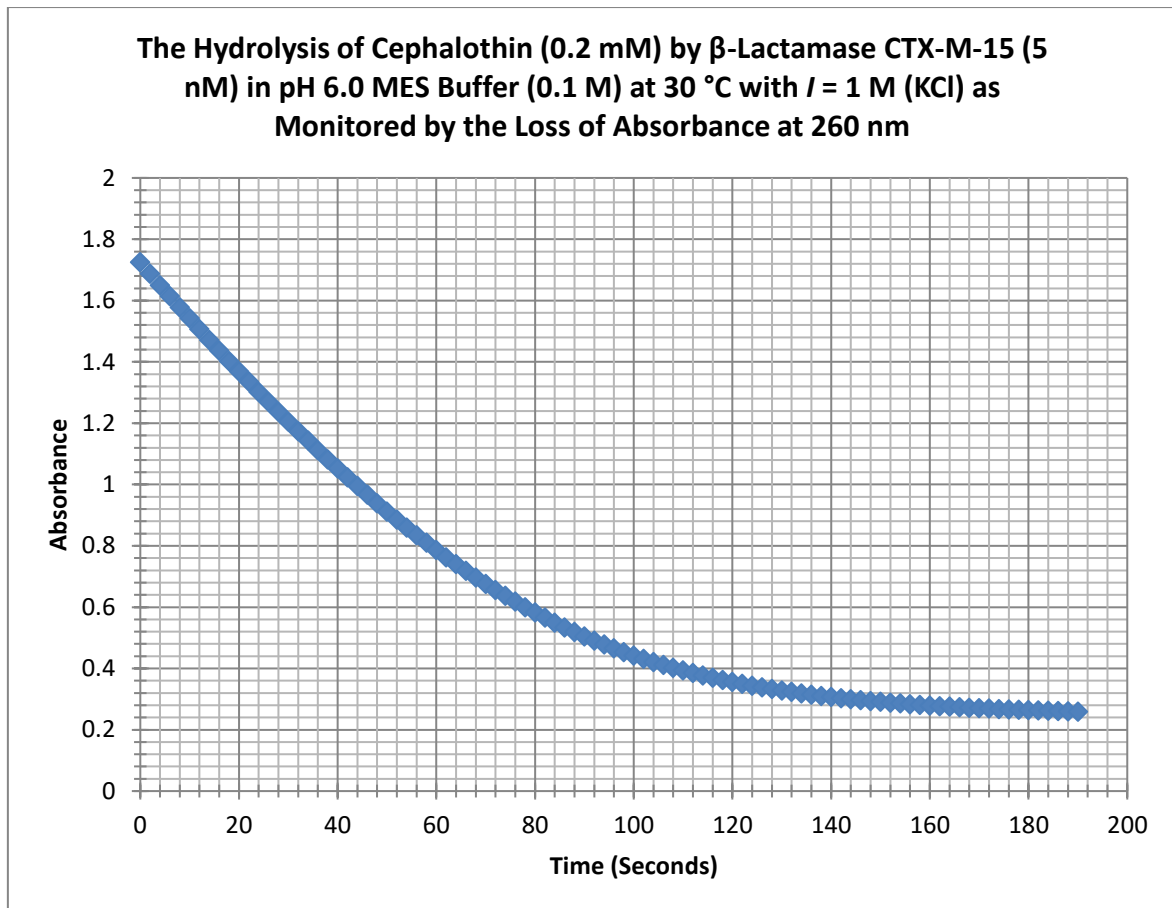


Figure 6.21: CTX-M-15 (5 nM) catalysed hydrolysis of cephalothin (0.2 mM) at pH 6.0.

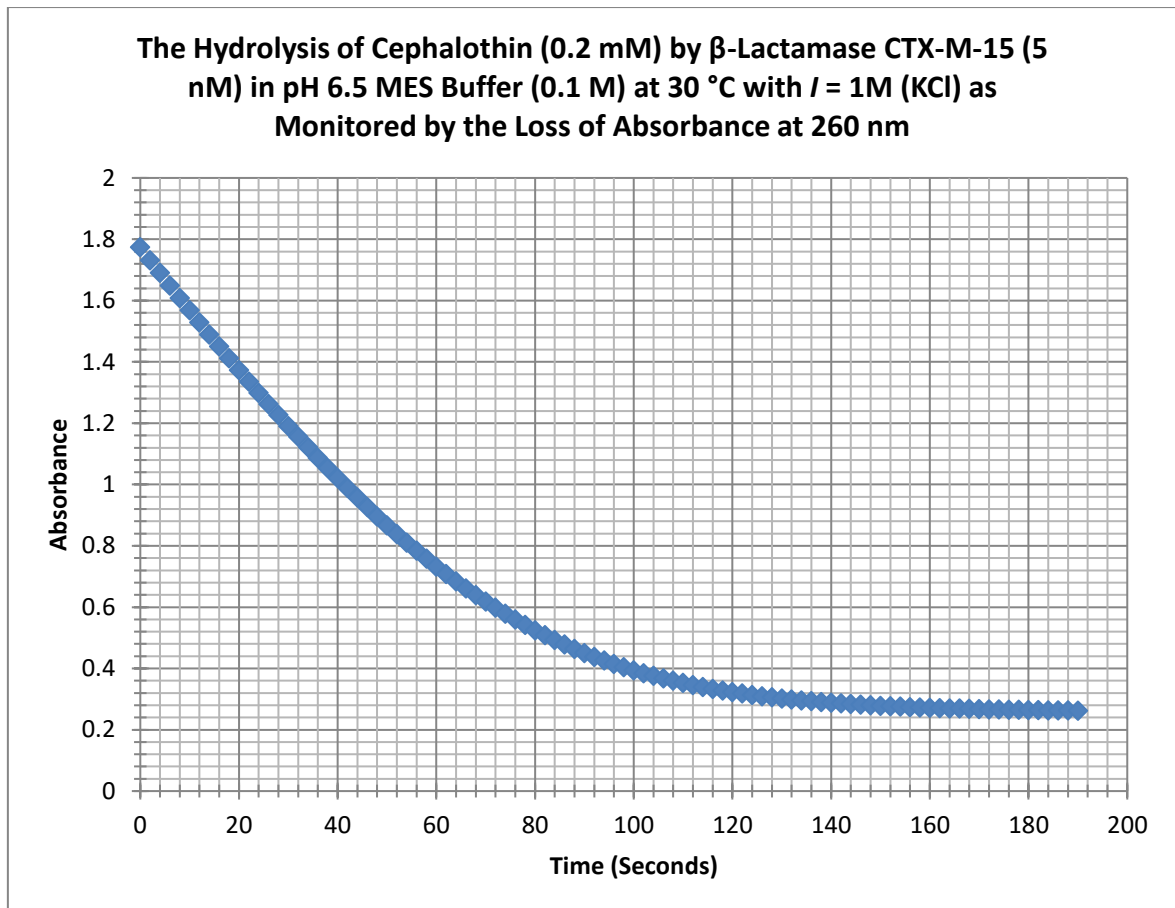


Figure 6.22: CTX-M-15 (5 nM) catalysed hydrolysis of cephalothin (0.2 mM) at pH 6.5.

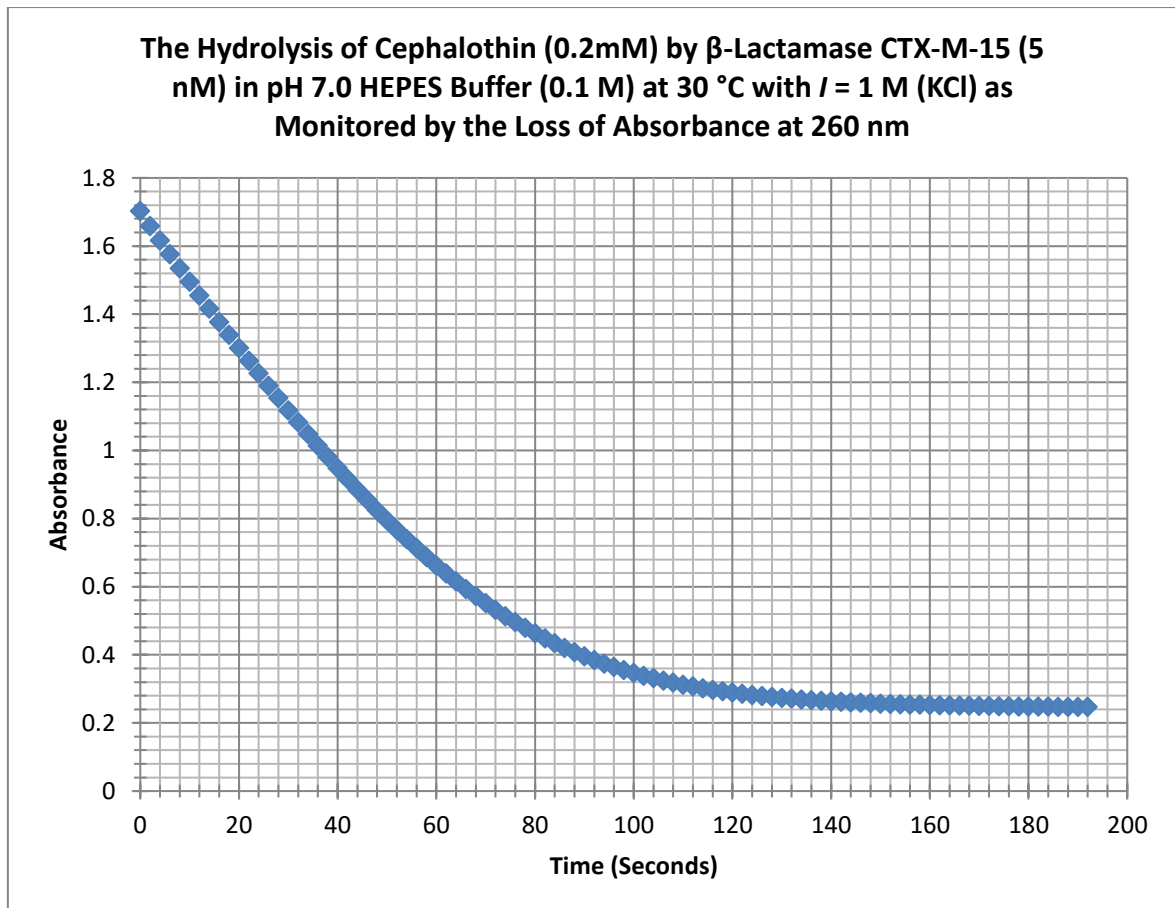


Figure 6.23: CTX-M-15 (5 nM) catalysed hydrolysis of cephalothin (0.2 mM) at pH 7.0.

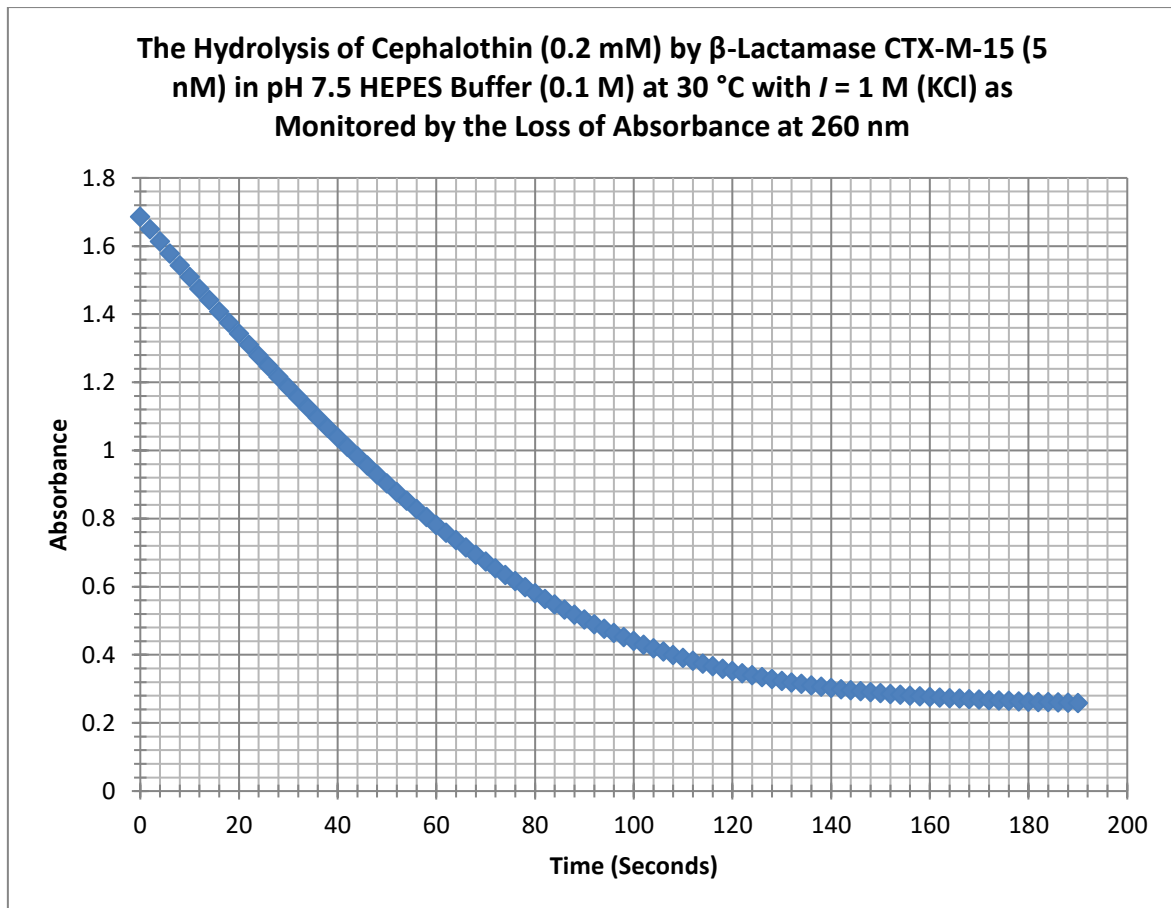


Figure 6.24: CTX-M-15 (5 nM) catalysed hydrolysis of cephalothin (0.2 mM) at pH 7.5.

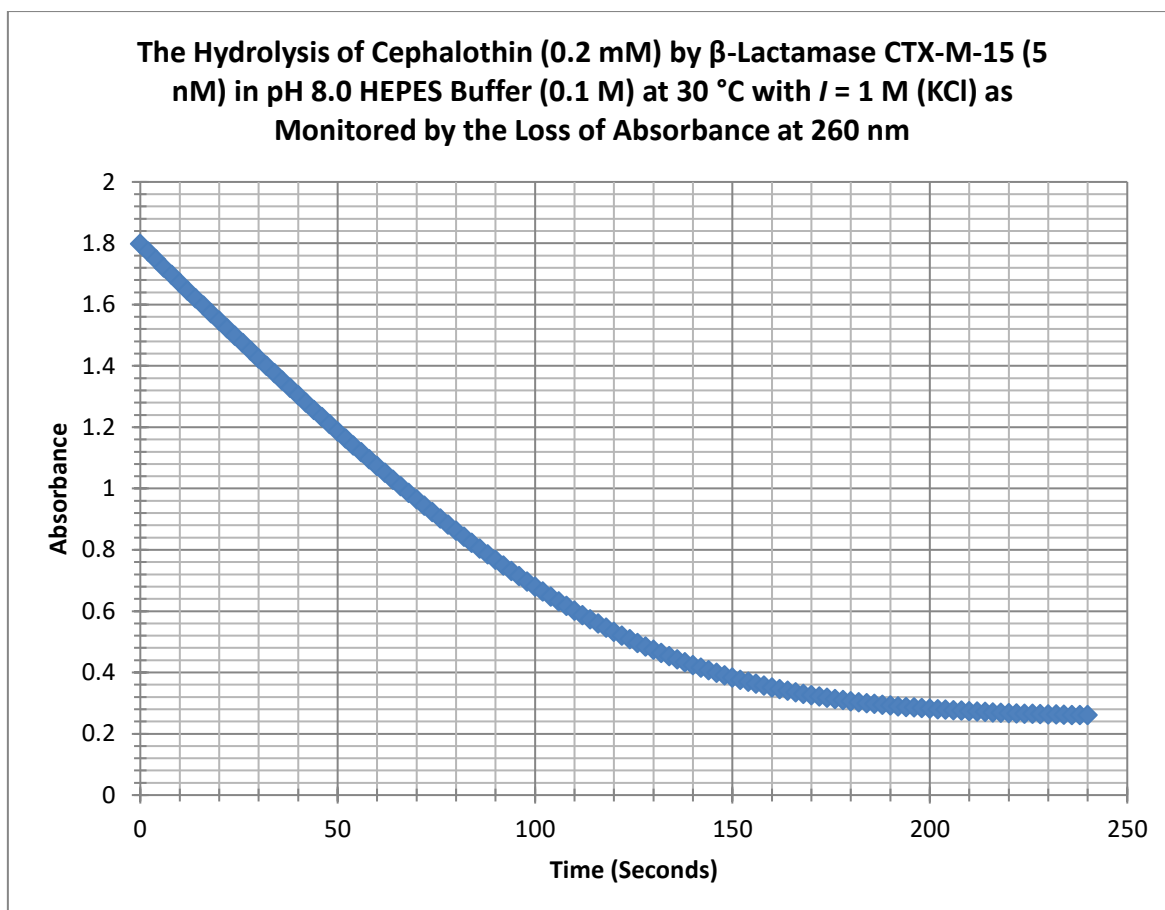


Figure 6.25: CTX-M-15 (5 nM) catalysed hydrolysis of cephalothin (0.2 mM) at pH 8.0.

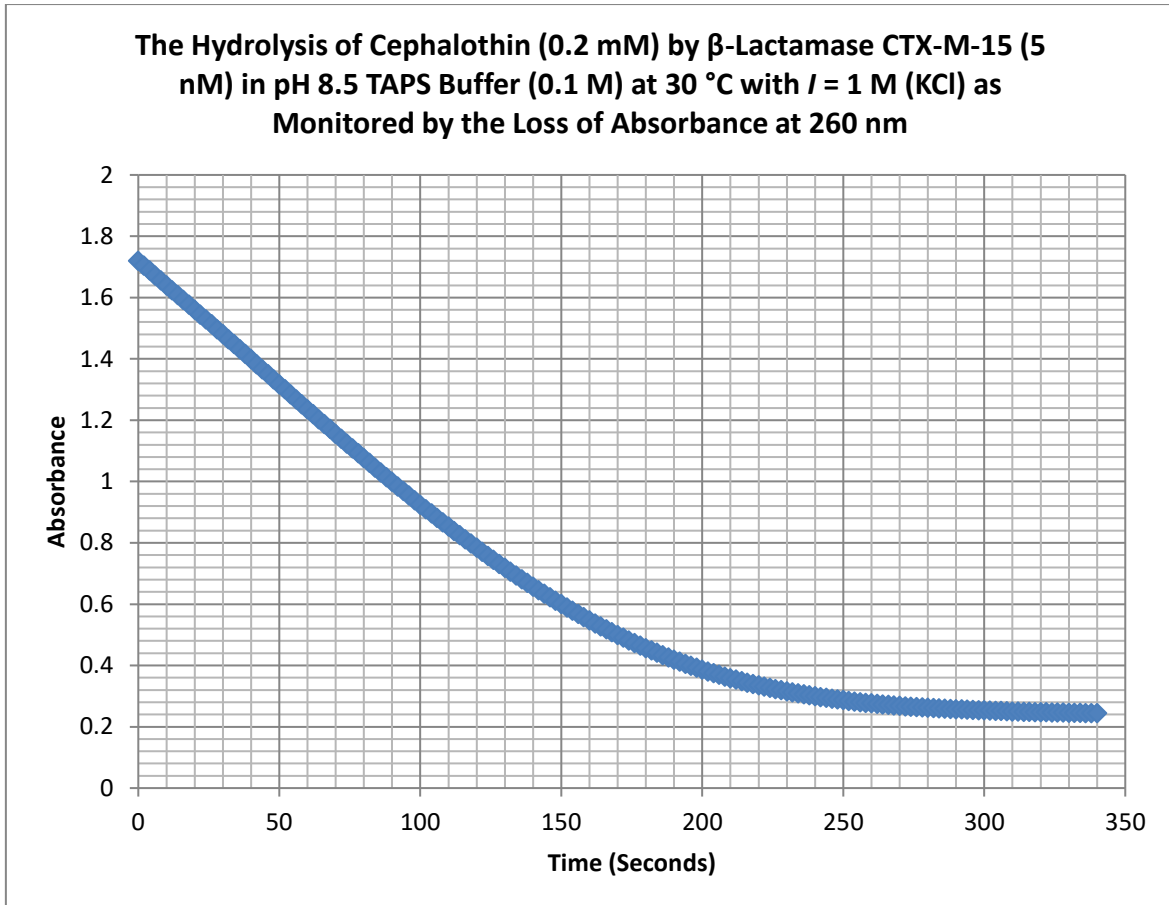


Figure 6.26: CTX-M-15 (5 nM) catalysed hydrolysis of cephalothin (0.2 mM) at pH 8.5.

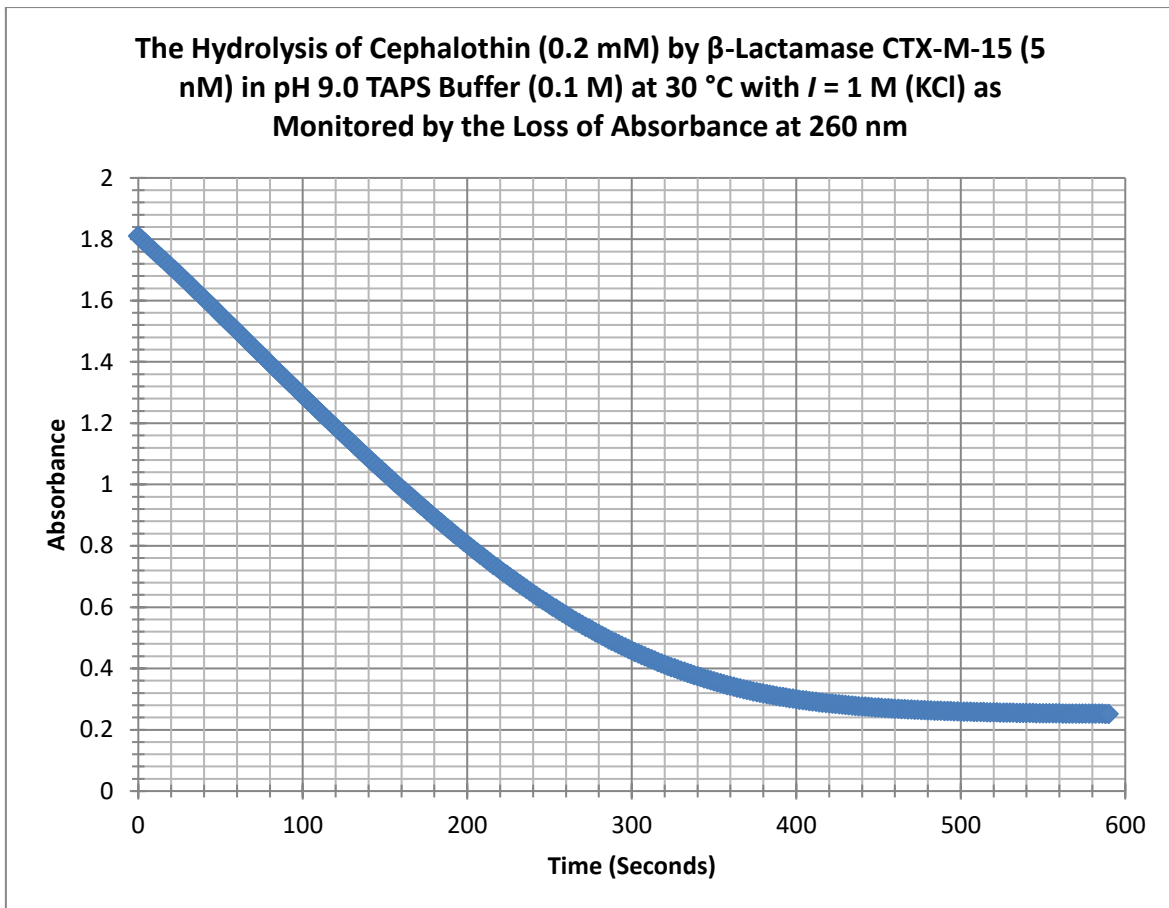


Figure 6.27: CTX-M-15 (5 nM) catalysed hydrolysis of cephalothin (0.2 mM) at pH 9.0.

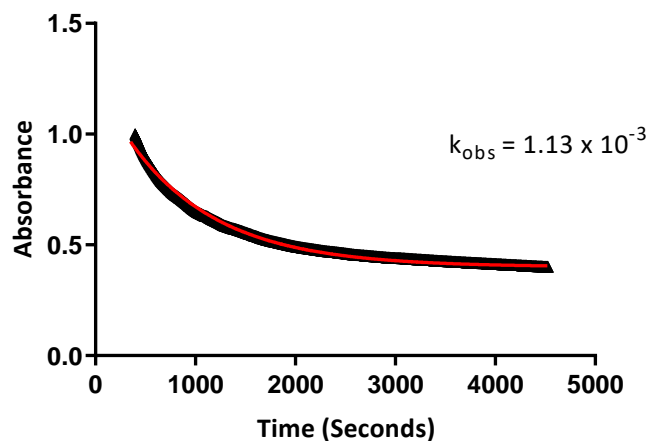
**Fit of the Hydrolysis of Cephalothin (0.2 mM) by CTX-M-15 (5 nM) at pH 4.0 at 30 °C and  $I = 1$  M (KCl)**

Figure 6.28: Curve fit of the hydrolysis of cephalothin (0.2 mM) catalysed by CTX-M-15 (5 nM) at pH 4.0 obtained using GraphPad Prism (black triangles = experimental data, red line = curve fit from software).

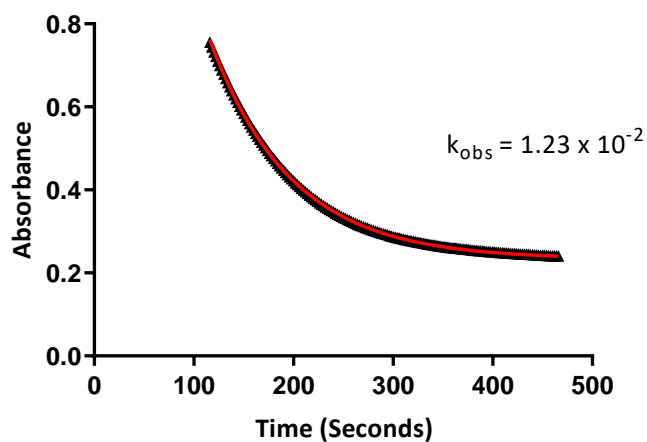
**Fit of the Hydrolysis of Cephalothin (0.2 mM) by CTX-M-15 (5 nM) at pH 4.5 at 30 °C and  $I = 1$  M (KCl)**

Figure 6.29: Curve fit of the hydrolysis of cephalothin (0.2 mM) catalysed by CTX-M-15 (5 nM) at pH 4.5 obtained using GraphPad Prism (black triangles = experimental data, red line = curve fit from software).

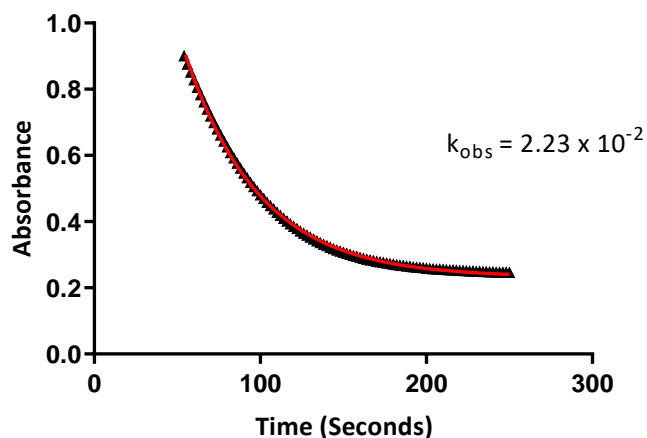
**Fit of the Hydrolysis of Cephalothin (0.2 mM) by CTX-M-15 (5 nM) at pH 5.0 at 30 °C and  $I = 1$  M (KCl)**

Figure 6.30: Curve fit of the hydrolysis of cephalothin (0.2 mM) catalysed by CTX-M-15 (5 nM) at pH 5.0 obtained using GraphPad Prism (black triangles = experimental data, red line = curve fit from software).

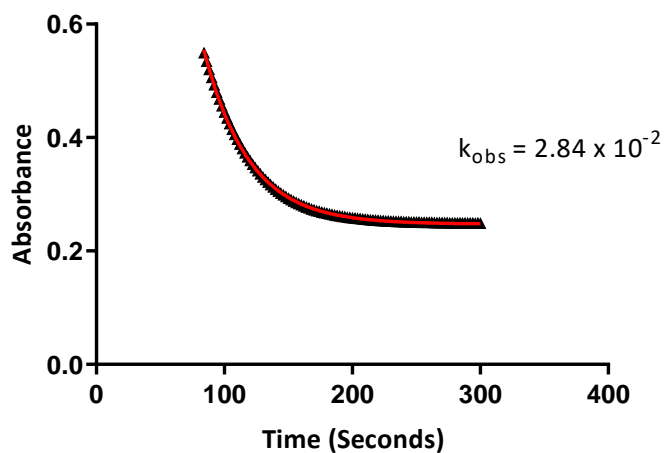
**Fit of the Hydrolysis of Cephalothin (0.2 mM) by CTX-M-15 (5 nM) at pH 5.5 at 30 °C and  $I = 1$  M (KCl)**

Figure 6.31: Curve fit of the hydrolysis of cephalothin (0.2 mM) catalysed by CTX-M-15 (5 nM) at pH 5.5 obtained using GraphPad Prism (black triangles = experimental data, red line = curve fit from software).

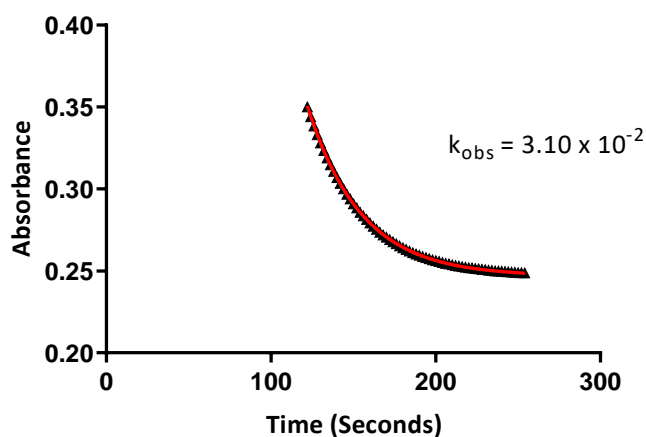
**Fit of the Hydrolysis of Cephalothin (0.2 mM) by CTX-M-15 (5 nM) at pH 6.0 at 30 °C and  $I = 1$  M (KCl)**

Figure 6.32: Curve fit of the hydrolysis of cephalothin (0.2 mM) catalysed by CTX-M-15 (5 nM) at pH 6.0 obtained using GraphPad Prism (black triangles = experimental data, red line = curve fit from software).

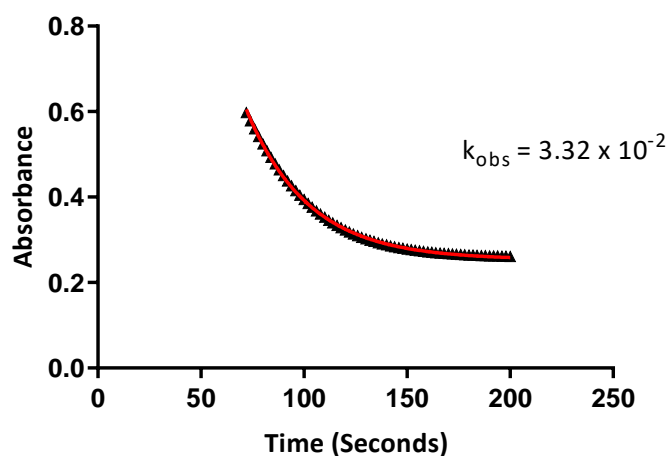
**Fit of the Hydrolysis of Cephalothin (0.2 mM) by CTX-M-15 (5 nM) at pH 6.5 at 30 °C and  $I = 1$  M (KCl)**

Figure 6.33: Curve fit of the hydrolysis of cephalothin (0.2 mM) catalysed by CTX-M-15 (5 nM) at pH 6.5 obtained using GraphPad Prism (black triangles = experimental data, red line = curve fit from software).

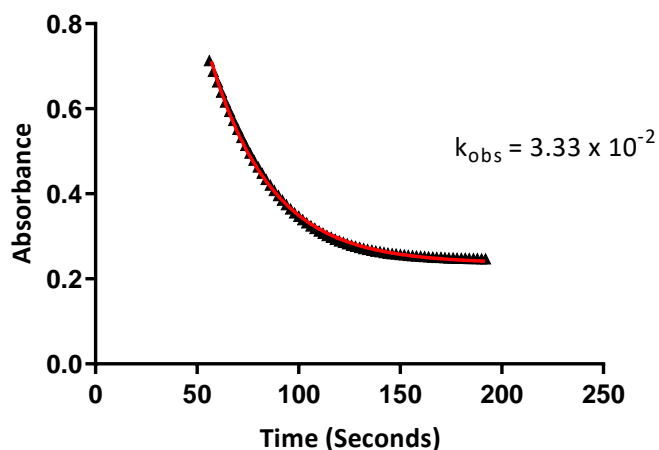
**Fit of the Hydrolysis of Cephalothin (0.2 mM) by CTX-M-15 (5 nM) at pH 7.0 at 30 °C and  $I = 1 \text{ M}$  (KCl)**

Figure 6.34: Curve fit of the hydrolysis of cephalothin (0.2 mM) catalysed by CTX-M-15 (5 nM) at pH 7.0 obtained using GraphPad Prism (black triangles = experimental data, red line = curve fit from software).

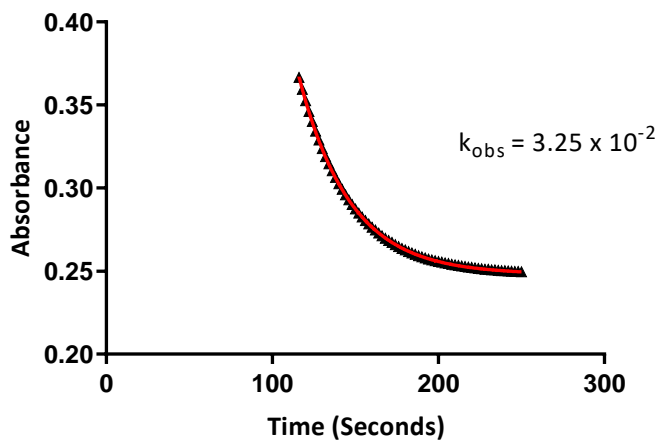
**Fit of the Hydrolysis of Cephalothin (0.2 mM) by CTX-M-15 (5 nM) at pH 7.5 at 30 °C and  $I = 1 \text{ M}$  (KCl)**

Figure 6.35: Curve fit of the hydrolysis of cephalothin (0.2 mM) catalysed by CTX-M-15 (5 nM) at pH 7.5 obtained using GraphPad Prism (black triangles = experimental data, red line = curve fit from software).

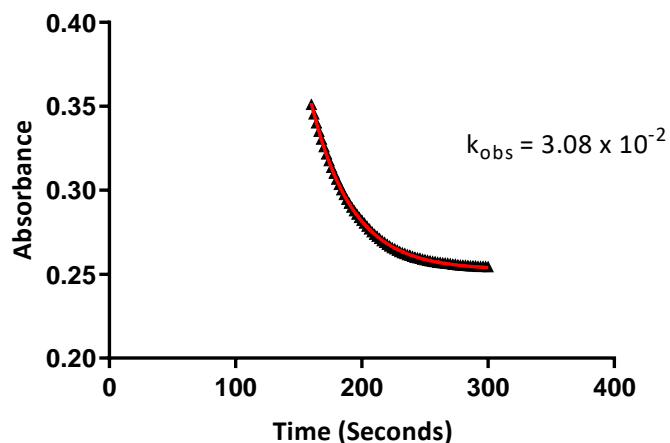
**Fit of the Hydrolysis of Cephalothin (0.2 mM) by CTX-M-15 (5 nM) at pH 8.0 at 30 °C and  $I = 1$  M (KCl)**

Figure 6.36: Curve fit of the hydrolysis of cephalothin (0.2 mM) catalysed by CTX-M-15 (5 nM) at pH 8.0 obtained using GraphPad Prism (black triangles = experimental data, red line = curve fit from software).

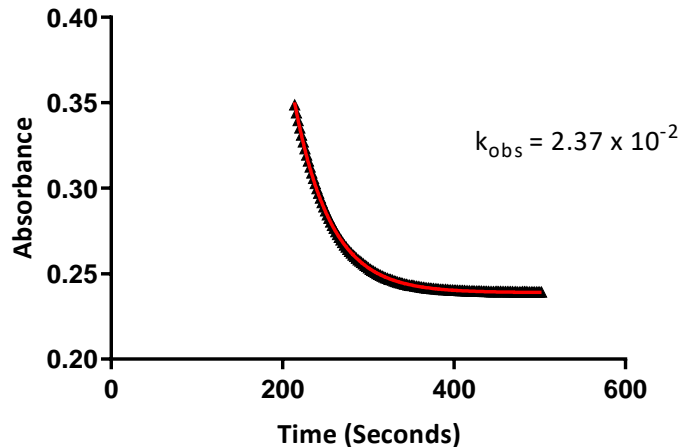
**Fit of the Hydrolysis of Cephalothin (0.2 mM) by CTX-M-15 (5 nM) at pH 8.5 at 30 °C and  $I = 1$  M (KCl)**

Figure 6.37: Curve fit of the hydrolysis of cephalothin (0.2 mM) catalysed by CTX-M-15 (5 nM) at pH 8.5 obtained using GraphPad Prism (black triangles = experimental data, red line = curve fit from software).

Fit of the Hydrolysis of Cephalothin (0.2 mM) by CTX-M-15 (5 nM) at pH 9.0 at 30 °C and  $I = 1\text{ M}$  (KCl)

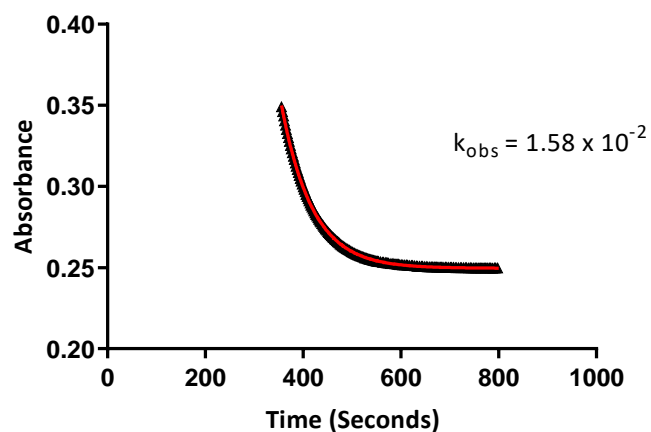


Figure 6.38: Curve fit of the hydrolysis of cephalothin (0.2 mM) catalysed by CTX-M-15 (5 nM) at pH 9.0 obtained using GraphPad Prism (black triangles = experimental data, red line = curve fit from software).

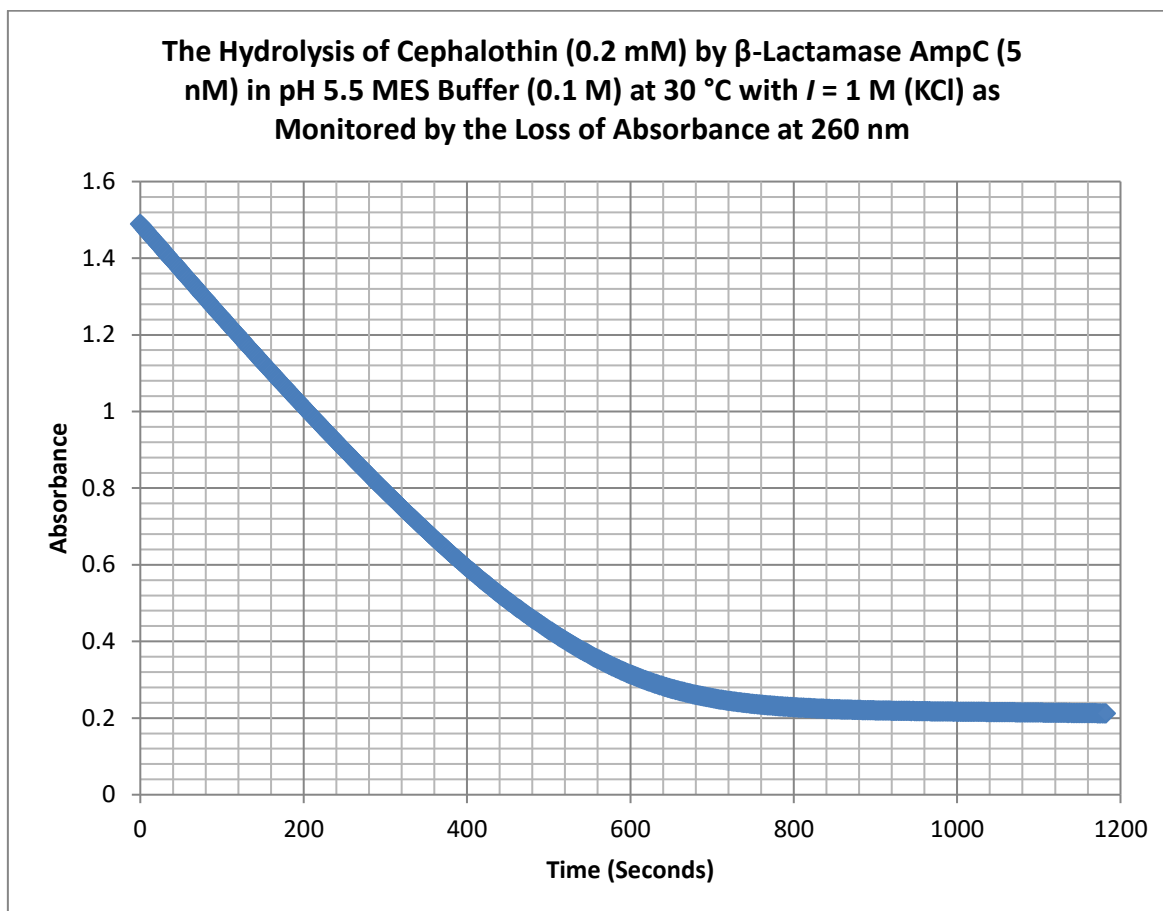
**6.10.3: AmpC Catalysed Cephalothin Hydrolysis Additional Data**

Figure 6.39: AmpC (5 nM) catalysed hydrolysis of cephalothin (0.2 mM) at pH 5.5.

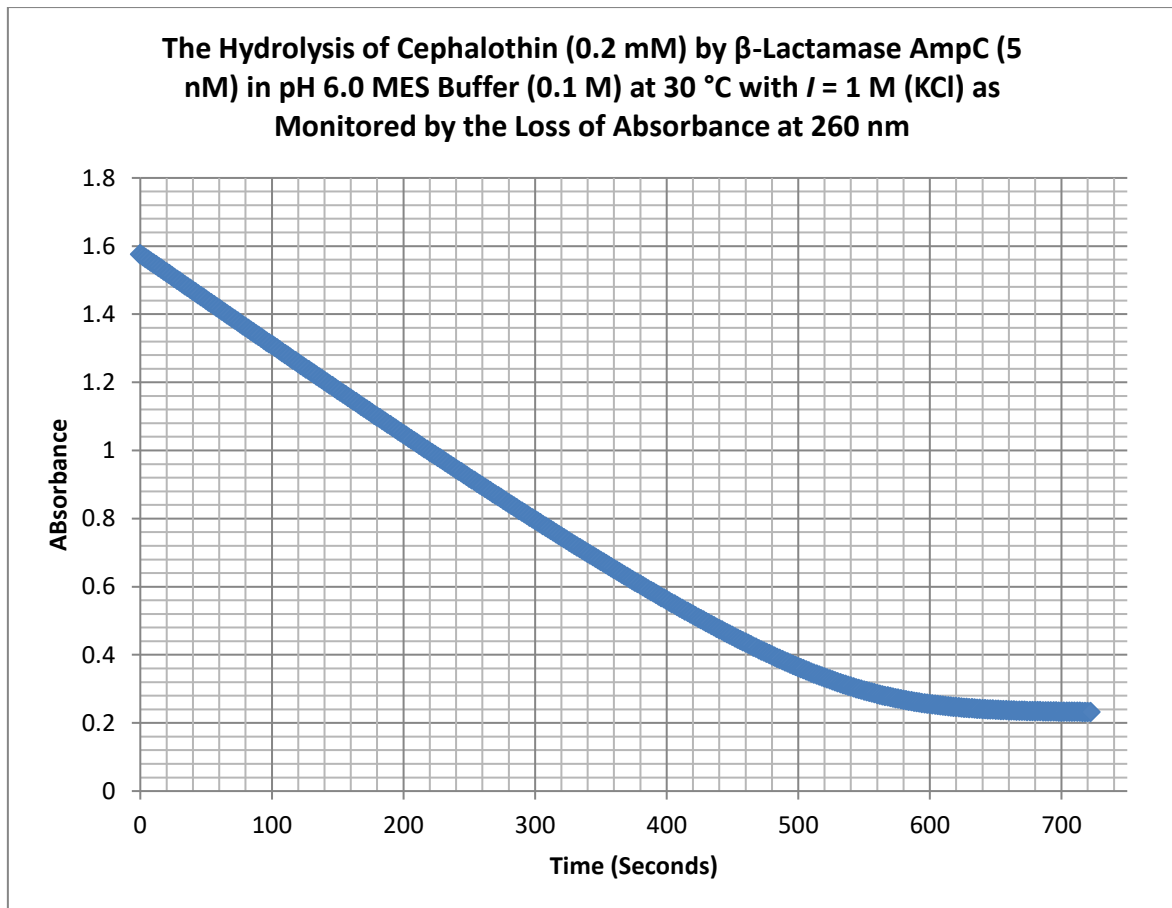


Figure 6.40: AmpC (5 nM) catalysed hydrolysis of cephalothin (0.2 mM) at pH 6.0.

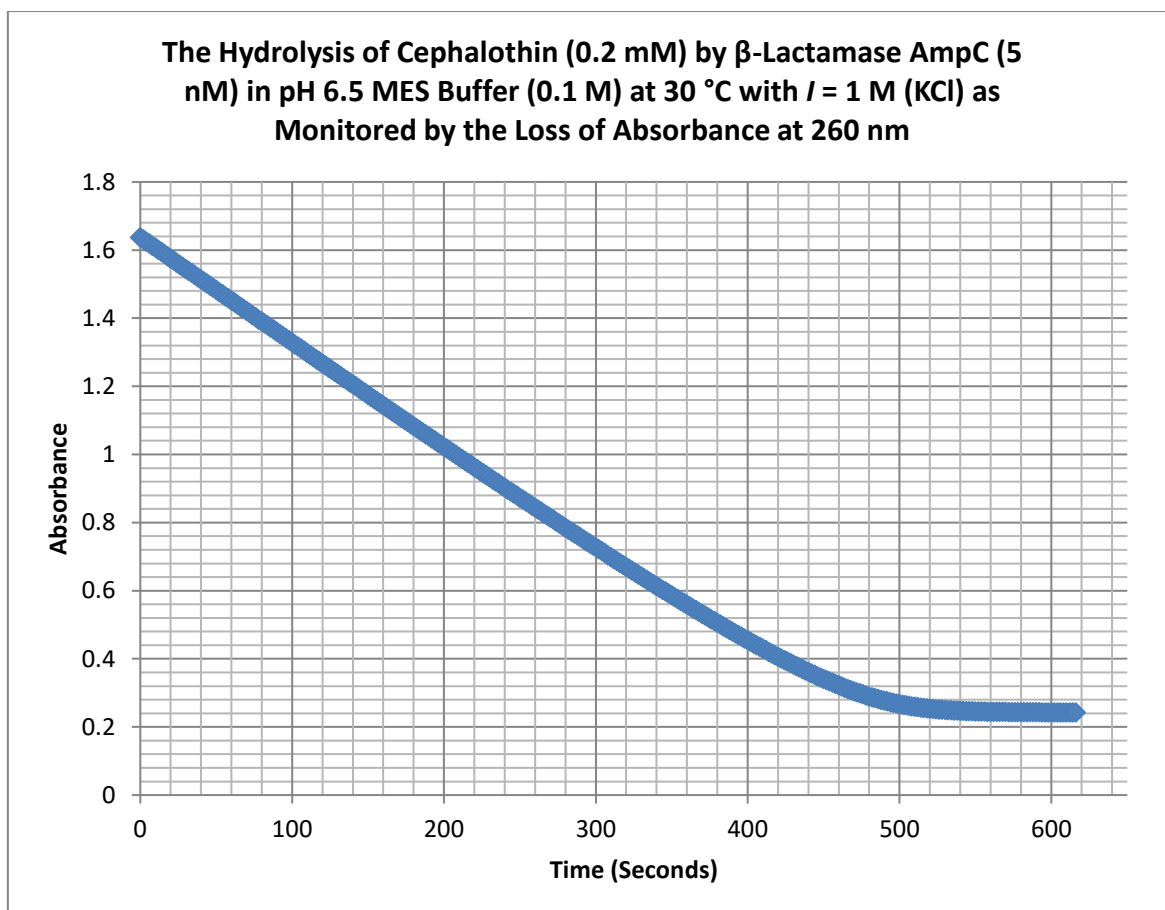


Figure 6.41: AmpC (5 nM) catalysed hydrolysis of cephalothin (0.2 mM) at pH 6.5.

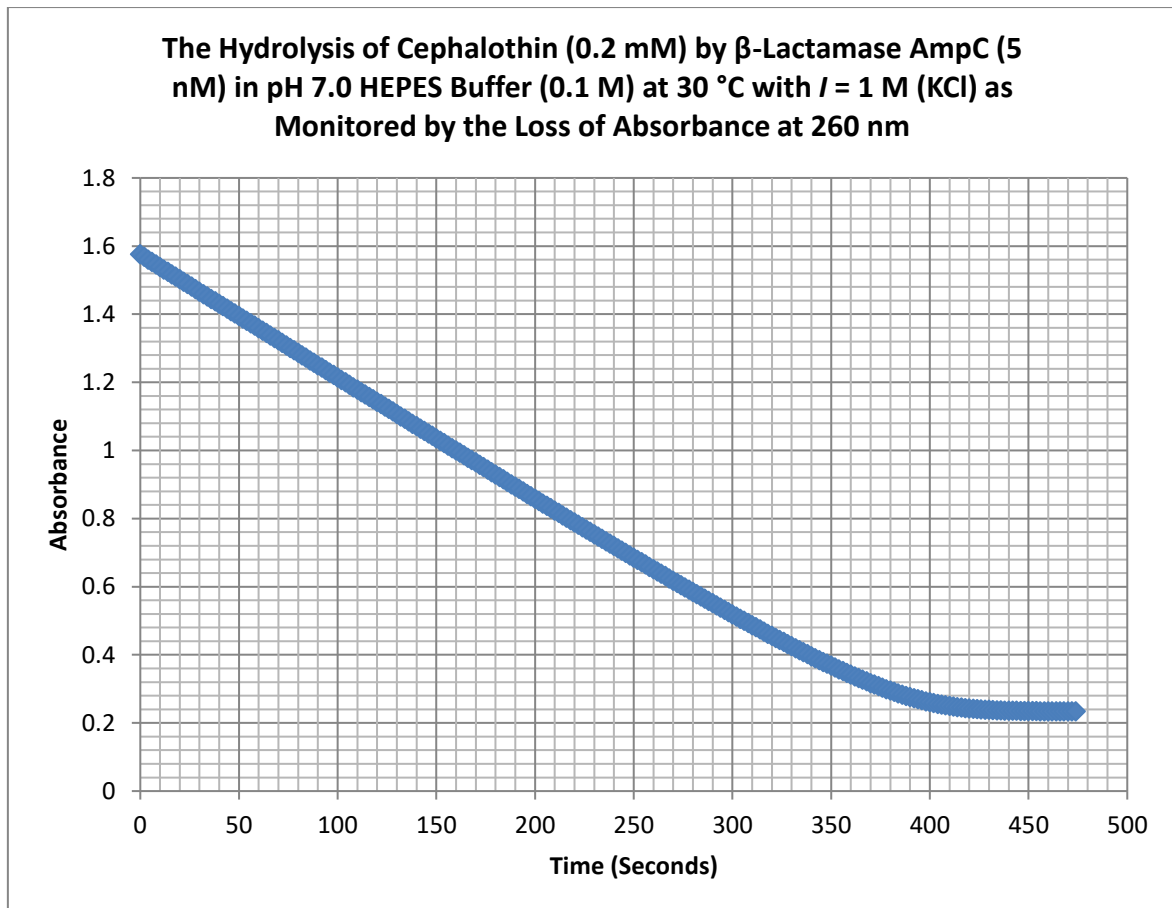


Figure 6.42: AmpC (5 nM) catalysed hydrolysis of cephalothin (0.2 mM) at pH 7.0.

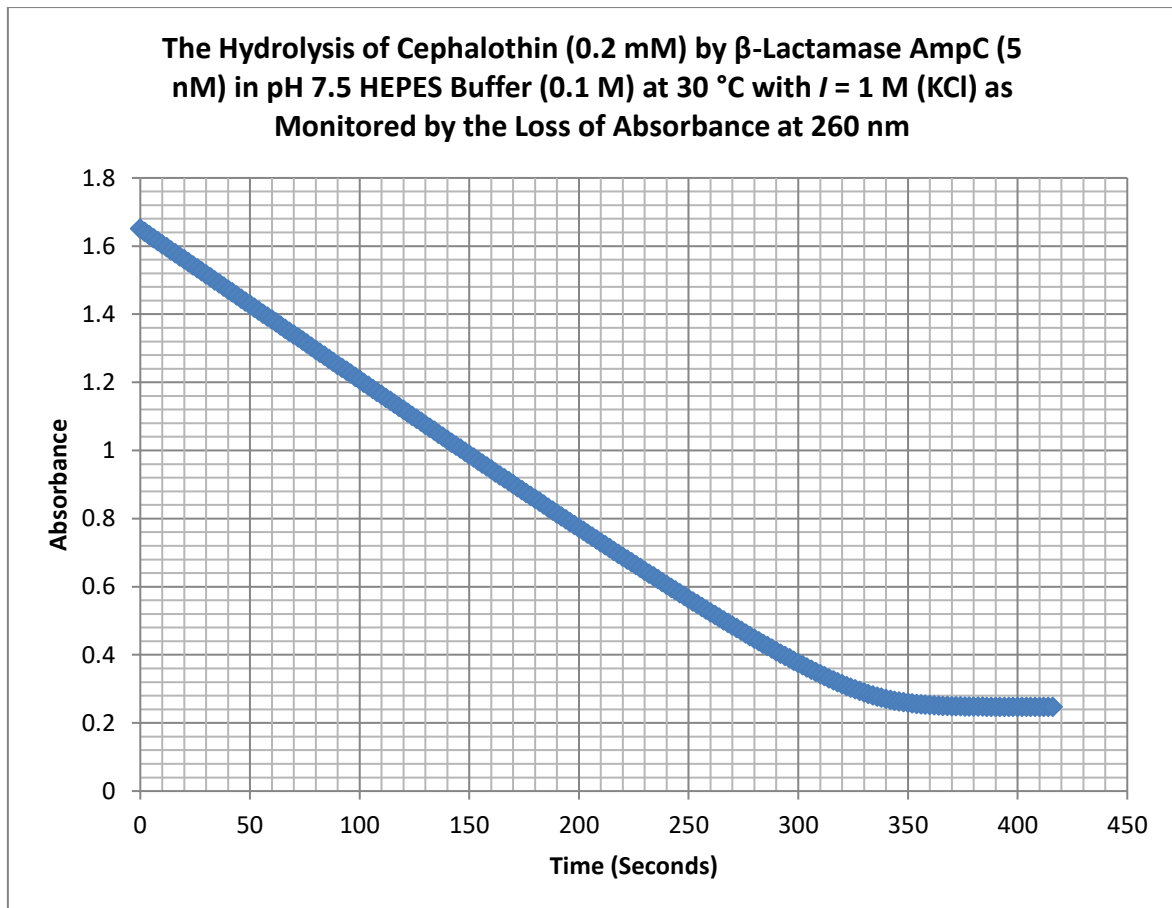


Figure 6.43: AmpC (5 nM) catalysed hydrolysis of cephalothin (0.2 mM) at pH 7.5.

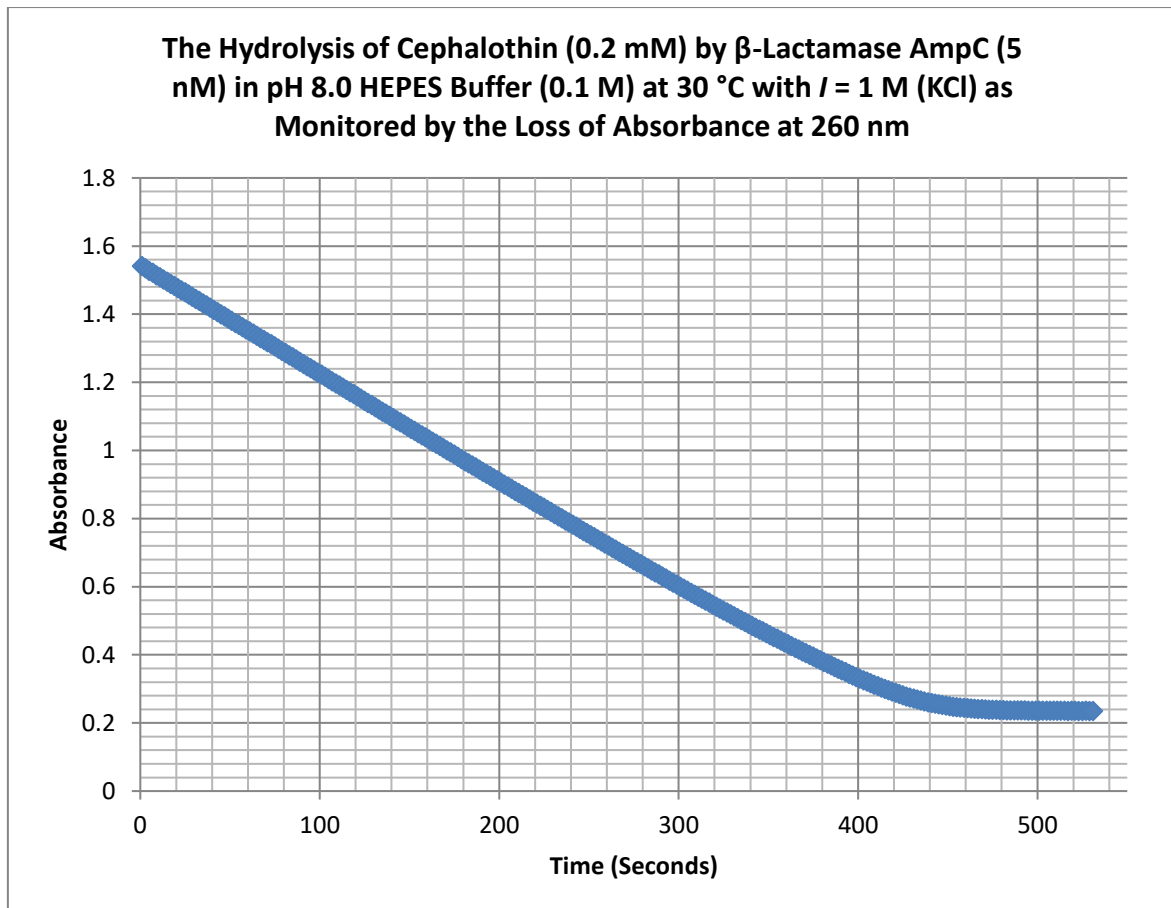


Figure 6.44: AmpC (5 nM) catalysed hydrolysis of cephalothin (0.2 mM) at pH 8.0.

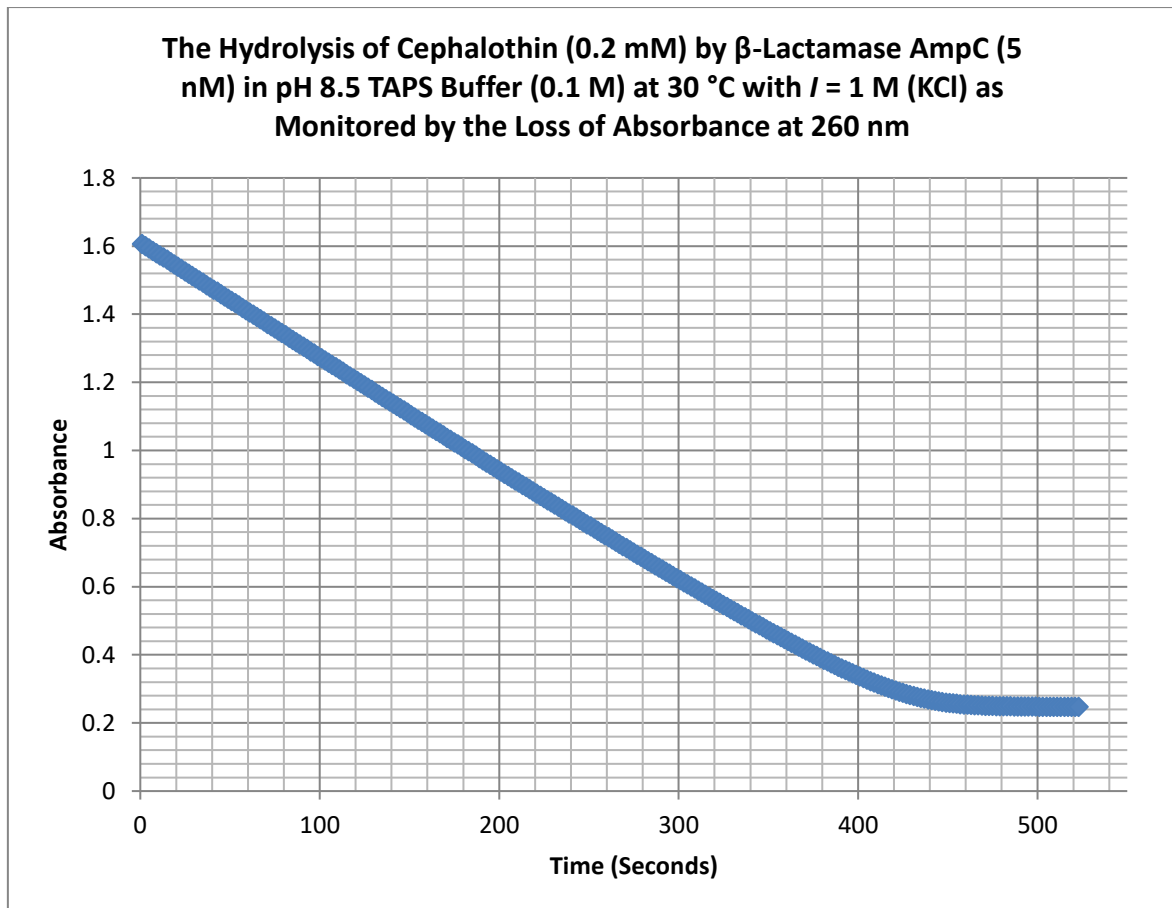


Figure 6.45: AmpC (5 nM) catalysed hydrolysis of cephalothin (0.2 mM) at pH 8.5.

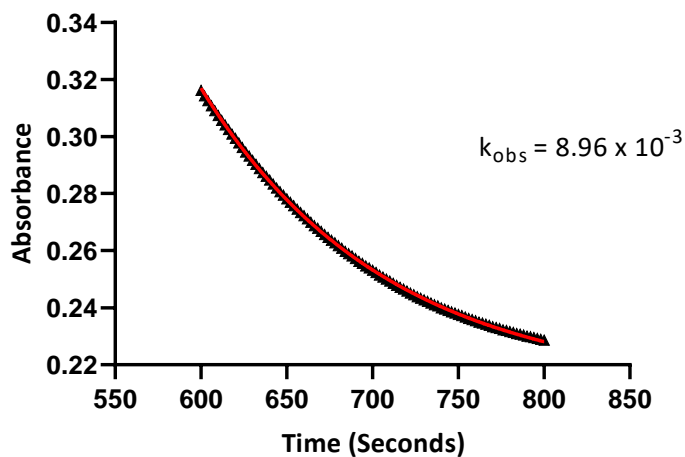
**Fit of the Hydrolysis of Cephalothin (0.2 mM) by AmpC (5 nM) at pH 5.5 at 30 °C and  $I = 1$  M (KCl)**

Figure 6.46: Curve fit of the hydrolysis of cephalothin (0.2 mM) catalysed by AmpC (5 nM) at pH 5.5 obtained using GraphPad Prism (black triangles = experimental data, red line = curve fit from software).

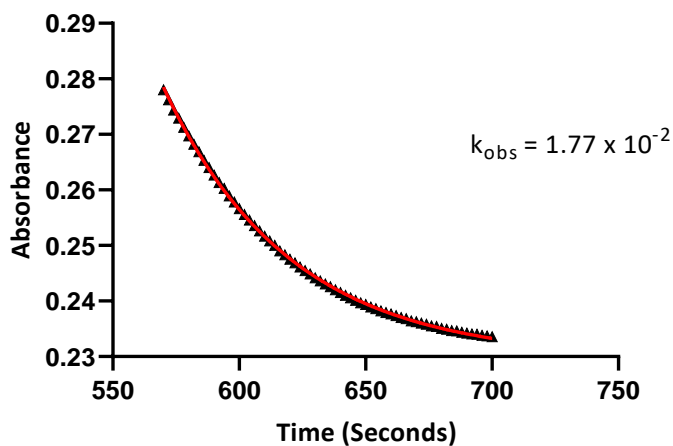
**Fit of the Hydrolysis of Cephalothin (0.2 mM) by AmpC (5 nM) at pH 6.0 at 30 °C and  $I = 1$  M (KCl)**

Figure 6.47: Curve fit of the hydrolysis of cephalothin (0.2 mM) catalysed by AmpC (5 nM) at pH 6.0 obtained using GraphPad Prism (black triangles = experimental data, red line = curve fit from software).

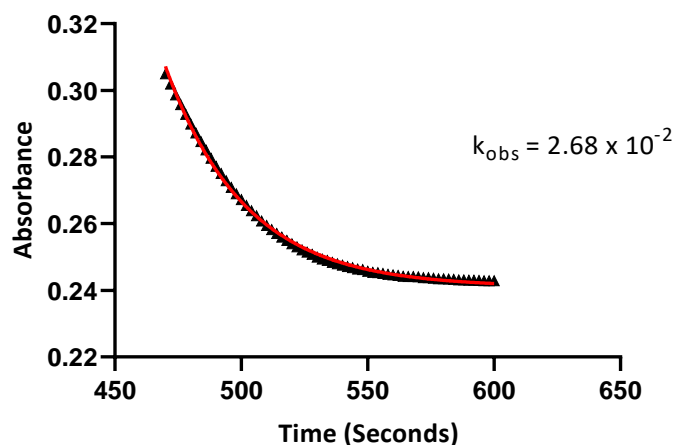
**Fit of the Hydrolysis of Cephalothin (0.2 mM) by AmpC (5 nM) at pH 6.5 at 30 °C and  $I = 1\text{ M}$  (KCl)**

Figure 6.48: Curve fit of the hydrolysis of cephalothin (0.2 mM) catalysed by AmpC (5 nM) at pH 6.5 obtained using GraphPad Prism (black triangles = experimental data, red line = curve fit from software).

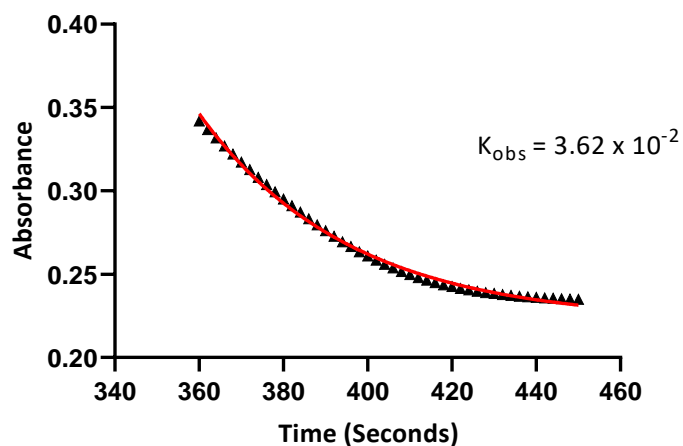
**Fit of the Hydrolysis of Cephalothin (0.2 mM) by AmpC (5 nM) at pH 7.0 at 30 °C and  $I = 1\text{ M}$  (KCl)**

Figure 6.49: Curve fit of the hydrolysis of cephalothin (0.2 mM) catalysed by AmpC (5 nM) at pH 7.0 obtained using GraphPad Prism (black triangles = experimental data, red line = curve fit from software).

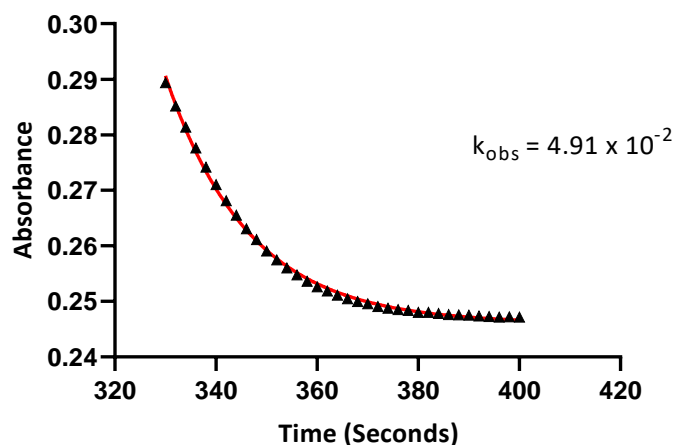
**Fit of the Hydrolysis of Cephalothin (0.2 mM) by AmpC (5 nM) at pH 7.5 at 30 °C and  $I = 1$  M (KCl)**

Figure 6.50: Curve fit of the hydrolysis of cephalothin (0.2 mM) catalysed by AmpC (5 nM) at pH 7.5 obtained using GraphPad Prism (black triangles = experimental data, red line = curve fit from software).

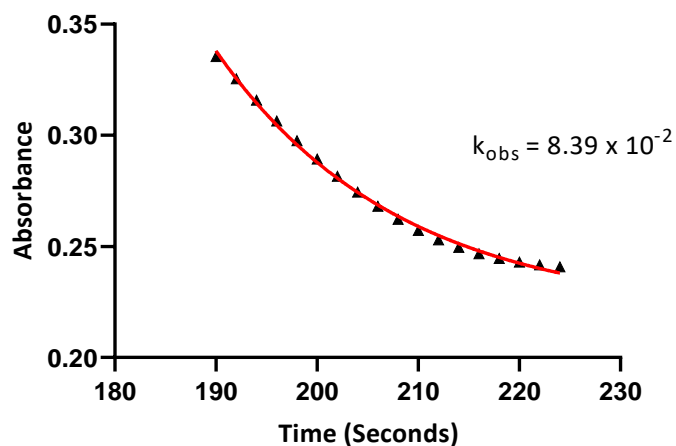
**Fit of the Hydrolysis of Cephalothin (0.2 mM) by AmpC (5 nM) at pH 8.0 at 30 °C and  $I = 1$  M (KCl)**

Figure 6.51: Curve fit of the hydrolysis of cephalothin (0.2 mM) catalysed by AmpC (5 nM) at pH 8.0 obtained using GraphPad Prism (black triangles = experimental data, red line = curve fit from software).

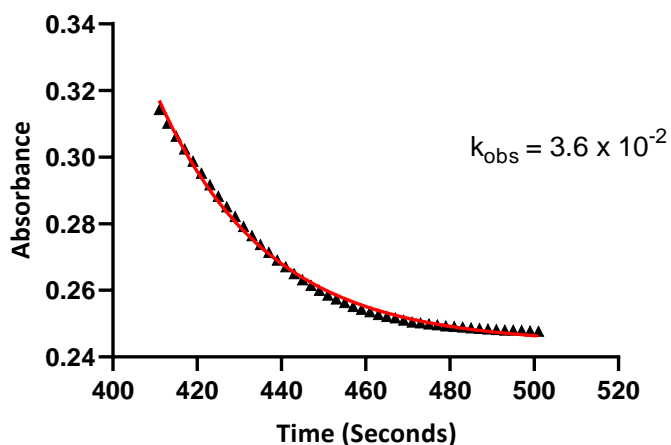
**Fit of the Hydrolysis of Cephalothin (0.2 mM) by AmpC (5 nM) at pH 8.5 at 30 °C and  $I = 1 \text{ M}$  (KCl)**

Figure 6.52: Curve fit of the hydrolysis of cephalothin (0.2 mM) catalysed by AmpC (5 nM) at pH 8.5 obtained using GraphPad Prism (black triangles = experimental data, red line = curve fit from software).

### 6.11: Scan UV Experiments

All scan UV experiments were performed on an Agilent Technologies Cary UV-Vis 4000 instrument in a quartz UV cell with a 1 cm path length, operated with Cary Win UV Scan software application. All samples were baseline blanked with all sample components minus the analyte (for example, cephalothin or carbamate inhibitor in the case of the carbamate hydrolysis experiments). The scan settings for the cephalothin experiments were as follows:

Table 6.9: UV scan parameters.

Parameter	Setting
Start wavelength (nm)	800
End wavelength (nm)	200
Average time (s)	0.100
Data interval (nm)	1.000
Scan rate (nm/min)	600
Source changeover (nm)	350
Thermostatted (°C)	30

### 6.12: pH Adjustments

All pH adjustments were performed using a Mettler Toledo FE20/FG2 pH meter coupled to a Mettler Toledo Inlab Routine Pro Electrode. The pH meter/probe were always subjected to a two point calibration prior to use using appropriate buffer solutions purchased from Fisher Scientific. Probes were washed with ultra-pure water and stored in 3 M KCl when not in use.

### 6.13: Enzyme Preparation and Purifications

As mentioned, the enzymes used in this thesis were a kind gift from Professor Schofield's group at the University of Oxford. However, their methods of production are summarised here (Cahill, 2017).

Enzyme proteins were produced in *E. coli* BL21 (DE3) at 37 °C using 2TY broth medium supplemented with 50 µg/ml<sup>-1</sup> ampicillin. Cells were grown until an optical density at 600

nm ( $OD_{600}$ ) of 0.6-0.7 was reached. Then, the bacterial cultures were taken out of the incubator and allowed to cool. They were then supplemented with ammonium iron(II) sulphate hexahydrate, the final concentration of which was adjusted to 50  $\mu$ M. The cells were incubated overnight at 37 °C in an orbital incubator and were harvested by centrifugation (10 minutes at 10,000 g).

To purify the enzymes, 20 g of the pellets were resuspended in 100 ml HisTrap Buffer A, supplemented with DNase I and PMSF (2  $g/L^{-1}$  final concentration), and lysed by sonication using a Vibra-Cell VCX 500 sonicator (SONICS, 10 minutes, 60 % amplitude, 10 seconds pulse, 10 seconds reset). The supernatant was loaded onto a 5 ml HisTrap HP column followed by extensive washing with HisTrap Buffer A before elution with a gradient of HisTrap buffer B in HisTrap Buffer A (20-500 mM imidazole). Fractions containing purified enzyme were concentrated by centrifugal ultrafiltration using an Amicon ultra 15 ml centricon with a 10 kDa molecular weight cut off (Millipore). The resultant solution was injected onto a Superdex S200 column (300 ml), pre-equilibrated with Gel Filtration Buffer, and eluted with an additional 300 ml of Gel Filtration Buffer. Fractions containing pure enzyme were incubated overnight at 4 °C with 3C protease. The 3C protease together with any uncleaved protein was removed from the digestion mixture with a second 5 ml HisTrap HP column, pre equilibrated with HisTrap Wash Buffer. Purified enzyme fractions, identified by SDS-PAGE analysis, were collected and concentrated by centrifugal ultrafiltration before buffer exchange into Exchange Buffer.

Polyacrylamide gels were made using the Mini-PROTEAN Tetra Cell system (Bio-Rad). In both running and stacking and gel preparation, tetramethylethylenediamine (TEMED) was added as the last component. During production, the running buffer was covered with a layer of propan-2-ol to prevent it from drying out whilst setting. This was subsequently

removed before pouring and setting of the stacking gel layer. SDS-PAGE gels were covered in wet tissue and stored at 4 °C until required.

20 µL of protein sample were mixed with 4 µL of SDS-PAGE Gel Loading Buffer. The samples were then heated at 100 °C on a hot block for 2 minutes before loading of up to 10 µL of each sample per well. Electrophoresis was carried out at a constant voltage of 160 V for 10 minutes followed by 180 V for 50 minutes using SDS-PAGE Running Buffer. Gels were subsequently stained for 10 minutes in SDS-Page Staining Solution and transferred into water. The gels were heated by microwaving until bands were visible before destaining overnight in water.

#### **6.14: NMR (Nuclear Magnetic Resonance) Analysis**

Proton NMR was used as a tool along with the LCMS experiments to confirm it was not avibactam that was carrying out the inhibition. Unfortunately, there was not enough time to fully characterise the HFA carbamate, but as was seen in the LCMS experiments, there was no sign of any avibactam. This, coupled with the fact that the HFA derivative was significantly more effective an inhibitor than avibactam, suggests that the HFA carbamate was correctly synthesised, but further work is needed to fully characterise the molecule.

NMR was carried out at 400 MHz Bruker 400 NMR instrument, and was used to the following parameters:

Table 7.0: NMR parameters.

NMR model	Bruker 400 MHz
Frequency	400 MHz
Probe	Z116098_0048
Pulse program	zg30
Size of FID	65536
Solvent	DMSO
Number of Scans	16
Dummy scans	2
Sweep Width	8223.685 Hz
Decay FID Res	0.250967 Hz
Acquisition time	3.985 sec
Receiver gain	25
Dwell time	60.800 $\mu$ sec
Pre-scan delay	10.69 $\mu$ sec
Temperature of acquisition	294.5 K
Delay time, D1	2 s
Nucleus	$^1\text{H}$ , $^{19}\text{F}$
90° pulse width	8.00 $\mu$ sec
Freq of observed channel	400.130 MHz

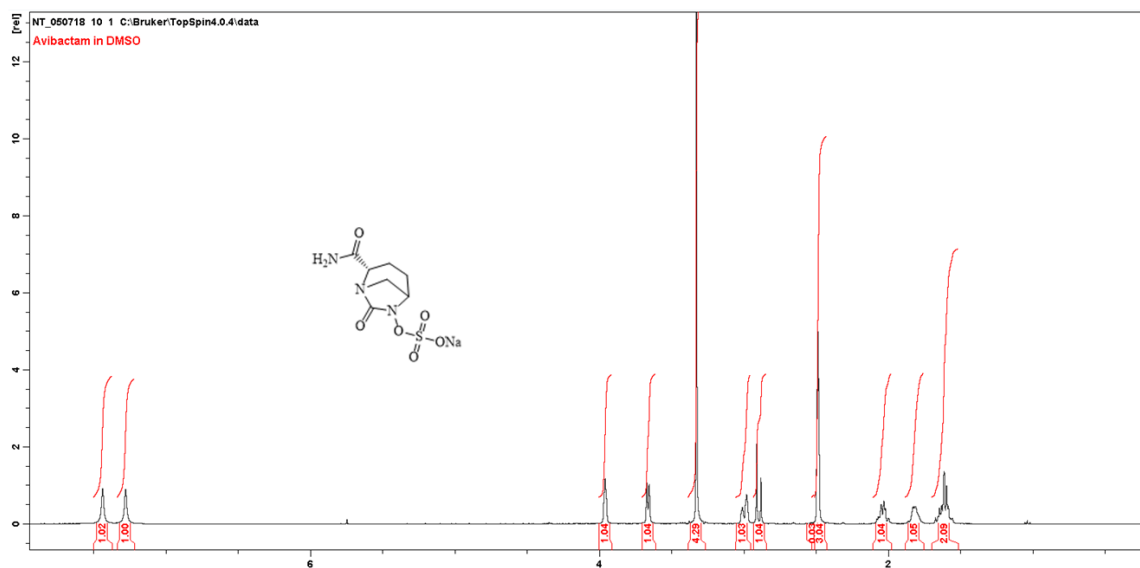


Fig 6.53: Proton NMR of avibactam.

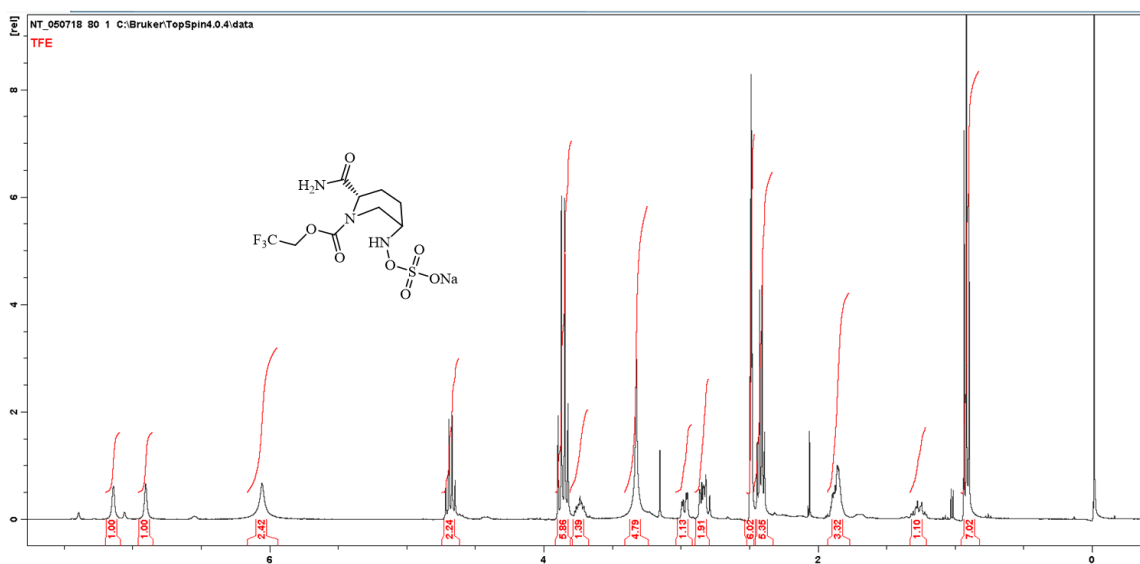


Figure 6.54: Proton NMR of TA carbamate.

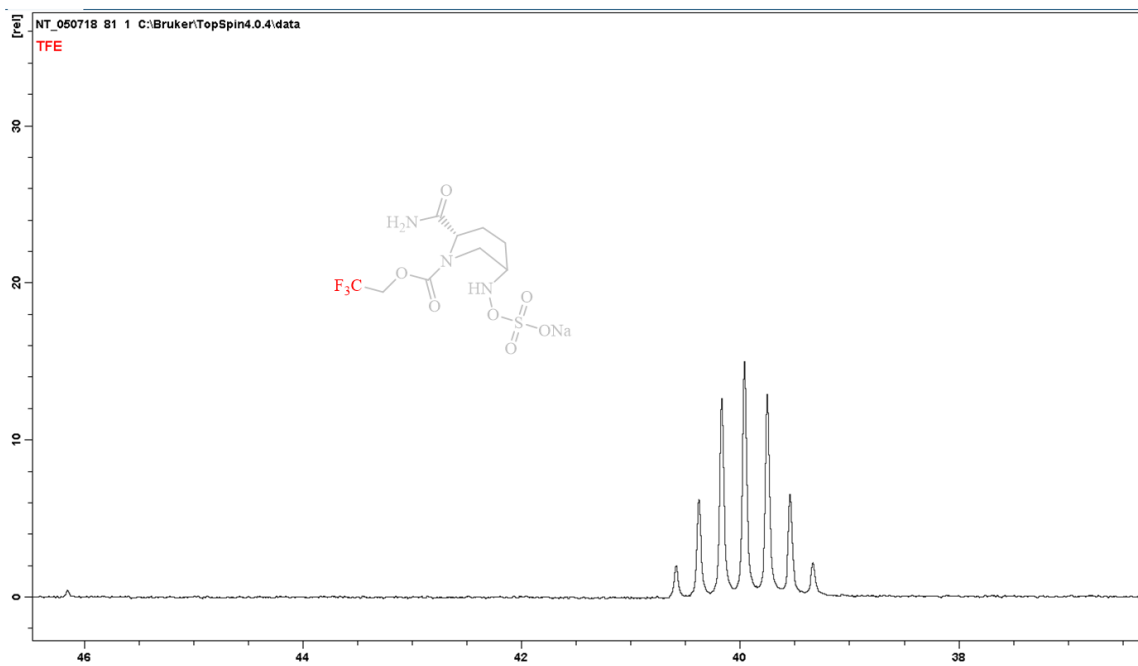


Figure 6.55: Fluorine NMR of TA carbamate.

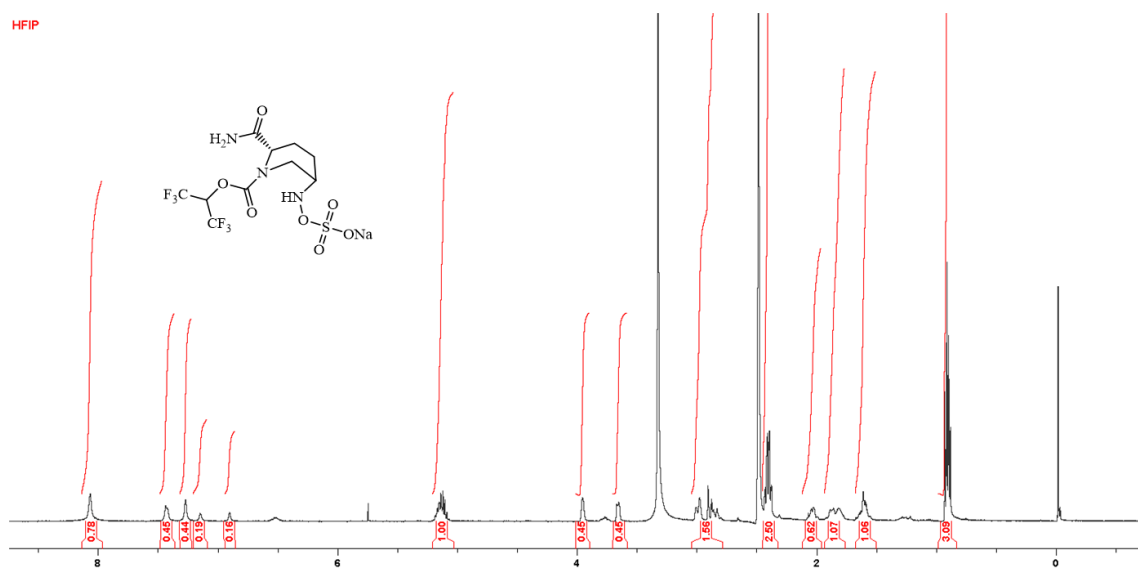


Figure 6.56: Proton NMR of HFIP carbamate.

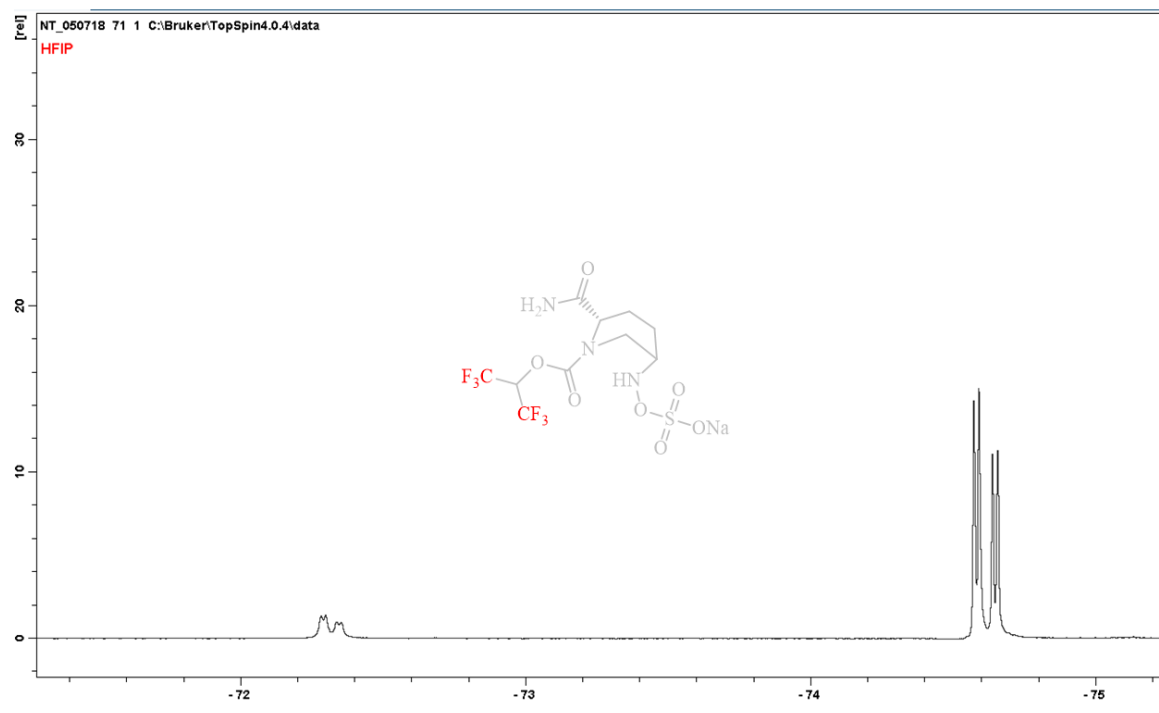


Figure 6.57: Fluorine NMR of HFIP carbamate.

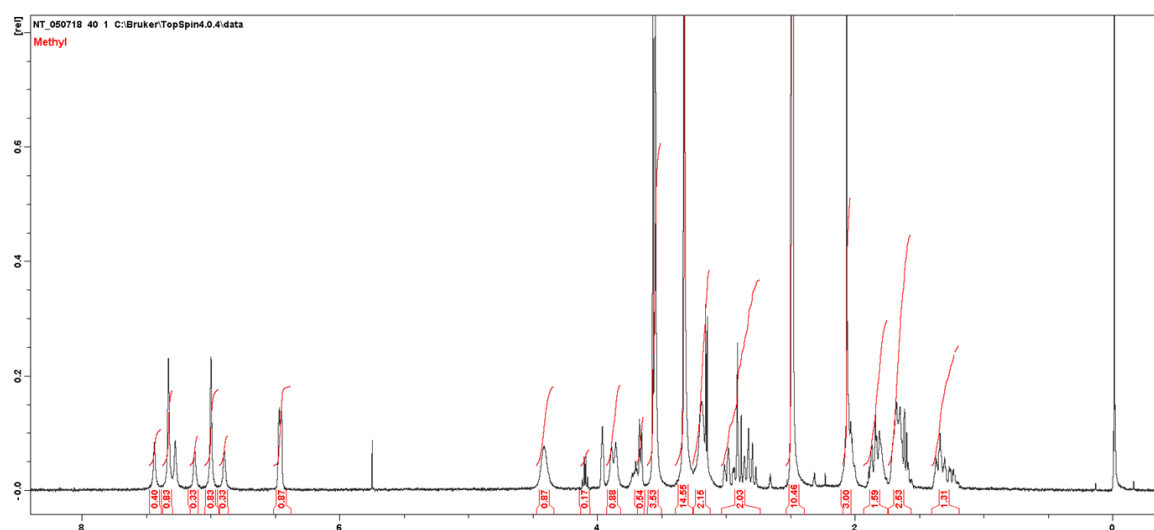


Figure 6.58: Proton NMR of MA carbamate.

### 6.15: Chapter Six References

Cahill, S.T. (2017). *Structural and Kinetic Studies on B-Lactamase Mechanism and Inhibition* (PhD Thesis). University of Oxford, Oxford.